UNIVERSIDAD COMPLUTENSE DE MADRID
FACULTAD DE MEDICINA
Departamento de Farmacología

TESIS DOCTORAL

Vasodilatadores en la hipertensión pulmonar: selectividad por el territorio vascular, por oxígeno y efectos antiproliferativos

MEMORIA PARA OPTAR AL GRADO DE DOCTOR

PRESENTADA POR

Daniel Morales Cano

Directores

Francisco Pérez Vizcaíno

Madrid, 2017

Universidad Complutense de Madrid

Facultad de Medicina

Programa de Doctorado en Investigación Biomédica

Departamento de Farmacología

Vasodilatadores en la hipertensión pulmonar: Selectividad por el territorio vascular, por oxígeno y efectos antiproliferativos

Daniel Morales Cano

Madrid, 2016

Universidad Complutense de Madrid

Facultad de Medicina

Programa de Doctorado en Investigación Biomédica

Departamento de Farmacología

Vasodilatadores en la hipertensión pulmonar: Selectividad por el territorio vascular, por oxígeno y efectos antiproliferativos

DANIEL MORALES CANO

Bajo la dirección de:

Dr. Francisco Pérez Vizcaíno

Dr. Ángel Cogolludo Torralba

Madrid, 2016

INDEX

LIST OF ABBREVIATIONS

$_i$[Ca^{2+}]: intracellular calcium concentration

5-HT: 5-hydroxytriptamine or serotonin

AA: arachidonic acid

AC: adenylate cyclase

Ach: acetilcholine

ADMA: asymmetric dimethylarginine

ALK: activin receptor like kinase

ALK-1: activin receptor-like kinase-1

ANOVA: analysis of variance

BH_4: tetrahydrobiopterin

BK_{Ca}: large-conductance calcium sensitive potassium channels

BMP: bone morphogenetic proteins

BMPR: bone morphogenetic protein receptor

BMPR2: bone morphogenetic protein receptor type 2

BrdU: 5-bromo-2-deoxyuridine

BSA: bovine serum albumin

BW: body weight

c-Abl: c-Abelson tyrosine kinase

Ca_L: L-type voltage-dependent Ca^{2+} channel

cAMP: cyclic adenosine monophosphate

CAV1: caveolin-1

CCB: calcium channel blocker

cdk2: cyclin-dependent kinase 2

cDNA: complementary DNA

cGMP: cyclic guanosine monophosphate

CKI: cyclin-dependent kinase inhibitor

CNS: central nervous system

CO: cardiac output

COPD: chronic obstructive pulmonary disease

co-Smad: co-mediator Smad

COX: cyclooxygenase

CTEPH: chronic thromboembolic pulmonary hypertension

DAG: diacylglycerol

DC: dendritic cells

DDAH: dimethylarginine dimethylaminohydrolase

DEA-NO: diethylamine NONOate sodium salt hydrate

dH_2O: double distilled water

DMEM: Dulbecco´s modified Eagle´s medium

DMSO: dimethyl sulfoxide

DTT: DL-dithiothreitol

EC: endothelial cells

ECE: endothelin-converting enzyme

ECM: extracellular matrix

EDHF: Endothelium-derived hyperpolarizing factor

EGF: epidermal growth factor

EIF2AK4: eukaryotic translation initiation factor 2 alpha kinase 4

Em: membrane potential

eNOS: endotelial nitric oxide sythase

ERA: endothelin receptor antagonist

ERK 1/2: extra-cellular regulated kinase 1/2

ET-1: endothelin 1

ET_A : endothelin receptor type A

ET_B : endothelin receptor type B

ETs: endothelins

FAD: flavin adenine dinucleotide

FBS: foetal bovine serum

FC: functional Class

FGF: fibroblast growth factor

FKBP12: tacrolimus binding protein 12

FMN: flavin mononucleotide

GC: guanylate cyclase

GDF: growth and differentiation factor

GPCR: G protein-coupled receptors

GPx: gluthatione peroxidase

GSH: gluthatione

H_2O_2 : hydrogen peroxide

HIF: hypoxia inducible factor

HIF-1α: hypoxia inducible factor -1α

hPA: Human Pulmonary artery

HPAH: hereditable pulmonary arterial hypertension

hPASMCs: human pulmonary artery smooth muscle cells

HPV: hypoxic pulmonary vasoconstriction

HR: heart rate

i.p.: intraperitoneal

i.v.: intravenous

ICAM-1: intercellular adhesion molecule

ID: internal diameter

IK_{Ca}: intermediated-conductance K_{Ca} channels

IL-1 β: interleukin-1 β

IL-1: interleukin-1

IL-6: interleukin-6

IL-8: interleukin-8

ILD: interstitial lung disease

iNOS: inducible nitric oxide sythase

IP: prostacyclin receptor

IP_3: inositol-1,4,5-trisphosphate

IPAH: idiophatic Pulmonary Hypertension

IPF: idiopathic pulmonary fibrosis

I-Smad: Inhibitory –Smad

JNK: c-Jun N-terminal kinase

K_2P: two-pore domain K+ channels

K_{ATP}: ATP-sensitive K+ channel

K_{Ca}: Ca^{2+} activated K+ channels

KCNK3: potassium channels subfamily K member 3

K_{ir}: inward rectifier K^+ channels

Kv: voltage -dependent potasium channels

LV+S: left ventricle plus septum

MAO_A: monoamino oxidase A

MAPK: mitogen-activated protein kinase

MAPKKK: mitogen-activated protein kinase kinase kinase

MCP-1: monocyte chemoattractan protein-1

MCT: monocrotaline

micro-CT: small-animal computer tomography

MLC: myosin Light Chain

MLCK: myosin light chain kinase

MLCP: myosin light chain phosphatase

mTOR: mammalian target rapamycin

MTT: 3-(4,5-dimethyltiazol 2-yl)-2,5-diphenyltetrazolium bromide

MYPT: myosin phosphatase-targeting subunit

NADH: reduced nicotinamide adenine dinucleotide

NADPH: reduced nicotinamide adenine dinucleotide phosphate

NFAT: nuclear factor of activated T cells

NF-κB: nuclear factor kappa-light chain-enhancer of activated β cells

nNOS: neuronal nitric oxide sythase

NO: nitric oxide

NOS: nitric oxide synthase

NOX: NADPH oxidase

NYAH: New York Hearth Association

O_2^-: supersoxide

$ONOO^-$: peroxynitrite

OS: oxygen selectivity

PA: pulmonary Arteries

PAEC: pulmonary artery endothelial cells

PAH: pulmonary arterial hypertension

PAI-1: plasminogen activator inhivitor-1

PAP: pulmonary artery pressure

PASMC: pulmonary smooth muscle cells

PCH: pulmonary capillary haemangiomatosis

PDE: cyclic nucleotide phosphodiesterases

PDE5: phosphodiesterase type 5

PDGF: platelet derived growth factor

PFA: paraformaldehyde

PG: prostanglandins

PGI_2: prostacyclin

PGI_2S: prostacyclin synthase

PH: pulmonary Hypertension

PHD: prolyl-hydroxylase

PI: propidium Iodide

PKA: cAMP-dependent protein kinase

PKC: protein kinase C

PKG: cGMP-dependent protein kinase

PLC: phospholipase C

PO_2: partial pressure of oxygen

PPAR: peroxisome proliferator-activated receptor

PS: pulmonary selectivity

PVDF: polyvinylidene fluoride microporous membrane

PVOD: pulmonary veno-occusive disease

PVR: pulmonary Vascular Resistance

qRT-PCR: quantitative real time-polymerase chain reaction

RHC: right heart catheterization.

rMA: rat mesenteric artery

RNS: reactive nitrogen species

ROCK: Rho Kinase

ROS: reactive oxygen species

rPA: rat pulmonary artery

rPASMCs: Rat Pulmonary Artery Smooth Muscle Cells

R-Smad: receptor-regulated Smads

RT: reverse Transcription

RV: right ventricle

RVP: right ventricular pressure

SAP: systemic arterial pressure

SDS: sodium dodecyl sulphate

SDS-PAGE: sodium dodecyl sulphate polyacrylamide gel electrophoresis

SEM: standard error of the mean

SERT: serotonin transporter

sGC: soluble guanylate cyclase

SMC: smooth muscle cells

SNAP: S-nitroso-N-acetylpenicillamine

SNP: sodium nitroprusside

SO_2: arterial saturation

SOD: superoxide dismutase

SPECT: single photon emission computed tomography

SR: sarcoplasmic reticulum

TAK-1: transforming growth factor-β activated kinase 1

TBS: tris buffer saline

TC: $CD8^+$ cytotoxic T cells.

TGF-β: transforming growth factor-β

TH: $CD4^+$ T helper cells

TNF-α: tumor necrosis factor-α

TP: thromboxane A_2 receptors

t-PA: tissue plasminogen activator

TPH: tryptophan hydrolase

Treg: $CD4^+$CD25hiFoxP3+CD127low T regulatory cells,

TRPC: canonical transient receptor potential

TTBS: tween tris buffer saline

TX: thromboxanes

TXA_2: Thromboxane A_2

TXB_2: 11-dehydro-TXB_2

TXS: TXA_2 synthase

V/Q: ventilation/perfusion

VCAM-1: vascular cell adhesion molecule

VEGF: vascular endothelial growth factor

VSMC: vascular smooth muscle cells

WHO: World Health Organization

XDH: xanthine dehydrogenase

XO: xanthine oxidase

RESUMEN

La Hipertensión Pulmonar (HP) es una enfermedad crónica y progresiva. La HP presenta una compleja fisiopatología caracterizada por vasoconstricción, remodelado vascular y trombosis. Las terapias actuales muestran efectos beneficiosos, sin embargo presentan también importantes limitaciones: 1) pobre selectividad pulmonar, 2) modesta eficacia vasodilatadora, 3) desacoplamiento de la ventilación/perfusión (V/Q) e 4) incapacidad para prevenir la progresión de la enfermedad.

La quercetina es un flavonoide natural que se consume en la dieta. Ejerce efectos *in vitro* como vasodilatador, antiagregante y antiproliferativo. Además, reduce la presión arterial, la hipertrofia cardíaca y el remodelado vascular en modelos animales de hipertensión arterial.

Hipótesis y objetivos

La **hipótesis general** de esta tesis es que los fármacos vasodilatadores sensibles al oxígeno con selectividad pulmonar son eficaces para reducir la presión arterial pulmonar (PAP) y para preservar o mejorar la oxigenación arterial. El **objetivo general** de esta tesis es analizar los efectos vasodilatadores y antiproliferativos de una amplia gama de fármacos con el fin de identificar aquellos que potencialmente presenten una mejor eficacia y menos efectos secundarios, basado en su capacidad para: 1) combinar los efectos como vasodilatador y antiproliferativo, 2) ejercer efectos vasodilatadores selectivos en la circulación pulmonar, evitando la hipotensión sistémica, 3) inducir vasodilatación selectiva en zonas bien oxigenadas (preservando la vasoconstricción pulmonar hipóxica-VPH) y 4) ejercer vasodilatación eficaz en condiciones de sensibilización al calcio.

Material y métodos

La selectividad pulmonar y por oxígeno se evaluaron utilizando arterias mesentérica y pulmonares (AP) de ratas y AP humanas bajo diferentes condiciones de oxigenación en un miógrafo isométrico. Las preparaciones se estimularon con una mezcla de serotonina, U46619 y endotelina-1 antes de realizar curvas concentración-respuesta a diferentes fármacos.

Los efectos antiproliferativos se estudiaron en células musculares lisas de arterias pulmonares (PASMC) humanas (hPASMCs) y de ratas control (rPASMCs) o con HP inducida por monocrotalina (rPASMCs-MCT) usando los ensayos de BrdU y MTT.

La PAP y la presión sistémica se evaluaron en ratas anestesiadas. El análisis de V/Q se realizó mediante micro-CT-SPECT en un modelo animal de fibrosis pulmonar inducido por bleomicina. Se evaluaron los efectos *in vivo* de la quercetina en el modelo de monocrotalina.

La expresión del ARNm y proteínas se midieron mediante qRT-PCR y Western blot, respectivamente. Las corrientes Kv se registraron en PASMC utilizando la técnica de patch-clamp.

Resultados

Nuestros resultados en el capítulo 1 indican que los fármacos estudiados mostraron poca selectividad pulmonar y por oxígeno. Algunos fármacos (treprostinil, nifedipino y levosimendan) fueron más eficaces en AP humanas y otros (sildenafilo, riociguat, hidroxifasudil y GW0742) en AP de rata. La quercetina relajó ambos vasos con la misma eficacia.

Las hPASMCs fueron más sensibles al efecto antiproliferativo de la mayoría de los fármacos. Algunos fármacos (BAY 41-2272, GW0742, sildenafilo y tadalafilo) mostraron mayores efectos en rPASMCs-MCT que en rPASMC. Cuando se examinaron los efectos sobre la incorporación de BrdU, la mayoría de los fármacos mostraron mayores efectos en rPASMCs que en hPASMCs, y, en rPASMCs-MCT, en comparación con rPASMC.

En cuanto al perfil vasodilatador/antiproliferativo, se observó que la mayoría de los fármacos actuaban principalmente como vasodilatadores, excepto el 5z-7-oxozeaenol, la rosiglitazona y la retigabina, que mostraron un perfil como antiproliferativos, y la quercetina, el imatinib y el levosimendan que fueron igual de eficaces para ambos efectos.

El sildenafilo y el riociguat (capítulo 2) reducen la contracción inducida por hipoxia o U46619 en AP de rata. *In vivo* ambos fármacos fueron más eficaces sobre el aumento de la PAP inducida por hipoxia global o por U46619 que por hipoxia unilateral. Ambos

fármacos inhibieron selectivavemente las respuestas pulmonares del U46619 y no empeoraron el acoplamiento V/Q en un modelo de fibrosis pulmonar.

La administración de quercetina *in vivo* (capítulo 3) aumentó la supervivencia y redujo la PAP, la hipertrofia cardiaca y el remodelado vascular. Estos efectos beneficiosos se asocian con un incremento de las corrientes Kv, una reducción de la expresión de 5-HT_{2A} y de la fosforilación de Akt. *In vitro* la quercetina ejerció efectos vasodilatadores en AP aisladas, inhibió la proliferación de PASMC y fibroblastos e indujo apoptosis.

Conclusiones

1. Los fármacos estudiados en esta tesis mostraron una baja selectividad pulmonar, siendo iguales o más eficaces como vasodilatadores en las arterias sistémicas que en las arterias pulmonares.

2. Los fármacos estudiados, con la excepción del GW0742 en arterias de rata, no mostraron selectividad por oxígeno, siendo iguales o más eficaces como vasodilatadores en condiciones de bajo nivel de oxígeno en comparación con alto nivel de oxígeno en rata o arterias pulmonares humanas.

3. La comparación de los efectos vasodilatadores frente a los efectos antiproliferativos indica que la mayoría de los fármacos estudiados, incluyendo los donadores de NO, los inhibidores de la PDE5, los activadores de sGC, el activador de la adenilato ciclasa forskolina, el agonista de PPARß/δ GW0742 y el inhibidor de ROCK1/2 hidroxifasudil ejercen un efecto principalmente como vasodilatadores. Algunos fármacos, como el sensibilizador al calcio levosimendan y los fármacos dirigidos a canales iónicos fueron igual de eficaces para ejercer ambos efectos.

4. El inhibidor de TAK-1 5z-7-oxozeaenol produce un efecto antiproliferativo en las células de músculo liso vascular pulmonar sin ningún efecto sobre el tono vascular. Por lo tanto, nuestros datos sugieren que TAK-1 puede representar una nueva diana para el tratamiento de la HP.

5. El riociguat fue un vasodilatador más eficaz en AP aisladas que el sildenafilo. La potencia de ambos fue similar en condiciones de alto oxígeno y en hipoxia. Ambos fármacos inhiben *in vitro* la respuesta vasoconstrictora a la hipoxia y al U46619. *In vivo*,

los dos fármacos fueron más eficaces en la inhibición del aumento de la PAP inducida por la hipoxia global o por el U46619 que en la inhibición de la respuesta a la hipoxia inducida por la obstrucción bronquial unilateral. Además, la fibrosis pulmonar se asoció con el desacoplamiento de la ventilación-perfusión y, aunque ambos fármacos aumentaron la perfusión pulmonar, no afectaron al acoplamiento ventilación-perfusión.

6. La quercetina indujo un efecto similar como vasodilatador y antiproliferativo *in vitro* en células de músculo liso pulmonar de rata y humano. En el modelo de HP, la quercetina aumentó la supervivencia mediante la reducción de la PAP, la hipertrofia del ventrículo derecho y el remodelado vascular. Aun cuando algunos marcadores biológicos clásicos de la hipertensión arterial pulmonar no se vieron afectados por quercetina, restauró la disminución de las corrientes Kv y redujo el aumento de la fosforilación de Akt y S6 inducida por monocrotalina. Por lo tanto, la quercetina podría ser útil en el tratamiento de la HP.

ABSTRACT

Pulmonary hypertension (PH) is a life-threatening chronic and progressive disease. PH exhibits a complex pathophysiology characterized by vasoconstriction, vascular remodeling and micro-thrombosis. Current therapies exert some beneficial effects; however they have a number of important limitations: 1) poor pulmonary selectivity 2) modest vasodilator efficacy, 3) ventilation/perfusion (V/Q) mismatch and 4) unability to prevent the progression of the disease.

Quercetin is a natural flavonoid consumed in the diet that exerts vasodilator, antiagregant and antiproliferative effects *in vitro*, and reduces blood pressure, cardiac hypertrophy and vascular remodelling in animal models of arterial hypertension.

Hypothesis and aim

The **general hypothesis** of this thesis is that oxygen-sensitive vasodilators with pulmonary selectivity are effective in lowering pulmonary arterial pressure (PAP) and preserve or improve arterial oxygenation. The **general aim** of this thesis is to analyze the vasodilator and antiproliferative effects of a wide range of drugs in order to identify those with potentially better efficacy and fewer side effects, based on their ability to: 1) combine both vasodilator and antiproliferative effects, 2) exert selective vasodilator effects in the pulmonary circulation, avoiding systemic hypotension, 3) induce selective vasodilator effects in the oxygenated lung areas (preserving hypoxic pulmonary vasoconstriction-HPV) and 4) exert effective vasodilator effects under calcium-sensitizing conditions.

Matherial and methods

Pulmonary and oxygen selectivity were assessed using mesenteric and pulmonary arteries (PA) from rats and human PA under different conditions of oxygenation. The preparations were stimulated with a mixture of serotonin, U46619 and endothelin-1 before the concentration-response curves to different drugs. In other set of experiments, HPV was recorded in rat PA. Vasodilator responses were evaluated in a wire myograph.

Antiproliferative effects were studied in primary cultures of pulmonary artery smooth muscle cells (PASMC) isolated from patients (hPASMCs), control rats (rPASMCs) or

monocrotaline-induced PAH rat model (rPASMCs-MCT) using the MTT and BrdU incorporation assays.

Systemic and PAP were assessed in anesthetized rats. V/Q analysis was performed by micro-CT-SPECT in an animal model of bleomycin-induced pulmonary fibrosis. The *in vivo* effects of quercetin were evaluated in a rat model of PAH-induced by MCT.

mRNA and protein expression were measured by qRT-PCR and Western blot, respectively. Kv currents were recorded in isolated PASMC using the patch clamp technique.

Results

Our results in chapter 1 indicate that the drugs studied showed low pulmonary and oxygen selectivity. Furthermore, some drugs (treprostinil, nifedipine and levosimendan) were more effective in hPAs, others (sildenafil, riociguat, hydroxyfasudil and GW0742) were better vasodilators in rPAs, and quercetin relaxed both vessels with the same efficacy.

When comparing their effects in rPASMCs versus hPASMCs cell viability it is observed that hPASMCs were more sensitive to the antiproliferative effect of most of the drugs. However, in rPASMCs versus rPASMCs-MCT we observed that some drugs (BAY 41-2272, GW0742, sildenafil and tadalafil) exhibited higher effects in rPASMCs-MCT. When we examined the effects on BrdU incorporation most of the drugs showed higher effects in rPASMCs than in hPASMCs, and, in rPASMCs-MCT as compared to rPASMC.

Regarding the vasodilator/antiproliferative profile, it is observed that most of the drugs tested act mainly as vasodilators except 5z-7-oxozeaenol, rosiglitazone and retigabine which showed an antiproliferative profile, and quercetin, imatinib and levosimendan were similarly effective to exert both effects.

In chapter 2, we found that sildenafil and riociguat reduced both the HPV and the contraction induced by U46619 in rat PAs. *In vivo* both drugs were more effective in inhibiting the increase in PAP induced by global hypoxia or by U46619 than in

inhibiting the unilateral hypoxia. Interestingly, both drugs showed a pulmonary selective inhibition of U46619-induced responses and they did not worsen V/Q coupling in a rat model of pulmonary fibrosis.

In chapter 3, we found that *in vivo* administration of quercetin led to a significant increase in survival and to a reduction of PAP, right ventricular hypertrophy and vascular remodelling. These beneficial effects were associated with an incrase in Kv currents, and a reduction 5-HT_{2A} expression and Akt phosphorylation. Furthermore, *in vitro* quercetin exerted effective vasodilator effects in isolated PA, inhibited PASMC and fibroblast proliferation and it induced apoptosis.

Conclusions

1. The drugs studied in this thesis showed low pulmonary selectivity, being equally or more effective as vasodilators in systemic (i.e. mesenteric) than in pulmonary arteries.
2. The drugs studied, with the exception of GW0742 in rat arteries, showed no oxygen selectivity, being equally or more effective as vasodilators under conditions of low oxygen as compared to high oxygen levels in rat or human pulmonary arteries.
3. The comparison of the vasodilator versus antiproliferative effects indicates that most of the drugs tested, including NO donors, PDE5 inhibitors, sGC activators, adenylate cyclase activator forskolin, the PPARβ/δ agonist GW0742 and the ROCK1/2 inhibitor hydroxyfasudil exert preferential vasodilator effects. Some drugs including the calcium sentitizer levosimendan and drugs targeting ion channels were similarly effective to exert both effects.
4. The TAK-1 inhibitor 5z-7-oxozeaenol produced strong and specific antiproliferative effects in pulmonary vascular smooth muscle cells without any effect on vascular tone. Thus, our data suggest that TAK-1 may represent a novel target for the treatment of PH.
5. Riociguat was a more effective vasodilator in isolated PA than sildenafil. The potency of both drugs was similar under conditions of high oxygen vs hypoxia. Both drugs inhibited *in vitro* the vasoconstrictor response to hypoxia and U46619. *In*

vivo, the two drugs were more effective in inhibiting the increase in PAP induced by global hypoxia or by U46619 than in inhibiting the response to unilateral hypoxia induced by bronchial obstruction. Furthermore, pulmonary fibrosis was associated with ventilation-perfusion uncoupling and although both drugs increased lung perfusion, they did not affect the ventilation-perfusion coupling.

6. Quercetin induced a strong vasodilator and antiproliferative effect in rat and human pulmonary smooth muscle *in vitro*. In the rat model of PH, quercetin increased the survival by lowering PAP, right ventricular hypertrophy and vascular remodeling. Even when some classic biomarkers of pulmonary arterial hypertension were unaffected by quercetin, it restored the decrease in Kv current and reduced the increase in Akt and S6 phosphorylation induced by monocrotaline. Therefore, quercetin could be useful in the treatment of PH.

INTRODUCTION

Pulmonary physiology

1.1. Functional organization

Lungs are the primary organs of respiration and constitute the only organ in the body that receives the entire cardiac output (CO). They are located within the rib cage occupying most of its space. The right lung is divided into three lobes (upper, middle and lower), each of them irrigated by a ramification of the right pulmonary artery (PA), while the left lung is divided into two lobes (upper and lower), each of them is irrigated by a ramification of the left pulmonary artery. The lobes of both lungs are further subdivided into bronchopulmonary segments which contain their own bronchus and branch of the pulmonary artery.

The vascular system plays a critical role for development as well as for tissue homeostasis and repair. It brings in an adequate supply of oxygen and nutrients, removes waste products, and transports cells through blood and lymphatic vessels (García de Vinuesa et al., 2016).

1.2. Pulmonary Circulation

The pulmonary circulation or “minor circulation” is normally a high flow, low resistance and low pressure system that carries blood into the pulmonary microcirculation whose main function is to facilitate gas exchange, (Mandegar et al., 2004). The pulmonary vasculature is comprised of three anatomic compartments connected in series: the arterial tree, an extensive capillary bed, and the venular tree (Townsley et al., 2012). In humans, there are 15 orders of pulmonary arteries between the main pulmonary artery and the capillaries and 15 orders of pulmonary veins between the capillaries and the left atrium (Kuhr et al., 2012).

The pulmonary circulation receives deoxygenated blood directly from the right ventricle (RV) of the heart through the main pulmonary artery which is divided into the left and right pulmonary arteries. Both arteries follow their conventional axial

pathway, parallel to the airway course, splitting progressively into smaller and smaller arterial branches, through the center of the lobe from the lung hilum to the peripheral lung pleural surface (Townsley et al., 2012).

This capillary network carries the blood to the alveoli allowing gas exchange by the contact between blood and air into the alveolar space, and allowing blood oxygenation. Based on direct measurement from cast of the pulmonary vasculature or from transmission electron microscopy, average capillary diameter ranges from 5-8 µm. However, their diameter may vary due to lung inflation and pulmonary arterial and venous pressure (Townsley et al., 2012). After blood is loaded with oxygen in the alveolar capillaries, the oxygen rich blood is transported through the pulmonary veins network. The left and right pulmonary veins join into a main pulmonary vein, which carries the blood to the left atrium of the heart and from there is pumped back into the systemic circulation.

1.3. Pulmonary arteries

At histological level, the pulmonary arteries are composed by tree different and concentric layers (Figure 1):

- **Intimal layer:** the innermost layer of the blood vessel is a non-fenestrated monolayer of endothelial cells lining the vessel lumen. These cells are attached to the underlying basement membrane and the internal elastic lamina composed by connective tissue matrix, which is characterized by frequent gaps, enabling endothelial projections into the media layer and facilitating myoendothelial communication.

- **Media layer:** the interlayer of the vessel. It is comprised by vascular smooth muscle cells (VSMC) and connective tissue. VSMC are able to modify the vessel diameter by contraction and relaxation, regulating the vascular tone and blood pressure. The external elastic lamina composed by elastic fibers is found between the medial layer and the adventitia.

- **Adventitia:** The outermost layer. In general, it is loosely organized, comprised by extracellular matrix of collagen and elastin fibers, fibroblast or other interstitial cells, and a neural network. A vascular network, i.e. *vasa vasorum,* is also present in the larger arteries. This layer contributes to the structural integrity of the vessel.

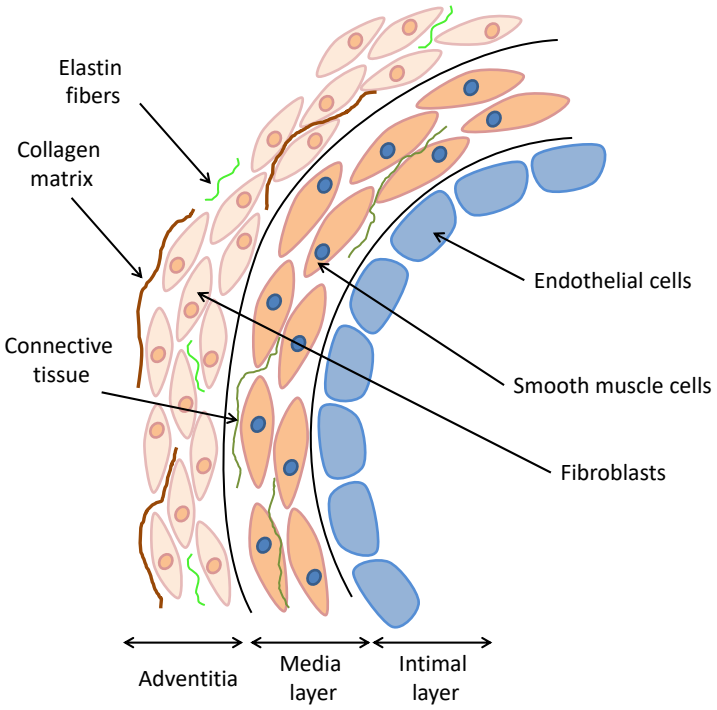

Figure 1: Schematic representation of cell types in the pulmonary vascular wall

The composition of the vascular wall, as well as the contribution of each layer varies from the proximal to the smaller extra-alveolar pulmonary arteries. Based on the presence of **elastic lamina** and the **degree of muscularity** (Figure 2), pulmonary arteries are classified into:

- **Elastic or large conduit arteries:** comprised of multiple layers of elastic lamina and VSMC, including the main pulmonary artery trunk, their ramifications and extralobular arteries. Their diameter is higher than 1 mm.

- **Muscular arteries:** comprised by a VSMC layer between the internal and external elastic lamina. This group includes pulmonary arteries that cross the lung lobes and follow the bronchus course, and determine the pulmonary vascular resistance (PVR). Their diameter is between 100 – 1000 µm.

- **Partially-muscular arteries:** characterized by an incomplete VSMC coat around the circumference of the vessel, the presence of intermediate cells and pericytes.

- **Precapillary non-muscular arteries:** adjacent to alveolar ducts. Their diameter is less than 100 μm.

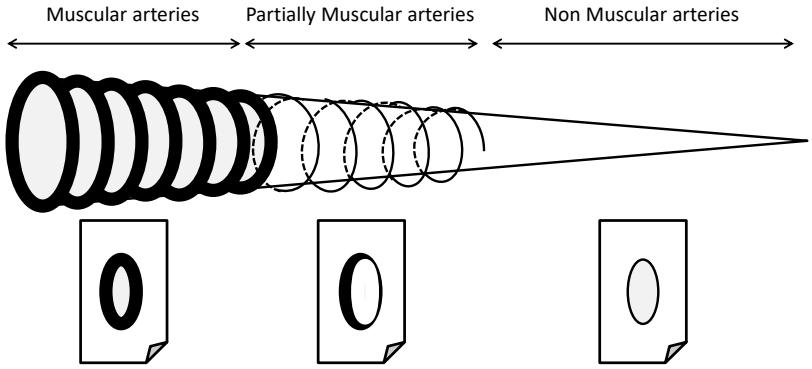

Figure 2: Schematic representation showing the graded structural changes in the media of the pulmonary arterial wall, moving from muscular arteries to precapillary non-muscular vessels and representative cross-sections of the media layer*. Adapted from Townsley et al., 2012.*

The transition among the different types of pulmonary arteries occurs in a progressive way, from muscular arteries to precapillary non-muscular vessel (Townsley et al., 2012).

1.4. Pulmonary arterial pressure

The pulmonary arterial pressure (PAP) is normally low under normal physiological conditions. The PAP is the product of CO and PVR as shown the following equation:

$$PAP = CO \times [PVR_{arteries} + PVR_{capillaries} + PVR_{veins}]$$

Where PVR is the vascular resistance of the pulmonary arteries, capillaries, and veins. (Mandegar et al., 2004).

In healthy individuals, the PAP is approximately 12-16 mmHg (2kPa), although these values vary with age, high altitude or during exercise or diving. When PAP rises due to

an increase of CO, the PVR decreases according to local mechanisms: pulmonary artery distension and capillary recruitment. Under normal conditions some capillaries are closed due to a low perfusion pressure and, when the blood flow and PAP increase (e.g. during exercise), these closed vessels open and decrease the PVR (capillary recruitment), being the main mechanism reducing PVR. Pulmonary artery distension is caused by dilation of the capillary segments due to the pulmonary capillaries are extremely thin and elastic (Kuhr et al., 2012; Kovacs et al., 2009).

Blood flow in the pulmonary circulation follows Poiseuille´s law:

$$PVR = 8L\eta/\prod \times 1/r^4$$

This equation states that PVR is inversely proportional to the fourth power of the radius of the blood vessel (*r*) and directly proportional to the length of the blood vessel (*L*) and viscosity of the blood (*η*). Therefore, small changes in the radius of the vessel can significantly change the PVR (Mandegar et al., 2004; Thenappan et al., 2016).

1.5. The Regulation of Pulmonary Vascular Tone

In contrast to the systemic arteries which regulate blood flow and oxygen delivery to the organs and tissue depending on their demands, PA regulate blood flow into the lung in order to achieve the highest oxygen saturation possible (Perez-Vizcaino et al., 2010). The regulation of vascular tone in the pulmonary circulation is a complex and multifactorial process that involves the distensibility of the pulmonary vasculature, the function of the heart, the concentration of oxygen in the blood and the capacity of the endothelium to release vasoactive substances (Chester et al., 2014). All these mechanisms together determine PVR and ensure that the pulmonary circulation is maintained as a low pressure and high blood flow circuit (Chester et al., 2014; Olschewski et al., 2014)

As in systemic circulation, the endothelium in the pulmonary circulation has a profound influence on vascular tone and remodelling. The endothelial cells (EC) release a variety of vasodilators as nitric oxide (NO), prostacyclin (PGI_2), and endothelium-

derived hyperpolarizing factor (EDHF), and vasoconstrictors, mainly endothelin-1 (ET-1) and thromboxane A_2 (TXA_2) (Cogolludo et al., 2007). The control of pulmonary vascular tone also involves a large number of factors acting through a wide variety of signalling pathways on many different targets within the pulmonary artery smooth muscle cells (PASMC) (Figure 3) (Cogolludo et al., 2007, Grassie et al., 2012).

At rest, a major contributor to pulmonary vascular tone is the activity of potassium channels by regulating resting membrane potential (*Em*), an important determinant of cytosolic intracellular calcium concentration ($[Ca^{2+}]_i$). When the voltage-dependent potassium channels (Kv) are closed or inactivated, membrane potential depolarizes, which leads to L-type voltage-dependent Ca^{2+} channel (Ca_L) opening, an increase in intracellular Ca^{2+} concentrations and sustained vasoconstriction (Kuhr et al., 2012, Cogolludo et al., 2007, Bonnet et al., 2007; Cogolludo et al., 2006).

Kv channels play a prominent role as a common target for several pulmonary vasoactive factors. Thus, hypoxia, TXA_2, ET-1 and serotonin (5-HT) decrease and NO and PGI_2 increase K^+ currents by inhibiting or activating, respectively, Kv channels (Cogolludo et al, 2007, Cogolludo et al., 2006).

In either systemic or pulmonary vessels, contraction is determined by phosphorylation/dephosphorylation at Ser 19 of the myosin light chain (MLC), which facilitates formation of the actin-myosin complex and cross-bridge cycling. MLC phosphorylation is dependent on the relative activity of the myosin light chain kinase (MLCK) and myosin light chain phosphatase (MLCP). Although MLCK is a Ca^{2+}/calmodulin dependent kinase, MLCP activity can be regulated independently of changes in i[Ca2+] (Grassie et al., 2012, Kuhr et al., 2012). Therefore, although i[Ca2+] is a major trigger for pulmonary vasoconstriction, the contraction and relaxation may also be regulated independently of changes in $[Ca^{2+}]_i$. Ca^{2+} sensitization (regulated by several kinases as Rho kinase (ROCK), protein kinase C (PKC), mitogen-activated protein kinase (MAPK), and non-receptor tyrosine kinases) and desensitization (triggered by cyclic nucleotides; cyclic adenosine monophosphate- cAMP and cyclic guanosine monophosphate-cGMP) of the contractile filaments also contribute to the control of pulmonary vascular tone (Cogolludo et al., 2007).

The increase in i[Ca2+] is mediated by two mechanisms: Ca^{2+} entry from the extracellular space and Ca^{2+} release from intracellular stores. Ca^{2+} influx through Ca_L channels is the main source of intracellular Ca^{2+}. Non-selective cation channels, encoded by the canonical transient receptor potential (TRPC) gene family, is an alternative Ca^{2+} influx pathway. Ca^{2+} release from intracellular stores from the sarcoplasmic reticulum (SR) is mediated by channels gated by Ca^{2+} (ryanodine-sensitive channels) and channels gated by the second messenger inositol-1,4,5-trisphosphate (IP_3). On the other hand, Ca^{2+} is sequestered into the SR against ionic gradient by the sarcoplasmic reticulum Ca^{2+} ATPase (SERCA) and extruded by the plasmalemmal Ca^{2+} ATPase (PMCA) or by facilitated diffusion systems such as the Na^{+}/Ca^{2+} exchanger (Cogolludo et al., 2007; Firth et al., 2013; Mandegar et al., 2004).

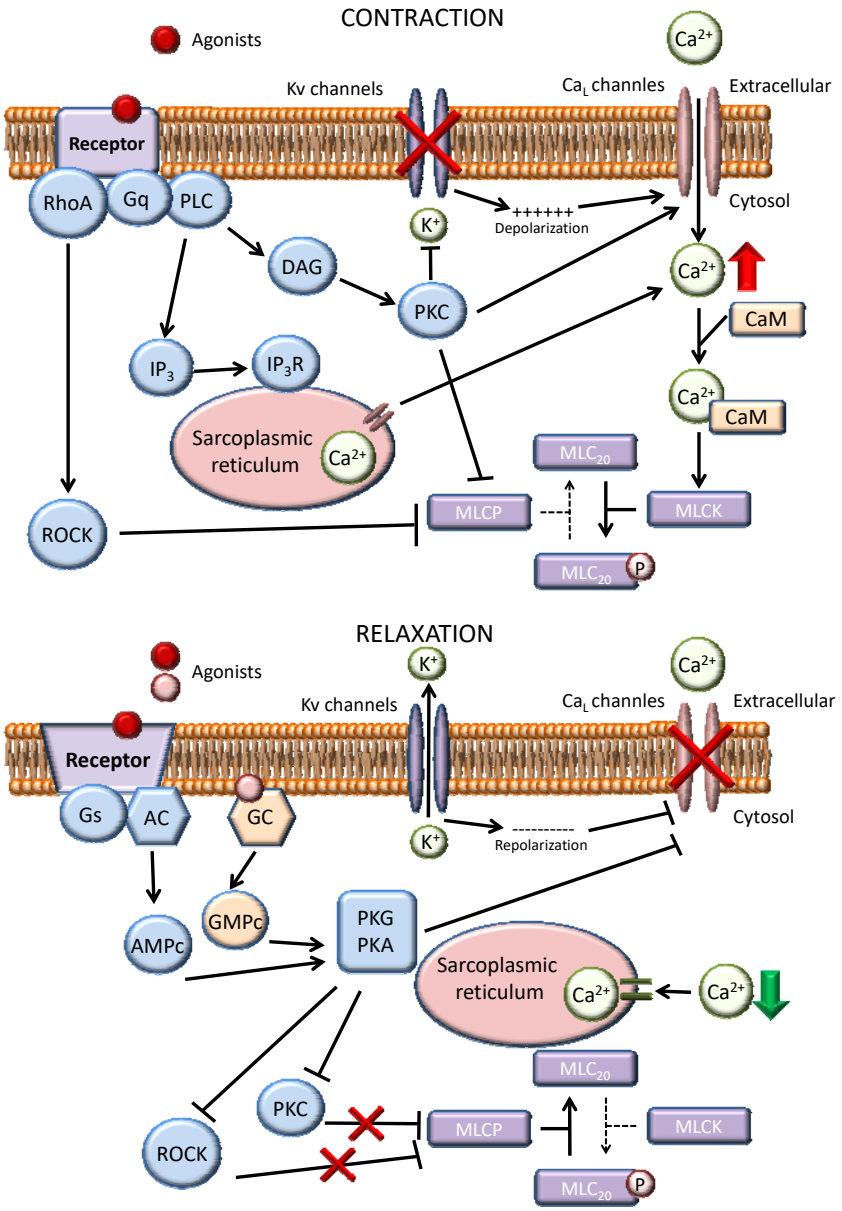

Figure 3: Schematic overview of the mechanisms controlling vascular tone regulation in PASMC*. Adapted from Cogolludo et al., 2006 and Cogolludo et al., 2007.*

In summary, the control of pulmonary vascular tone involves the activation of a wide variety of signalling cascades modulating Ca^{2+} homeostasis, Ca^{2+} sensitivity or both.

2. Pulmonary Hypertension

Pulmonary hypertension (PH) is a progressive pathophysiological disorder that affects the lung vasculature including the PA, pulmonary veins and pulmonary capillaries, resulting in an increase of pulmonary pressure. This increased pulmonary pressure

causes hypertrophy of the RV, whose function progressively declines, leading to heart failure and eventually death. This progressive dysfunction of the RV leads to decreased exercise tolerance and shortness of breath (Galie et al., 2015; Kim et al., 2015; Selej et al., 2015).

2.1. Definition and classification

PH is defined as an increase in mean pulmonary arterial pressure (PAP) ≥ 25mmHg at rest as assessed by right heart catheterization (RHC). The normal mean PAP at rest is 14 ± 3 mmHg with an upper limit of normal of approximately 20 mmHg (Galie et al., 2015).

PH classification includes multiple clinical conditions that show a similar clinical presentation such as: shortness of breath, fatigue, non-productive cough, weakness, angina pectoris, syncope and peripheral edema. The different classes of PH have been recently categorized more precisely in the firth symposium of PH held in Nice, France, in 2013 (Table 1). This classification subdivides PH into five groups according their similar clinical presentation, pathological finding, hemodynamic characteristics and treatment strategy (Galie et al., 2015).

In addition, the New York Heart Association (NYAH) and the World Health Organization (WHO) classify PH into four functional classes (FC) that share a similar degree of exercise limitation, symptoms and prognosis. Class I includes patients without any limitation or symptoms. Patients in class II and III show a progressive deterioration of their daily physical activity and patients in class IV have severe limitations, even at rest, resulting in inability to carry out any physical activity without symptoms. (Table 2) (Lammers et al., 2011, Saglam et al., 2015, Mackenzie et al, 2015). This classification is useful because it provides a link between the symptoms and functional limitations of patients, which allows studying and monitoring the progression of the disease regardless of the etiology of PH, being considered one of the best predictors of survival.

Table 1: Clinical classification of pulmonary hypertension

1. Pulmonary arterial hypertension (PAH)
1.1 Idiopathic (IPAH) 1.2 Heritable (HPAH) 1.2.1 BMPR2 mutation 1.2.2 Other mutation 1.3 Drug and toxins induced 1.4 Associated with 1.4.1 Connective tissue disease 1.4.2 Human immunodeficiency virus (HIV) infection 1.4.3 Portal hypertension 1.4.4 Congenital heart disease 1.4.5 Schistosomiasis
1´. Pulmonary veno-occusive disease (PVOD)and/or pulmonary capillary haemangiomatosis (PCH)
1´.1 Idiophatic 1´.2 Heritable 1´.2.1 EIF2AK4 mutation 1´.2.2 Other mutation 1´.3 Drugs, toxins and radiation induced 1´.4 Associated with: 1´.4.1 Connective tissue disease 1´.4.2 HIV infection
1´´. Persistent pulmonary hypertension of the newborn
2. Pulmonary hypertension due to left heart disease
2.1 Left ventricular systolic dysfunction 2.2 Left ventricular diastolic dysfunction 2.3 Valvular disease 2.4 Congenital/acquired left heart inflow/outflow tract obstruction and congenital cardiomyophaties 2.5 Congenital/acquires pulmonary veins stenosis
3. Pulmonary hypertension due to lung disease and/or hypoxia
3.1 Chronic obstructive pulmonary disease 3.2 Interstitial lung disease 3.3 Other pulmonary diseases with mixed restrictive and obstructive pattern 3.4 Sleep-disordered breathing 3.5 Alveolar hypoventilation disorders 3.6 Chronic exposure to high altitude 3.7 Developmental lung disease
4. Chronic thromboembolic pulmonary hypertension (CTEPH) and other pulmonary artery obstruction
4.1 Chronic thromboembolism pulmonary hypertension 4.2 Other pulmonary artery obstruction 4.2.1 Angiosarcoma 4.2.2 Other intravascular tumors 4.2.3 Arteritis 4.2.4 Congenital pulmonary arteries stenosis 4.2.5 Parasites (hydatidosis)

5. Pulmonary hypertension with unclear and/or multifactorial mechanism
5.1 Haematological disorders: chronic haemolytic anemia, myeloproliferative disorders, splenectomy 5.2 Systemic disorders, sarcoidosis, pulmonary histiocytosis, lymphangioleiomyomatosis 5.3 Metabolic disorders: glycogen storage disease, Gaucher disease, thyroid disorders 5.4 Other: pulmonary tumoral thrombothic microangiopathy, fibrosis mediastinitis, chronic renal failure (with/without dialysis), segmental pulmonary hypertension

Table 2: Functional classification of pulmonary hypertension in adults based on The New York Heart Association classification and WHO.

Class	Symptoms
I	Patients with pulmonary hypertension but without limitation of physical activity. Ordinary physical activity does not cause undue dyspnea, fatigue chest pain or near syncope
II	Patients with pulmonary hypertension resulting in slight limitation of physical activity. Comfortable at rest. Ordinary physical activity causes undue dyspnoea, fatigue, chest pain or near syncope
III	Patients with pulmonary hypertension resulting in marked limitation of activity. Comfortable at rest. Less than ordinary activity causes dyspnea or fatigue, chest pain or near syncope
IV	Patients with pulmonary hypertension resulting in inability to carry out any physical activity without symptoms. These patients manifest symptoms of right heart failure. Dyspnoea and/or fatigue may be present even at rest. Discomfort is increased by any physical activity undertaken. Syncope or near syncope can occur

2.2. Epidemiology

Epidemiological studies on PH are complex for two reasons. First, PH diagnosis is difficult because it requires an invasive RHC. Second, patients with PH are often not referred to specialist centres, limiting the availability of their records in a suitable database (McGoon et al., 2013). Therefore, the knowledge about the incidence and prevalence of PH at the global level is poor. In the UK, a prevalence of 97 cases per million population has been reported. Epidemiologic studies report a greater incidence of the disease in females; depending on the disease classification the female-to-male ratio can be as great as 4:1 (Mair et al., 2014). Epidemiological data of the different groups of PH are not widely available, showing different values. Thus, in Europe, the

prevalence and incidence of class I (PAH) are in the range of 15-60 cases per million population and 5-10 cases per million per year, respectively. Regarding the class 4 (CTEPH), in the Spanish PH registry, CTEPH incidence and prevalence were 3.2 cases per million and 0.9 cases per million per year, respectively. It is should be noted that, although patients belonging to classes 2 (PH due to left hearth disease) and 3 (PH due to lung disease and/or hypoxemia) represent an important part of the clinical practice, there is little information about the demographics and clinical course of this PH population, being their prevalence and incidence related with the progression of FC impairment Furthermore, we need to consider schistosomiasis- associated PAH and high altitude-related PH as an important source of patients that currently they are not well studied (Galie et al., 2015)

2.3. Diagnosis

The diagnosis of PH requires a clinical suspicion based on symptoms and physical examination, due to different pathologies that comprehend the PH term, it is necessary to make a distinction between the various groups of patients with PH because they differ in etiology, prognosis, histological appearance, and response to various therapies (Stenmark et al., 2009; Galie et al., 2015). For that reason, several screening tools are used to diagnose the patients. Among them, non-invasive assessments include: electrocardiogram, chest radiograph, pulmonary function test and arterial blood gases, transthoracic echocardiography (the most important noninvasive tool to assess the possibility of PH), ventilation/perfusion (V/Q) lung scan, high resolution computed tomography, contrast-enhanced computed tomography and cardiac magnetic resonance imaging.

Unfortunately, invasive testing including pulmonary angiography and RHC are required to confirm the diagnosis of PH and assess the severity of haemodynamic impairment (Galie et al., 2015; Hoeper et al., 2013). In all patients suspected to suffer PAH the pulmonary vasoreactivity testing is recommended. Short-acting vasodilators, such as *i.v.*administration of adenosine (50 to 350 μg/min) and epoprostenol (2 to 12 ng/Kg/min), inhaled iloprost (5 μg), inhaled NO (10 to 20 part per million) are used as

the gold standard for vasoreactivity testing. This vasoreactivity testing allows identification of "responder". In all other forms of PAH or PH, pulmonary vasoreactivity testing is not recommended since the results can be misleading and "responders" are relatively rare. A positive acute response is defined as a reduction in mean PAP ≥ 10 mmHg to reach an absolute value of mean PAP ≤ 40 mmHg with either no change or an increase in CO (Agarwal et al., 2011; MacKenzie et al., 2015; Hoeper et al., 2013).

2.4. Genetics of PAH: BMPR2 and other TGFβ family members

Regarding group 1 (PAH), the identification of a heterozygous mutation in the bone morphogenetic protein receptor type 2 (BMPR2) gene in the year 2000 was a step forward in the understanding of the pathobiology of PAH (Morrel et al., 2013). BMPR2 is a receptor belonging to the transforming growth factor-β (TGF-β) family (Machado et al., 2015). 668 mutations have been identified in the BMPR2 gene that account for approximately 75% of patients of HPAH and up to 25% of sporadic cases of IPAH (Soubrier et al., 2013; Galie et al., 2015). By contrast, BMPR2 mutations are not found in associated PAH (scleroderma and connective tissue diseases, portal hypertension, and human immunodeficiency virus infection) with the exception of some reports in congenital heart disease (Soubrier et al., 2013). The majority of BMPR2 mutations are nonsense or truncated mutations, leading to a state of haploinsufficiency. Likewise, additional gene mutations in PAH have been described, such as activin receptor-like kinase-1 (ALK-1), the type I receptor accessory protein endoglin, the bone morphogenetic protein receptor type 1 beta (BMPR1B) and the canonical downstream bone morphogenetic protein (BMP) signalling intermediaries, Smad1 and 8. All together support the role for TGF-β pathway in PAH. Other rare heterozygous mutations in genes encoding for proteins such as caveolin-1 (CAV1) and the potassium channels subfamily K member 3 (KCNK3) have been found in cases of HPAH and IPAH (Soubrier et al, 2013; Galie et al., 2015). Finally, a bi-allelic mutation in eukaryotic translation initiation factor 2 alpha kinase 4 (EIF2AK4), which encodes a serine threonine kinase present in all eukaryotes, has been reported in heritable PVOD/PCH

(Galie et al., 2015). This mutation was presented in all familial PVOD/PCH and in 25% of histologically confirmed sporadic PVOD/PCH.

2.5. Pathogenesis of the pulmonary hypertension

Although the initial trigger leading to PH is still poorly understood, a complex interplay among different factors are thought to contribute to the sustained vasoconstriction, vascular remodelling, in situ thrombosis and arterial wall stiffening, which result in elevated PVR (Kuhr et al., 2012, Morrel et al., 2009).

As shown in the angiogram (Figure 4), examination of the pulmonary vasculature reveals significant differences between PH patients and normal subjects. Thus, all patients with PH share common pathological features such as precapillary arteriopathy; increased thickness of the intima, media and adventitia of peripheral arteries; muscularization of the precapillary arterioles and capillaries; obliteration of small vessels; and a significant decreased in the number of small vessels (Kuhr et al., 2012)

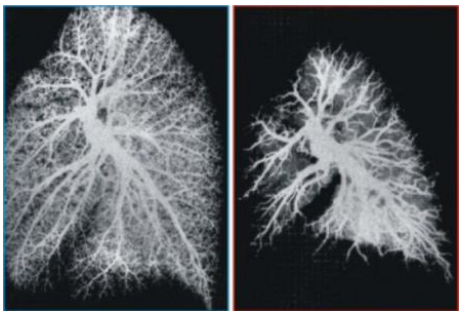

Figure 4: Pulmonary vascular angiogram*. Pulmonary vasculature angiogram from a healthy patient (left panel) versus a patient with PAH (right panel). Adapted from Kuhr et al., (2012) with permission.*

The more important characteristics related with the disease are described below, although is difficult to differentiate among them, due to existence of a complex interplay among the different processes. These processes are influenced by both genetic and environmental factors that alter vascular structure and function (Ma et al., 2014).

- **Vasoconstriction**

Vasoconstriction is a result of an imbalance in tissue and circulating levels of vasoactive mediators. This imbalance include a decrease in the production of vasodilators/growth inhibitors such as NO and PGI_2, while there is an increase in the production of the vasoconstrictor/pro-mitogens such as ET-1, TXA_2 and 5-HT (Morrel et al., 2009; Rabinovitch et al., 2012). This imbalance is a well-characterized contributory mechanism of endothelial dysfunction (Morrel et al., 2009).

The control of pulmonary vascular tone involves a large number of factors acting through a wide variety of signalling pathways on many different targets. As mentioned above the control the vascular tone is regulated by prostanoids (PGI_2 and TXA_2), NO, ET-1, 5-HT, K^+ channels/Ca^{2+} channels and hypoxia (Cogolludo et al., 2007; Wilkins et al., 2012). All of these mediators will be discussed in the following sections of this thesis.

- **Vascular remodelling**

The thickness and tissue mass of the pulmonary arterial walls are maintained by a balance between cell proliferation and apoptosis. A disruption of this balance in favor of proliferation leads to muscularization of distal, normally nonmuscular PAs, associated with differentiation of pericytes into smooth muscle cells (SMC). The progressive thickening of the more proximal intraacinar and preacinar muscular arteries and the obliteration associated with neointimal formation are attributed to increased proliferation and migration of cells considered to be SMCs because they are positive to α-SMC staining (Rabinovitch et al., 2012; Kuhr et al., 2012). This process involves all cell types within the three layers of vessel wall. SMCs are initially hyperplastic and hypertrophic. Adventitial fibroblasts proliferate and migrate from the adventitia to the media layer, which shows a phenotype like. EC, after the initial damage, start to growth abnormally by monoclonal endothelial expansion within the plexiform lesions (Clapp et al., 2015). In addition to this increase of proliferation and migration, changes in extracellular matrix (ECM) composition also take place. These changes likely contribute to a decrease in compliance of the large vessels, a functional

change increasingly thought to be important in disease progression (Pugliese et al., 2015).

- **Thrombosis**

Thrombosis in small peripheral PA contributes to PH. This is a complex process characterized by interaction of EC with both soluble elements (e.g. plasma coagulation proteins) and cellular elements of blood (e.g. platelets). In a healthy state, a balance exists between ongoing thrombosis and prevention of clot formation by both antithrombotic and fibrinolytic system (Berger et al., 2009). EC facilitate the thrombotic process by activating factor X, which participates in the formation of the thrombin-activating prothrombinase complex and activates the extrinsic pathway of coagulation. In addition, ECs release the von Willebrand factor, which attracts and activate platelets. At the same time, ECs release NO and PGI_2 which are potent inhibitors of platelet aggregation. In addition, expression of thrombomodulin on the surface of the ECs prevents cleavage of fibrinogen to fibrin, and also rapidly activates protein C. Furthermore, ECs also synthesize and release plasminogen activator inhibitor-1 (PAI-1), an inhibitor of tissue plasminogen activator (t-PA) (Nogueira-Ferreira et al., 2014; Berger et al., 2009). On the other hand, PAH patients showed an increased levels of PAI-1, von Willebrand factor, TXA_2 and 5-HT, and decreased levels of t-PA, thrombomodulin, NO and PGI_2 (Nogueira-Ferreira et al., 2014). Thus, PAH patients show a hypercoagulant phenotype.

Thus, the intrapulmonary arteries in PH manifest endothelial dysfunction, inflammation, excess of proliferation, impaired apoptosis, and disordered metabolism. Several factors are involved in these deregulated signalling pathways, which are discussed below.

3. Role of endothelial dysfunction on the pathogenesis of pulmonary hypertension

EC exert a delicate and constant influence on the underlying PASMC. As previously mentioned EC release a number of vasoactive substances and play a major role in the control of vascular structure, vascular tone and platelet aggregation. Endothelial dysfunction in PH is reflected by reduced production of the vasodilators/growth inhibitors NO and PGI_2 and increased production of the vasoconstrictor/pro-mitogens, ET-1, TXA_2 and 5-HT which mediate PASMC proliferation. Thus, this excessive release of soluble factors, act either as growth factors to induce PASMC proliferation or as chemokines to recruit circulating inflammatory cells which initiate or enhance pulmonary vascular remodelling and inflammation (Morrel et al., 2009, Rabinovitch et al., 2012; Gao et al., 2016; Perez-Vizcaino et al., 2006).

3.1. The NO/cGMP signalling pathway.

NO is a highly reactive and gaseous molecule synthesized by a family of enzymes known as NO synthases (NOS): endothelial (eNOS), inducible (iNOS) and neuronal (nNOS), all of which are expressed in the lung. These isoforms function as homodimers, which convert L-arginine to L-citruline and NO (Figure 5). This reaction requires several cofactors: flavin adenine dinucleotide (FAD), flavin mononucleotide (FMN), molecular oxygen, reduced nicotinamide adenine dinucleotide phosphate (NADPH) and tetrahydrobiopterin (BH_4). Both nNOS and eNOS are constitutively expressed. An increase in $_i[Ca^{2+}]$ stabilize the binding of calmodulin to eNOS and nNOS, and activates the enzyme to produce NO, which is implicated in the control of vascular tone. In contrast, iNOS expression gene is induced by exposure to microbial products, such as lipopolysaccharide or proinflammatory cytokines such as interleukin-1 (IL-1) or tumor necrosis factor-α (TNF-α). Binding of calmodulin to iNOS is tight even at low $[Ca^{2+}]i$, and therefore, iNOS is also considered as a calcium-independent isoform. iNOS releases high levels of NO for prolonged periods, being their main role to kill invading microorganisms by the combination of the NO produced with superoxide (O_2^-) to form

peroxynitrite ($ONOO^-$) (Korhonen et al., 2005; Perez-Vizcaino et al., 2010; Tabima et al., 2012; Wilkins et al., 2008; Potter et al., 2011). Thus, there are both direct effects of NO, that are mediated by the NO molecule itself, and indirect effects of NO, that are mediated by reactive nitrogen species (RNS) produced by the interaction of NO with O_2^- (that form $ONOO^-$) or with oxygen (responsible of the S-nitrosylation by the nitrosonium ion) (Korhonen et al., 2005).

NO diffuses rapidly into the adjacent PASMC, where it stimulates soluble guanylate cyclase (sGC) and increases cGMP production (Figure 5). This cGMP plays a major role in relaxing PASMC, preventing fibrosis, inhibiting platelet aggregation, modulating inflammation, and controlling vascular permeability (Potter et al., 2011; Nossaman et al., 2013; Dasgupta et al., 2015; Perez-Vizcaino et al., 2006).

The sGC is a cytosolic, heterodimeric protein consisting of a large α subunit and a smaller β subunit with a prosthetic heme group (heme-binding domain). It is necessary for full sGC activation the binding of NO to the ferrous (Fe^{2+}) heme ring to form an intermediate six-coordinate complex, which induces a subsequent cleavage and dissociation of the Fe^{2+} of histidine (His105) bond, leading to conformational reorganization to a five-coordinate state. The conformational change in the H-NOX domain is propagated to the heterodimeric catalytic domain, where cGMP production is in turn increased. It should be noted that carbon monoxide can also activate sGC by binding heme to form a six-coordinated complex, however, NO activates the enzyme 100-200 fold, whereas carbon monoxide only activates it about 4 fold (Follmann et al., 2013; Potter et al., 2011; Schermuly et al., 2008).

The second messenger cGMP exhibits their vasodilator actions through the reduction of i[Ca2+] and desensitization of the contractile apparatus by phosphorylation mediated by cGMP-dependent protein kinase (PKG) to target proteins, such as the myosin phosphatase-targeting subunit (MYPT). One of the mechanism leading to i[Ca2+] reduction involves a PKG dependent activation of large-conductance calcium sensitive potassium channels (BK_{Ca}), which lead to hyperpolarization of PASMCs membrane potential and inhibition of Ca^{2+} influx through Ca_L and IP_3 receptor

associated cGMP kinase substrate (IRAG) (Dasgupta et al., 2015; Wilkins et al., 2008; Rybalkin et al., 2003).

The biological activity of cyclic nucleotides, cAMP and cGMP, is governed by their rates of synthesis and degradation (Rybalkin et al., 2003; Maurice et al., 2014).The family of cyclic nucleotide phosphodiesterases (PDE) catalyzes the hydrolysis of the cyclic phosphate bound in cAMP and cGMP to generate the inactive products 5´-AMP and 5´-GMP (Figure 5) (Francis et al., 2011). This family of PDEs comprise 11 different gene families (PDE1-11), which are structurally related but with different cellular functions, primary structure, affinities for cAMP and cGMP, catalytic properties and response to specific activators or inhibitors, as well as in their mechanism of regulation (Maurice et al., 2014). Certain PDEs are highly specific for cAMP (PDEs 4, 7 and 8), cGMP (PDEs 5, 6 and 9), or both (PDEs 1, 2, 10 and 11). Furthermore, some genes encoding for the different PDEs present multiple promoters with several alternative mRNA splicing and distinct regulatory or transcriptional processes, which together generate close to 100 PDE isozymes (Rybalkin et al., 2003; Maurice et al., 2014; Francis et al., 2011). PDEs share a common structural organization, with a conserved carboxy-terminal catalytic domain and a variable amino-terminal sequence that acts as regulatory region of PDE. This last region is implicated in subcellular localization, the incorporation of PDEs into compartmentalized signalosomes, the interaction with signalling molecules and molecular scaffolds, and in the regulation of PDEs activity. X ray crystal structure of isolated catalytic domains of nine PDE families (PDE1-5 and PDE7-10) have demonstrated that they share approximately 350 amino acids, and the active site forms a deep hydrophobic pocket that contains a common motive of $HD(X_2)H(X_4)N$ (Maurice et al., 2014; Francis et al., 2011).

The major PDEs present in PASMC are PDE1A, 1B, and 1C, PDE3A and 3B, and PDE5. Under basal conditions (low calcium levels), the most active PDE hydrolyzing cGMP in SMC is PDE5. In contrast, under higher calcium conditions (e.g., during muscle contraction), the PDE1 variants can become the predominant PDEs. Although PDE3 does not have as great a total catalytic capacity as the other two, it may still play a role in controlling cAMP. This enzyme is strongly inhibited by cGMP and has been termed the cGMP-inhibited PDE. In all cases, these PDEs do not necessarily share the same

subcellular localization and therefore different functional compartments in the cell can be identified (Francis et al., 2011).

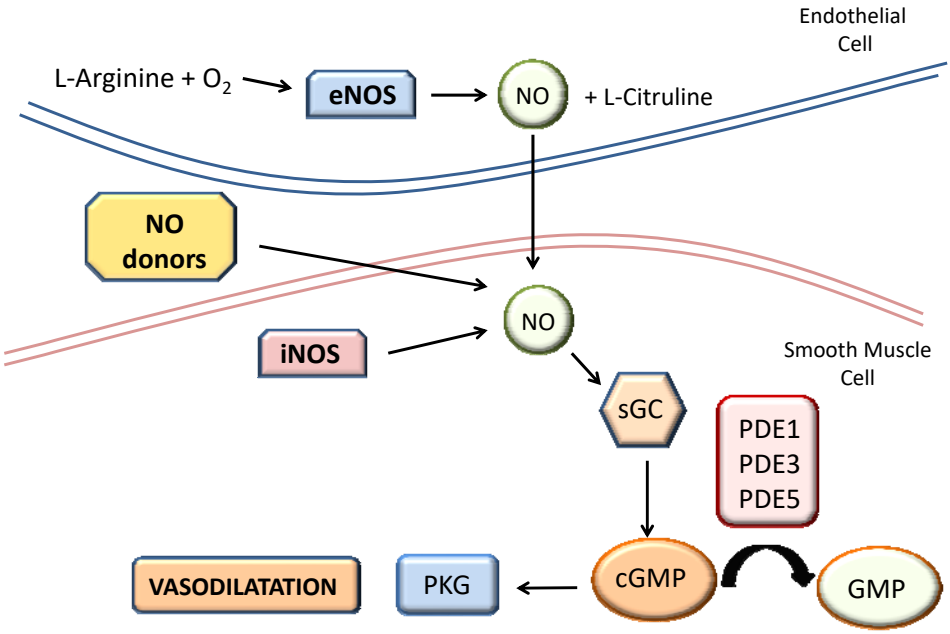

Figure 5: Intracellular signalling pathway of nitric oxide (NO: A simplified overview of NO signalling and effects in the pulmonary vasculature.

3.1.1. Role of NO/cGMP signalling pathway in pulmonary hypertension

As mentioned above, the NO-sGC-cGMP pathway plays important physiologic roles. This pathway requires the activation of eNOS in ECs leading to NO synthesis, diffusion of NO to the adjacent SMC, NO-induced activation of sGC leading to cGMP synthesis and activation of PKG (Ignarro et al., 2001). All this steps in the signalling pathway have been reported to be impaired in PH.

Reduced NO production in PH can be due to decreased expression of eNOS, inhibition of eNOS enzymatic activity or a decreased synthesis of NO by eNOS. Regarding these processes, in patients with IPAH, it has been observed that the expression of eNOS is downregulated in small arterioles, while it is upregulated in plexiform lesions (Mason et al., 1998). Likewise, high arginase II levels and activity, which compete with eNOS for L-arginine, is increased in PAH ECs (Morrel et al., 2009; Rabinovitch et al., 2012). Furthermore, elevated levels of asymmetric dimethylarginine (ADMA), which is an

endogenous competitive inhibitor of NOS, have been found in patients with IPAH, CTEPH, PAH related to sickle cell disease and PAH related to systemic sclerosis. In addition, lung tissues from patients with IPAH also show decreased expression of dimethylarginine dimethylaminohydrolase (DDAH), the enzyme responsible for the hydrolysis and degradation of ADMA (Wilkins et al., 2012). Once NO is produced, its bioavailability is regulated by levels of other reactive species in the surrounding medium, which act as scavengers of NO, such as O_2^-, which reacts with NO extremely rapid, yielding the oxidant $ONOO^-$, which oxidizes the NOS cofactor BH_4 to dihydrobiopterin (BH_2). This process alter the electron flow through eNOS to molecular oxygen rather than L-arginine, yielding O_2^- rather than NO, a condition referred to as eNOS uncoupling (Nisbet et al., 2007; Perez-Vizcaino et al., 2006).

Another step impaired in the pathogenesis of PH is sGC, which is oxidized under conditions of oxidative stress. This oxidation is due to a change in the oxidation status of sGC from the normal heme iron (Fe^{2+}) to an oxidized heme (Fe^{3+}), rendering it less responsive to NO and dissociation of heme group from sGC (Dasgupta et al., 2015). It should be noted, that in the PA from IPAH patients, sGC expression is upregulated compared to healthy donors. A similar observation was made in experimental models of PH induced by chronic hypoxia in mice and in MCT-induced PAH in rats (Schermuly et al., 2008).

An important aspect of NO pathway is that PDE5 is overexpressed in the intima lesions and neomuscularised distal vessels, as well as in SMC in the media layer of remodeled PA from IPAH patients. Furthermore, PDE1, which is normally expressed at low levels in pulmonary tissue, is upregulated in precapillary pulmonary arterial resistance vessels in PH (Wilkins et al., 2008; Murray et al., 2007).

In summary, chronic PAH disrupts NO-sGC-cGMP signalling pathway by decreasing eNOS expression or activity, increasing NO catabolism, reducing sGC responsiveness, and increasing PDE5 activity (Tabima et al., 2012; Nossaman et al., 2013).

3.2. Prostanoids

Prostanoids are arachidonic acid (AA) metabolites that can be classified into prostanglandins (PG), which contain a cyclopentane ring, and thromboxanes (TX), which contain a cyclohexane ring (Mubarak et al., 2010; Gryglewski et al., 2008). Their biosynthesis comprises three stages. The first and limiting step is the stimulus-induced mobilization of AA from cell membrane by phospholipase A_2 action. There are numerous stimuli, such as, ADP, angiotensin II, bradykinin, chatecolamines, histamine, thrombin, shear forces or hypoxia that induce AA release. Then, AA is oxidized by the action of the cyclooxygenases, COX-1 and COX-2, which are constitutive and inducible isoforms, respectively. This process involves two sequential actions of the enzymes: firstly, the conversion of AA to the endoperoxide PGG_2, and subsequently, the conversion of PGG_2 into the endoperoxide PGH_2. Thereafter, PGH_2 is the substrate of prostacyclin synthase (PGI_2S) to generate PGI_2 (Mitchell et al., 2014; Mubarak et al., 2010; Gryglewski et al., 2008), and of TXA_2 synthase (TXS) to generate TXA_2 (Figure 6) (Sellers et al., 2008; Delannoy et al., 2010; Nakahata et al., 2008).

3.2.1. Prostacyclin

PGI_2 is produced mainly endogenously by ECs, although PASMC produce a smaller amount, about 1/7-1/10 of that produced by ECs (Chu et al., 2015). PGI_2 presents a half-life of 3 minutes, being rapidly hydrolyzed in aqueous media into the stable and biological inactive metabolite 6-keto-PGF1α which is subsequently converted into 2,3-dinor-6-keto-PGF1α, the major PGI_2 metabolite excreted in urine (Luo et al., 2016). Due to their stability, this latter metabolite is used to measure the PGI_2 production.

The actions of PGI_2 are mainly mediated through its specific cell surface prostacyclin receptor (IP) (Figure 6), which is abundantly expressed in multiple organs including the heart, lungs, nerves and the gastrointestinal system, as well as in blood vessels, leukocytes and platelets (Gomberg-Maitland et al., 2008; Lang et al., 2015). The IP receptor is a member of the seven transmembrane-spaning G protein coupled receptor (GPCR) superfamily, which is predominantly coupled to G proteins and

activates adenylyl cyclase (AC), which converts ATP to the second messenger cAMP. The biological effect of cAMP is mediated by activation of cAMP-dependent protein kinase (PKA) and exchange protein activated by cAMP (EPAC) (Mitchell et al., 2014; Reid et al., 2015). Activation of the IP receptor inhibits platelet aggregation, exerts cytoprotective and antiproliferative activities and induce potent vasodilation of all vascular beds by reduction of the $_i[Ca^{2+}]$ (Galie et al., 2015; Clapp et al., 2015; Mitchell et al., 2008).

In Addition to the IP, PGI_2 can act as an agonist of PPARβ/δ, a member of the peroxisome proliferator-activated receptor (PPAR) family or nuclear receptors, particularly at elevated concentrations (Reid et al., 2015; Ali et al., 2006; Li et al., 2012).

As with other prostanoids, PGI_2 is not highly specific to the IP receptor, it can cross over with other prostanoids receptors, such as TXA_2 receptors (TP), EP1, EP3 (PGE_2 receptor subtypes 1 .and 3) and FP ($PGF_2\alpha$ receptor) receptors yielding vasoconstriction, as well as EP2, EP4 (PGE_2 receptor subtypes 2 and 4) and DP1 (PGD_2 receptor) receptors, with a similar effect than IP receptor, yielding vasorelaxation (Clapp et al., 2015; Mitchell et al., 2014). Furthermore, the signalling pathways mediating IP receptor is regulated by desensitization. This process involves both PKA and PKC phosphorylation and receptor internalization.

3.2.2. Thromboxane A_2

TXA_2 is produced mainly by the platelets and monocytes/macrophages (Smyth et al., 2010). Since TXA_2 is very unstable (half-life of about 30 seconds), its production is determined by measuring of the inactive form 11-dehydro-TXB_2 (TXB_2) (Nakahata et al., 2008).

TXA_2 acts by binding with the TP (Figure 6), which are widely distributed among different tissues such as thymus, spleen, lung, kidney, heart and brain. In addition, TP receptors are expressed in many types of cells within the cardiovascular system,

including EC, cardiac myocytes, VSMC and platelets (Nakahata et al., 2008; Huang et al., 2004).

In humans, TP receptors exist in two isoforms, TPα (with 343 amino acid) originally cloned from placenta, and TPβ (with 407 amino acid) cloned from endothelium, which arise from alternative splicing. Both isoforms share the first 328 amino acids, while the unique difference is the length of the extended C-terminal cytoplasmic domain. Both TP receptors belong to the family of GPCRs (Capra et al., 2014; Nakahata et al., 2008; Huang et al., 2004).

Activation of these receptors induces potent platelet activation, constriction of vascular smooth muscle cells and cell proliferation (Cogolludo et al., 2003). TXA_2 contracts VSMC by binding to specific Gq/11 protein–coupled receptors. Stimulation of Gq/11 protein activates phospholipase C (PLC), resulting in increased IP_3 and diacylglycerol (DAG), which leads to an increase in i[Ca2+] and sensitization of the contractile proteins to Ca^{+2}.

Furthermore, the signalling pathways mediating TP receptors involve the activation of several protein kinases, such as PKC, PKA, PKG, ROCK and tyrosine kinases (Cogolludo et al., 2003; Huang et al., 2004), which participate in the receptor desensitization by phosphorylation, and subsequent sequestration of the receptor away from the plasma membrane. Besides this phosphorylation, TP receptors can be modulated by other GPCRs. Hetero-dimerization of TPα and IP receptors, which enhances the cAMP generation, has also been reported (Wilson et al., 2004; Nakahata et al., 2008; Huang et al., 2004).

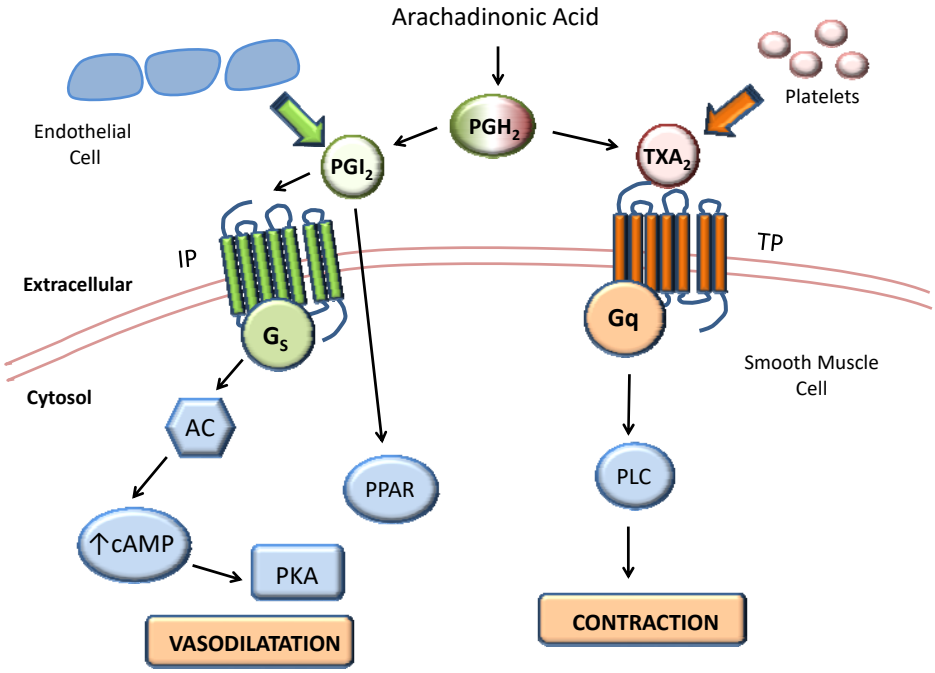

Figure 6: Prostanoids signalling: *A schematic overview of prostanoids (PGI_2 and TXA_2) signalling and effects in the pulmonary vasculature.*

3.2.3. Role of prostanoids in pulmonary hypertension

As mentioned above, both prostanoids, PGI_2 and TXA_2, have an important role in cardiovascular homeostasis due to their effects in platelet aggregation, vascular tone, local inflammatory response and leukocyte-endothelial cell adhesion (Kawabe et al., 2010). Studies in the 1990´s demonstrated that pathological conditions may be associated with an imbalance in prostanoid excretion. Thus, reduced levels of the of the PGI_2 urinary marker, 2,3-dinor-6-keto-PGF1α, was found in patients with IPAH and PH associated with congenital heart disease (Christman et al., 1992). Furthermore, in patients with severe PH, there is a progressive loss of the endogenous PGI_2S expression in ECs and PASMCs from large and small pulmonary arteries vessels (Tuder et al., 1999; Clapp et al., 2015; Mitchell et al., 2014). This finding is in line with the subsequent decreased levels of circulating PGI_2 in these patients. Loss of PGI_2 production aggravates the vascular damage (Chu et al., 2015). On the contrary, the major urinary metabolite of TXA_2, TXB_2, is elevated in patients with PH compared with healthy volunteers (Robbins et al., 2001; Christman et al., 1992; Robbins et al., 2006).

These results are in line with the imbalance between production of vasoconstrictors and vasodilators, activators versus inhibitors of SMC growth and migration, and prothrombotic and antithrombotic mediators, which contributes to endothelial dysfunction in PH (Morrel et al, 2009, Rabinovitch et al., 2012).

3.3. Peroxisome proliferator-activated receptors

Peroxisome proliferator-activated receptors are members of the nuclear hormone receptor superfamily, which heterodimerize with the retinoid X receptor (RXR) and bind to specific DNA regions of target genes (AGGTCAXAGGTCA, with X as random nucleotide) termed as peroxisome proliferator hormone response elements. PPARs modulate the function of many target genes involved in the regulation of metabolism, inflammation, cell differentiation, cell growth and angiogenesis. Three members PPAR family, PPARα, PPARβ/δ and PPARγ have been described in mammalian cells and are activated by fatty acids as endogenous ligands (Chu et al., 2015; Quintela et al., 2012; Braissant et al., 1996).

PPARα is predominantly expressed in tissues with high rates of fatty acid catabolism such as liver, heart, kidney, skeletal muscle, brown adipose tissue and the intestine. It is also expressed in various cell types within the cardiovascular system such as cardiomyocytes, EC, VSMCs and monocytes/macrophages, where it regulates genes involved in lipid and lipoprotein metabolism. PPARβ/δ are ubiquitously expressed at much higher levels than the others PPARs, markedly in brain, adipose tissue and skin. This isoform stimulates fatty acid oxidation (Jasińska-Stroschein et al., 2014). PPARγ is abundantly expressed in many tissues including white and brown adipose tissue and the gut. Furthermore, significant expression has also been detected in cells within the vessel wall such as monocytes/macrophages, EC, and VSMCs. PPARγ is an important regulator of genes involved in lipid and glucose metabolism (Nisbet RE, 2007; Jasińska-Stroschein et al., 2014).

In addition to their metabolic effects, both PPARβ/δ and PPARγ are important regulators of genes involved in cell differentiation, cell growth, inflammation, apoptosis and angiogenesis (Nisbet et al., 2007).

3.3.1. Role of PPAR in pulmonary hypertension

PPARγ is ubiquitous expressed in lung, especially on EC and VSMCs and a decrease of PPARγ expression and function has been found in patients with severe PH (Ameshima et al., 2003) in the chronic hypoxic (Nisbet et al., 2010) and MCT models of PAH (Jasińska-Stroschein et al., 2014). PPARγ modulates additional responses related with PH pathogenesis including vasoconstriction, vascular remodelling and inflammation. Thus, PPARγ reduces vascular production of TXA_2 and increases endothelial NO release by reducing the inhibitory interaction between eNOS and caveolin (Mathew et al., 2014), and by decreasing the serum levels of ADMA, the endogenous inhibitor of NOS (Wakino et al., 2005). In addition, PPARγ may increase the NO bioavailability by downregulating NADPH oxidase type 4 (NOX4) and reducing reactive oxygen species (ROS) production as reported in hypoxia-induced PH (Nisbet et al., 2007). Furthermore, *in vitro* studies have revealed that PPARγ ligands inhibit ET-1 secretion by ECs (Martin-Nizard et al., 2002) and the vasoconstrictor effect of ET-1 (Nisbet et al., 2007). Accordingly, PPARγ ligands reduced ET-1 expression in cardiac and vascular tissues derived from an *in vivo* model. Furthermore, activation of PPARγ reduce the activation of platelet derived growth factor (PDGF) induced by hypoxia in a mouse model of PH *in vivo*, and inhibits PDGF stimulated VSMC migration *in vitro* (Jasińska-Stroschein et al., 2014).

Whereas PPARγ and their potential in PH have been extensively reviewed (Green et al., 2011; Sutliff et al., 2010), the vascular actions of PPARβ/δ and its effectiveness as a therapeutic target in the treatment of PH remain less investigated. Interestingly, PGI_2 and its analogs act as agonists of PPARβ/δ receptors (Reid et al., 2015; Ali et al., 2006), which may underpin some of their beneficial effects in PH. Similar to PPARγ, activation of PPARβ/δ also exhibit antiinflammatory properties in the vessel wall (Quintela et al., 2012), antiproliferative effect on VSMCs (Han et al., 2015; Kang et al., 2011),

vasodilator effect in several blood vessels such as the aorta, pulmonary and mesenteric arteries contracted with U46619 (Harrington et al., 2010) as well as improved NO bioavailability, among other potential beneficial effects on endothelial function (Quintela et al., 2012) that could be useful for PH treatment.

3.4. Serotonin

Serotonin, 5-hydroxytriptamine or 5-HT in the periphery is produced mainly by the enterochromaffin cells of the gut yielding about 95% of the total amount in the body (Egermayer et al., 1999; Fidalgo et al., 2013). However, 5-HT is also locally released from pulmonary neuroendrocrine cells and neuroepithelial bodies distributed through the airways (MacLean et al., 2000). 5-HT is also produced in the serotonergic neurons of the raphe nuclei of the brainstem and hypothalamus in the central nervous system (CNS) and in the gut, from which it is stored in dense granules of the platelets (Namkung et al., 2015; Fidalgo et al., 2013).

5-HT is synthetized from the essential amino acid tryptophan obtained from the diet. The initial step is produced by the action of tryptophan hydrolase (TPH) (Figure 7) and followed by the action of the aromatic amino acid decarboxylase (Fidalgo et al., 2013). Monoamino oxidase A (MAO_A) is the enzyme responsible for the breakdown of 5-HT to 5-hydroxyindolacetic acid (5-HIAA) (MacLean et al., 2009). TPH is the rate-limiting enzyme in the synthesis of the 5-HT. There are two isoforms of TPH, termed TPH1 and TPH2. TPH1 is present mainly in the gut and mediates generation of 5-HT in the periphery, whereas TPH2 is expressed in the CNS (MacLean et al., 2009).

Normally, plasma levels of free 5-HT are extremely low (<1nM) (MacLean et al., 2009) due to its rapid uptake into the platelet and storage into the dense granules or its degradation by MAO_A (MacLean et al., 2000; Fidalgo et al., 2013). 5-HT uptake by platelets involves the activation of the serotonin transporter (SERT) in the plasma membrane and the transport across the dense granules via the vesicular monoamine transporter (VMAT) (Jedlitschky et al., 2012).

Currently, there are at least 14 structurally distinct 5-HT receptors, grouped into 7 families (5-HT_{1-7}) (MacLean et al., 2009) according to the signalling mechanism, which are widely expressed in mammalian tissues (Namkung et al., 2015). In PA, the most important receptors belonging to these families are the 5-HT_{2A}, 5-HT_{2B} and 5-HT_{1B} receptors, although the effect of each one is different depending on the species studied (Morrell et al., 2009; MacLean et al., 2009).

5-HT is involved in regulation of cell proliferation, vascular tone and microthrombosis (MacLean et al., 2000; Fidalgo et al., 2013). The vasoconstrictor effect of 5-HT is mediated mainly in human small and large PA by the 5-HT_{1B} (MacLean et al., 2009) and 5-HT_{2A} receptors, although this last receptor only contributes to vasoconstriction when 5-HT concentrations are much higher than the physiological range. In most nonhuman mammals, the 5-HT_{2A} receptor mediates vasoconstriction in both the systemic and pulmonary circulation (Morrell et al., 2009; Cogolludo et al., 2006). Finally, although 5-HT_{2B} receptors are upregulated in PA from PH patients, and their deletion abolishes the development of hypoxia-induced PH, there are not current evidences on their role in mediating constriction or proliferation of human PASMCS (hPASMCs) or pulmonary arterial fibroblasts (Dempsie et al., 2008).

In contrast to the constriction of 5-HT, the mitogenic effect in PASMC and pulmonary arterial fibroblasts involve the internalization of the SERT, activation of the 5-HT_{1B}, generation of ROS and extra-cellular regulated kinase 1/2 (ERK1/2) activation, which after phosphorylation is translocated to the nucleus and activates DNA binding of transcription factors such as GATA-4, cyclin D1, Egr-1 and Elk-1, and thus increase the expression of proteins involved in cellular proliferation as S100A4/Mts1 (Dempsie et al., 2008; Thomas et al., 2013). Activation of RhoA/ROCK patway has also been implicated in both the vasoconstrictor and the mitogenic effects of 5-HT (Dempsie et al., 2008).

3.4.1. Role of serotonin in pulmonary hypertension

The "serotonin hypothesis" of PAH arose in the 1960s, when there was an epidemia of cases of PAH in women taking the appetite suppressant drug aminorex. In the 1980s the new generation of anorexigens, fenfluramine and derivatives were also associated with cases of PAH, and more recently, in 2009 benfluorex, a drug that shares similar structural and pharmacological characteristics with fenfluramine derivatives and have a common metabolite, norfenfluramine. This metabolite itself is a trigger for PAH, due to its properties as an agonist at 5-HT_{2A}, 5-HT_{2B} and 5-HT_{2C} receptors (MacLean et al., 2008; Seferian et al., 2013).

Accordingly with the "serotonin hypothesis", 5-HT is a potent vasoconstrictor and mitogen, and patients with PAH have increased circulating 5-HT levels, even after heart-lung transplantation (Morrell et al., 2009), and a low level in platelets (Nogueira-Ferreira et al., 2014). This increase in 5-HT levels is derived from several sources. Thus, expression of the TH1 gene is increased in lungs and pulmonary artery endothelial cells (PAEC) from patients with IPAH, and knockout TH1 mice are protected from chronic hypoxia-induced pulmonary vascular remodelling and hypertension, indicating that *de novo* synthesis is essential for the development of hypoxia-induced PH (MacLean et al., 2008; Thomas et al., 2013). Likewise, polymorphisms in the gene-encoding SERT affect their expression and function. An increased rate SERT transcription has been associated with exaggerated PAH in patients with chronic obstructive lung disease and increased risk to develop PAH at high altitude. Accordingly, mice overexpressing SERT are more susceptible to hypoxia induced PH, and inhibition of SERT protects against hypoxia or MCT (MacLean et al., 2008).

In addition, upregulation of the 5-HT_{1B} receptors has been found in PA from PAH patients, MCT treated rats and chronic hypoxic-mice (MacLean et al., 2008). In the same way, several studies show that the use of several receptor antagonists such as fluoxetine (5-HT_{1B}) and ketanserin (5-HT_{2A}) or mice deficient for the 5-HT_{2B} receptor inhibits the effect of hypoxia induced vasoconstriction and vascular remodelling (MacLean et al., 2008; Morrell et al., 2009). Another consequence of the high 5-HT level is that 5-HT, in rat PASMCs through the 5-HT_{2A} receptor, inhibits native Kv1.5

current, and this may contribute to vasoconstriction observed in the disease (Cogolludo et al., 2006).

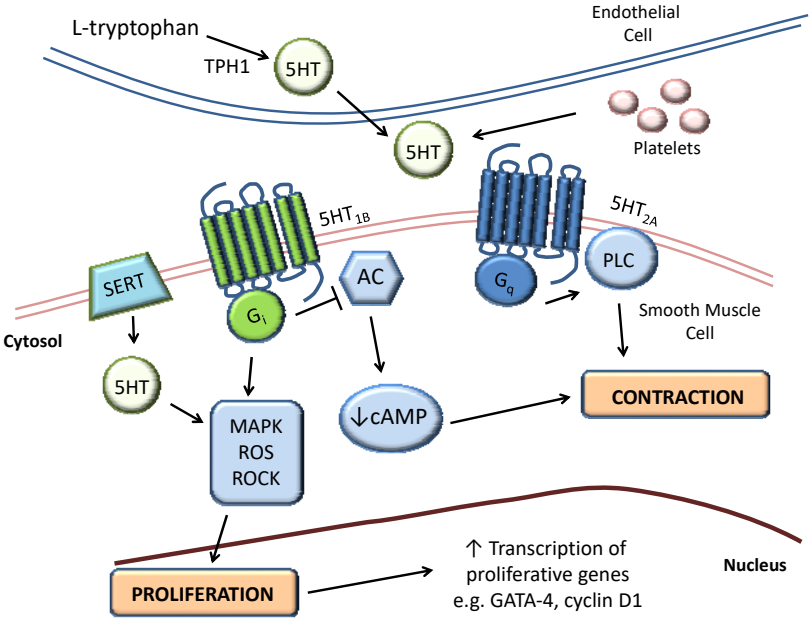

Figure 7: Serotonin signalling: *A schematic overview of serotonin (5HT) signalling and effects in the pulmonary vasculature*.

3.5. Endothelin-1

Endothelins (ETs) represent a family of 3 isopeptides (ET-1, ET-2 and ET-3) that share a similar structure to the sarafotoxins which are found in the venom of Israeli Mole Viper (*Atractaspis engaddensis*). They are encoded by three different genes located on chromosomes 6, 1 and 20, respectively. The three forms are 21 amino acid peptides with a high level of homology and similar structure (Shao et al., 2011; Chester et al., 2014). ET-1 was isolated and characterized in pulmonary and systemic EC in 1988 by Yanagisawa *et al.* (1988). ET-1 was soon defined as the most potent and long-lasting endogenous vasoconstrictive substance yet discovered. ETs have been found to be involved in multiple physiologic functions in the nervous, renal, cardiovascular, respiratory, gastrointestinal and endocrine systems. Furthermore, they have been implicated in carcinogenesis, bronchoconstriction, fibrosis, heart failure and PH (Galié et al., 2004).

Although ETs are mainly produced by vascular EC, a range of other cells types have also been shown to express ETs including cardiac myocytes, fibroblasts, lung epithelium, glomerular kidney cells, mesangial cells, leukocytes and macrophages (Shao et al., 2011; Chester et al., 2014). Of the three subtypes, ET-1 is the predominant ET isoform that is expressed in the cardiovascular system, whereas ET-2 and ET-3 are mainly expressed in the gastrointestinal tract and the brain, respectively (Selej et al., 2015).

ET-1 is not stored in secretory granules within EC. Around 75%-80% of ET-1 synthesized in the EC is released towards the underlying muscular media (Selej et al., 2015). The ET-1 gene encodes for a larger 203 amino acid precursor peptide called preproendothelin, which is cleaved to a smaller 38 amino acid peptide Big-ET-1 or pro-endothelin-1 by the enzyme furin convertase. Big-ET-1 then is transformed to the mature and active 21 amino acid peptide ET-1 by the action of the endothelin-converting enzyme (ECE) (Chester et al., 2014; Galié et al., 2004). A number of stimulus can enhance ET-1 production, such as hypoxia, cytokines, growth factors, oxidized LDL cholesterol and mechanical forces (shear stress or pulsatile stretch and flow). In contrast, NO, PGI_2, estrogens or atrial natriuretic peptides, can all reduce the amount of ET-1 released (Shao et al., 2011; Chester et al., 2014).

ETs exert their effects in the cardiovascular system through binding to the two types of endothelin receptors called type A (ET_A) and type B (ET_B) ET receptors (Figure 8). The two subtypes show distinct ligand preference; ET_A receptors are ET-1 selective, with an affinity order of ET-1 ≥ ET-2 > ET-3, whereas ET_B receptors exhibit similar affinities for the ETs (Shao et al., 2011). ET_A receptors are found in VSMC, while ET_B receptors are also located on VSMC and endothelial cells. These receptors are GPCRs, which activate different downstream signalling pathways by association with different Gα proteins. Activation of ET_A or ET_B receptors on VSMC mediates vasoconstriction responses via the activation of PLC beta (Selej et al., 2015), which leads to an increase of IP_3 and DAG, and a subsequent increase in $_i[Ca^{2+}]$. The increase of DAG and calcium also stimulates different PKC isoforms, which mediate the mitogenic effect of ET-1 (Chester et al., 2014, Galié et al., 2004). On the other hand, the activation of ET_B receptors on EC stimulate the release of local vasodilators, such as NO and PGI_2. Additional effects of ET_B receptors are linked to a reduction in ECE expression and inhibition of apoptosis.

Endothelial ET_B receptors also contribute to the clearance and the reuptake of ET-1 from the circulation by internalizing the receptor once ET-1 has bound; removing about 50% - 80% of circulating ET-1 (Shao et al., 2011; Chester et al., 2014).

Although ET-1 is able to affect numerous tissues and organs throughout the body, the lungs represent a primary target. In healthy adults, ET-1 plasma levels are low (1-2 pg/mL) although ET-1 is highly expressed in the lung, with levels of ET-1 mRNA being at least 5 times greater than in other organs. In addition, lungs represent a site for ET-1 metabolic pathways (Galié et al., 2004; Chester et al., 2014)

ET-1 in the pulmonary circulation produces an intense and maintained vasoconstriction of the PA and veins at low concentrations, with a greater efficacy and potency than 5-HT, noradrenaline and the TXA_2 mimetic, U46619 (Chester et al., 2014; Pérez-Vizcaino et al., 1996). When administered intravenously, ET-1 causes a biphasic response in the pulmonary circulation with initial mild vasodilatation due to the release of NO and by activation of potassium channels, followed by sustained vasoconstriction mediated by both ET_A and ET_B receptors (Galié et al., 2004). In addition, ET-1 has mitogenic effects on PAEC, PASMC and fibroblast (Shao et al., 2011; Biasin et al., 2014). ET-1 also shows positive ionotropic and chronotropic effects in the myocardium, induces cardiac hypertrophy, platelet aggregation and stimulates the production of cytokines, growth factors and ECM proteins (Galié et al., 2004, Chester et al., 2014).

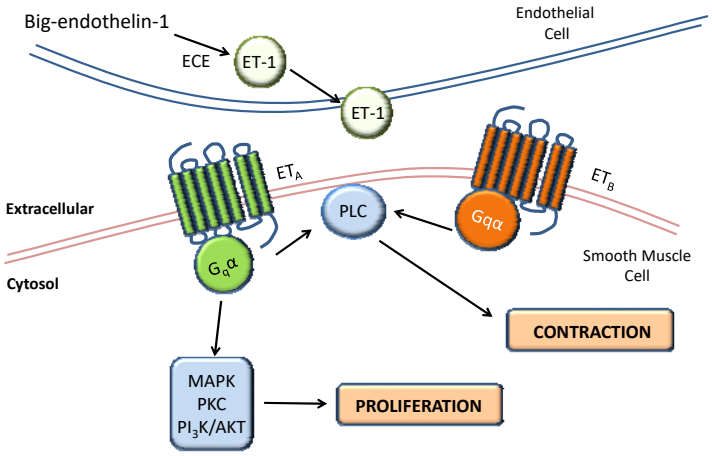

Figure 8: Endothelin-1 signalling: *A schematic overview of endothelin-1 (ET-1) signalling and effects in the pulmonary vasculature.*

3.5.1. Role of endothelin-1 in pulmonary hypertension

The abundance of ET-1 within the lung makes dysregulation of the ET-1 system as a prime candidate for involvement in the onset and progression of the disease. In 1991, a study by Stewart et al. showed that circulating plasma levels of ET-1 were increased in patients with PAH and this was related with an enhanced ability of the lung to release ET-1 (Selej et al., 2015). This effect is most likely due to a combination of increased production and reduced clearance of ET-1. This increased level of ET-1 in the plasma and lugs of patients have also been correlated with increased right atrial pressure, increased PVR, decreased pulmonary artery oxygen saturation, vascular remodelling and increased mortality in patients with PAH (Shao et al., 2011; Selej et al., 2015). Nevertheless, it is not clear if the increase in ET-1 plasma levels are a cause or a consequence of PAH (Galié et al., 2004; 2015). ET receptors are also upregulated in PH, although the relative proportion (60% ET_A and 40% ET_B) seems to remain constant in patients with IPAH and PAH associated with congenital heart disease (Shao et al., 2011; Galie et al., 2015; Humbert et al., 2016).

In addition, ET-1 expression may also be modulated by BMPR2 ligands. Mutations that interfere with the ligand binding to the BMPR2 or their kinase activity have been linked to the familiar form of the disease. The BMPR2 ligands BMP7 and BMP4 were shown to suppress the ET-1 release from VSMC and inhibit the contractile response of the ET-1. Changes in the function of BMPR2 could either directly or indirectly influence the release and response to ET-1 (Chester et al., 2014).

4. Oxidative stress

The term "*oxidative stress*" has been widely used to describe the consequence of an imbalance in ROS homeostasis due to either the over-production of these species and/or decreased capability of antioxidant defenses (Aggarwal et al., 2013; Tabima et al., 2012; Perez-Vizcaino et al., 2010). ROS include free radicals (substances containing one or more unpaired electrons) that are naturally formed as by products of oxygen metabolism, such as hydroxyl (OH·), O_2^-, peroxyl (RO_2·) and hidroperoxyl (HO_2·), and

non-radical species, such as hydrogen peroxide (H_2O_2) and other peroxides (ROOH) (Perez-Vizcaino et al., 2010). In parallel, the term reactive nitrogen species (RNS) is widely used to identify highly reactive substances containing nitrogen (and oxygen too) such as NO, (a free radical) and NO derived substances such as $ONOO^-$ (Perez-Vizcaino et al., 2010).

ROS serve as important intracellular and intercellular second messengers, regulating a variety of cellular signalling pathways through reaction with protein residues, mainly cysteine. The main ROS involved in cell signalling pathways are O_2^- and H_2O_2. The effect of ROS in cellular signalling include activation and regulation of many major cell signalling pathways such as p38 MAPK, PI3K/Akt, nuclear factor kappa-light chain-enhancer of activated β cells (NF-κB), ERK, c-Jun N-terminal kinase (JNK), RhoA/ROCK, COX and ion channels (Tabima et al., 2012; Perez-Vizcaino et al., 2010).

4.1. Sources of ROS in the pulmonary vasculature

ROS is produced by all vascular cell types, including EC, VSMC, and adventitial fibroblasts, from both metabolic and enzymatic sources. The main sources involved in generating ROS include: NADPH oxidases, xanthine oxidase, uncoupled NOS, mitochondria and COX (Tabima et al., 2012; Perez-Vizcaino et al., 2010).

- **NADPH oxidases**

The NADPH oxidase system is a multi-subunit enzymatic complex that is capable of producing O_2^- by catalyzing a one electron reduction of molecular oxygen, using reduced nicotinamide adenine dinucleotide (NADH) or NADPH as a donor, being almost the most important source of ROS in the pulmonary vasculature. In humans, seven isoforms of NOX have been identified: NOX1-5 and DUOX1-2. NOX1-4 have been detected in VSMC, endothelium and adventitia, playing an important role in the regulation of vascular tone (Tabima et al., 2012; Perez-Vizcaino et al., 2010).

NOX can be activated by growth factors (PDGF, epidermal growth factor [EGF], and TGF-β1), cytokines (TNF-α, IL-1, and platelet aggregation factor), mechanical forces

(cyclic stretch, laminar and oscillatory-shear stress), metabolic factors (hyperglycemia, hyperinsulinemia, free fatty acids), G-protein-coupled receptor agonists (5-HT, ET-1, TXA_2, Angiotensin-II) and changes in oxygen levels. Likewise, NOX isoforms are down-regulated by statins, PPAR agonist, and estradiol (Aggarwal et al., 2013; Perez-Vizcaino et al., 2010; Tabima et al., 2012).

- **Xanthine oxidase**

Xanthine oxidades (XO) is a flavoprotein that catalyzes the terminal steps in purine degradation. The process consists in transformation of hypoxanthine and xanthine to uric acid with concomitant release of O_2^-/H_2O_2 as products. Initially, XO exists as a xanthine dehydrogenase (XDH) form, where substrate-derived electrons reduce NAD^+ to NADH. However, during inflammatory conditions, it can be easily converted into XO by reversible thiol oxidation of the cysteine residues or irreversible proteolysis. Therefore, the ratio of XO to XDH in the cell is critical to determine ROS production generated by this enzyme (Aggarwal et al., 2013; Tabima et al., 2012).

- **COX**

The metabolism of AA may also cause the generation of O_2^- during the second stage of the synthesis of prostanoids, due to its peroxidase activity (Perez-Vizcaino et al., 2010).

- **Mitochondria**

Mitochondria are the cellular organelles that produce energy (ATP) through oxidative phosphorylation. Electrons flow down the redox gradient on the electron transport chain from the NADH and FADH2 as electron donors, creating the mitochondrial membrane potential used by ATP synthase to produce ATP. Oxidation of NADH by complex I and FADH2 by complex II reduces ubiquinone to ubiquinol and thus reoxidized by complex III. Oxidation of ubiquinol to ubiquinone involves the formation of ubisemiquinone and takes two cycles within complex III with the two electrons of ubiquinol being sequentially transferred to complex IV, where oxygen is reduced by cytochrome c oxidase to H_2O. Under physiological conditions the major sources of mitochondrial ROS are complex I, II and III, although complex I and III seems to be the main sites (Perez-Vizcaino et al., 2010; Tabima et al., 2012). In the pulmonary

vasculature, mitochondria are an important source of ROS production under physiological conditions and play a role as an oxygen sensor (Freund-Michel et al., 2014; Ryan et al., 2015).

- **Uncoupled eNOS**

Other source of O_2^- generation is eNOS. Under conditions of substrate (L-arginine) or cofactor (BH_4) deficiency eNOS is dysfunctional; electrons flowing from NADPH through the NOS reductase domain to the oxygenase domain are diverted to molecular oxygen rather than to L-arginine and yield O_2^- instead of NO (Aggarwal et al., 2013; Tabima et al., 2012).

4.2. ROS scavengers in the pulmonary vasculature

Antioxidant enzymes play a critical role in the regulation of the oxidant levels in the vasculature. The major vasculature enzymatic antioxidants are superoxide dismutase (SOD), catalase and glutathione peroxidase (GPx).

- **Superoxide dismutase**

SOD exists as three isoforms: Cu/ZnSOD (SOD1) in the cytoplasm, MnSOD (SOD2) in the mitochondria, and the extracellular EC-SOD (SOD3). SOD is a universally expressed enzyme and all the three isoforms are expressed in the lung. This enzyme catalyzes the conversion of $O_2^{\cdot-}$ into H_2O_2 (Aggarwal et al., 2013).

- **Catalase**

Catalase is mainly located in cellular peroxisomes and the cytosol. It contains a molecule of Fe^{3+} at its active site and catalyzes the decomposition of H_2O_2 to H_2O and O_2. This enzyme is very effective during high levels of oxidative stress and has the highest turnover rate of all these antioxidant enzymes, as each molecule can degrade 40 million molecules of H_2O_2 in 1 second (Aggarwal et al., 2013).

- **Glutathione peroxidase**

GPx exists in eight isoforms. GPx requires 2 molecules of gluthatione (GSH) to reduce 1 molecule of H_2O_2 to 2 molecules of H_2O and in this process GSH is oxidized to GSSG (Aggarwal et al., 2013).

4.3. Role of ROS in pulmonary hypertension

Many ROS and NO signalling pathways are simultaneously disrupted in PAH, including increased expression of NADPH oxidase and XO, uncoupling of eNOS, and reduction in mitochondrial number, as well as impaired mitochondrial function (Tabima et al., 2012).

In the chronic hypoxia-induced PH model the expression of NOX4 in PASMCs is increased and the inhibition or knockdown of NOX4 reverses PH through reduction of ROS formation and SMC proliferation (Tabima et al., 2012). Furthermore, elevated plasma XO levels have been reported in PA from patients with IPAH, in lamb model of congenital heart disease with increased pulmonary blood flow and in a rodent model of hypoxia induced PH (Aggarwal et al., 2013; Tabima et al., 2012).

Besides the increase in ROS generation, deregulation of antioxidant enzymes has been implicated in the pathology of systemic and PH (Aggarwal et al., 2013). In PH of different etiologies, the expression and/or activity of these isoforms are decreased, which contributes to oxidative stress and vascular remodelling. SOD1 has been found diminished in PA from hypoxia induced PH piglets. SOD2 protein level and activity are attenuated in the plexiform lesions of PA from PH patients and in PAECs isolated from patients with IPAH (Aggarwal et al., 2013).

In addition, as mentioned above, mitochondria are major sources of ROS production under physiological conditions playing a role as an oxygen sensor in PA and, conversely, mitochondrial dysfunction plays a role in pathogenesis of PH.

Suppression of oxidative phosphorylation of glucose and subsequent increase in glycolysis has been evidenced in PH in all pulmonary arterial layers (ECs, PASMC and

fibroblasts). This metabolic shift results from activation of transcription factors such as the hypoxia inducible factor-1α (HIF-1α) and contributes to the hyperpolarized mitochondrial membrane potential observed in patients with PH and in several animal models of PH (Tabima et al., 2012; Freund-Michel et al., 2014; Ryan et al., 2015).

5. Potassium channels

Ion channels play an important role in multiple functions of VSMCs, including contractile state, size, and rate of proliferation and apoptosis through their ability to alter *Em* and intracellular ion levels and cell volume (Bonnet et al., 2007). The concentration of intracellular K^+ (≈ 140 mM) is much higher than in the extracellular space (≈ 5 mM). Therefore, transmembrane K^+ current, which is generated by K^+ efflux through K^+ channels, is a key determinant of the *Em* in VSMCs (Mandegar et al., 2002; Lai et al., 2015; Olschewski et al., 2014). K^+ channels are found on both plasma membrane and internal membranes of many cell types where they respond to a variety of stimuli.

Four functional classes of K+ channels have been identified in VSMC: the voltage-dependent K^+ channels (Kv), the Ca^{2+} activated K^+ channels (K_{Ca}), the inward rectifier K^+ channels (K_{ir}) and the two-pore domain K^+ channels (K_2P) (Burg et al., 2008; Mandegar et al., 2002; Gutman et al., 2005).

- **Inward rectifier channels**

K_{ir} channels consist of only two membrane-spanning domains (S) with a membrane reentrant loop that contains the elements for ion selectivity (P-domain). This P-domain and the S2 contribute to the permeation pore structure. The term inward rectifier describes the increased K^+ influx through the channels during membrane hyperpolarization.

The K_{ir} family comprises 15 members in mammals and it has been divided into four subfamilies according to their biophysical properties and physiological role: classical K_{ir} (Kir2.x), G protein gated Kir (Kir3.x), ATP-sensitive K^+ channel or K_{ATP} channels

(Kir6.x/sulfonylurea receptor (SURx)), and K^+-transport channels (Kir1.1, Kir4.x, kir5.1, and Kir7.1). K_{ir} channels are blocked by low concentrations of Ba^{2+} and Cs^+ (Sepúlveda et al., 2015; Bonnet et al., 2007; Ohya et al., 2016).

K_{ATP} channels are inhibited by intracellular ATP levels, with an inverse relationship between the channel opening probability and the ATP concentration. There are many inorganic compounds that can promote or inhibit K_{ATP} channel opening. The pharmacological agents which directly can activate the K_{ATP} channels include cromakalim, levcromakalim (lemakalim), aprikalim, nicorandil and pinacidil. While, all types of K_{ATP} channels are inhibited by sulfonylureas (Foster et al., 2016; Sobey et al., 2001).

- **Kv channels**

The Kv channel family forms the most diverse group, including 38 members grouped in 12 families (Kv1-Kv12) with a high level of similarity. Each Kv channel gene encodes one α subunit. Kv channels are usually a homotetrameric structure (4 identical α subunits), although, some channels can be heterotretameric. The α subunit consist of six membrane-spanning domains (S1-S6). These domains form two structurally and functionally different parts of the channel. The segment located between S5-S6 is the potassium ion-conducting domain (P-domain), and the S4 segment represents the sensor of the channel. They have been divided into delayed-rectifier and rapidly-inactivating K^+ channels based on differences in activation and inactivation kinetics (Grizel et al., 2014; Bonnet et al., 2007; Gutman et al., 2005; Lai et al., 2015; Ohya et al., 2016; Olschewski et al., 2014).

Functional diversity of Kv channels activity is further enhanced by several factors such as heteromultimerization with other α-subunits, association with the accessory β-subunits which provide a surface interaction with several proteins that include protein kinases and phosphatases, an alternative mRNA splicing and post-translational modification as phosphorylation, glycosylation or ubiquitination (Gutman et al., 2005; Boucherat et al., 2015).

- **The Ca^{2+} activated K^+ channels**

There are 5 members of Ca^{2+}-sensitive channels ($K_{Ca}1$-$K_{Ca}5$). These consist of six or seven membrane-spanning domains and one P-domain. Based on their single channel conductance these channels have been divided into: large-conductance K_{Ca} channels (BK_{Ca}), small-conductance K_{Ca} channels (K_{Ca}), and intermediated-conductance K_{Ca} channels (IK_{Ca}). The ubiquitous BK_{Ca} channel is structurally unique, with 7 membrane-spanning domains and a calcium binding region, which causes its opening when cytosolic calcium rises (Bonnet et al., 2007; Ohya et al., 2016; Sobey et al., 2001; Olschewski et al., 2014).

- **The two-pore domain K^+ channels**

There are about 15 members of K_{2P} channels belonging to the K_{2P} family, named TWIK, due to their two P-domains in tandem, rather than the usual single P-domain, and four membrane-spanning domains (S1-S4) in a weak inward rectifying K^+ channel. They form homodimers, and sometimes heterodimers, where each monomer contributes two P-domains and S2 and S4 to the conduction pore. TWIK-related acid-sensitive K^+ channels (TASK) and TWIK-related alkaline pH-activated K^+ channels (TALK) belong to this family. These channels contribute to leak or background K^+ conductance, and are regulated by several factors such as, intra and extracellular pH, membrane stretch, temperature, oxygen and polyunsaturated acids (Sepúlveda et al., 2015; Bonnet et al., 2007; Ohya et al., 2016).

PASMCs have a resting *Em* of around -65 to -50 mV *in vitro*, close to the predicted equilibrium potential for K^+ ions. Although this resting potential is maintained by the four classes of K^+ channels described above (Weir et al., 2006), TASK and Kv channels, seem to play a determinant role in regulating pulmonary vascular tone through the control of the *Em*, and subsequently of i[Ca2+] in PASMCs (Burg et al., 2008; Sobey et al., 2001; Boucherat et al., 2015).

When either expression or activity of functional Kv channels decline, the whole K^+ current decrease. Then it results in a less negative *Em*, leading to cellular membrane depolarization (Mandegar et al., 2002; Boucherat et al., 2015).

5.1. Role of potassium channels in pulmonary hypertension

As mentioned above, Kv channels are implicated in control of the vascular tone and in the maintenance of cellular homeostasis and proliferation in SMCs. When Kv channel expression or activity is impaired, positively charged K^+ ions accumulates inside the cells, which inhibits caspases activation and apoptosis. This renders the interior of the cell more positive, resulting in membrane depolarization and activation of voltage-activated Ca^{2+} channels, leading to an increase in $[Ca^{2+}]_i$. This increased i[Ca2+] stimulates vasoconstriction and both cellular proliferation and migration (Wilkins et al., 2012; Mandegar et al., 2002; Boucherat et al., 2015; Burg et al., 2008).

Reduced expression and activity of Kv channels (most notably TASK1, Kv1.5 and Kv2.1) is a common denominator of human and experimental PH models, such as MCT or chronic hypoxia (Foris et al., 2013; Yuan et al., 1998), which highlights their role in the pathogenesis of several forms of PH. In addition, inhibition of Kv channels contributes to the contraction induced by key pulmonary vasoconstrictors, such as hypoxia, 5-HT, ET-1 and TXA_2,and activation of K channels participates in the relaxant response induced by NO and PGI_2. Other factors involved in PAH pathogenesis such as acute and chronic hypoxia and ROS also inhibit the activity and mRNA and protein expression of several K^+ channels, such as Kv1.5 (Cogolludo et al., 2006; Cogolludo et al., 2003; Boucherat et al., 2015; Burg et al., 2008; Bonnet et al., 2007; Olschewski et al., 2014).

6. Bone morphogenetic proteins

The activity of BMP was first observed in the mid-1960s when it was identified in extracts from bone matrix that could induce ectopic bone formation when implanted subcutaneously in rats. It was not until the 1980s when the first BMPs were characterized and cloned (Wang et al., 2014; Lowery et al., 2010; Wozney et al., 1988).

BMP signalling is critical in embryogenesis and many processes in early development of many organ systems. Furthermore, BMP signalling has been associated with regulation of early heart development and morphogenesis. In adult tissue, BMPs show an

important role in maintaining cell homeostasis on proliferation, apoptosis, and differentiation in a variety of tissues (García de Vinuesa et al., 2016; Cai et al., 2012).

The BMP family consists of about 20 ligands, which belong to the TGF-β superfamily. BMPs can be subdivided into at least four groups based on sequence similarity and affinities for specific receptors: the BMP2/4, the BMP5/6/7, the BMP9/10 and the GDF5-7 (growth and differentiation factor) subgroups (García de Vinuesa et al., 2016).

BMPs are synthesized as large precursor proteins with an amino N-terminal signal peptide, a prodomain for folding and secretion, and a bioactive carboxy C-terminal mature peptide. BMP precursor proteins are produced in the cytoplasm as dimeric pro-protein complex, which are cleaved by pro-protein convertases (serine endoproteases) to generate N- and C- terminal mature peptide. The C-terminal mature fragment is capable of binding to its receptor, while the non-covalently associated prodomain plays a regulatory role (Cai et al., 2012; Wang et al., 2014).

6.1. BMP signalling: canonical and non-canonical pathways

Like others members of the TGF-β family, BMPs bind to two types of serine-threonine kinase receptors, known as type I and type II receptors (BMPRs). Type I receptors include activin receptor-like kinases: ALK1, ALK2 (also known as ACTR1A), ALK3 (also known as BMPR1A) and ALK6 (also known as BMPR1B). Type 2 BMP receptor include BMPR2, type 2 activin receptor (ActR2A), and type 2B activin receptor (ActR2B). BMPRs form an heterotetrameric complex comprising two dimers of type I and type 2 receptors. While ALK3, ALK6, and BMPR2 are specific to BMPs, ALK2, ActR2A and ActR2B can function as receptor for activin, another member of the TGF-β superfamily (Lowery et al., 2010; Cai et al., 2012).

BMPs can signal through both canonical and non-canonical pathways. In the canonical signalling pathway, BMP ligands bind to the cell surface receptor which forms the heterotetrameric complex. Thereafter, the constitutively active type II receptor transphosphorylate the type I receptor which, in turn, phosphorylates the receptor-regulated Smads (R-Smad) which include Smad1, Smad5 and Smad 8 (Wang et al.,

2014). The R-Smads interact with the co-mediator Smad (co-Smad) Smad4, and this complex translocates into the nucleus where it regulates gene expression (Lowery et al., 2010; Cai et al., 2012; Wang et al., 2014). The non-canonical or Smad-independent signalling pathway involves the MAPK (ERK, p38-MAPK and JNK), PI3K/Akt, PKC signalling pathway, and Rho-GTPases.

6.2. BMP signalling pathway in pulmonary arterial hypertension

An heterozygous germline mutation in BMPR2 is found in more than 70% of patients with HPAH and 20% of patients with IPAH (Wang et al., 2014). Currently, there are a total of 668 germline variants of BMPR2 gene underlying PAH, being the major causal gene for familiar cases of PAH. The spectrum of variants include variants leading to amino acid substitution, nonsense mutations, defects resulting from small insertion/deletions, splice-site variation, major gene rearrangements and single-nucleotide mutation in the 5-prime untranslated region (5´UTR) (Machado et al., 2015). These mutations have been found in various regions of the protein, including the ligand-binding domain, the key catalytic region of the kinase domain, or the long cytoplasmic tail (Cai et al., 2012).

Genetic manipulation of BMPR2 expression in mice has provided information regarding the mechanism by which BMPR2 mutations are involved into the PAH. Mouse models of BMPR2 deficiency and associated PAH have proved difficult to generate. The main reason is that BMPR2 null homozygotes are embryonic lethal, whereas heterozygote littermate do not develop robust PAH, being necessary a second hit such as 5-HT or hypoxia to develop the disease (Upton et al., 2013).

In the ECs, BMP2/4 stimulates BMPR2 and induces eNOS phosphorylation and activity leading to PAEC proliferation, survival and migration. However, in the presence of BMPR2 mutations, BMP2/4 cannot induce eNOS activation, contributing to the phenotype of PAH (Gangopahyay et al., 2011; Long et al., 2006; Lowery et al., 2010). Likewise, endothelial injury and enhanced inflammatory response characterized by focal infiltration of inflammatory cells around distal PA are found in ECs from BMPR2

deleted mice and in patients with PAH (Lowery et al., 2010). Disruption of BMPR2 in PASMCs results in an activation of the p38-MAPK pathway, leading to aberrant proliferation (Wang et al., 2014). This disruption of BMPR2 reduce the antiproliferative effect of BMP2/4, while signalling by BMP6/7 is enhanced, leading to proliferation of PASMCs by activation of p38-MAPK (Yu et al., 2005). BMPR2 could also interact with the cytoskeleton, and its deficiency may cause cytoskeletal defects related to the development of PAH (Wang et al., 2014).

7. Hypoxic Pulmonary Vasoconstriction

Hypoxic pulmonary vasoconstriction (HPV), also known as the von Euler-Liljestrand mechanism, is a physiological and highly conserved mechanism unique to the lung as a response to decreased partial pressure of oxygen (PO_2) below 160 mmHg (<21% O_2). HPV is important since it optimizes the ventilation-perfusion (V/Q) matching and prevents arterial hypoxemia by diverting the desaturated, mixed venous blood flow from poorly ventilated areas into a better ventilated areas of the lung (Weir et al., 2006; Kuhr et al., 2012; Firth et al., 2013).

Whereas most systemic arteries dilate during hypoxia, PA constrict (Sommer et al., 2008). Furthermore, this response is produced particularly into the resistance PA (<300 µm), and although the endothelium alters this vasoconstriction via release of vasoactive substances, HPV persist in endothelium denuded PA rings and isolated PASMC (Michelakis et al., 2004; Ward et al., 2009; Veit et al., 2015).

The effects of alveolar hypoxia on the pulmonary circulation can be divided into three phases: the acute phase (30 seconds to < 20 minutes), the sustained phase (>30 minutes to hours-days), and the chronic phase, characterized by refractory vasoconstriction and vascular remodelling (Veit et al., 2015), which by the subsequent pulmonary vasoconstriction and increase in PVR contributes to PH.

7.1. Regulation of hypoxic pulmonary vasoconstriction

A number of hypotheses have been exposed to explain how PASMC are able to sense variations on the oxygen levels. There are several mechanisms involved in HPV that are activated in parallel or sequentially, leading to contraction of the PASMCs. These pathways converge in a critical increase of i[Ca2+] and/or enhanced calcium sensitivity of the actin-myosin associated with inhibition of MLCP by ROCK (Weir et al., 2006, Sommer et al., 2008; Swenson et al., 2013). i[Ca2+] is increased by hypoxia-induced inhibition of several potassium channels, particularly the Kv1.5 and Kv2.1 channels, leading to membrane depolarization and extracellular calcium entry through Ca_L. In addition a release of calcium from the SR occurs, with consequent further influx through store-operated calcium channels (SOCC) (which are activated by depletion of the calcium from the SR), receptor-operated calcium channels (ROCC), and TRPC channels, which are non-selective cation channels, but carry predominantly Ca^{2+} ions. Moreover, sensitivity to calcium of the contractile elements is enhanced via a hypoxia-induced increase in ROCK activity (Veit et al., 2015; Swenson et al., 2013; Olschewski et al., 2014).

Currently there are two controversial models to explain the importance of ROS regulation during HPV. The **"redox hypothesis"** proposes that decreased generation of mitochondrial ROS (from complex I/III) and a more reduced cytosolic redox state initiates HPV by inhibition of K^+ channels opening, membrane depolarization and an increase in Ca^{2+} influx via Ca_L mediated by redox couples, such as GSH/GSSG and NADH/NAD ratio. Whereas, in contrast, the **"ROS hypothesis**" proposes that the response is due to an increased generation of ROS from the complex I/III of the electron transport chain of the mitochondria or activation of NADPH oxidases, which leads to increase Ca^{2+} concentration via Kv, TRCP, Ca_L and/or intracellular release from the SR (Ward J et al., 2009). Alternatively, our group has proposed a unifying model in which hypoxia induces an increase in mitochondrial-derived ROS which in turn activates a redox amplification pathway involving neutral sphingomyelinase-derived ceramide and NADPH oxidase (Cogolludo et al., 2009; Frazziano et al., 2011; Moreno et al., 2014). In addition, it has been suggested that hypoxia elevates the cytosolic AMP/ATP ratio, which activates AMP-activated kinase (AMPK) and stimulates

production of cyclic ADP ribose (cADPR), an endogenous activator of ryanodine receptors (RyRs) leading to Ca^{2+} release from the SR (Connolly et al., 2010; Sommer et al., 2008; Veit et al., 2015; Ward et al., 2009; Sylvester et al., 2012).

7.2. Role of hypoxia in the pathogenesis of pulmonary hypertension

PH associated with lung diseases (group 3) is much more common than PAH (group 1) (Pugliese et al., 2015). The most frequent lung diseases associated with group 3 are chronic obstructive pulmonary disease (COPD), interstitial lung disease (ILD), other pulmonary diseases with mixed restrictive and obstructive pattern, sleep-disordered breathing (sleep apnea), alveolar hypoventilation disorders, chronic exposure to high altitude and developmental lung disease (Galie et al., 2015). Regardless of the pathological mechanism of each disease, all of them share the common feature of chronic hypoxia. Chronic hypoxic exposure induces changes in the structure of PAs, as well as biochemical and functional changes of the different vascular cell types (Stenmark et al., 2006; Pugliese et al., 2015). Thus, chronic hypoxia induces a decrease in the production and/or activity of PGI_2 and NO, as well as increased production of ET-1, 5-HT, TXA_2 and inflammatory cytokines (IL-1, IL-6) by PAEC. These signals are able to induce the recruitment of adventitial or circulating cells, and induce proliferation and contraction of the PASMC, and increase the deposition of ECM proteins such as collagen and elastin within the adventitia layer (Stenmark et al., 2006; Pugliese et al., 2015; Paffett et al., 2007).

As mentioned above, hypoxia induces changes in the activity and expression pattern of Kv channels. A change in K^+ channel function is observed under acute hypoxia, whereas under chronic hypoxia, PASMCs show downregulation of Kv channel gene and protein expression. Kv channel downregulation leads to depolarization of PASMCs and inhibition of apoptosis. The resultant membrane depolarization results in an increase of calcium influx across the membrane, leading to vasoconstriction and cell proliferation (Weir et al., 2006). Interestingly, ROS produced under hypoxic conditions plays an important role in the inhibition of Kv channels in PASMC (Cogolludo A et al.,

2009; Frazziano et al., 2011), and this seems to be involved in chronic hypoxia-induced pulmonary vascular remodelling and PH (Stenmark et al., 2006; Pugliese et al., 2015; Paffett et al., 2007).

The hypoxia-inducible factor (HIF) is a heterodimeric transcription factor consisting either HIF-1α or HIF-2α and HIF-1β, which under hypoxic conditions participates as a master regulator of hypoxic responses. Under normoxic conditions, HIF-1α subunits are hydroxylated by the prolyl-hydroxylase (PHD) enzyme in two residues of proline. Then it is recognized by the von Hippel-Lindau (VHL) E3 ubiquitin-ligase complex and degraded by the proteasome. On the contrary, under hypoxic conditions, hydroxylation by PHD activity is inhibited and results in an accumulation of stable HIF-1α, which is translocated into the nucleus and binds to the regulatory regions containing a hypoxia-response element (HRE), initiating or enhancing the transcription of hypoxia-responsive genes, such as ET-1 or VEGF. Furthermore, it has been shown an inverse relationship between nuclear HIF-1 translocation and Kv1.5 expression in PASMCs (Bonnet et al., 2006; Stenmark et al., 2006; Pugliese et al., 2015; Paffett et al., 2007; Cottrill et al., 2013).

8. Inflammation and Immunity in Pulmonary hypertension

Inflammation has been defined as a complex series of interactions among soluble factors and cells that can arise in response to traumatic, infectious, post ischemic, toxic or autoimmune injury (Nathan et al., 2002). Soluble factors implicated in this process are cytokines and chemokines (soluble cytokines that act as chemoattractants, which play a role in leukocyte recruitment and trafficking). Both mediators are produced by inflammatory cells of the innate immune system as well as by any of the cells of the vascular wall (Price et al., 2012; Rabinovitch et al., 2014). Inflammatory and immune cells involved in these processes are T and B lymphocytes, monocytes/macrophages, mast cells and dendritic cells (DC) (Savai et al., 2015; Price et al., 2012; Rabinovitch et al., 2014)

- **T lymphocytes**

T lymphocytes are a key component of the adaptive immune response. Three subsets of T lymphocytes exist: $CD4^+$ T helper (TH) cells, $CD4^+CD25hiFoxP3^+CD127low$ T regulatory (Treg) cells, and $CD8^+$ cytotoxic T (TC) cells. Moreover, $CD4^+$ T cells are divided into TH1, TH2 and TH17. TH cells stimulate B cell differentiation and macrophage activation, and TC cells bind to major histocompatibility complex class I and kill infected cells. Treg cells control other T cells response and also regulate monocytes, macrophages, DC, natural killer cells and B cells (Price et al., 2012; Rabinovitch et al., 2014).

- **B lymphocytes**

B lymphocytes play a key role in cell mediated immune regulation by production of antibodies to specific antigen epitopes. In addition, B lymphocytes participate on antigen presentation, cytokine production, differentiation of effector T lymphocytes and collaboration with DC and lymphoid organogenesis (Price et al., 2012; Kherbeck et al., 2013)

- **Monocytes/Macrophages**

Monocytes/macrophages are invoved in the pathogen defense by phagocytosis (Price et al., 2012; Kherbeck et al., 2013).

- **Dendritic cells**

DCs are antigen-presenting cells that are also responsible for the initiation of the inflammatory response, displaying antigen bound to major histocompatibility complex class 2. Furthermore, these cells have the ability to differentiate into other cell phenotypes, including ECs (Price et al., 2012; Kherbeck et al., 2013).

- **Mast cells**

Mast cells are bone marrow derived cells resident in many tissues, containing well-characterized granules rich in histamine and heparin. They are important in hypersensitivity reactions; wound healing and pathogens defense (Price et al., 2012).

As mentioned above, interaction between EC, PASMC, fibroblast and leukocytes are important in the inflammatory processes, and involve successive events (e.g., rolling, adhesion, and extravasation of leukocytes) in response to cytokines and chemokines. These processes are also influenced by growth factors which activate several signalling pathways involved in inflammation, cellular proliferation, migration and resistance to apoptosis (El Chami et al., 2012; Rabinovitch et al., 2014).

8.1. Role of Inflammation and Immunity in pulmonary hypertension

Altered immunity and inflammation are known features of PH. In addition to the changes caused by the anomalous growth of vascular cells, the perivascular infiltration of various inflammatory cells, which comprise T and B lymphocytes, macrophages, DC and mast cells represents a common finding in patients with PAH as well as in animal models of PH (Savai et al., 2015). Beyond these histological findings circulating levels of cytokines, chemokines and growth factors are abnormally elevated. In addition, circulating levels of certain autoantibodies directed against antinuclear antigens, EC and fibroblasts have been found in idiopathic and systemic sclerosis-associated PAH. These cytokines and chemokines include interleukin-1β (IL-1 β), interleukin-6 (IL-6), interleukin-8 (IL-8), TNF-α, fractalkine (CX3CL1), monocyte chemoattractan protein-1 (MCP-1 or CCL2) which are increased in plasma of PAH patients, as well as in EC and PASMCs (Nogueira-Ferreira et al., 2014). These cytokines affect proliferation, migration and differentiation of pulmonary vascular cells as well as contribute to the recruitment of inflammatory cells (Hu et al., 2015; Morrell et al., 2013). Moreover, several growth factors are released from VSMC, EC and inflammatory cells, including PDGF, VEGF or EGF, which modulate cell proliferation and migration into the vessel wall (Rabinovitch et al., 2014; Price et al., 2012; El Chami et al., 2012). Isoforms of the transcription factor nuclear factor of activated T cells (NFAT) plays a pivotal role in the inflammatory response. Among them, NFATc3 is expressed in PASMCs and is activated by chronic hypoxia in a calcineurin-dependent manner (de Frutos et al., 2007) and NFATc2 is increased in leukocytes and PASMCs from PAH patients (Bonnet et al., 2007;

Rabinovitch et al., 2012). In line with this, an inhibitor of the NFAT family, FK506 (tacrolimus), was reported to reverse severe PH in the SUGEN/hypoxia model by restoring BMPR2 expression (Spiekerkoetter et al., 2013).

Other pathway implicated in the inflammatory and immune responses is the mammalian target rapamicyn (mTOR), which leads to both DNA and protein synthesis, mediating PASMC growth (Kudryashova et al., 2015). Many cell types with augmented growth properties and/or diminished apoptotic response, show activation of the PI3K and Akt/mTOR signalling pathways (Morrell et al., 2013). Accordingly, inhibition of mTOR pathway with rapamycin have shown that ameliorate the MCT induced PAH (Houssaini et al., 2013).

9. Treatment of pulmonary hypertension

The right diagnosis for this disease is crucial since the prognosis and management of each group of patients is different. The treatment of PH cannot be considered as a mere prescription of drugs, but should include an initial evaluation of the severity and the subsequent response to treatment (Galie et al., 2015; MacKenzie et al., 2015). Currently, the pharmacological treatment of PAH include different drugs: Calcium channel blockers (CCB), endothelin receptor antagonist (ERAs), phosphodiesterase type 5 (PDE5) inhibitors, sGC stimulators and IP agonists (Figure 9). Additional experimental compounds and strategies are being tested, including ROCK inhibitors, VEGF receptor inhibitors, tyrosine kinase inhibitors or 5-HT antagonist among others (MacKenzie et al., 2015; Agarwal et al., 2011; Galie et al., 2015).

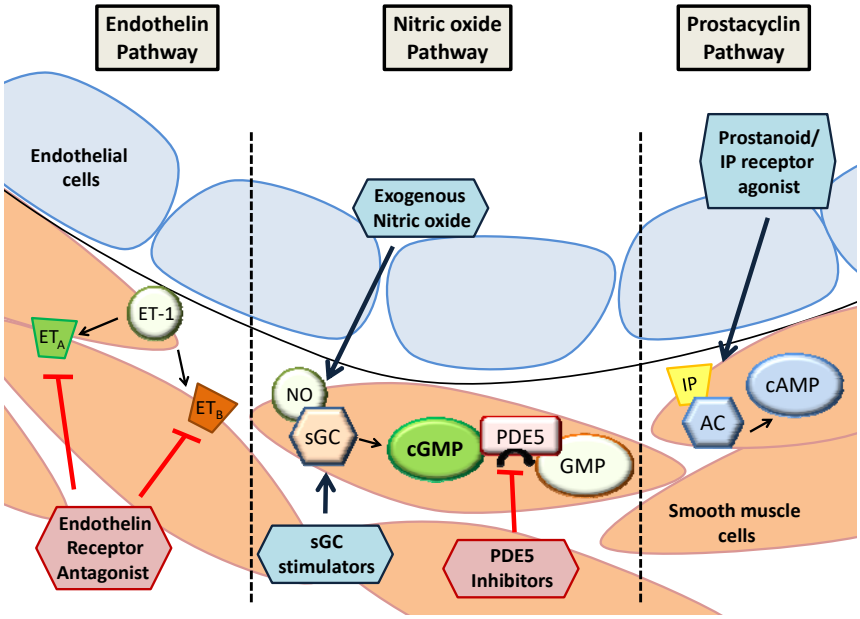

Figure 9: Target of current PH treatments:

9.1. Current treatments

9.1.1. Calcium Channel Blockers (CCBs):

Vasoconstriction of PASMCs is primarily governed by the availability of intracellular Ca^{2+}. As previously described, Ca^{2+} enters SMCs via Ca_L and initiates a vasoconstrictive cascade increasing PVR. Thus the ability to prevent Ca^{2+} influx by blocking the Ca_L represents an approach to suppress SMC vasoconstriction and promote vasodilation. CCB include nifedipine, amlodipine and diltiazem. CCBs are administrated only to a small number of patients with IPAH, which are “responders” to pulmonary vasoreactivity testing. These drugs are contraindicated in non-responders (Agarwal et al., 2011). The daily doses of these drugs showing efficacy in IPAH are relatively high (120-240 mg for nifedipine, 240-720 mg for diltiazem and up to 20 mg for amlodipine). Thus, side effects are frequent including systemic hypotension and lower limb peripheral oedema (Galie et al., 2015).

9.1.2. Prostanoids

As previously mentioned PGI_2 is the most potent endogenous inhibitor of platelet aggregation and also shows vadodilator, cytoprotective and antiproliferative activities (Galie et al., 2015). Deregulation of the PGI_2 metabolic pathway has been shown in patients with PAH as assessed by a reduction of PGI_2S expression in the PA and of PGI_2 urinary metabolites (Humbert et al., 2016).

The main target of PGI_2 and its analogues (prostanoids) is the IP that activates AC and increase cAMP levels (Agarwal et al., 2011), which increases PKA activity and finally vasodilatation (Humbert et al., 2016). Headache, jaw pain, flushing, nausea, diarrhea and musculoskeletal pain are the most common side effects of prostanoids (MacKenzie et al., 2015). Prostanoids available for PAH treatment include:

- Epoprostenol is a synthetic salt of PGI_2 with a short half-life (3-5 minutes) and is stable at room temperature for only 8 hours. It requires continuous *i.v.* administration using an infusion pump and a permanent tunneled catheter. It was the first prostanoid to be tested in patients with PAH (Humbert et al., 2016). Currently, it is the first line preferred treatment for WHO FC III-IV PAH patients and often serves as rescue therapy. Long-term use improves symptoms, exercise capacity, haemodynamic and quality of life. Serious adverse events related to the delivery system include pump malfunction, local site infection, catheter obstruction and sepsis (Galie et al., 2015; MacKenzie et al., 2015; Agarwal et al., 2011).

- Iloprost is a chemically stable PGI_2 analogue available for *i.v*. or aerosol administration. It has a longer half-life (20-30 minutes) compared with epoprostenol. Inhaled Iloprost is approved in USA for patients with PAH in WHO FC II-III, and in Europe and other countries for patients with PAH in WHO FC III (Humbert, 2016). Iloprost provides initial symptomatic improvements; however, only a minority of patients achieves long term-stability, particularly if it is used as monotherapy (Galie et al., 2015).
- Beraprost is a stable and orally active prostanoid, with a half-life of 35-40 minutes. Beraprost improves exercise capacity but without haemodynamic

improvements. It is only available in Japan, South Korea and other South-East Asian countries such as Indonesia for treatment of PAH in patients in WHO FC III (Galie et al., 2015; MacKenzie et al., 2015; Humbert et al., 2016).

- Treprostinil is a tricyclic benzidine analogue of epoprostenol, with similar pharmacological action, and improved chemical stability and longer half-life (4-5 hours). These features allow the administration of the compound by subcutaneous*, i.v*., inhaled and oral routes. Subcutaneous route is approved in the USA for patients with PAH WHO FC II-IV, and in Europe for WHO FC III (Humbert et al., 2016). Inhaled and oral routes are only approved in USA but not in Europe. The effect of treprostinil in PAH showed improvements in exercise capacity, haemodynamics and symptoms (Galie et al., 2015; MacKenzie et al., 2015; Agarwal et al., 2011).
- Selexipag is a novel orally active, selective and non-prostanoid IP receptor agonist. It is rapidly metabolized to an active form with a half-life of 7.9 hours. Although selexipag and its metabolite share similar mechanism of action to the endogenous prostacyclin, they are chemically distinct.

9.1.3. Endothelin Receptor Antagonists (ERA)

ET-1 is a potent vasoconstrictor and promoter of PASMCs proliferation by binding to two distinct receptor isoforms of the endothelin receptors, ET_A and ET_B in PASMC. Thus, the use of ET_A antagonists causes vasodilatation while ET_B antagonists may cause vasoconstriction by inhibition of local vasodilators release from EC. In addition, the blockade of both receptors attenuates the vasodilator effect of ET_A antagonism alone (Shao et al., 2011; Agarwal et al., 2011).

- Bosentan is the first molecule of this class to be synthesized. It is an oral active and nonselective dual ET_A and ET_B antagonist that received approval in 2001 for patients with PAH in WHO FC II-IV in the USA and other regions, and in patients in WHO FC II-III in Europe. Bosentan improves exercise capacity, FC, haemodynamics, echocardiographic and time to clinical worsening in PAH patients. The major toxicity associated with bosentan is hepatocellular injury by

increased levels of liver transaminases in approximately 10% of patients, thus requiring monthly liver function monitoring (Galie et al., 2015, Humbert et al., 2016; Agarwal et al., 2011).

- Ambrisentan is an oral active and selective ET_A antagonist with a ratio of ET_A to ET_B receptor selectivity of 77:1 (Agarwal et al., 2011), that has a longer half-life than bosentan (9h vs 5.4h respectively). It is approved for the treatment of patients with PAH in WHO FC II-III in the USA, Europe and other regions (Humbert et al., 2016). Ambrisentan has demonstrated efficacy on symptoms, exercise capacity, haemodynamics and time to clinical worsening (Galie et al., 2015). Unlike bosentan, ambrisentan was not associated with elevated liver toxicity, offering an alternative for patients in whom bosentan was not tolerated due to their hepatocellular injury (Agarwal et al., 2011). An increased incidence of peripheral oedema has been reported (Humbert et al., 2016; Galie et al., 2015).
- Macitentan is the newest dual ERA, administrated orally with the longest duration of blockade, and with a half-life of 16h (Selej et al., 2015; Enderby et al., 2015). It is approved for the treatment of PAH of WHO FC II-III in the USA and Europe (Humbert et al., 2016). While no liver toxicity was shown, decreased haemoglobin levels have been reported (Galie et al., 2015).

9.1.4. The NO/cGMP signalling pathway

9.1.4.1. Phosphodiesterase 5 (PDE5) inhibitors

PDE5 is abundantly expressed in the PASMCS and is upregulated in PASMCs from PAH patients, and in the RV cardiomyocytes; which may result in increased cGMP hydrolysis and impairment of pulmonary vasorelaxation. PDE5 inhibitors prevent cGMP degradation, and enhance cGMP effects, prolonging their vasodilator responses in the pulmonary vasculature (Agarwal et al., 2011; Wilkins et al., 2008). However, the efficacy of PDE5 inhibitors depends on availability of NO and cGMP (Humbert et al., 2016).

- Sildenafil is an oral active and selective PDE5 inhibitor, initially approved to treat erectile dysfunction (Agarwal et al., 2011). It is approved for the treatment of WHO FC II-III PAH patients in Europe and WHO FC II-IV in the USA (Humbert et al., 2016). Most side effects of sildenafil are mainly related to its vasodilator effect, such as headache and flushing, visual changes, dyspepsia and epistaxis (Galie et al., 2015; Agarwal et al., 2011).
- Tadalafil is an oral and once–daily administered selective PDE5 inhibitor, originally approved for erectile dysfunction (Agarwal et al., 2011), which presents a longer half-life than sildenafil. It is approved in the USA, Europe and other countries for patients with PAH WHO FC II-III (Humbert et al., 2016). The side-effect profile is similar to that of sildenafil (Galie et al., 2015).

9.1.4.2. Stimulators of soluble guanylate cyclase (sGC)

sGC is expressed in the VSMCs of the pulmonary vasculature, platelets, RV and other tissues as brain and kidney (Potter et al., 2011). When bound to NO, sGC catalyses the conversion of GTP to cGMP, which promotes vasodilatation, and inhibits SMC proliferation, leukocyte recruitment, inflammation, fibrosis, platelet aggregation and vascular remodelling (Humbert et al., 2016). The mechanism of action includes sensitizing sGC to endogenous NO by stabilizing NO-sGC binding, thereby acting in synergy with NO and and also directly stimulates sGC, independently of NO, increasing the cGMP levels (Enderby et al., 2015). The sGC stimulator riociguat is the first member of this novel class of drugs approved.

- Riociguat.iIs the only drug approved in the USA, Europe and other countries for group 1 PAH patients and for group 4 PH patients with inoperable CTEPH, or persistent/recurrent PH after pulmonary endarterectomy in WHO FC II-III (Enderby et al., 2015; Humbert et al., 2016). The reported adverse events are haemoptysis, pulmonary haemorrhage and syncope. (MacKenzie et al., 2015; Enderby et al., 2015; Galie et al., 2015).

The introduction of these drugs has improved symptoms, quality of life and survival of PH patients. Unfortunately, these treatments only appear to relieve symptoms, improve exercise capacity, prevent hospitalizations, but the functional limitation and survival of these patients remains unsatisfactory (Selej et al., 2015). All this current treatments are directed against the vasoconstrictor component of the disease. However, as previously mentioned, pathologic studies also show that obliteration of vessels caused by inflammation, smooth muscle proliferation and fibrosis within vessel wall represent other important part of the pathophysiology underlying of the disease. Thus, our knowledge on the cellular and molecular mechanisms implicated in the pathobiology of PH has remarkably increased, and based on this, new classes of drugs targeting these new mechanisms have been suggested as a new therapeutic option. (Morrel et al., 2013; Hu et al., 2015; Selej et al., 2015).

9.2. Novel molecular targets for pulmonary hypertension

9.2.1. Novel approaches to reversing sustained vasoconstriction: ROCK inhibitors

RhoA is a member of the Rho (Ras homologous) family of small monomeric G-protein. This protein acts as a signal transducer with it downstream substrate ROCK. Activation of ROCK produces vasoconstriction by phosphorylation of MLC independently of the MLCK pathway and phosphorylation of MLCP. These effect leads to inhibition of MLCP, which prolongs actin-myosin interaction and increases vascular tone in face of constant or even declining levels of cytosolic Ca^{2+}(calcium sensitization) (Morrell et al., 2013; Hu et al., 2015; McMurtry et al., 2010). In small PAs and lungs from human PAH patients and animal models of PAH, there are an increase in RhoA activity and expression of ROCK1/2, suggesting that RhoA/ROCK signalling plays a key role in the pathogenesis of PH (Do et al., 2009).

Fasudil was the first ROCK inhibitor approved in 1995 for the treatment of subarachnoid hemorrhage-induced brain vessel vasospasm. Clinical trials have shown

that intravenous administration of fasudil has acute beneficial vasodilatory effect on the pulmonary circulation, causing a decrease in PA pressure (Hu et al., 2015).

9.2.2. Agents that target proliferation, apoptosis and cell metabolism

Currently, the hyperproliferative phenotype and other characteristics found in PASMCs isolated from patients with PH, strongly suggest that the disease shares common features with cancer. Accordingly, cells of this disease show: genomic instability, sustained proliferative signalling, evasion of growth suppressors, resistance against cell death, induction of angiogenesis, tumour promoting inflammation, evasion of immune destruction and reprogramming of energy metabolism, eight out of ten “hallmarks of cancer”, defined by Hanahan and Weinberg. (Morrell et al., 2013; Hanahan et al., 2011).

Among drugs targeting these features we found: growth factor receptor inhibitors, statins, elastase inhibitors or kinase inhibitors.

9.2.3. Tyrosine Kinase Inhibitors

Receptor tyrosine kinases are a class of high-affinity cell surface receptors for a variety of growth factors, hormones, and cytokines ligands. These include PDGF, EGF, fibroblast growth factor (FGF), VEGF, c-Kit and bcl-Abl. Tyrosine kinase inhibitors reduce proliferation and migration of pulmonary SMCs and ECs (Hu et al., 2015; Morrell et al., 2013).

Imatinib was initially developed for the treatment of chronic myeloid leukemia, which inhibits the activity of the PDGF receptor kinase, c-Kit tyrosine kinase cell surface receptor and bcl-Abl oncoprotein (Homsi et al., 2007). It has shown to inhibit proliferation and migration of PASMC from IPAH patients (Nakamura et al., 2012).

9.2.4. Mitochondria-metabolic dysfunction

A shift from glucose oxidation to glycolysis, known as "Warburg effects" is a well-known metabolic abnormality in cancer cells. Interestingly, a similar glycolytic shift is found in PASMCs and ECs isolated from PAH patients and animal models (Morrell et al., 2013). As a result, mitochondrial pyruvate dehydrogenase kinase (PDK) activity is increased (which phosphorylate and inhibits pyruvate dehydrogenase-PDH), leading to attenuation of Krebs cycle and oxidative metabolism. Other consequence of deregulation of the mitochondrial function is the disruption of mitochondrial dynamics. This process due to a reduction of factors that increase the mitochondrial biogenesis or improve the mitochondrial oxidative capacity, as the PPARs (Paulin et al., 2014). Patients with IPAH have reduced lung expression of PPARγ (Ameshima et al., 2003) and PPARγ agonist have been proposed as potential therapies of PAH due to their anti-inflammatory and apoptotic effects (Jasińska-Stroschein et al., 2014).

9.2.5. Inflammatory and immune targets

Perivascular inflammation and vascular infiltration of inflammatory cells, as T and B lymphocytes and monocytes/macrophages are involved in the pathogenesis of PAH. It was found that inflammation precedes vascular remodelling in PAH animal models, which suggest that altered immunity is the cause rather a consequence of the vascular disease (Hu et al., 2015; Morrell et al., 2013; Nogueira-Ferreira et al., 2014). Inflammatory processes are also increasingly recognized as important components of pulmonary remodelling in humans with IPAH or PAH related with other inflammatory syndromes, such as connective tissue diseases, viral diseases (e.g. HIV, γHerpes virus 8 or Kaposi sarcoma-associated herpes virus and chronic active Epstein-Barr virus infection) or parasites as schistosomiasis (Savai et al., 2015; Price et al., 2012; Rabinovitch et al., 2014).

As previously mentioned, inflammation is associated with increased circulating levels of cytokines and chemokines such as IL-1 β, IL-6, IL-8 or TNF-α (Nogueira-Ferreira et al., 2014). These cytokines affect proliferation, migration and differentiation of pulmonary vascular cells (Hu et al., 2015; Morrell et al., 2013).

9.2.6. Flavonoids

Flavonoids were discovered in the 1930s and were initially considered as vitamins (vitamin P), due to their first biological property described were related to the barrier function on capillary permeability of the endothelium. This consideration as vitamin was discontinued in the 1950s. The term flavonoid comprises several thousand of compounds found in plants, which share a common skeleton of phenylchromane (molecules possessing two phenols joined by a pyran carbon ring structure). This basic structure allows a multitude of substitution patterns leading to several flavonoids subclasses, such as flavanols, flavones, flavanones, flavanols, anthocyanidins, isoflavones, dihydroflavonols and chalcones. Flavonoids are widely distributed in the plant kingdom, being present in variable amount in fruits, vegetables, nuts, seed, herbs, spices, tea and red wine. The average of daily intake in the occidental diet of flavonols plus flavones has been estimated to be 22-23 mg (although this amount depends of the population studied). Quercetin represents about 60-75% of the total dietary intake. Epidemiological studies have shown an inverse association between dietary flavonoid intake and mortality from cardiovascular disease (Perez-Vizcaino et al., 2006).

In addition to the classical antioxidant effect of this class of compounds, there are a huge number of enzymes whose activity is modulated by quercetin (mostly inhibited). Several *in vitro* studies have shown that quercetin presents direct effects on vascular tone, showing direct endothelium-independent vasodilator effect in isolated arteries such as coronary and PA contracted with different stimuli such as noradrenaline, ET-1, TXA_2, PKC activator (phorbol esters) and depolarizing agents (KCl) (Duarte et al., 1993; Gryglewski et al., 1897; Menendez et al., 2010). In addition, quercetin exerts protective effect on NO and endothelial function under conditions of oxidative stress, where high O_2- concentration reacts with quercetin as antioxidant. Quercetin, in the low micromolar range, may not act only as scavenger of O_2^-, but also as a XO and NADPH oxidase inhibitor (Jimenez et al., 2015) or as a strategy to prevent BH_4 oxidation and eNOS uncoupling. Additionally, quercetin inhibits ET-1 release and transcription of prepro-endothelin-1 in human endothelial umbilical veins and in the bovine aortic EC. Furthermore, quercetin reduces the expression of adhesion molecules and other

inflammatory markers, such as vascular cell adhesion molecule-1 (VCAM-1), intercellular adhesion molecule-1 (ICAM-1) and MCP-1 induced by TNF-α in human EC and VSMCs. Then, quercetin prevents endothelial dysfunction, reduces blood pressure, oxidative status and end-organ damage in animal models of hypertension (Perez-Vizcaino et al., 2009) As mentioned above, quercetin may interact over several enzymes and pathways. As a pan-inhibitor of MAPKs (e.g. ERK1/2, p38-MAPK, JNK and Akt) quercetin may control cell proliferation, migration and viability, and the TGF-β pathway (Nakamura et al., 2011; Stoclet et al., 2004).

A large body of *in vitro* and *in vivo* evidences support a protective effect of quercetin in the cardiovascular system. However, the possible protective effect of quercetin in PH remains unknown.

HYPOTHESIS AND AIMS

Pulmonary hypertension (PH) is a progressive pathophysiological disorder that affects the lung vasculature. PH may involve multiple clinical conditions and can complicate the majority of cardiovascular and respiratory diseases. Although the initial trigger leading to PH is still poorly understood, a complex interplay among different factors are thought to contribute to the sustained vasoconstriction, vascular remodelling, *in situ* thrombosis and arterial wall stiffening, which results in elevated PVR. These processes are influenced by both genetic and environmental factors that alter vascular structure and function.

A number of new drugs have been developed for some forms of PH in recent years which improve clinical symptoms and slow the progression of the disease but the prognosis of the patients is still poor. The effectiveness of current vasodilator drugs are limited by lack of pulmonary selectivity, ventilation-perfusion uncoupling and low efficacy when pulmonary artery contraction involves mechanisms of calcium sensitization.

The **general hypothesis** of the present thesis is that oxygen-sensitive vasodilators with pulmonary selectivity are effective in lowering PAP and preserve or improve arterial oxygenation. Therefore, they would offer a new therapeutic approach for patients with PH, especially for those in group 3, (i.e., PH owing to lung diseases and/or hypoxia), for which treatments are not currently available.

The **general aim** of this thesis is to analyse the vasodilator and antiproliferative effects of a wide range of drugs in order to identify those with potentially better efficacy and fewer side effects, based on their ability to: 1) combine both vasodilator and antiproliferative effects, 2) exert selective vasodilator effects in the pulmonary circulation, avoiding systemic hypotension, 3) induce selective vasodilator effects in the oxygenated lung areas (preserving hypoxic pulmonary vasoconstriction) and 4) exert effective vasodilator effects under calcium-sensitizing conditions.

The specific aims of this Thesis are:

1. *In vitro* analysis of the pulmonary- and oxygen- selectivity in rat isolated arteries of a wide range of vasodilators including those: 1) currently used in

PH (Ca^{2+} channel blockers, PDE5 inhibitors, prostacyclin derivatives), 2) under development for PH (Rho kinase inhibitors, soluble guanylate cyclase activators) and 3) other drugs with potential interest (mainly quercetin and derivatives, P2Y purinoceptor agonists, adenylate cyclase activators, K^+ channel openers, NO and several NO donors belonging to different chemical classes). (Chapter 1).

2. *In vitro c*onfirmation of the pulmonary- and oxygen-selectivity of selected drugs in human arteries. (Chapter 1).

3. *In vitro* analysis of the antiproliferative effects of drugs in pulmonary artery smooth muscle cells derived from control (rPASMCs) and MCT-induced PAH rat models (rPASMCs-MCT) or from human donors (hPASMCs). (Chapter 1).

4. *In vivo* analysis of the acute effects of selected drugs on pulmonary and systemic hemodynamics and gas exchange in rats and the response to acute unilateral and bilateral lung hypoxia and to a contractile agonist thromboxane A_2 mimetic U46619. (Chapter 2).

5. *In vivo* analysis of the chronic effects of quercetin in a rat model of PAH induced by monocrotaline on systemic and pulmonary hemodynamics, right ventricular hypertrophy, pulmonary artery remodelling and survival. (Chapter 3).

MATERIAL AND METHODS

1. Ethical statement

All experimental procedures utilizing animals were carried out according to the Royal Decree 1201/2005 and 53/2013 on the Care and Use of Laboratory Animals and all procedures were approved by the institutional Ethical Committee of the Universidad Complutense de Madrid (Madrid, Spain) and the University of Valencia (Valencia, Spain).

Human samples were provided by Dr. José Ángel Lorente (Hospital Universitario de Getafe, Spain) and Dr. Julio Cortijo (Hospital Universitario de Valencia). The Human Research Ethics Committees from both Hospitals approved their use, after informed consent, of lung tissue discarded by pathologist following thoracic surgery. Lung tissues were obtained from 33 adult patients undergoing lung carcinoma surgery.

2. IN VIVO studies

2.1. Animals models

All animals used in this thesis were pathogen-free male Wistar rats, which were obtained from Harlan Iberica (Barcelona, Spain) and maintained in the general animal facility of Universidad Complutense of Madrid (ANUC) or University of Valencia (Valencia, Spain). Rats were housed, five per cage, with free access to water and food *ad libitum* under standard conditions: at a constant temperature (24 ± 1°C), with a 12-hours light/dark cycle.

2.1.1. Haemodynamic Measurements

Male rats Wistar were anesthetized by intraperitoneal (*i.p.)* administration with a mixture of 80 mg/kg ketamine (Mearial Lyon, France) plus 8 mg/kg xylacine (KVP Pharma und Veteriär-Produkte GmbH, Kiel, Germany). Before initiation of surgical procedure, general anesthesia was confirmed by assessing the absence of response to any stimulus. Then, animals were placed in a supine position on a thermostatically controlled electric heating blanket (Homeothemic Blanket Control Unit, Harvard Apparatus, March-Hugstetten, Germany) to maintain body temperature at 38°C. The tracheostomy was performed by a ventral neck incision followed by insertion of a 2.1

mm catheter internal diameter (ID) in the trachea (14 GA, BD Insyte, USA) as shown in Figure 10. This catheter is attached on a ventilator (Nemi Scientific Inc, Medway, USA) and ventilated with room air (tidal volume 9 mL/kg, 60 breaths/min, and a positive end-expiratory pressure of 2 cm H_2O). Arterial saturation (SO_2) was continuously recorded using a pulsioxymeter (StarrOx) placed in the lower extremity of the animal.

Figure 10: Tracheostomy. *Catheter placement into the trachea to ventilate the animal.*

The internal jugular vein was exposed and was cannulated using a catheter (PE-50). This vein was used for administration of drugs. The left carotid artery was exposed and cannulated using an heparinized saline filled polypropylene cannula (Intramedic Polyethylene Tubing I.D 0.58mm-0.023´´ and O.D 0.965mm-0.038´´, Beckton Dickinson, USA) attached to a pressure transducer (Bentley Trantec, Model 60-800; American Edwards Laboratories, Santa Ana, CA, USA) and fixed with silk suture. This left carotid artery was used to measure the systolic, diastolic and mean systemic arterial pressures (SAP) and heart rate (HR). On the other hand, the right carotid artery was cannulated using a probe MLT1402 T-type Ultra-Fast Thermocouple probe (AD instruments, Clifton NJ, USA) for CO estimation by the thermodilution method (Sato et el, 1982; Muller et al, 1981; Graudins et al, 2006). Briefly, 150 µL cold saline solution was injected via the internal jugular vein and a thermodilution curve was recorded from the carotid thermistor probe on PowerLab Chart Software. CO was calculated by measuring the area under the curve using the Cardiac Output Module from Power-Lab Chart Software.

After sternotomy, a heparinized saline-filled cannula attached to a pressure transducer (Bentley Trantec, Model 60-800; American Edwards Laboratories, Santa Ana, CA, USA)

was advanced by means of a 0.9-mm-ID catheter (22 GA, BD Insyte, USA) into the RV to measure the right ventricular pressure (RVP) and advanced through the main PA to measure the systolic, diastolic and mean PAP (Figure 11 and 12). Pressure measurements were then recorded using the LabChart v7 software (AD instruments).

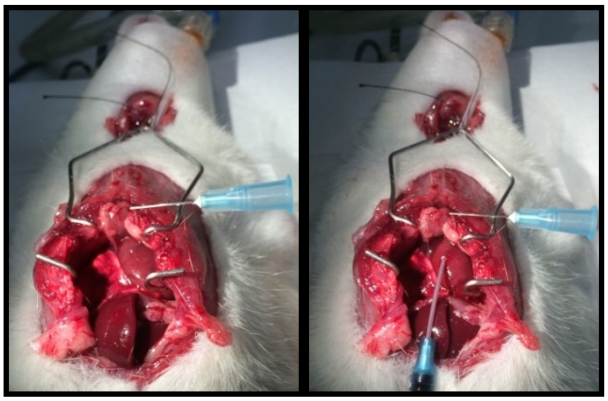

Figure 11: Right hearth cathaterization. *Catheter placement to measure Right Ventricular Pressure (RVP) and Pulmonary Arterial Pressure (PAP).*

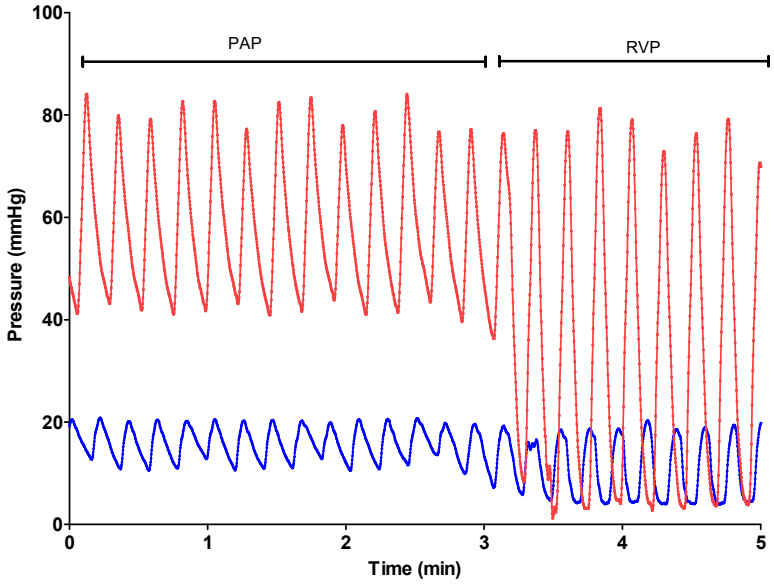

Figure 12: Representative recording of Pulmonary Arterial Pressure (PAP) and Right Ventricular Pressure (RVP). *PAP was recording by placing the catheter in the pulmonary artery and then the catheter was retracted to the right ventricle to measure RVP in a non-PH (Blue) and PH (Red) rats.*

2.1.2. Acute drug effect*:* regional and global hypoxia

The rats were anesthetized, ventilated and instrumented for hemodynamic measurements as described above. The experimental design for the acute *in vivo* study

is shown in Figure 13. After a 10 minutes stabilization period under normoxic (room air) ventilation, rats were exposed to global hypoxia (10 % O_2, I, GH) for 5 minutes followed by a 20 minutes recovery period of normoxia. Thereafter, rats were exposed to unilateral hypoxia by advancing the tracheal tube into the right bronchium (and obstructing the left bronchium) for 5 minutes (II, UH) followed by a 20 minutes recovery period of normoxia. Then vehicle (dimethyl sulfoxide (DMSO), 500 µl), riociguat (0.1 mg/kg) or sildenafil (0.5 mg/kg) were infused manually over a period of 5 minutes through the jugular vein, and after 40 minutes rats were again exposed to GH (III) and UH (IV). Finally rats were treated with U46619 (U4) (0.003 mg/kg) for 5 minutes.

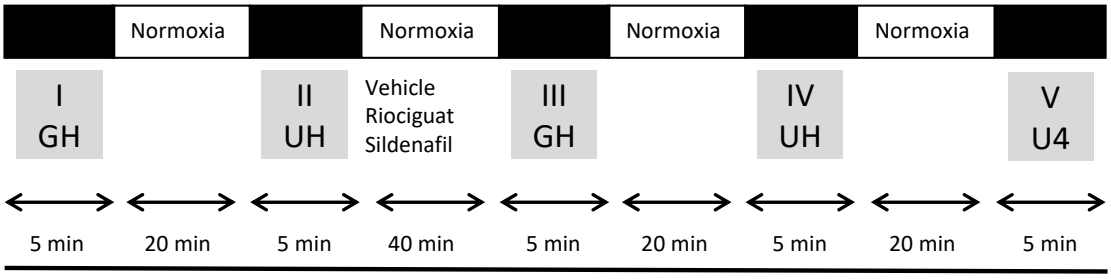

Figure 13: Experimental protocol.

2.2. Chronic models of Pulmonary Hypertension.

2.2.1. Monocrotaline model

Male Wistar rats obtained from Harlan Iberica (Barcelona, Spain) at 8 weeks of age and 225-250 g of body weight (BW) were maintained in the general animal facility of Universidad Complutense (ANUC), five per cage, at a constant temperature (24 ± 1°C), with a 12-hour light/dark cycle, on a standard chow and water *ad libitum*.

Animals were randomly divided into a control and a pulmonary arterial hypertensive group. PAH was induced by a single *i.p.* injection of 60 mg/kg monocrotaline (MCT) (Sigma-Aldrich) dissolved in 0.9 % (w/v) NaCl sterile saline solution (control animals were injected with saline). MCT is a pyirrolizidine alkaloid derived from *Crotalaria spectabilis* seeds*.* The MCT alkaloid is activated to the reactive pyrrole metabolite dehydromonocrotaline in the liver by the enzyme cytochrome P-450 (CYP3A4). This reactive metabolite initiates endothelial injury in the pulmonary vasculature leading to

obstructive pulmonary vascular remodelling characterized by narrowing/obliteration of the vascular lumen and RV hypertrophy (Gómez-Arroyo et al. 2012; Maarman et al. 2013).

Twenty one days after MCT injection, i.e. after the animals have developed a marked increase in PAP, rats from both groups were randomly assigned to vehicle or quercetin treatment (10 mg/kg once daily 9:00-11:00 AM, dissolved in 1 mL of 1% methylcellulose) by gastric gavage for an additional period of 11 days. The experimental design for the acute *in vivo* study is shown in Figure 14. This dose has been shown to be effective in systemic hypertension in rats (Perez-Vizcaino et al., 2009). The treatment period was chosen because in the 4-6th week is the period of maximal worsening of the disease and higher mortality in this model. The number of rats in each group was adjusted to reach a similar number of surviving rats in all groups at the end of the treatment based on the expected and actual mortality.

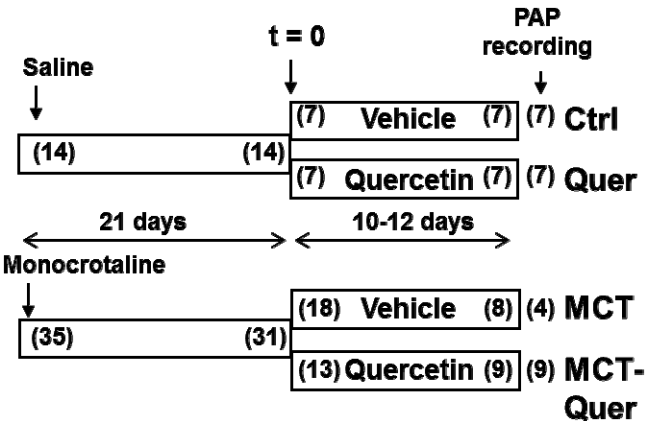

Figure 14: Study protocol. *Numbers in parenthesis indicate the number of rats which started and finished each period. The numbers at the far right indicate the number of rats in which pulmonary arterial pressure could be recorded; the missing animals in the monocrotaline (MCT) group died during the anesthesia or surgery.*

2.2.2. Bleomicin model of lung fibrosis

Male Wistar rats obtained from Harlan Iberica (Barcelona, Spain) at 12 weeks of age and 325-350 g of BW which are reported to mount a robust early inflammatory response followed by PH and fibrotic remodelling secondary to bleomycin (Moeller et al., 2008) and were maintained in the general animal facility of University of Valencia

(Valencia, Spain). Rats were anaesthetized with ketamine/medetomidine and then a single dose of bleomycin at 3.75 U/kg (dissolved in 200 µL of saline solution) was administered intratracheally via the endotracheal route. This dose of bleomycin reproducibly generated pulmonary fibrosis in previous experiments (Almudéver et al., 2013). Sham control treated rats received the identical volume of intratracheal saline instead of bleomycin. This procedure, fixed experimentation day 1 and was synchronously coupled with the initiation of single drug administration at day 21. In both sham control and bleomycin groups, sildenafil at 0.5 mg/kg or riociguat at 0.1 mg/kg were administered via i.p. After 2 hours of administration it was evaluated the V/Q ratio using a micro-CT-SPECT.

2.2.2.1. Analysis of ventilation and perfusion by micro-CT-SPECT images

Radioisotopic perfusion scanning provides a safe and highly sensitive test for chronic thromboembolism, PH and alterations of pulmonary vascular perfusion. Perfusion lung imaging depends on the embolization of 99mTc-labelled 10-40 µm human albumin macroaggreagates (MAA-$Tc99^{m}$), for which the pulmonary arterioles act as a sieve so that the amount of particulate matter impacted is proportional to the pulmonary artery flow in the terminal arterioles and other precapillary vessels of that region (Jobse et al., 2013). *In vivo* imaging and quantitative analysis were performed in rat lug tissue using small-animal computer tomography (micro-CT) and single photon emission computed tomography (Albira micro-CT-SPECT-PET Imaging System (Oncovision®, Spain).

2.2.2.2. Lung Ventilation/Perfusion scanning (V/Q scan)

V/Q SPECT imaging is a well-established nuclear medicine technique that provides spatial information regarding the 2 core processes of respiratory gas exchange, ventilation of alveolar units and perfusion of the pulmonary capillary beds. SPECT V/Q is commonly used in the diagnosis of pulmonary embolism but has been shown to be sensitive to early indicators of COPD and ILD in addition to being capable of identifying

comorbid disease (such as PH) and distinguishing pathophysiologic changes. Furthermore, coregistration of nuclear imaging data to CT images allows for greater insight into the anatomic position of lung dysfunction and structural information such as the distribution of emphysema (in COPD) or pulmonary fibrosis (in ILD). Although V/Q imaging techniques hold great promise in providing a better understanding of chronic respiratory illnesses such as COPD or ILD, these techniques can also be used in preclinical research to study disease pathogenesis and evaluate the efficacy of therapies. Preclinical models for investigating COPD associated PH or ILD associated PH include a host of different agents to elicit pathologies such as inflammation, pulmonary artery remodelling, lung fibrosis and emphysema.

In this protocol, the V/Q study was started 2 hours after drug *i.p*. administration. First, the rats were tracheally intubated through the oral cavity after anesthetization with ketamine and xylazine (90 and 6 mg/kg, respectively). The animals were then ventilated (20 mL/min, 125 strokes/min) on a rodent ventilator (model 683; Harvard Apparatus) with diethylene-triamine-pentaacetate DTPA-$Tc99^{m}$) (Molipharma, Valencia, Spain) (10 mCi) for 15 minutes. After DTPA-$Tc99^{m}$ delivery, the animals were removed from the ventilator and allowed to breathe freely. SPECT scans were acquired on an ALBIRA micro-CT-PET-SPECT system (Oncovision®) using pinhole collimators and a radius of rotation of 3.5 cm. After the ventilation SPECT scan, rats were injected with 0.5–1 mCi of MAA-$Tc99^{m}$ via the tail vein. Perfusion imaging entailed a SPECT scan.

The relationship between ventilation and perfusion data was determined with PMOD™ software analyzing the intensity of radiation (arbitrary units) of each volume of interest (VOI) of the whole lung region selected of 256 image sections for each animal study corrected by the maximal activity. Corrected radiation intensities of ventilation (V) and perfusion (Q) studies were represented.

2.3. Cardiovascular remodelling

2.3.1. Right Ventricular Hypertrophy

After the hemodynamic measurements, animals were sacrificed by overdose of anesthesia. The hearts were then excised and the RV was carefully dissected. Next, both RV and the left ventricle plus septum (LV+S) were weighed. The ratio RV/BW and the Fulton Index [RV/(LV+S)] were calculated to assess the right ventricular hypertrophy.

2.3.2. Lung histology

The right lung was inflated in situ with 5 mL of 4% paraformaldehyde (PFA) saline solution through the right bronchus, removed, introduced in PFA and embedded in paraffin. Lung sections were stained with haematoxylin and eosin technique and examined by light microscopy, and elastin was visualized by its green autofluorescence. Briefly, hematoxilin is a dark blue or violet dye (basic/positively charged) that binds to basophilic substances (acid and negatively charged, such nucleic acid; DNA in chromatin) while eosin, is a red or pink dye (acid/negative charged) that binds to acidophilic substances as positively charged proteins in the cytoplasm. Small arteries (25–100 μm outer diameters) were analyzed in a blinded fashion and categorized as muscular, partially muscular or nonmuscular (Meyrick et al., 1978). Briefly, the outside diameter (external elastic lamina) and inside diameter (internal elastic lamina) of PA were measured using ImageJ (Ver 1.41, NIH, Bethesda, MD, USA). Five or six vessels with an external diameter ranging from 25 to 75 μm were analyzed from each animal. The medial wall thickness (calculated as external elastic lamina diameter minus the internal lamina diameter), the cross-sectional medial wall area and the total cross-sectional area were calculated. In order to quantify vascular remodelling the following two indices were used: percentage medial wall thickness (medial wall thickness/internal diameter × 100) and percentage medial wall area (cross-sectional medial wall area/total cross-sectional area × 100) (Moral-Sanz et al, 2012).

3. IN VITRO studies

For the *in vitro* procedures, animals were sacrificed by decapitation under general anesthesia with a mixture of ketamine/xylazine (80 mg/8 mg/kg, *i.p*.).

3.1. Tissue isolation

Each tissue was processed on different way according to the technic that was to be used. In the following sections of material and methods are described in details treatments and solutions used in the development of each experiment performed with these tissues.

3.1.1. Rat vessel isolation

After animal sacrifice, the left lung and mesenteric plexus were removed and immediately immersed and washed in Krebs solution containing (in mmol/L): NaCl 118, KCl 4.75, $CaCl_2$ 2.0, $MgSO_4$ 1.2 , $NaHCO_3$ 25, KH_2PO_4 1.2 and glucose 11. This solution was filtered through a filter of 0.2 μm pore.

Left lung and mesenteric plexus were dissected to isolate the intrapulmonary arteries (rPA) and mesenteric arteries (rMA) respectively. rPA and rMA rings (2-3 mm length and approximately 0.5-0.8 mm of internal diameter) were carefully dissected in Krebs solution.

3.1.2. Human vessel isolation

Human Pulmonary arteries (hPA) were isolated from human lung tissue obtained from subjects undergoing lung carcinoma surgery, after informed consent, in the Hospital Universitario de Getafe (Madrid, Spain) (Dr. José Ángel Lorente) and from Hospital Universitario de Valencia (Dr Julio Cortijo) (Figure 15).

Human lung tissue was obtained from 33 patients (20 men, 6 women and 7 N/A, mean age 66.96±2.1 years) undergoing lobectomy or pneumonectomy during resection of lung carcinoma.

hPA rings (2-3 mm length y and approximately 0.5-0.8 mm of internal diameter) were carefully dissected in Krebs solution containing (in mmol/L): NaCl 118, KCl 4.75, $CaCl_2$ 2.0, $MgSO_4$ 1.2, $NaHCO_3$ 25, KH_2PO_4 1.2 and glucose 11. This solution was filtered through a filter of 0.2 µm pore.

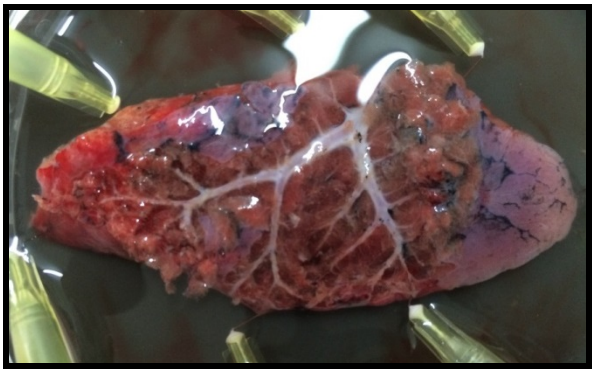

Figure 15: Arterial tree image from human lung section obtained from subjects undergoing lung carcinoma surgery.

3.2. Cell culture

All cell culture experiments were performed under sterile conditions using a laminar flow cabinet Cruma 870FL. Cell cultures were maintained in a humidified incubator (CO_2 Memmet), maintaining a 99% of humidity, a temperature of 37°C and a continuous supply of 5% CO_2 and 95% O_2.

3.2.1. Rat Pulmonary Artery Smooth Muscle Cell and Rat Pulmonary Fibroblast Culture

Rat pulmonary artery smooth muscle cell (rPASMCs) and rat pulmonary fibroblast primary cell cultures were used in this study. Briefly, rPASMCs and fibroblast were isolated from rPA (approximately 0.5-0.8 mm of internal diameter) derived from MCT-PAH induced rat model (21 days after administration of MCT *i.p.*) and control male rats. rPA were dissected in a Ca^{2+} free PSS containing (in mmol/L): NaCl 130, KCl 5, $MgCl_2$ 1.2, glucose 10 and HEPES 10 (pH 7.3 adjusted wth NaOH). The adventitia was carefully dissected, and used to obtain fibroblast culture. For rPASMC, adventitia and endothelium were removed and rPAs were cut longitudinally and digested into an enzymatic solution containing (in mg/mL): collagenase 1.125, elastase 0.1, albumin 1 for 4 minutes at 4°C followed by 1 minute at 37°C. Following digestion, tissues were

washed in Ca^{2+} -free PSS three times and followed for three further washes with Dulbecco´s modified Eagle´s medium (DMEM) containing 20 % (v/v) heat-inactivated foetal bovine serum (FBS), pyruvate (1.1 mg/mL), 1% non-essential amino acids, streptomycin (100 mg/mL), penicillin (100 U/mL) and amphotericin B (250 ng/mL). Explants of adventitia and digested rPAs were placed onto 35 mm petri dishes and incubated in a humidified atmosphere of 5% CO_2 in air at 37°C in DMEM 20% (v/v) FBS. The rPASMCs and fibroblast start to migrate from the tissue fragments within 2-5 days. After 1 week, when the cells reach 80-90% confluence close to the explant, cells were trypsinized (trypsin-EDTA solution 1% (v/v) in Hank´s solution, Sigma-Aldrich) for 1 minute at 37°C into the incubator. The rPASMCs and fibroblasts were harvested and re-suspended in DMEM medium to neutralize the trypsin effect. Following, cells suspension were centrifuged at 1500 rpm for 10 minutes and the cell suspension was subcultured in 75 cm^2 sterile flask in DMEM supplemented with 10% FBS. rPASMCs and fibroblasts were used within passages 2-3. Cell phenotype was determined in preliminary experiments by cell shape and for rPASMC by immunocytochemistry using primary antibodies against α-actin and secondary fluorescent-labeled (FITC) antibodies and visualized under a fluorescent microscope.

3.2.2. Human Pulmonary Artery Smooth Muscle Cell Culture

Human pulmonary artery smooth muscle cells (hPASMCs) primary cell cultures were used in this study. Briefly, hPASMCs were isolated from hPA (approximately 0.5-0.8 mm of internal diameter) derived from 11 non-PAH patients (7 men, 1 women and 3 N/A, mean age 72.62±1.47 years) undergoing lung carcinoma surgery as described above. hPA were dissected in a in Krebs solution containing (in mmol/L): NaCl 118, KCl 4.75, $CaCl_2$ 2.0, $MgSO_4$ 1.2 , $NaHCO_3$ 25, KH_2PO_4 1.2 and glucose 11. This solution was filtered through a filter of 0.2 µm pore. After carefully dissection of the adventitia, vessels were cut longitudinally and endothelium was removed. Explants of these arteries were placed in a 75 cm^2 culture flasks and maintained in Smooth Muscle Cell Growth Medium supplemented with Smooth Muscle Cell Growth Supplement (Cell Applications, Inc). The hPASMCs start to migrate from the tissue fragments within 5-7 days. After 2 weeks, when the cells reach 80-90% confluence close to the explant, cells were trypsinized (trypsin-EDTA solution 1% (v/v) in Hank´s solution, Sigma-Aldrich) for

1 minute at 37°C into the incubator. The hPASMCs were harvested and re-suspended in Smooth Muscle Cell Growth Medium to neutralize the trypsin effect. Then, cell suspension was centrifuged at 1500 rpm for 10 minutes and subcultured in 75 cm^2 sterile flask in Smooth Muscle Cell Growth Medium. hPASMCs were used within passages 2-3.

3.3. Vascular reactivity

Intrapulmonary artery rings (2–3 mm long, 0.5–0.8 mm internal diameter) were dissected from human or rat lung tissue, and mesenteric arteries rings (2–3 mm long, 0.5–0.8 mm internal diameter) were dissected from rat mesenteric beds.

3.3.1. Vasodilator effects of different drugs in arterial rigns contracted with a cocktail of ET-1, U46619 and 5-HT

To analyse the vasodilator effects of the different drugs *in vitro*, preparations were mounted in a wire myograph (model 610M or 620M, Danish Myo Technology, Aarhus, Denmark) in Krebs buffer solution, maintained at 37°C and continuously bubbled the chamber with 95% O_2 and 5% CO_2 (oxygen) or 95% N_2 and 5% CO_2 (hypoxia), yielding approx. 2-4% O_2 in the buffer, due to contact with room air (Cogolludo et al., 2009). The wire myograph is attached on a digital system to recorder the vessel tension. (PowerLab, ADINSTRUMENTS)

After equilibration period of 30 minutes, arterial rings were firstly stimulated with KCl (80 mmol/L) to obtain the maximum contraction of the vessel. Thereafter, preparations were washed three times and after an equilibration period of 20 minutes, arterial rings were contracted with 5-HT ($1x10^{-5}$ M) for 10 minutes, and when a plateau was reached, a single concentration of acetylcholine (Ach) ($1x10^{-6}$ M) was added to analyse the endothelium-dependent vasodilatation and washed three times again. After other equilibration period of 20 minutes, arterial rings were contracted with a cocktail of pulmonary vasoconstrictors: ET-1 ($3x10^{-9}$M), the thromboxane A_2 mimetic U46619 ($3x10^{-8}$ M) and 5-HT ($3x10^{-6}$ M) for 20 minutes. Following this, when a plateau was reached, the different drugs were added in a cumulative fashion (Figure 16). The

vasodilator effect induced by the each drug is normalized (%) with respect to the initial precontraction with the cocktail of vasoconstrictors.

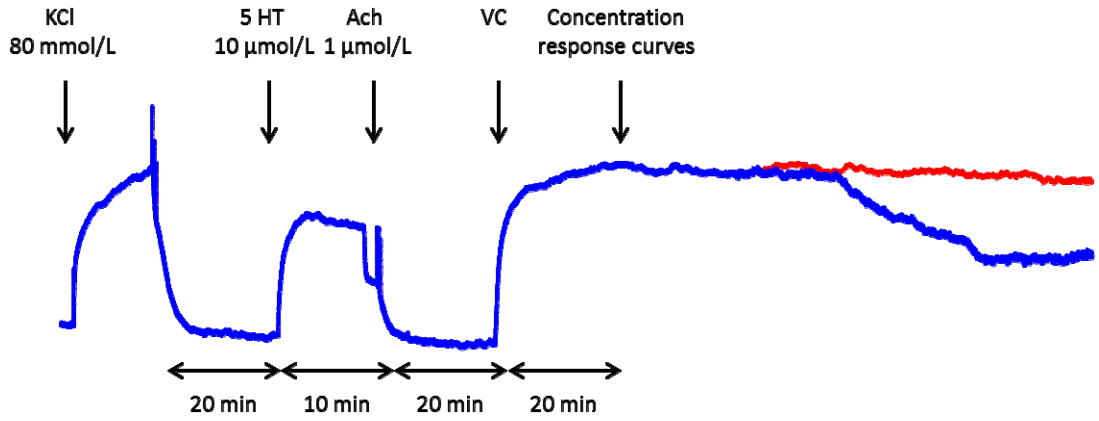

Figure 16: Representative traces of the protocol used to analyze the vasodilator effect of the different drugs used in this thesis*. Vehicle trace is represented as a red line and drug tested as a blue line.*

3.3.2. Endothelium dependent relaxation and serotonin response

In other set of experiments intrapulmonary artery rings (2–3 mm long, ~0.5–0.8 mm internal diameter) were dissected from the four animal groups (Ctrol, Querc, MCT and MCT-Quer) and mounted in Krebs solution bubbled with 21%O_2 and 5% CO_2 under 0.75 g of resting tension in in a wire myograph (Cogolludo et al., 2007). After equilibration, arterial rings from the four animal groups were firstly stimulated with KCl (80 mmol/L). Thereafter, preparations were washed and after 45 minutes were contracted by phenylephrine ($1x10^{-7}$ M), and concentration–response curves to Ach (10^{-9}-$3×10^{-4}$ M) were performed by cumulative addition. In different rings a concentration–response curves to 5-HT ($3×10^{-8}$-10^{-4} M) were performed by cumulative addition.

To analyze the effects of quercetin on vascular tone, pulmonary arterial rings were mounted in Krebs solution bubbled with 21%O_2 and 5% CO_2 (normoxia) or 95% N_2 and 5% CO_2 (hypoxia) in a wire myograph (Cogolludo et al., 2007) and contracted with U46619 (10^{-7} M). Following, when a plateau was reached, quercetin was added in a cumulative fashion.

3.3.3. Hypoxia and U46619 inhibition

To analyze the effects of the different drugs *in vitro*, preparations were mounted in a wire myograph in Krebs buffer solution maintained at 37°C bubbling the chamber with 21% O_2, 74%N_2 and 5% CO_2 (Cogolludo et al., 2007). After equilibration, arterial rings were first stimulated with KCl (80 mmol/L) and then every vessel was exposed to hypoxia for 15 minutes (by bubbling the chamber with 95 % N_2 and 5% CO_2, yielding approx. 2-4% O_2, in the buffer due to contact with room air (Cogolludo et al., 2009)), with a 5 minutes recovering period of normoxia. Thereafter, preparations were washed three times and after an equilibration period of 30 minutes, the arterial rings were treated with vehicle (DMSO) or drugs and exposed again to hypoxia for 15 minutes and followed by other recovering period of normoxia for 5 minutes. Thereafter, preparations were washed three times and after another equilibration period of 30 minutes, finally, arterial rings were contracted with the thromboxane A_2 mimetic U46619 ($1x10^{-7}$ M) for 15 minutes.

3.4. Pulmonary and oxygen selectivity

The drug concentration that induced a 50% of relaxation from the basal level (IC_{50}), was calculated from the adjustment of the concentration-response curve on each experiment. With this value, we calculated the pulmonary selectivity (PS) of each drug defined as the ratio of IC_{50} values in MA and the IC_{50} values in PA both under oxygen conditions. On the other hand, the oxygen selectivity (OS) was defined as the ratio of IC_{50} values in PH under hypoxia and the IC_{50} values in PH under oxygen**.**

3.5. Cell Viability and Cell Proliferation

3.5.1. Treatments

rPASMC, rPASMCs derived from MCT-PAH induced rat model and hPASMCs, were seeded at 30.000 cell/mL (approximately 50% confluence) in 96 well plates, the

following day cells were growth arrested by an exposure for 24 hours to 0.1% (v/v) FBS medium in order to maintain cells quiescent and synchronise cell cycle. Following, PASMCs were then exposed to different drugs (Table 3) or vehicle (0.1% DMSO) in DMEM (rPAMCs and rPASMCs-MCT) or Smooth Muscle Cell Growth Medium (hPASMCs) containing 1% (v/v) FBS plus a mixture of 5-HT ($3x10^{-6}$ M), the thromboxane A_2 mimetic U46619 ($3x10^{-8}$ M) and ET-1 ($3x10^{-9}$ M) for 48 hours. Each experimental condition was performed at least in triplicate.

In other set of experiments, rPASMCs and fibroblasts derived from MCT-PH induced rat model (21 days after administration of MCT *i.p.*) and control male rats were seeded at 30.000 cell/mL (approximately 50% confluence) in 96 well plates, the following day cells were growth arrested by an exposure for 24 hours in 0.1% (v/v) FBS medium to maintained cell quiescent and synchronise cell cycle. Then, cells were exposed to different drugs or vehicle (0.1% DMSO) in DMEM (rPAMCs and fibroblasts) containing 10% (v/v) FBS for 24 and 48 hours. Each experimental condition was performed at least in triplicate.

3.5.2. Cell viability

Cell viability was assessed by the MTT assay (Sigma-Aldrich). It is a colorimetric assay that measure the cell viability and proliferation of cells by reduction of the yellow tretrazolium ((3-(4,5-dimethyltiazol 2-yl)-2,5-diphenyltetrazolium bromide) by metabolically active cells, by the action of NADPH-dependent cellular oxidoreductase enzymes, to generate purple formazan, that can be solubilized and quantified. Briefly, 100 µL of (1mg/mL) MTT solution prepared in cell culture medium was added to each well (except for the blank control wells). After 30 minutes of incubation period (rPASMCs, rPASMCs-MCT and fibroblasts) or 1 hour (hPASMCs), the content of each well was removed by aspiration and replaced by 50 µL of solubilization solution (100 % DMSO) to dissolve the purple formazan product and subsequently incubated at 37°C for 5 minutes in the dark. The amount of formazan product (presumably directly related to the number of viable cells) is measured by recording the absorbance of each well using a plate reader (EZ Read 400 Microplate Reader, Biochrom) at a wavelength

of 540 nm. Data were expressed as percentage relative to values of time 0 or to the vehicle.

3.5.3. Cell proliferation

Cell proliferation was measured by incorporation of the thymidine analog BrdU (5-bromo-2'-deoxyuridine) into newly synthesized DNA during cell proliferation and its subsequent detection according to the manufacturer's protocol (Roche Applied Science). Briefly, cells (rPASMCs, rPASMCs-MCT and hPASMCs) were labeled with a 10 μM BrdU solution, prepared in cell culture medium, in the last 6 hour of the experiment time or during the first 24 hours of treatment. Following this, the content of the well plate was removed by aspiration and, cells were fixed using FixDenat solution for 30 minutes. This solution acts to fix, permeabilize and denature the DNA of the cells to improve the accessibility of the incorporated BrdU to the detection antibody. After that period, the content of the well plate was removed by inversion and 100 μL of anti-BrdU antibody (mouse monoclonal antibody, clone BMG 6H8, fragment Fab, conjugated with peroxidase) was added in each well at room temperature for 90 minutes. Each well was washed 3 times with 150 μL washing solution (PBS 1x). After the last wash, 100 μL of Substrate solution (TMB, tetramethylbenzidine) was added to each well and incubated at room temperature for 30 minutes in the dark. We added such as stop solution a solution of 1M H_2SO_4 to each well and incubated for 1 minute on a shaker. The absorbance was measured using a spectrophotometric plate reader (EZ Read 400 Microplate Reader, Biochrom) at dual wavelength of 450-620 nm. The magnitude of the absorbance for the developed color is proportional to the quantity of BrdU incorporated into cells, which is a direct indication of cell proliferation Results were normalized (%) with regarding to the vehicle.

3.5.4. Nuclear morphology analysis-Hoechst 33258/PI

Analysis of nuclear morphology was assessed on rPASMCs using chambers with 8 wells attached to a specially treated standard glass microscope slide (Lab-Tek® II Chamber Slide System ™ 154534, Thermo Scientific) after 24 or 48 hours of treatment, using the same number of cells used in the MTT and BrdU assay. Briefly, after removal the

culture medium and washing three times with HEPES solution warmed at 37°C, cells were incubated at 37°C for 40 minutes in an humidified incubator with a solution containing the nucleic acid dye Hoechst 33258 (4 µg/mL) and propidium iodide (PI, (20 µg/mL) prepared in HEPES solution. The blue fluorescent dye Hoechst 33258 is a cell permeable nucleic acid stain with binding selectivity for adenine-thymine rich regions in the minor groove of the double strand of DNA. Consequently, it stains DNA, chromosomes and nuclei of viable and non-viable cells. The red-fluorescent PI dye does not permeate through intact cell membranes; it only stains apoptotic or necrotic cells. PI binds to DNA by intercalation between the bases with little or no sequence preference. After the incubation period, chambers were washed 3 times with HEPES solution and cells were observed under the fluorescence microscope using 355/460 nm and 530/620 nm excitation/emission filters for Hoechst 33258 and PI, respectively (Perez-Vizcaino F, 2006).

Table 3: List of drugs tested in this thesis.

Chemical classes	Drug	Mechanism
NO donors	Sodium nitroprusside (SNP)	NO donors
	S-Nitroso-N-acetyl-DL-penicillamine (SNAP)	NO donors
	Diethylamine NONOate sodium salt hydrate (DEA NONOate)	NO donors
	Formaldoxime	NO donors
	Acetohydroxamic acid	NO donors
sGC stimulators	YC-1	sGC stimulators
	BAY-41-2272	sGC stimulators

	Riociguat	sGC stimulators
PDE inhibitors	Sildenafil	PDE5 inhibitor
	Tadalafil	PDE5 inhibitor
	Dipyridamol	PDE5 inhibitor
Kinase Inhibitors	Imatinib	Tyrosine-kinase inhibitor
	5z-7-oxozeaenol	TAK-1 Inhibitor
	Hydroxyfasudil	ROCK1/2 inhibitor
	Quercetin	Flavonoid, pan-inhibitor of MAPKs and the TGF-β pathway
Ion Channels	Nifedipine	Voltage-dependent Ca^{2+} channel blocker
	Flupirtine	Kv7 channel agonist
	Retigabine	Kv7 channel agonist
	Pinacidil	ATP-sensitive potassium channels activator
PPAR agonist	GW0742	PPARβ/δ agonist
	L165041	PPARβ/δ agonist
	Rosiglitazone	PPARγ agonist
Adenylate cyclase	Treprostinil	Prostacyclin analog

activators		
	Forskolin	Adenylate cyclase activator
Others	Tacrolimus	Calcineurin inhibitor
	2 Me-SADP	Purinergic $P2Y_1$ receptor agonist
	Levosimendan	Calcium sensitizer

4. Protein expression

4.1. Protein Extraction and Preparation

Whole Lung and PA were homogenized using a lysis buffer containing Trizma® Pre-set crystals pH 7.5 (Sigma-Aldrich), DL-dithiothreitol (DTT) 1M (Sigma-Aldrich), the surfactant agent NP40 1% (v/v) (Roche Diagnostics GmbH, Alemania) and supplemented with protease (Protease inhibitor cocktail tablets, Roche Diagnostics GmbH, Alemania) and phosphatase inhibitors (PhosSTOP, Roche Diagnostics GmbH, Alemania). Lysis buffer allows proteins to be released and solubilized from the tissue. The protease inhibitors prevent proteolysis, dephosphorylation and denaturation of the protein sample. Sample homogenates were then maintained at 4°C for 30 minutes to allow disassociation of proteins. Then, samples were centrifuged at 4°C for 10 minutes at 10.000 rpm. After centrifugation, the supernatant was transferred into a new eppendorf and stored in a freezer at –80°C.

4.2. Total protein determination (Lowry Method)

To determine total protein concentration (whole lung or PA), a colorimetric assay based on the Lowry method (BioRad) was used. The assay is based on the reaction of protein with an alkaline copper tartrate solution and Folin reagent. As with the Lowry assay, there are 2 steps which lead to color development: the reaction between

protein and copper at alkaline pH, and the subsequent reduction of Folin reagent by the copper-treated protein. Color development is primarily due to the amino acids tyrosine and tryptophan, and to a lesser extent cystine, cysteine, and histidine present in the proteins. These amino acids reduce the Folin reagent, yielding several possible reduced species that have a characteristic blue color.

The sample protein concentration was evaluated by comparison against a range of bovine serum albumin (BSA) standards (0 – 0.8 mg/mL BSA solution diluted in double distilled H_2O (dH_2O) and lysis buffer). Briefly, 20 µL of each concentration of BSA solution (in triplicate) and simple dilution (in duplicate) were added into a 96 well plate. Assay solution was prepared by adding 1 mL of reagent A (alkaline solution of copper tartrate, Bio-Rad, USA) and 25 µL of reagent S (surfactant solution, Bio-Rad, USA). Thereafter, 20 µL of this solution and 160 µL of reagent B (reagent folin diluted, Bio-Rad, USA) were added to each well. The plate was then maintained for 15 minutes in the dark at room temperature and then read at 750 nm using a plate reader (EZ Read 400 Microplate Reader, Biochrom).

4.3. Sodium Dodecyl Sulphate Polyacrylamide Gel Electrophoresis

Protein samples were separated according to their molecular weight using a Sodium Dodecyl Sulphate Polyacrylamide Gel Electrophoresis (SDS-PAGE). Protein samples (10 µg) were then denatured and reduced by heating at 99°C for 5 minutes. This process is necessary to unfold the tridimensional conformation of the proteins and allow the antibody recognition. The sodium dodecyl sulphate (SDS) of the sample buffer binds to the protein and negatively charges the protein, allowing separate the protein accordingly to their size.

Samples were loaded into a mini-gels system (Bio-Rad, USA) of acrylamide/bisacrilamide (10%-15%, accordingly the molecular weight of the protein). Following the Laemli method with a protein molecular weight standard of mixture of ten multicolored recombinant proteins (10–250 kD) (Precision Plus Protein

Kaleidoscope Standards, Bio-Rad, USA). The protein standard allowed the observation of the electrophoresis progression and determination of protein size.

Samples were separated at 90 Volts at room temperature until adequate migration and separation of protein samples. For the electrophoresis process was used a Tank Buffer solution containing 0.3% (w/v) Tris (Trizma base minimum), 0.144 % (w/v) Glicine and 0.1% (v/v) SDS in dH_2O.

4.4. Protein Transfer and visualitation

After electrophoresis, proteins were transferred onto a polyvinylidene fluoride microporous membrane (PVDF) (Immun-Blot PVDF, Bio-Rad) using a wet transfer method. To activate de PVDF membrane, it was submerged in 100% methanol for several seconds and kept in a Transfer buffer solution containing 0.3% (w/v) Tris (Trizma base minimum), 0.144 % (w/v) Glicine, 0.1% (v/v) SDS and 20 % (v/v) methanol in dH_2O.

The transfer process was run for 2 hours at 400 mA on ice. To check the successful transfer process, the membrane was immersed in 0.1% (w/v) Ponceau red and in 1% (v/v) acetic acid solution to visualize protein bands on the membrane and to allow the right fixation of the proteins on the membrane.

Before antibody detection with the right antibody, the membranes were rinsed in tween tris buffer saline (TTBS) buffer solution containing NaCl 0.5M, Tris 0.02M (pH 7.5), 0.1% (v/v) Tween 20 in dH_2O twice for 5 minutes to remove the excess of Ponceau solution. Then, the membranes were blocked with a Blocking Buffer solution containing 5% (w/v) non-fat milk or 5% (w/v) BSA in TTBS solution to prevent the nonspecific binding of primary and secondary antibodies. Then, the membranes were incubated on a shaker for 1 hour at room temperature.

4.5. Immunoblotting

For specific protein analysis, membranes were incubated overnight on a shaker at 4°C. The next day, the membranes were then washed in TTBS (4x10 minutes) to remove the excess of unbound primary antibody. Then, the membranes were incubated for 1 hour

on a shaker at room temperature with the appropriate secondary antibody conjugated with horseradish peroxidase (HRP) diluted in 1% (w/v) nonfat milk or 1% (w/v) BSA in TTBS. Afterwards; the membranes were washed in TTBS (4x10 minutes) and finally washed with TBS solution containing NaCl 0.5M, Tris 0.02M (pH 7.5) in dH_2O. The specific bands of each protein were detected by enhanced chemiluminescence (ECL, Amersham Pharmacia Biotech, UK or SuperSignal West Femto Chemiluminescent Substrate, Thermo Scientific, USA). Quantification of protein expression was carried out by densitometry analysis using Quantity One software (Bio-Rad Laboratories).

Membranes were then washed in TTBS for 10 minutes before the stripping process. This process allows the removal of the primary and secondary antibodies used before without causing a significant loss of antigen released from the membrane. This process uses a combination of a detergent, a reducing agent and heat. Briefly, we carried out a harsh striping using a striping solution containing 4% (v/v) SDS, Tris-HCl 125 mmol/L (pH 6.7) and 1.56 % (v/v) β-mercaptoethanol. The membranes were kept deep in the striping solution at 50°C for 30 minutes in a water bath. Afterwards, membranes were then washed in TTBS (2x15 minutes) and re-probed with other specific antibodies. The values of each experimental protein were corrected with the housekeeping protein β-actin and for phosphorylated proteins values obtained with the antibody against the phosphorylated protein were normalized by the total protein. All values were expressed as a percentage of the control samples.

The primary and secondary antibodies used are listed below (Tables 4 and 5, respectively).

Table 4: Information of the Primary antibodies used for immunoblotting

Primary antibody	Protein	Specie	Supplier	Reference	Dilution
Anti-β-actin	β-actin (clon AC-15)	Mouse	Sigma-Aldrich	A1978	1:5.000
Anti-survivin	survivin	Mouse	Santa-Cruz	Sc-17779	1:200
Anti-total Akt	Akt	Rabbit	Cell Signalling	#9272	1:1000
Anti-p-Akt	Phospho-Akt (ser 473)	Rabbit	Cell Signalling	#9271S	1:1000
Anti-total Erk 1/2	Erk (42/44)	Rabbit	Cell Signalling	#9102	1:1000
Anti-p-Erk 1/2	Phospho-Erk (42/44)	Rabbit	Cell Signalling	#3510S	1:1000
Anti-S6	S6 Ribosomal Protein (5G10)	Rabbit	Cell Signalling	#2217	1:1000
Anti-pS6 235-236	Phospho-S6 Ribosomal Protein (ser 235/236)	Rabbit	Cell Signalling	#2211	1:1000
Anti-pS6 240-244	Phospho-S6 Ribosomal Protein (ser 240/244)	Rabbit	Cell Signalling	#2215	1:1000
Anti-p38	p38	Rabbit	Cell Signalling	#9212	1:1000
Anti-p-p38	Phospho-p38 (Thr 180/Tyr 182)	Rabbit	Santa-Cruz	Sc-17852-R	1:1000

Table 5: Information of the Secondary antibodies used for immunoblotting (WB)

Secondary antibodies	Specie	Supplier	Reference	Dilution
Anti-mouse-HRP	Goat	Calbiochem	401215	1:10.000
Anti-rabbit-HRP	Goat	Calbiochem	401315	1:10.000

5. Analysis of RNA expression

RNA expression was analyzed using quantitative real time-polymerase chain reaction (qRT-PCR).

5.1. RNA extraction

For RNA, whole lung lobes or PAs derived from these lungs lobes were isolated. Upon dissection, tissue was immediately snap-frozen in liquid nitrogen and stored at –80 °C. Extraction and purification of RNA was performed using the RNeasy Fibrous Tissue Mini Kit according to the manufacturer's protocol (Qiagen, Hilden, Germany). Briefly, sample homogenate with homogenization buffer was centrifuged at 10.000 rpm for 3 minutes. The sample supernatant was then mixed by pipetting with the same volume of 70% ethanol to allow the precipitation the RNA. The RNA is captured in the column supplied by the kit according to the manufacturer's protocol. To remove any residual genomic DNA DNase I was added for 15 minutes at room temperature. Finally, RNA was eluted from the column by adding 30 µL of sodium citrate (pH 6.4) pipetted directly on the membrane column for 2 minutes, and then each column was centrifuged and the residue added again on the membrane the RNA eluted. RNA eluted was immediately stored at –80°C. The concentration and quality of RNA isolated was measured using a NanoDrop 1000 spectrophotometer (Thermo scientific, USA) at a wavelength of 260 nm.

5.2. Reverse Transcription

For the mRNA analysis, the complementary DNA (cDNA) derived from rat whole lungs and PAs was obtained by reverse transcription (RT) of 300 ng of RNA, according to the manufacturer's protocol of the iScript cDNA synthesis kit (BioRad, Hemel Hempstead, UK). Each reaction contain 1x iScript reaction mix, iScript reverse transcriptase, 300 ng of total RNA and RNase free H_2O.

Then, 30 µL of the reaction were prepared in a 0.2 mL Eppendorf tube. RT was performed using the Thermociclator (MJ Mini personal thermal cycler, Bio-Rad, Hemel

Hempstead, UK) with the following steps: 25°C for 5 minutes, 42°C for 30 minutes, 85°C for 5 minutes and then maintained at 4°C. The cDNA was stored –20 °C.

5.3. Quantitative Real Time Polymerase Chain Reaction analysis.

The cDNA samples were amplified by qRT-PCR using a Taqman ® system (TaqMan PCR Master mix, Applied biosystems) in the Genomic Unit of Universidad Complutense de Madrid using a "7.900HT Fast Real-time CR System". Briefly, for mRNA expression, 10 µl of reaction mix were incubated in a 384 well plate following the cycle conditions: 95°C for 10 minutes, followed by 40 cycles of 95°C for 15 seconds and 60°C for 1 minute. Details of the primers used are shown in Tables 6 and 7.

Each sample was performed in triplicate and data were corrected by the relative expression of the housekeeping β-actin and expressed as relative expression of target genes in control animals using the delta-delta Ct method (RQ).

Table 6: Sequences designed of primers used in this thesis.

Primers Designed			
Gen	**Protein**	**Primer Forward 5´- 3´**	**Primer Reverse 5´- 3´**
Actb	β-Actin	5´-GCCCTAGACTTCGAGCAAGA-3´	5´-TCAGGCAGCTCATAGCTCTTC-3´
Kcna5	Kv1.5	5´-GGAAGAACAAGGCAACCAGA-3´	5´-AGCTGACCTTCCGTTGACC-3´
Nos2	iNOS	5'-TTGGAGTTCACCCAGTTGTG-3'	5'-ACATCGAAGCGGCCATAG-3'
Nos3	eNOS	5'-GGTATTTGATGCTCGGGACT-3'	5'-TGTGGTTACAGATGTAGGTGAACA-3'
Cav1	Caveolin-1	5'-GGGCATGAAGGCAGGTTAT –3'	5'-AGTGAGGACAGCAACCAACTC –3'
Bmpr2	BMPR2	5'-CGGGCAGGATAAATCAGGA-3'	5'-CAGGAAAGTAAATTCGGGTGA-3'
Htr2a	5 HT_{2A}	5'-CTGCTCAATGTGTTTGTCTGG-3'	5'-AACAACGTATATACCAGTGGATTGA-3'

Table 7: List of Taqman assays used in this thesis.

Gen	Protein	Taqman Assay
Birc5	Survivin	Rn00574012_m1
Kcnb1	Kv2.1	Rn00755102_m1
Kcnq1	Kv7.1	Rn00583376_m1
Ncnq5	Kv7.5	Rn015112013_m1

6. Electrophysiological recording of Kv currents

The patch-clamp technique allows the high fidelity measurement of small scale ionic current. The rationale of this technique is based upon the formation of a high resistance (gigaohm) seal with the cell studied using a recording electrode or "patch pipette". Pipettes are pulled to a fine tip of approximately 1-4 µm from borosilicate glass capillary tubes. The "patch pipette" is filled with a filtered internal solution (0.2 µm pore) containing (in mmol/L): KCl 110, $MgCl_2$ 1.2, Na_2ATP 5, HEPES 10, EGTA 10, (adjusted to pH 7.3 using KOH). The pippete is sealed onto a patch on the surface of the cell membrane to keep the voltage constant while measuring the current flowing across the membrane of a cell or even form a single channel localized in the membrane patch. Several configurations of the patch-clamp technique have been developed. Potassium currents were recorded using the whole-cell configuration of the patch clamp technique. This technique allows study the response of all ion channels within the cell membrane. This configuration is obtained by applying negative pressure to the recording pipette after create the seal between the tip of the electrode and the cell membrane. This manipulation ruptures the path membrane inside the tip of the electrode, thereby making the intracellular space contiguous with the internal pipette solution and allowing the dialysis of the cell cytosol. The membrane of the whole cell is voltage clamped, and the recorded currents are a composite of the currents flowing through all the active channels.

6.1. Smooth Muscle Cell isolation

For smooth muscle cells isolation, endothelium-denuded PA were cut into small segments and placed in Ca^{2+} -free physiological salt solution containing (in mg/ml) 1 papain, 0.8 DTT and 0.7 albumin. Tissues were incubated in this solution at 4˚C for 10 minutes and then shaked for 7 minutes at 37˚C. Afterwards, tissues were washed in Ca^{2+} -free physiological salt solution and disaggregated using a wide bore smooth-tipped pipette. Cells were stored at 4˚C and used within 8 hours of isolation

6.2. Ionic current recording

A suspension of cells was placed on a 500 µL chamber mounted on the stage of an inverted microscope (Leica). After a period of 15 minutes to allow cells to settle in the bottom of the chamber, it is perfused with Ca^{2+}-free physiological saline solution (described above).

Currents were recorded using the whole-cell configuration of the patch-clamp technique by using an Axopatch 200B amplifier (Axon Instruments, Burlingame, CA, U.S.A). Experiments were performed at room temperature. Current recordings were low pass-filtered and sampled at 2 kHz with an analog-to-digital converter DigiData 1322A (Axon Instruments, Burlingame, CA, U.S.A) (data acquisition system). Command voltages and data storage were controlled with Clampex software (Molecular Devices). Patch electrodes were pulled from borosilicate glass capillaries (GD-1, Narishige Scientific Instruments, Tokio, Japan) with a DMZ Universal puller (Zeitz DMZ Puller, AutoMate Scientific). The cells were continuously perfused with the internal solution.

7. Reagents

All chemicals and reagents were supplied by Sigma-Aldrich (Madrid, España), except Riociguat (Chemexpress, Shangai, China), Retigabine (Axon, Groningen, The Netherlands), GW0742 (Tocris, Bristol, UK), Treprositinil and Imatinib (mesilate) (Cayman, Michigan, USA) and Rosiglitazone (Selleck Chemicals, Munich, Germany). Drugs were dissolved in DMSO and final vehicle concentrations were ≤ 0.1%.

8. Statistical analysis

Results are expressed as means ± standard error of the mean (SEM) of n measurements where n identifies the number of animals. Individual cumulative concentration-response curves were fitted to a logistic equation. For the concentration-response of vasodilators, the maximal responses (E_{max}) were expressed as percent of inhibition of the contraction induced by the mixture of vasoconstrictors (ET-1, U46619, 5-HT) and the pIC_{50} and pIC_{30} were defined as the negative $logIC_{50}$ (concentration of the drug that produces 50% inhibition of the contraction) and the negative $logIC_{30}$ (concentration of the drug that produces 30% inhibition of the contraction), respectively. Statistical analysis for vasodilatation studies were performed comparing drug-induced responses with PA oxygen using two-way analysis of variance (ANOVA) followed by Bonferroni post hoc test for rat arteries and unpaired Student's t-test for human arteries. For antiproliferative studies drug-induced responses were compared with vehicle using one-way ANOVA followed by Dunnett´s post hoc test.

Results derived from the MCT-induced PAH model were compared by one-way ANOVA followed by Bonferroni's post hoc test except for mortality which was assessed using a Kaplan-Meier analysis and for the PA muscularization study using a $\chi 2$ test. Current-voltage relations were analysed by two-way repeated-measures ANOVA with the Bonferroni post hoc test. A value of $P<0.05$ was considered statistically significant.

RESULTS

CHAPTER 1

1. Drug Screening

1.1. Vasodilatation studies.

The effects of vasodilators tested in this thesis were analyzed on the contraction induced by a mixture of vasoconstrictors (the thromboxane A_2 mimetic U46619, ET-1 and 5-HT) in mesenteric arteries, as a prototype of systemic vessels, and in PA under hypoxia (95% N_2-5%CO_2) or high oxygen (95% O_2-5%CO_2) conditions. The rationale for this protocol is that these three vasoconstrictors are the main vasoactive factors known to be involved in the pathogenesis of PH (Selej et al., 2015; Morrell el al., 2009; Christman et al., 1992) and that the possible differences in the potency or efficacy of the vasodilators may be influenced by the vasoconstrictor stimuli. First, we tested the vasoconstrictor responses induced by U46619 ($1x10^{-9}$ – $3x10^{-6}$ M) (Figure R1-A), ET-1 ($3x10^{-11}$ – $3x10^{-8}$ M) (Figure R1-B) and 5-HT ($3x10^{-8}$ – $1x10^{-4}$) (Figure R1-C) in a cumulative fashion. The maximal contractile responses reached by U46619, ET-1 and 5HT were 105.385 ± 5.385%, 118.222 ± 7.202% and 40.066 ± 7.202% of the initial response to KCl (80mM), respectively. In order to choose the final concentration of the vasoconstrictors in the mixture, we selected submaximal effective concentrations of each agent inducing ≈50% of its individual maximal response, which were $3x10^{-8}$ M for U46619, $3x10^{-9}$ M for ET-1 and $3x10^{-6}$ M for 5-HT, respectively (Figure R1-D). It should be noted that the contractile response induced by this pan-constrictor cocktail was higher than that induced by each vasoconstrictor separately and sustained along the duration of the experiment. After the contraction reached a steady-state, the vasodilators were added in accumulative fashion. The parameters derived from these concentration-response curves in rat and human arteries are shown in Table R1-2 respectively.

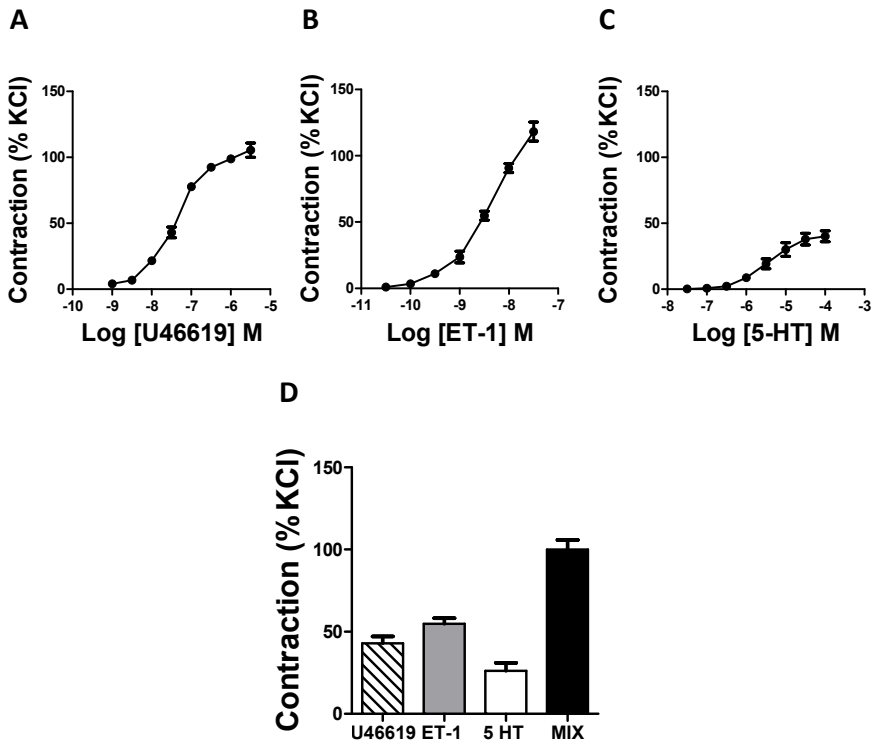

***Figure R1. Contractile responses induced by vasoconstrictors and the mixture**. Mean contractile responses to U46619 (A; n=2), ET-1 (B; n= 5) and 5-HT (C; n=13) in freshly isolated PA bubbled with 95% O_2-5% CO_2. Average values of the contractile responses induced by U46619 ($3x10^{-8}$ M), ET-1 ($3x10^{-9}$ M), 5-HT ($3x10^{-6}$ M) and the mixture of these submaximal effective concentrations (D). Data are expressed as a percentage of initial responses to KCl. Results are means ± SEM.*

1.1.1. Vasodilator effects of NO donors.

As shown in figure R2, we examined the effect of several chemical classes of NO donors in rat arteries pre-contracted with the mixture of vasoconstrictors. Addition of the NO donor sodium nitroprusside (SNP) (Figure R2-A), S-nitroso-N-acetylpenicillamine (SNAP) (Figure R2-B), diethylamine NONOate sodium salt hydrate (DEA-NO) (Figure R2-C), formaldoxime (Figure R2-D) and acetohydroxamic acid (Figure R2-E) induced a relaxant response in a concentration-dependent manner in all vessels with different potency (SNP> DEA-NO> SNAP> acetohydroxamic acid> formaldoxime).

SNP induced a similar relaxation in pulmonary arteries under high oxygen, pulmonary arteries under hypoxia and mesenteric arteries. DEA-NO and SNAP caused a more pronounced relaxant effect in mesenteric arteries than in pulmonary arteries. Again,

both compounds showed a similar effect in pulmonary arteries independently of the oxygen levels.

Formaldoxime and acetohydroxamic acid (Figure R2-D and E, respectively) produced a weak relaxant effect, which was stronger in mesenteric than in pulmonary arteries.

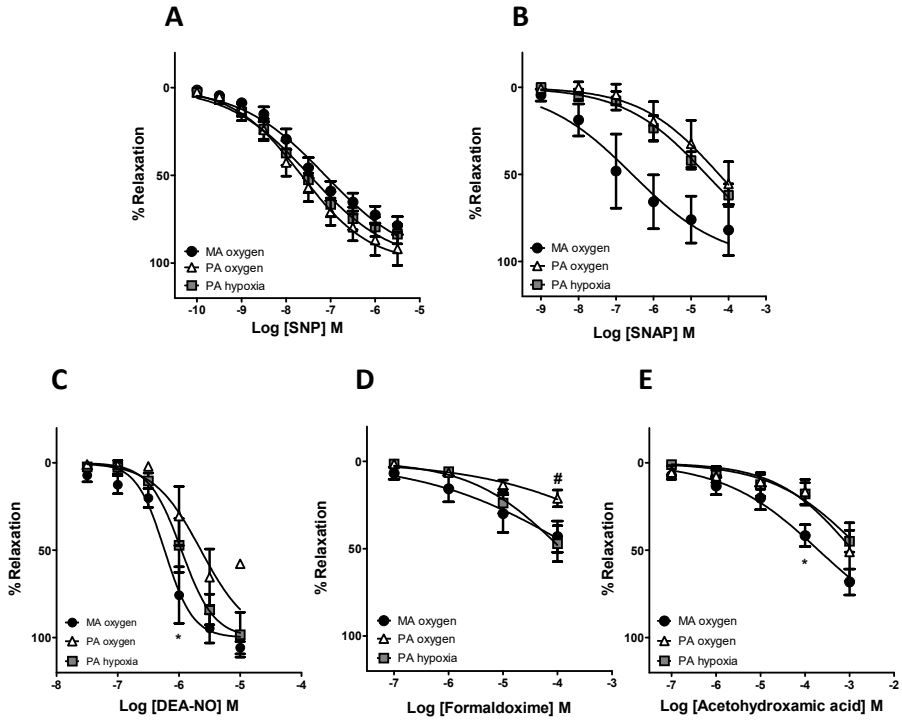

Figure R2. Effects of NO donors on vascular tone. *Concentration-dependent relaxation induced by the NO donors SNP (A; n= 7-9), SNAP (B; n=4), DEA-NO (C; n=3-5), formaldoxime (D; n=3-5) and acetohydroxamic acid (E; n=3) in rat mesenteric arteries (MA oxygen) and pulmonary arteries under high oxygen (PA oxygen) or hypoxic (PA hypoxia) conditions. Arteries were initially stimulated with a cocktail of U46619 ($3x10^{-8}$ M), 5-HT ($3x10^{-6}$ M) and ET-1 ($3x10^{-9}$ M). Results are means ± SEM. Drug-induced responses were compared with PA oxygen using two-way ANOVA followed by Bonferroni post hoc test. * indicates P<0.05 MA oxygen vs PA oxygen. # indicates P<0.05 PA hypoxia vs PA oxygen.*

1.1.2. Vasodilator effects of PDE5 inhibitors.

We examined the effect of different PDE5 inhibitors in rat arteries pre-contracted with the mixture of vasoconstrictors. Addition of the PDE5 inhibitors sildenafil and tadalafil, and the non-selective PDE inhibitor dipyridamole (Figure R3-A, B and C, respectively) caused a concentration-dependent relaxation in pulmonary and mesenteric arteries. All the three compounds caused a similar relaxation in pulmonary arteries under high

oxygen vs. hypoxic conditions. A higher efficacy of sildenafil and tadalafil was observed in mesenteric arteries when compared to pulmonary arteries, indicating an inverse pulmonary selectivity, while the response to dipyridamole was similar in the two vessels. The relaxant response of sildenafil was also examined in human pulmonary arteries (Figure R3-D). Sildenafil induced a concentration-dependent relaxation, which was more potent when pulmonary arteries were exposed to hypoxia.

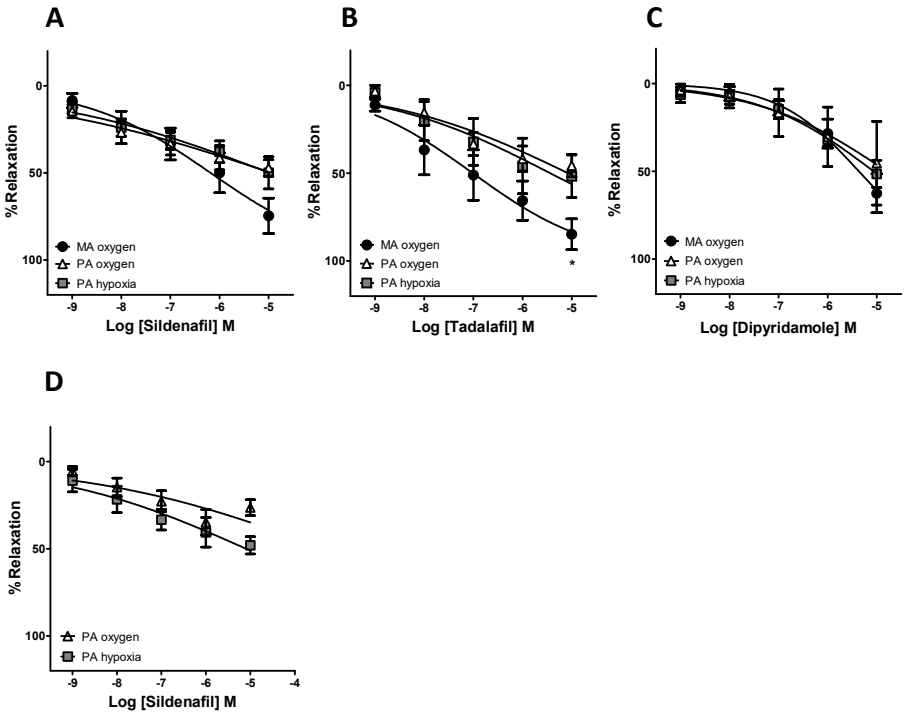

Figure R3.. Effects of PDE5 inhibitors on vascular tone. *Concentration-dependent relaxation induced by the PDE5 inhibitors sildenafil (A; n=5-7) and tadalafil (B; n=3-4), and the non-selective PDE inhibitor dipyridamole (C; n=3) in rat mesenteric arteries (MA oxygen) and pulmonary arteries under high oxygen (PA oxygen) or hypoxic (PA hypoxia) conditions. Concentration-dependent relaxation induced by the PDE5 inhibitors sildenafil (D; n=4-5) in human pulmonary arteries under high oxygen (PA oxygen) or hypoxic (PA hypoxia) conditions. Arteries were initially stimulated with a cocktail of U46619 ($3x10^{-8}$ M), 5-HT ($3x10^{-6}$ M) and ET-1 ($3x10^{-9}$ M). Results are means ± SEM. Drugs induced responses were compared with PA oxygen using two-way ANOVA followed by Bonferroni post hoc test for A, B and C and unpaired Student's t-test for D. * indicates P<0.05 MA oxygen vs PA oxygen.*

1.1.3. Vasodilator effects of sGC stimulators.

As shown in figure R4, we examined the effect of different sGC stimulators in rat arteries pre-contracted with the mixture of vasoconstrictors. Addition of the sGC stimulators YC-1, BAY 41-2272 and riociguat (Figure R4-A, B and C, respectively) caused a strong relaxant response in pulmonary and mesenteric arteries, with some differences in potency depending on the artery and the oxygen levels. YC-1 (Figure R4-A) produced a similar relaxant effect in mesenteric and pulmonary arteries under high oxygen and hypoxia. On the other hand, the relaxant response to BAY 41-2272 (Figure R4-B) was ≈3 fold more potent in pulmonary arteries under hypoxia than in mesenteric and pulmonary arteries under high oxygen levels. The relaxant effect of riociguat (Figure R4-C) in mesenteric and pulmonary arteries under hypoxia was slightly more effective than in pulmonary arteries under high oxygen. In addition, YC-1 was less potent (<pIC_{50}) that the other two sGC stimulators in mesenteric and pulmonary arteries, although all the three compounds did not show differences in their E_{max} (Table R1). In human pulmonary arteries pre-contracted with the mixture of vasoconstrictors, cumulative addition of riociguat (Figure R4-D) produced a concentration-dependent relaxation. Human pulmonary arteries under hypoxia were more sensitive to riociguat.

As compared to PDE5 inhibitors, sGC stimulators showed, in general, higher vasodilator efficacy, reaching a full relaxant response in most rat vessels.

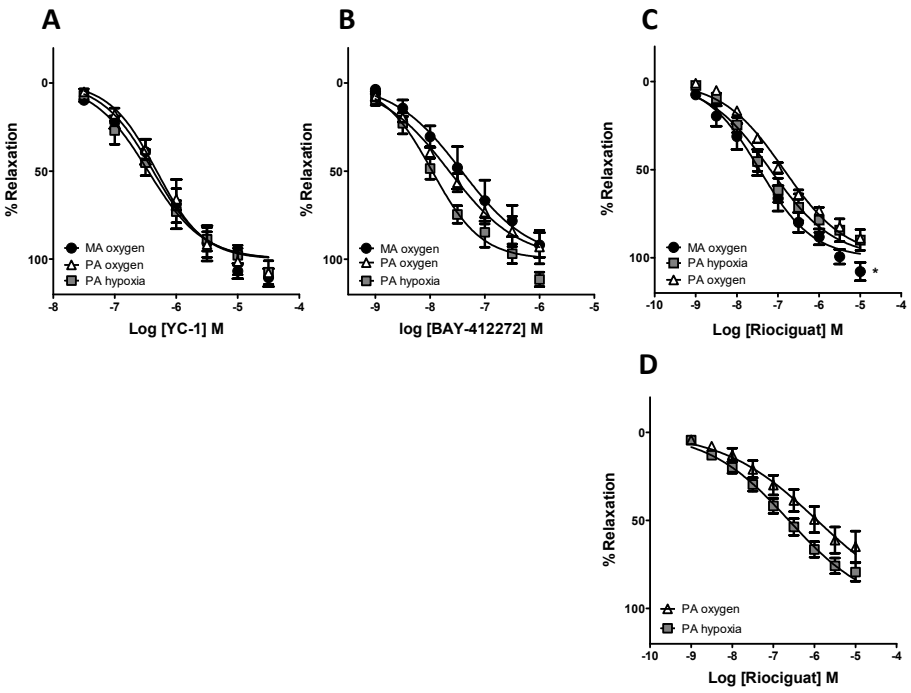

FigureR4. Effects of sGC stimulators on vascular tone. *Concentration-dependent relaxation induced by the sGC stimulators YC-1 (A; n=5-6), BAY 41-2272 (B; n=6) and riociguat (C; n=6) in rat mesenteric arteries (MA oxygen) and pulmonary arteries under high oxygen (PA oxygen) or hypoxic (PA hypoxia) conditions. Concentration-dependent relaxation induced by the sGC stimulator riociguat (D; n=10-11) in human pulmonary arteries under high oxygen (PA oxygen) or hypoxic (PA hypoxia) conditions. Arteries were initially stimulated with a cocktail of U46619 ($3x10^{-8}$ M), 5-HT ($3x10^{-6}$ M) and ET-1 ($3x10^{-9}$ M). Results are means ± SEM. Vasodilator responses were compared with PA oxygen using two-way ANOVA followed Bonferroni post hoc test for A, B and C and unpaired Student's t-test for D. * indicates P<0.05 MA oxygen vs PA oxygen.*

1.1.4. Vasodilator effects of drugs targeting ion channels.

As shown in figure R5, we examined the effect of several drugs targeting ion channels in rat arteries pre-contracted with the mixture of vasoconstrictors. The Kv7 channel agonists flupirtine (Figure R5-A) or retigabine (Figure R5-B) relaxed mesenteric arteries but had no effect on pulmonary arteries independently of the oxygen level. The ATP-sensitive potassium channel activator pinacidil (Figure R5-D) induced a relaxation in a concentration-dependent manner in all vessels. Again, the maximal relaxant effect was reached in mesenteric arteries, where pinacidil showed a higher pIC_{50} and E_{max} than in pulmonary arteries. (Table R1).

The CCB nifedipine (Figure R5-D) caused a relaxation in a concentration-dependent manner in all vessels. However, the relaxant response to nifedipine was significantly higher in mesenteric arteries, reaching a full relaxation. By contrast, nifedipine produced only a weak relaxant effect in pulmonary arteries, independently of the oxygen level.

The relaxant responses of CCB nifedipine were also examined in human pulmonary arteries (Figure R5-E). Addition of nifedipine to pulmonary arteries resulted in a concentration-dependent relaxation. However, the relaxant effect of nifedipine was similar under oxygen and hypoxia conditions. It should be noted, that nifedipine showed higher pIC_{50} and E_{max} values in human pulmonary arteries than in rat pulmonary arteries (Table R1 and 2).

Taken together, these data suggest that K^+ channel activators and voltage-dependent Ca^{2+} channel blockers act mainly as systemic vasodilators, with a poor relaxant effect in pulmonary arteries.

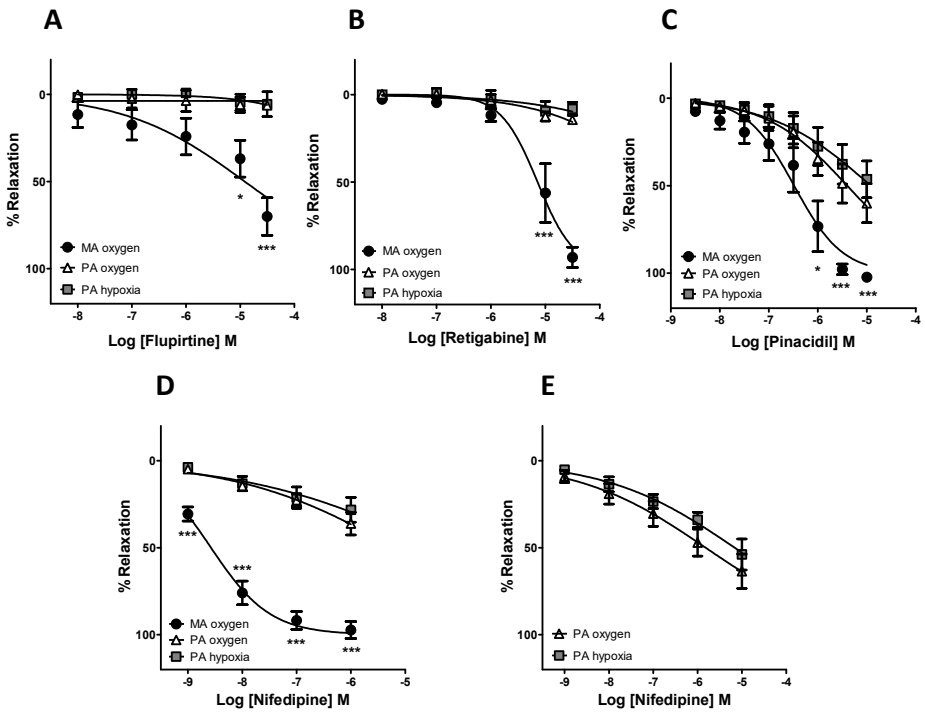

Figure R5. Effects of drugs targeting ion channels on vascular tone. *Concentration-dependent relaxation induced by the Kv7 channels agonists flupirtine (A; n=3) and retigabine (B; n=3), the ATP-sensitive potassium channel activator pinacidil (C; n=5) and the CCB nifedipine (D; n=8-9) in rat mesenteric arteries (MA oxygen) and pulmonary arteries under high oxygen (PA oxygen) or hypoxic (PA hypoxia) conditions. Concentration-dependent relaxation induced by nifedipine (E; n=6) in human pulmonary arteries under high oxygen (PA oxygen) or hypoxic CO2 (PA hypoxia) conditions. Arteries were initially stimulated with a cocktail of U46619 ($3x10^{-8}$ M), 5-HT ($3x10^{-6}$ M) and ET-1 ($3x10^{-9}$ M). Results are means ± SEM. Vasodilator responses were compared with PA oxygen using two-way ANOVA followed Bonferroni post hoc test for A, B, C, E and F and unpaired Student's t-test for D. * and *** indicates P<0.05 and P< 0.001 MA oxygen vs PA oxygen.*

1.1.5. Vasodilator effects of the adenylate cyclase activators.

As shown in figure R6, we also examined the effects of drugs that enhance AC activity such as forskolin and treprostinil in rat arteries precontracted with the mixture of vasoconstrictors. The relaxant effects of forskolin (Figure R6-A) and treprostinil (Figure R6-B) were significantly more pronounced in mesenteric arteries than in pulmonary arteries (Table R1). Furthermore, their relaxant responses were similar in pulmonary arteries under high oxygen and hypoxic conditions.

In human pulmonary arteries (Figure R6-C), treprostinil induced a slightly stronger effect in pulmonary arteries under hypoxia than under high oxygen conditions (Table

R2). It should be noted, that these relaxant effects were stronger than in rat pulmonary arteries under the same conditions.

Taken together, these data suggest that the activation of adenylate cyclase causes relaxation, with a higher efficacy in systemic than in pulmonary arteries.

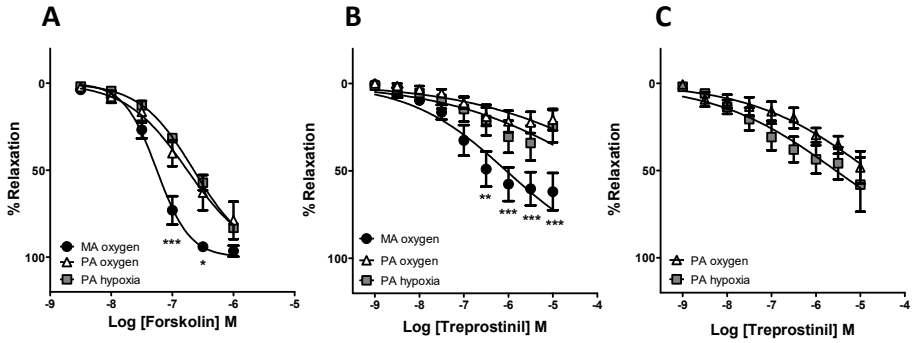

FigureR6. Effects of adenylate cyclase activator on vascular tone. *Concentration-dependent relaxation induced by the PGI_2 mimetic treprostinil (A; n=6-8) and the adenylate cyclase activator forskolin (B; n=3) in rat mesenteric arteries (MA oxygen) and pulmonary arteries under high oxygen (PA oxygen) or hypoxic (PA hypoxia) conditions. Concentration-dependent relaxation induced by treprostinil (C; n=6) in human pulmonary arteries under high oxygen (PA oxygen) or hypoxic (PA hypoxia) conditions. Arteries were initially stimulated with a cocktail of U46619 ($3x10^{-8}$ M), 5-HT ($3x10^{-6}$ M) and ET-1 ($3x10^{-9}$ M). Results are means ± SEM. Vasodilator responses were compared with PA oxygen using two-way ANOVA followed by Bonferroni post hoc test for A and B and unpaired Student's t-test for C. *, ** and ***indicate P<0.05, P<0.01 and P<0.001 MA oxygen vs PA oxygen.*

1.1.6. Vasodilator effects of PPAR agonists.

As shown in figure R7, we examined the effect of the several PPAR agonists in rat arteries pre-contracted with the mixture of vasoconstrictors. Addition of chemically distinct PPARβ/δ agonists, GW0742 and L165041, and the PPARγ agonist rosiglitazone (Figure R7-A, B and C, respectively) caused a relaxant response in a concentration-dependent manner in pulmonary and mesenteric arteries. The relaxant effects of PPAR agonists were in general more prominent in mesenteric arteries. The relaxant responses induced by L165041 or rosiglitazone in pulmonary arteries were independent of oxygen levels. Of note, GW0742 showed higher relaxant response in pulmonary arteries under high oxygen as compared to hypoxic conditions (Figure R7-

A). Unfortunately, the relaxation induced by GW0742 in human pulmonary arteries was similar under oxygen and hypoxia conditions (Figure R7-D) (Table R2).

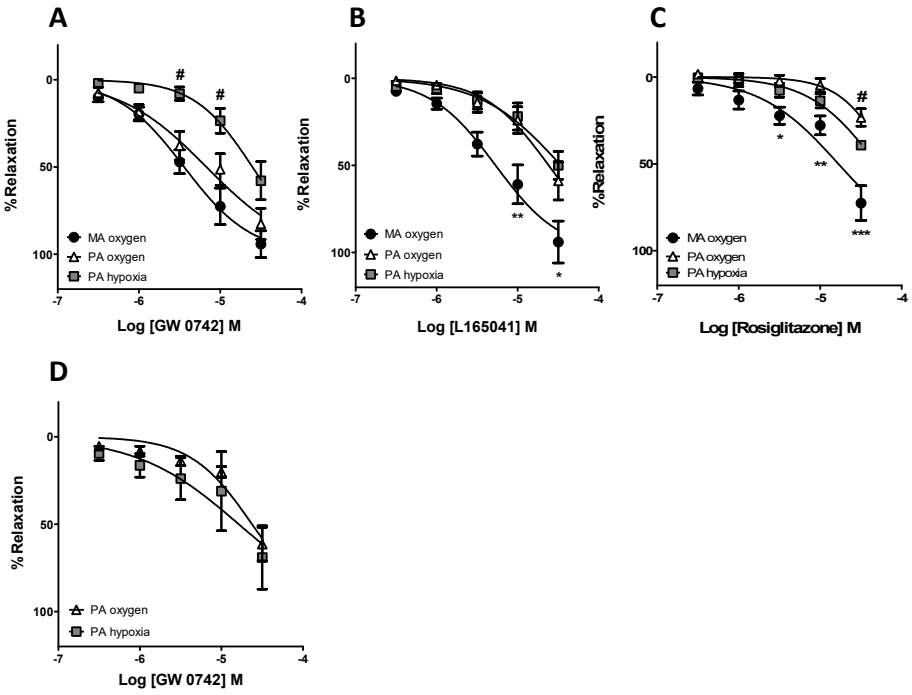

Figure R7. Effects of PPAR agonists on vascular tone. *Concentration-dependent relaxation induced by the PPARβ/δ agonists GW0742 (A; n=7-10) and L165041 (B; n=7-8) and the PPARγ agonist rosiglitazone (C; n=4) in rat mesenteric arteries (MA oxygen) and pulmonary arteries under high oxygen (PA oxygen) or under hypoxic (PA hypoxia) conditions. Concentration-dependent relaxation induced by the PPARβ/δ agonist GW0742 (C; n=3-5) in human pulmonary arteries under high oxygen (PA oxygen) or hypoxic (PA hypoxia) conditions. Arteries were initially stimulated with a cocktail of U46619 ($3x10^{-8}$ M), 5-HT ($3x10^{-6}$ M) and ET-1 ($3x10^{-9}$ M). Results are means ± SEM. Vasodilator induced responses were compared with PA oxygen using two-way ANOVA followed by Bonferroni post hoc test for A, B and C and unpaired Student's t-test for D. * , **and *** indicate P<0.05, P< 0.01 and P<0.001 MA oxygen vs PA oxygen. # indicates P<0.05 PA hypoxia vs PA oxygen.*

1.1.7. Vasodilator effects of kinase inhibitors.

As shown in figure R8, we examined the effects of several kinase inhibitors in rat arteries pre-contracted with the mixture of vasoconstrictors. The ROCK1/2 inhibitor hydroxyfasudil (Figure R8-A) induced a relaxation in a concentration-dependent manner in all vessels. The relaxant response to hydroxyfasudil was more potent in mesenteric arteries than in pulmonary arteries (Table R1). Moreover, pulmonary arteries were more sensitive to hydroxyfasudil under hypoxia than under high oxygen.

On the other hand, the flavonoid quercetin (Figure R8-B), that acts as a pan-inhibitor of MAPKs and the TGF-β pathway, caused a full relaxation in mesenteric and pulmonary arteries. However, mesenteric and pulmonary arteries under hypoxia were more sensitive to quercetin than pulmonary arteries under high oxygen condition (Table R1).

The transforming growth factor-β activated kinase 1 (TAK-1) inhibitor, 5z-7-oxozeaenol (Figure R8-C) had no effect as vasodilator in rat pulmonary arteries independently of the oxygen level.

The tyrosine kinase inhibitor imatinib (Figure R8-G) induced a concentration-dependent relaxation in all vascular beds. However, this relaxant effect was stronger in mesenteric arteries than in pulmonary arteries (Table R1). In addition, in pulmonary arteries, the relaxant effect induced by imatinib was independent of the oxygen level (Table R1).

The relaxant responses of these drugs were also examined in human pulmonary arteries. The relaxation by hydroxyfasudil and quercetin (Figures R8-D and E, respectively) in pulmonary arteries was similar under oxygen and hypoxia conditions (Table R1). It should be noted, that the relaxant effects induced by hydroxyfasudil and quercetin were less potent in human pulmonary arteries than in rat pulmonary arteries under the same conditions (Table R1 and R2). The drug 5z-7-oxozeaenol (Figure R8-F) did not show any effect in human pulmonary arteries.

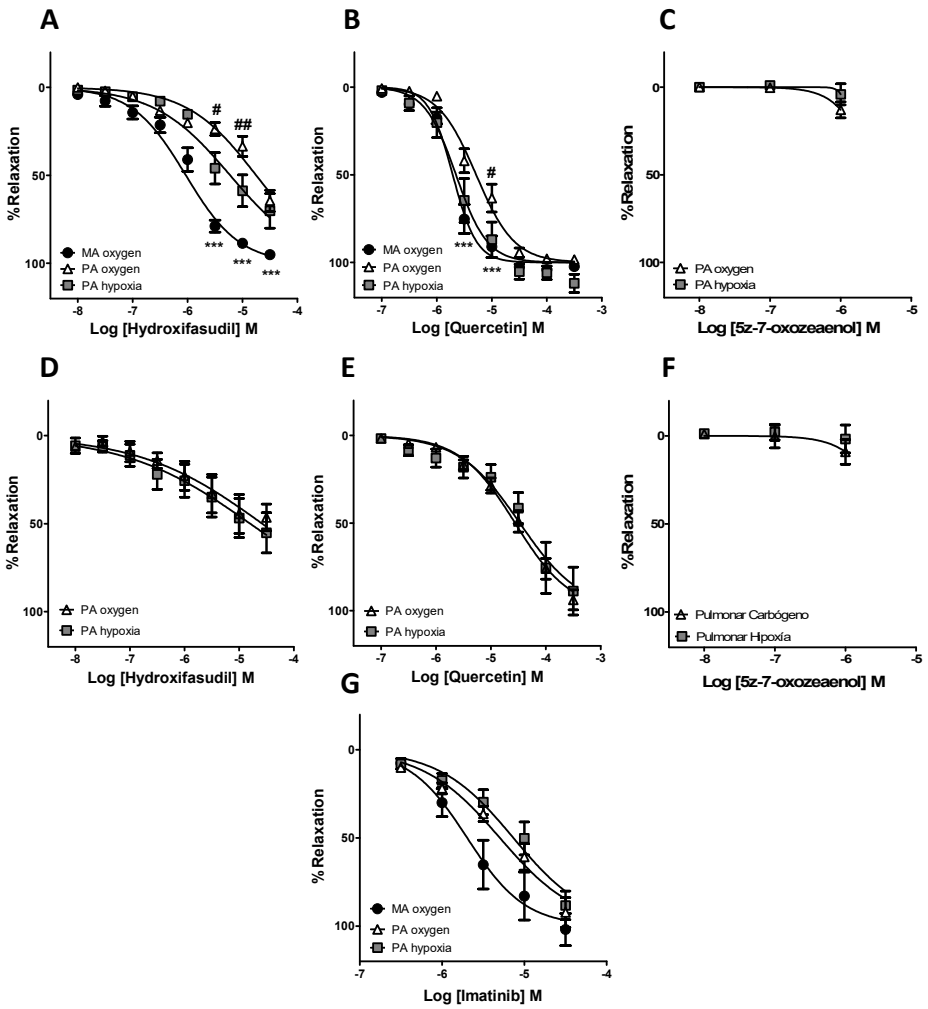

Figure R8. Effects of kinase inhibitors on vascular tone. *Concentration-dependent relaxation induced by the ROCK inhibitor hydroxyfasudil (A; n=7-8), the flavonoid quercetin (B; n=6) the TAK-1 inhibitor 5z-7-oxozeaenol (C; n=3-4), and the tyr-kinase inhibitor imatinib (G; n=5-6) in rat mesenteric arteries (MA oxygen) and pulmonary arteries under high oxygen (PA oxygen) or hypoxic (PA hypoxia) conditions. Concentration-dependent relaxation induced by the ROCK inhibitor hydroxyfasudil (D; n=5-6), the flavonoid quercetin (E; n=6-8) the TAK-1 inhibitor 5z-7-oxozeaenol (F; n=3-4) in human pulmonary arteries under high oxygen (PA oxygen) or hypoxic (PA hypoxia) conditions. Arteries were initially stimulated with a cocktail of U46619 ($3x10^{-8}$ M), 5-HT ($3x10^{-6}$ M) and ET-1 ($3x10^{-9}$ M). Results are means ± SEM. Vasodilator responses were compared with PA oxygen using two-way ANOVA followed by Bonferroni post hoc test for A, B, C and G and unpaired Student's t-test for D, E and F. *** indicates P<0.001 MA oxygen vs PA oxygen. $^{\#}$ and $^{\#\#}$ indicate P<0.05 and P<0.01 PA hypoxia vs PA oxygen.*

1.1.8. Vasodilator effects of other drugs.

As shown in figure R9, we examined the effect of drugs that could be useful such as novel strategies in the treatment of the PH. Addition of the calcineurin inhibitor tacrolimus (Figure R9-A) caused a weak relaxant response in pulmonary and mesenteric arteries. Moreover, the relaxant response was similar independently of the oxygen level in pulmonary arteries. We also assessed the effect of the $P2Y_1$ receptor agonist 2-MeSADP (Figure R9-B). Increasing concentrations of 2-MeSADP caused a minimal effect in mesenteric arteries and pulmonary arteries under hypoxia, whereas in pulmonary arteries under high oxygen 2-MeSADP did not show effect. The calcium sensitizer levosimendan (Figure R9-C) caused a relaxant effect that was stronger in mesenteric arteries than in pulmonary arteries (Table R1). In pulmonary arteries its relaxant effect was independent of oxygen level (Table R1).

In human pulmonary arteries, the relaxant response of levosimendan was similar under oxygen and hypoxic conditions (Figure R9-D and Table R2). The vasodilation induced by levosimendan was more potent in human than in rat pulmonary arteries under the same conditions (Tables R1 and R2).

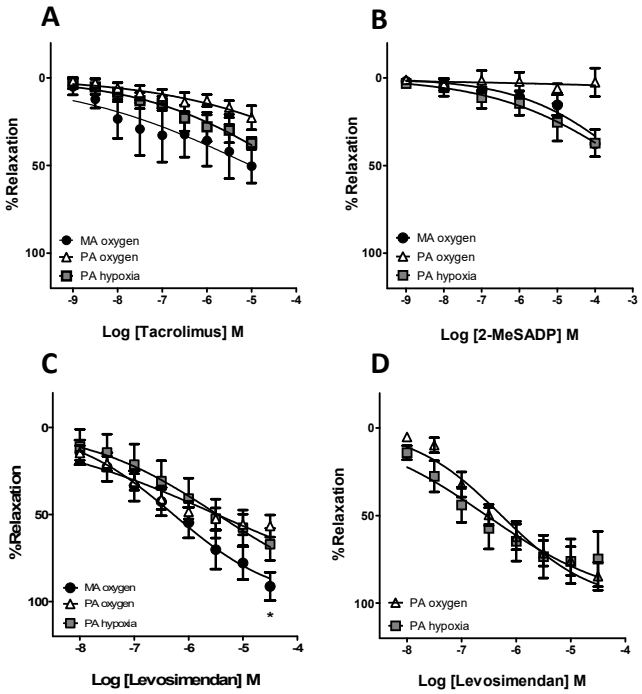

Figure R9. Effects of drugs used for other indications on vascular tone. *Concentration-dependent relaxation induced by the calcineurin inhibitor tacrolimus (A; n=3), the P2Y1 receptor agonist 2-MeSADP (B; n=2-3) and the calcium sensitizer levosimendan (C; n=4-15) in rat mesenteric arteries (MA oxygen) and pulmonary arteries under high oxygen (PA oxygen) or hypoxic (PA hypoxia) conditions. Concentration-dependent relaxation induced by the calcium sensitizer levosimendan (D; n=5) in human pulmonary arteries under high oxygen (PA oxygen) or hypoxic (PA hypoxia) conditions. Arteries were initially stimulated with a cocktail of U46619 ($3x10^{-8}$ M), 5-HT ($3x10^{-6}$ M) and ET-1 ($3x10^{-9}$ M). Results are means ± SEM. Vasodilators responses were compared with PA oxygen using two-way ANOVA followed by Bonferroni post hoc test for A, B and C and unpaired Student's t-test for D. * indicates P< 0.05 MA oxygen vs PA oxygen.*

As shown in figure R10 and Tables R1 and R2, the data obtained from the individual cumulative concentration-response curves for each drug exhibited different efficacy (E_{max}) and potency (pIC_{50}) in rat mesenteric and pulmonary arteries (Figure R10-A and Table R1) and in human pulmonary arteries (Figure R10-B and Table R2). Thus, quercetin was more efficient to relax rat and human pulmonary arteries, while 5z-7-oxozeaenol was the less effective drug in both vessels under high oxygen level (Figures R10-A and R10-B, respectively).

Table R1. Parameters derived from the concentration-response curves induced by different drugs in rat pulmonary and mesenteric arteries.

Drug	Mesenteric artery			Pulmonary artery					
				Hypoxia			Oxygen		
	pIC_{50}	*Emax*	n	pIC_{50}	*Emax*	n	pIC_{50}	*Emax*	n
Sildenafil	6.18±0.26	≥ 74.62±10.13 [a]	5	4.98±0.48	≥ 49.93±9.26	5	4.94±0.54	≥ 47.13±4.66	7
Tadalafil	7.01±0.29 [a]	≥ 84.85±8.82 [a]	4	5.44±0.53	≥ 51.80±12.11	3	5.08±0.40	≥ 45.68±6.40	4
Dipirydamole	5.37±0.16	≥ 62.61±11.07	3	5.07±0.20	≥ 51.49±7.78	3	4.80±0.71	≥ 45.38±23.87	3
YC-1	6.38±0.09	110.52±5.05	5	6.46±0.07	107.45±1.98	6	6.32±0.06	107.68±6.73	6
BAY41-2272	7.42±0.10	91.88±6.98	6	7.96±0.07 [c]	111.44±4.07	6	7.65±0.08	93.11±9.54	6
Riociguat	7.45±0.08 [b]	107.82±5.23 [a]	6	7.19±0.09 [c]	89.95±5.91	6	6.86±0.04	88.98±1.76	6
Hydroxyfasudil	6.03±0.05 [b]	95.08±1.41 [b]	7	5.23±0.10 [d]	≥ 70.20±9.81	7	4.75±0.07	≥ 64.50±6.02	8
Imatinib	5.70±0.10 [b]	101.95±9.15	5	5.13±0.08	≥ 88.33±8.13	5	5.30±0.07	≥ 92.32±8.47	6
Quercetin	5.71±0.04 [b]	102.32±2.71	6	5.65±0.07 [d]	111.90±5.20 [c]	6	5.28±0.04	98.34±1.79	6
5Z-7-oxozeaenol	N/A	N/A	N/A	N/A	≥ 4.12±6.00	4	N/A	≥ 12.91±4.57	3
GW0742	5.44±0.07	94.26±7.68	7	4.60±0.07 [d]	≥ 57.86±10.94	9	5.17±0.09	≥ 82.61±8.93	10
L165041	5.27±0.09 [b]	94.04±12.03	8	4.47±0.11	≥ 50.04±7.99	7	4.62±0.08	≥ 58.98±10.92	7
Rosiglitazone	4.78±0.09	≥ 72.59±9.99	4	N/A	≥ 39.25±1.47	4	N/A	≥ 23.29±5.05	4
SNP	7.12±0.08 [b]	78.67±5.09	9	7.48±0.09	83.50±5.55	7	7.66±0.10	91.91±9.55	8
SNAP	6.57±0.35 [b]	81.95±14.66	4	4.60±0.14	≥ 61.94±6.43	4	4.25±0.25	≥ 55.55±12.75	4
DEA-NO	6.24±0.07 [b]	94,75±8,3	5	5.96±0.07	83.93±8.75	5	5.71±0.09	≥ 65.43±16.13	3
Acetohydroxamic acid	3.70±0.16	≥ 68.19±7.45	3	N/A	≥ 44.85±6.24	3	N/A	≥ 50.98±16.68	3
Formaldoxime	N/A	≥ 43.12±8.99	5	N/A	≥ 47.14±10.24	5	N/A	≥ 21.20±4.84	3
Treprostinil	6.05±0.15	≥ 61.90±10.67 [b]	7	N/A	≥ 24.49±9.26	6	N/A	≥ 20.64±6.11	8
Forskolin	7.25±0.04 [b]	96.55±3.20	3	6.65±0.03	≥ 83.20±1.78	3	6.76±0.08	≥ 78.87±10.82	3
Nifedipine	8.78±0.10	97.34±4.86 [b]	8	N/A	≥ 28.26±7.14	8	N/A	≥ 36.18±6.52	9
Retigabine	5.14±0.11	93.02±5.78 [b]	3	N/A	≥ 8.13±3.71	3	N/A	≥ 14.41±1.55	3
Flupirtine	4.92±0.28	≥ 70.08±10.79 [b]	3	N/A	≥ 5.62±7.10	3	N/A	≥ 6.36±1.54	3
Pinacidil	6.49±0.11 [b]	102.31±1.34 [b]	5	N/A	≥ 46.37±10.53	5	5.40±0.15	≥ 60.02±11.16	5
2Me-SADP	N/A	≥ 15.50±5.91	4	N/A	≥ 25.40±10.61	4	N/A	≥ 6.05±2.68	4
Tacrolimus	5.01±0.60	≥50.39±9.66	3	N/A	≥ 37.16±3.11	3	N/A	≥ 22.76±6.87	3
Levosimendan	6.28±0.14	*91.28±8.11* [a]	4	5.47±0.23	≥ 67.13±9.32	7	5.48±0.18	≥ 56.60±6.36	15

The maximal responses (E_{max}) are expressed as percent of the mixture of vasoconstrictors (ET-1, U4, 5HT)-induced contraction and the pIC_{50} is defined as the negative $logIC_{50}$ (concentration of the drug that produces 50% inhibition of the contraction). Values are expressed as mean ± SEM, (n) indicates the number of experiments from different animals assessed. N/A, minimum or no effect. Data were obtained from the individual cumulative concentration-response curves fitted to a logistic equation and compared using unpaired Student's t-test. [a] and [b] P<0.05 and P<0.01 Mesenteric artery vs Pulmonary artery oxygen. [c] and [d] P<0.05 and P<0.01 Pulmonary artery hypoxia vs Pulmonary artery oxygen.

Table R2. Parameters derived from the concentration-response curves induced by different drugs in human pulmonary arteries under hypoxia or oxygen conditions.

Drug	Human pulmonary artery hypoxia			Human pulmonary artery oxygen		
	pIC_{50}	*Emax*	*n*	pIC_{50}	*Emax*	*n*
Hydroxyfasudil	4.80±0.24	≥55.19±11.41	6	4.58±0.24	≥46.47±7.59	5
Nifedipine	5.16±0.23	≥53.89±8.92	6	5.82±0.25	≥63.54±9.90	6
Sildenafil	5.09±0.52	≥47.99±4.95 [c]	4	N/A	≥26.38±4.58	5
Quercetin	4.47±0.11	88.82±13.69	6	4.56±0.05	93.82±5.72	8
GW0742	4.79±0.22	≥69.04±18.14	3	4.63±0.07	≥61.46±9.65	5
Levosimendam	6.54±0.22	74.82±15.78	5	6.27±0.11	84.72±7.93	5
Riociguat	6.62±0.07 [d]	≥79.34±5.24	11	5.93±0.12	≥64.96±8.90	10
Treprostinil	5.55±0.21	≥58.04±15.54	3	4.79±0.23	≥48.23±9.28	5
5Z-7-oxozeaenol	N/A	≥1.79±7.88	4	N/A	≥9.12±7.00	3

The maximal responses (E_{max}) are expressed as percent of inhibition of the contraction induced by the mixture of vasoconstrictors (ET-1, U4, 5HT) and the pIC_{50} is defined as the negative $logIC_{50}$ (concentration of the drug that produces 50% inhibition of the contraction). Values are expressed as mean ± SEM, (n) indicates the number of experiments from different lung samples assessed. N/A, minimum or no effect. Data were obtained from the individual cumulative concentration-response curves fitted to a logistic equation and compared using unpaired Student's t-test. [c] and [d] P<0.05 and P<0.01 Pulmonary artery hypoxia vs Pulmonary artery oxygen.

For drugs that did not reach a 50% inhibition of the contraction, their pIC_{30}, which is defined as the negative $logIC_{30}$ (concentration of the drug that produces 30% inhibition of the contraction), was calculated (Table R3).

Table R3. Parameters derived from the concentration-response curves induced by different drugs in rat pulmonary and mesenteric arteries.

Drug	Mesenteric artery		Pulmonary artery			
			Hypoxia		Oxygen	
	pIC_{30}	n	pIC_{30}	n	pIC_{30}	n
Rosiglitazone	5.18±0.09 [b]	4	4.65±0.05	4	N/A	4
Acetohydroxamic acid	4.60±0.16 [a]	3	3.56±0.16	3	3.65±0.20	3
Formaldoxime	4.85±0.30	5	4.63±0.16	5	N/A	3
Treprostinil	6.97±0.17	7	5.39±0.33	6	N/A	8
Nifedipine	9.03± 0.13 [b]	8	5.96±0.41	8	6.43±0.18	9
Pinacidil	6.90±0.13 [b]	5	5.78±0.17	5	6.10±0.14	5
Tacrolimus	6.78±0.39	3	5.61±0.18	3	N/A	3

Values are expressed as mean ± SEM, (n) indicates the number of experiments from different lung samples assessed. N/A, minimum or no effect. Data were obtained from the individual cumulative concentration-response curves fitted to a logistic equation and compared using unpaired Student's t-test. [a] and [b] P<0.05 and P<0.01 Mesenteric artery vs Pulmonary artery oxygen.

In order to determine the correlation between the data obtained in rPA and hPA we have plotted (Figure R10-C) the E_{max} effect in rPA (abscissa axis) versus the E_{max} effect in hPA (ordinate axis). A dotted line was drawn from 0 to 100%. Thus, drugs appearing below the line act as batter vasodilators in rPAs, while drugs appearing above the line are essentially better vasodilators in hPAs. Thus, treprostinil, nifedipine and levosimendan were better vasodilator in hPAs, whereas, sildenafil, riociguat, hydroxyfasudil and GW0742 were better vasodilators in rPAs. In addition, 5z-7-oxozeaenol did not show any effect as vasodilator in both vessels and, in contrast, quercetin relaxed both vessels with the same efficacy.

Therefore, our data suggest that, at least under our experimental conditions, we have observed different sensitivity for each drug in rPA and hPA under high oxygen level, although in general, the drug behavior pattern followed the same trend in both species. However, only we can establish a right correlation between the vasodilator effects observed in rat and human pulmonary arteries under high oxygen level for quercetin and 5z-7-oxozeanol.

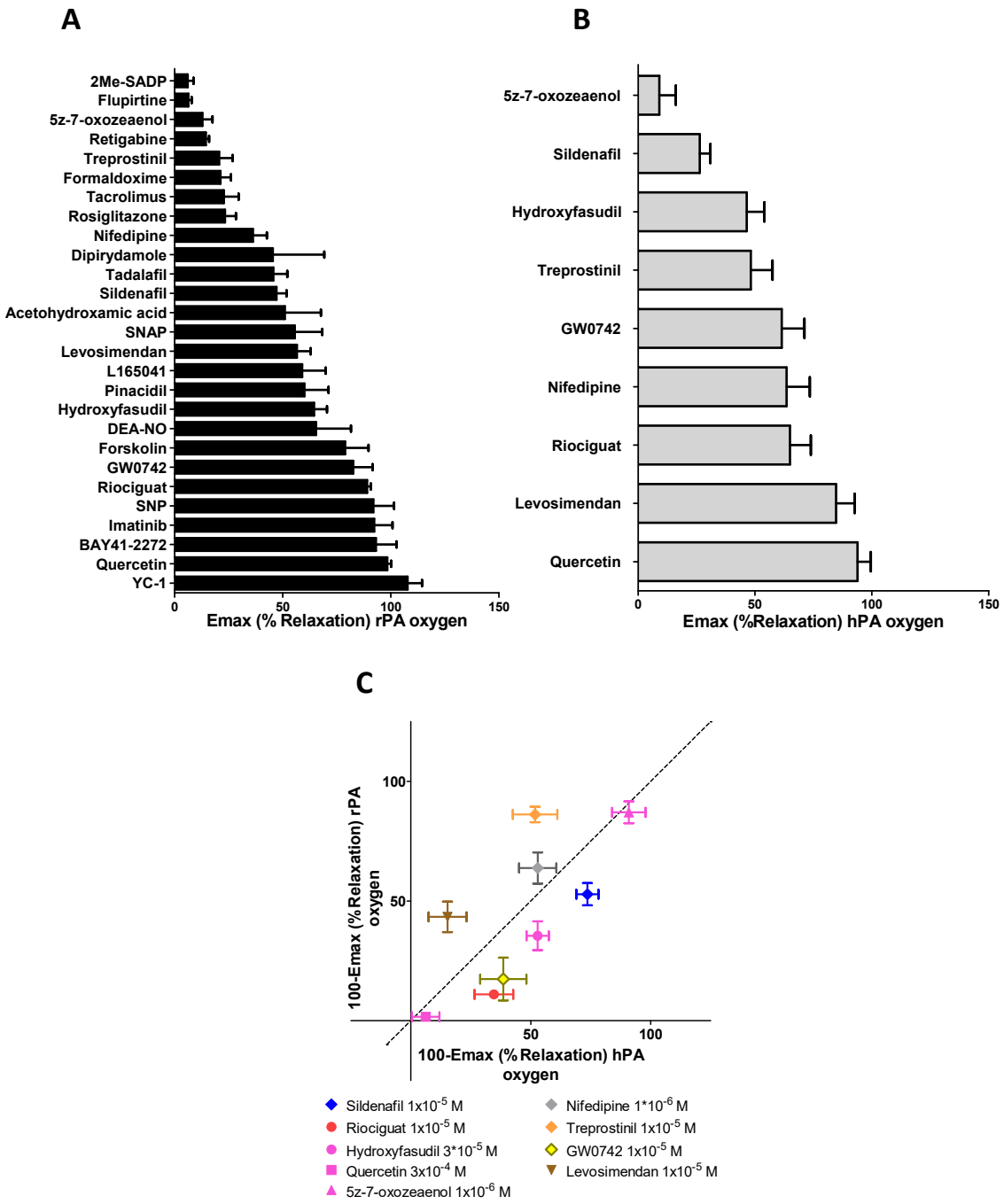

Figure R10: Efficacy of vasodilators used. *Bar graph representing the percent of maximal relaxation (E_{max}) of several vasodilator drugs on contractile tone in rat pulmonary arteries (A) and human pulmonary arteries (B) bubbled with 95% O_2-5% CO_2 (PA oxygen). Comparison of the E_{max} effects of several drugs in rat and human pulmonary arteries (C). Abcissa, vasodilatation on hPA (100 –E_{max} (% relaxation)); ordinate, vasodilatation on rPA (100 –E_{max} (% relaxation)).*

1.2. Oxygen and pulmonary selectivity.

We calculated the pulmonary and oxygen selectivity for each drug as described in the material and method section. As shown in figure R11-A, regarding pulmonary selectivity (PS), we have found that in rat arteries pre-contracted with the mixture of vasoconstrictors, several drugs tested showed higher selectivity for mesenteric arteries than for pulmonary arteries. For other drugs there was no difference between the effects in pulmonary and mesenteric arteries and none of the drugs was significantly selective for pulmonary arteries.

Regarding oxygen selectivity (OS) (Figure R11-B), most drugs were similarly effective under high oxygen or hypoxia. Only hydroxyfasudil and quercetin were more potent under hypoxia than under high oxygen conditions. On the other hand, GW0742 was the only drug that was more potent as vasodilator under high oxygen than under low levels of oxygen. Unfortunately, the oxygen sensitivity of GW0742 was not observed in human pulmonary arteries (Figure R11-C). Similarly, the selectivity of hydroxyfasudil or quercetin under hypoxia was not reproduced in human arteries. Despite some apparent trends in Figure R11-C, the effects of all other drugs were not statistically different under oxygen or hypoxic conditions.

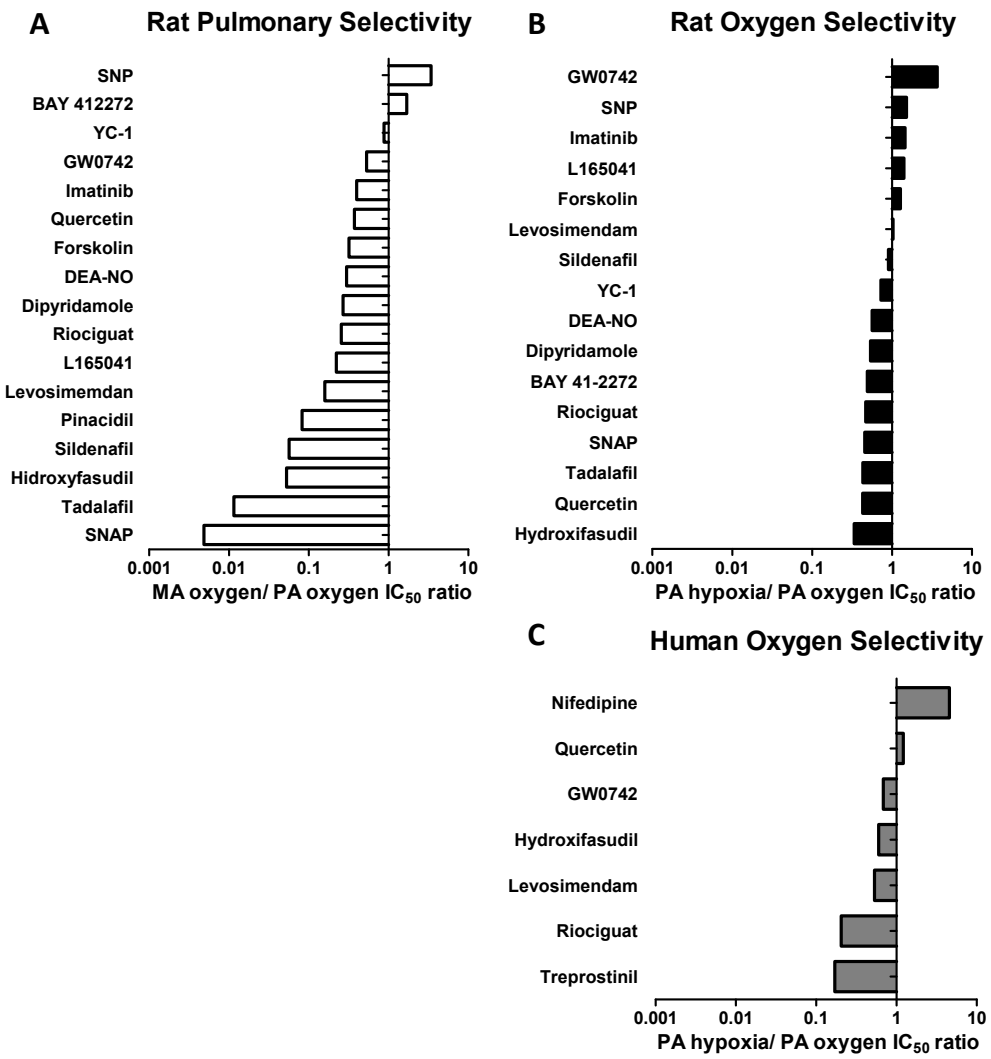

Figure R11. Selectivity of drugs for pulmonary vessels and oxygen*. Relative pulmonary selectivity (A) and oxygen selectivity (B) of different vasodilator drugs in rat arteries. (C) Relative oxygen selectivity in human pulmonary arteries. Data are expressed as relative potency (pIC_{50}) in mesenteric vs pulmonary arteries and under conditions of high and low oxygenation, respectively. Values >1 indicate greater selectivity for PA oxygen in panels A, B and C; while values <1 indicate greater selectivity for MA oxygen in panel A or PA hypoxia in panels B and C.*

As previously mentioned, several drugs did not reach the 50% of the inhibition of the contraction. In this case, we have assessed their PS and OS using the pIC_{30} values.

As shown in figure R12-A, we have found that acetohydroxamic acid and pinacidil and specially nifedipine, showed a higher selectivity for mesenteric arteries than for pulmonary arteries. Nifedipine was more potent to induce vasodilation in pulmonary arteries exposed to high oxygen levels (Figure R12-B). However, it should be noted that

the concentration inducing a 30% relaxation was much higher in pulmonary than in mesenteric arteries (Table R3).

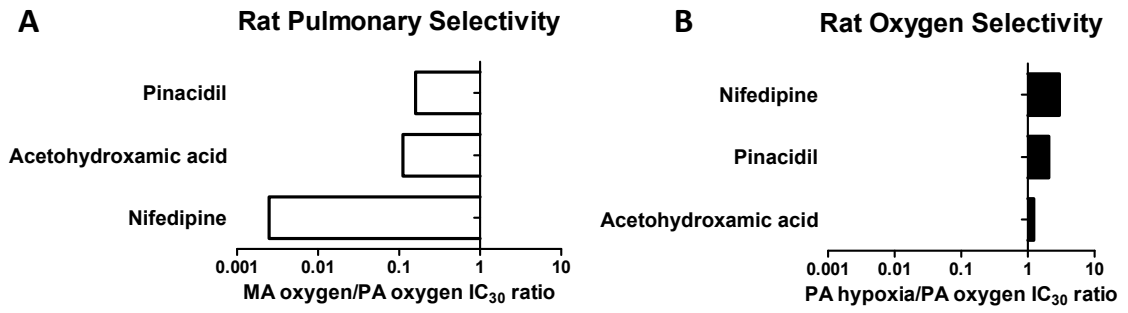

Figure R12: Selectivity of drugs*. Pulmonary selectivity (A) and oxygen selectivity (B) of different vasodilator drugs in rat arteries (MA oxygen) and pulmonary arteries under high oxygen (PA oxygen) or hypoxic (PA hypoxia) conditions. Data are expressed as relative pIC_{30} values in mesenteric vs pulmonary arteries and under conditions of high vs low oxygenation, respectively. Values >1 indicate greater selectivity for PA oxygen; while values <1 indicate greater selectivity for MA (A) or PA hypoxia (B).*

1.3. Antiproliferative studies.

In order to select the conditions, we first assessed the mitogenic effects of the mixture of vasoconstrictors used in vascular reactivity experiment ($3x10^{-8}$ M U46619, $3x10^{-9}$ M ET-1 and $3x10^{-6}$ M 5-HT). The *in vitro* studies of antiproliferative effects were carried out in rPASMCs, rPASMCs-MCT or hPASMCs. Figure R13 shows the time course of PASMCs proliferation mediated by low serum (1% FBS) with or without the mixture of vasoconstrictors for 24 and 48 hours. We have used as a positive control cell proliferation mediated by high serum (10% FBS for rPASMCs and rPASMCs-MCT, and HPA medium for hPASMCs). The MTT and the BrdU incorporation assays were used as complementary approaches. The first one estimates the number of viable cells, i.e. the balance between proliferation and apoptosis/necrosis. The second is an estimate of DNA synthesis.

As shown in figure R13, cell viability (Figure R13-D) and DNA synthesis (Figure R13-E) were significant increased by the mixture of vasoconstrictors plus 1% FBS after 48 hours. It should be noted that the proliferative response was similar in the three cell types studied, i.e. viable cells were approximately doubled in 48 hours.

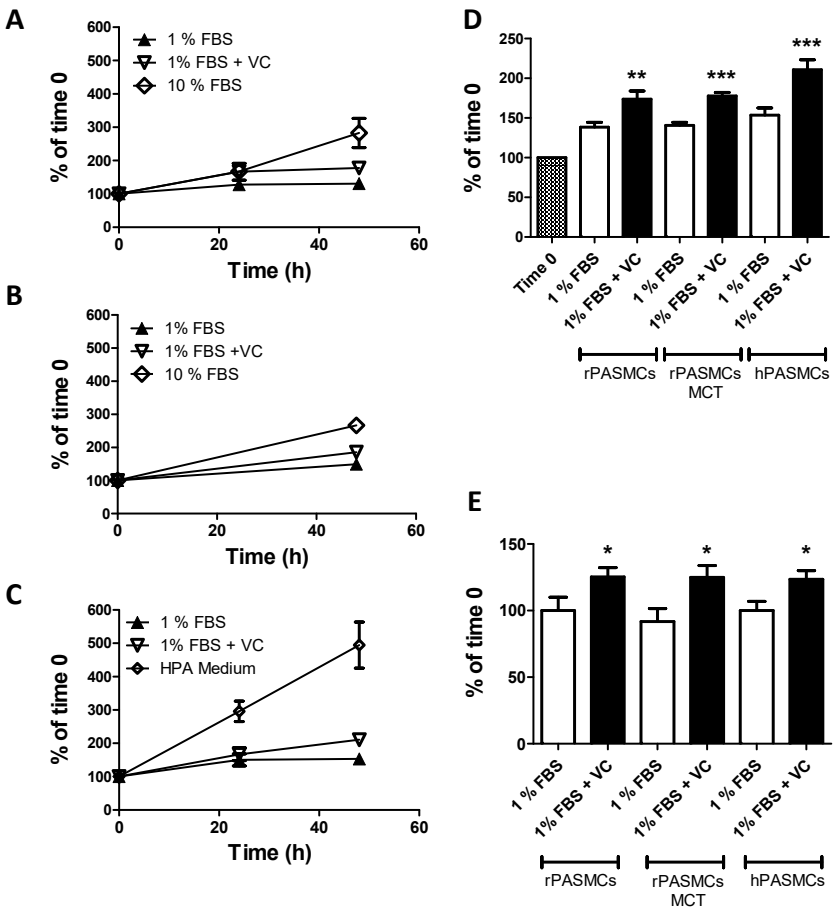

***Figure R13**: **The mixture of vasoconstrictors stimulates cell viability and DNA synthesis in PASMCs**. Time course of the cell viability induced by 1%FBS, 1%FBS + VC and either 10% FBS or HPA medium in rPASMCs (A), rPASMCs-MCT (B) and hPASMCs for 24 and 48 hours. Cell viability was estimated by the MTT assay, and DNA synthesis was determined by the BrdU incorporation assay. Bar graphs show average of cell viability (D) and BrdU incorporation (E) for 48 hours. Data represent mean ± SEM. All experiments were performed in triplicates and results are expressed as % of time 0 for panels A, B and C and % of 1% FBS for panels D and E of at least three independent experiments. The effects of the vasoconstrictor mixture were compared using unpaired Student's t-test. * and ** indicate P<0.05 and P< 0.01 versus 1% FBS.*

1.3.1. Effects of NO donors.

As show in figure R14, SNP had no effect on cell viability in rPASMCs (Figure R14-A), whereas it significantly inhibited cell viability in hPASMCs and rPASMCs-MCT in a concentration-dependent manner. Moreover, it should be noted that hPASMCs were more sensitive to SNP. Likewise, the other NO donors had minor (SNAP) or no effect (DEA-NO, formadoxime and acetohydroxamic acid) on rPASMCs cell viability (Figure

R14-C, D and E, respectively). SNP significantly inhibited the BrdU incorporation in rPASMCs and rPASMCs-MCT but not in hPASMCs.

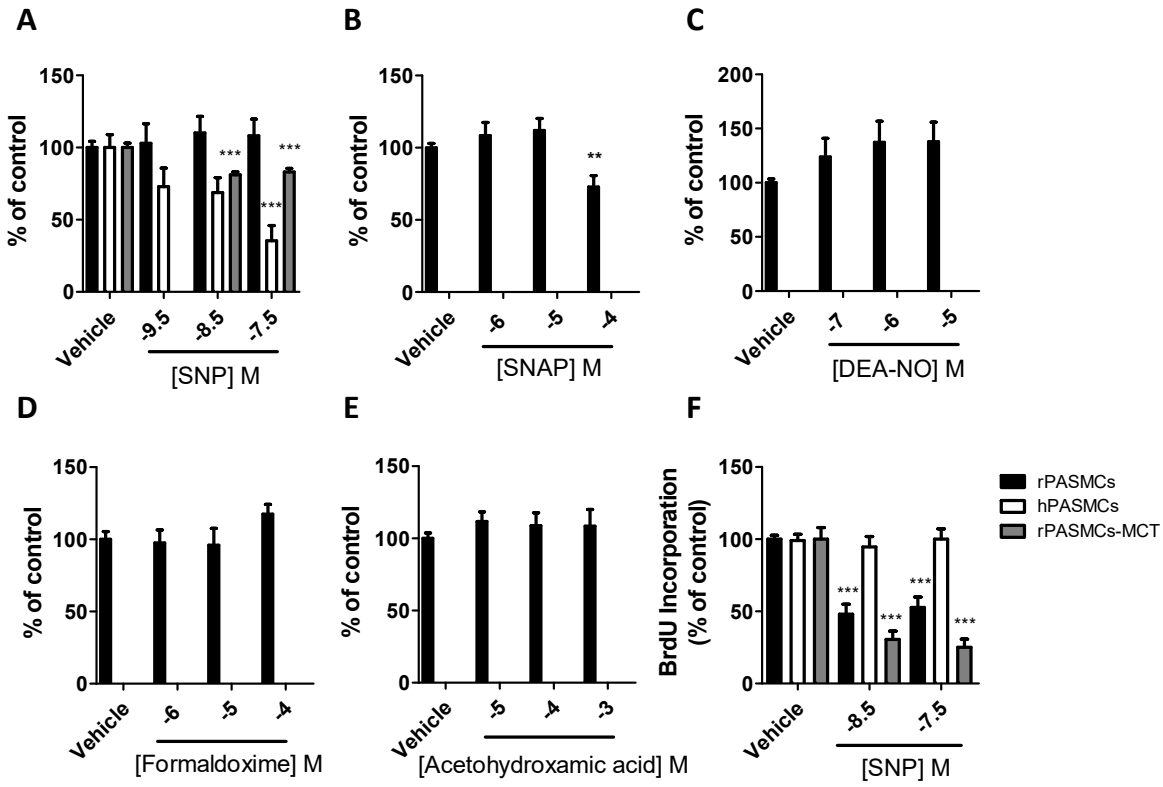

Figure R14. Antiproliferative effects of NO donors in PASMCs*. Concentration-dependent inhibition of cell viability induced by SNP (A), SNAP (B) DEA-NO (C), formaldoxime (D) and acetohydroxamic acid (E) in rPASMCs (black bars), rPASMCs-MCT (grey bars) and hPASMCs cells (white bars) for 48 hours. Concentration-dependent inhibition of BrdU incorporation induced by SNP (F) in rPASMCs (black bars), rPASMCs-MCT (grey bars) and hPASMCs cells (white bars) for 48 hours. Data represent mean ± SEM of 3-6 experiments performed in triplicate. Results are expressed as % of vehicle (DMSO 0.1%+VC). Drug-induced responses were compared with vehicle using one-way ANOVA followed by Dunnett´s post hoc test. *, ** and *** indicate P<0.05, P< 0.01 and P<0.001, respectively.*

1.3.2. Effects of PDE5 inhibitors.

Sildenafil (Figure R15-A) and tadalafil (Figure R15-B) significantly inhibited cell viability in rPASMCs-MCT and hPASMCs, while they had no effect in rPASMCs from healthy animals. Interestingly, tadalafil showed a higher effect than sildenafil in hPASMCs. Dipyridamole did not show any effect in rPAMCs or hPASMCs (FigRXC). In addition, both sildenafil (Figure R15-D) and tadalafil (Figure R15-E) significantly inhibited the BrdU incorporation in all cell types.

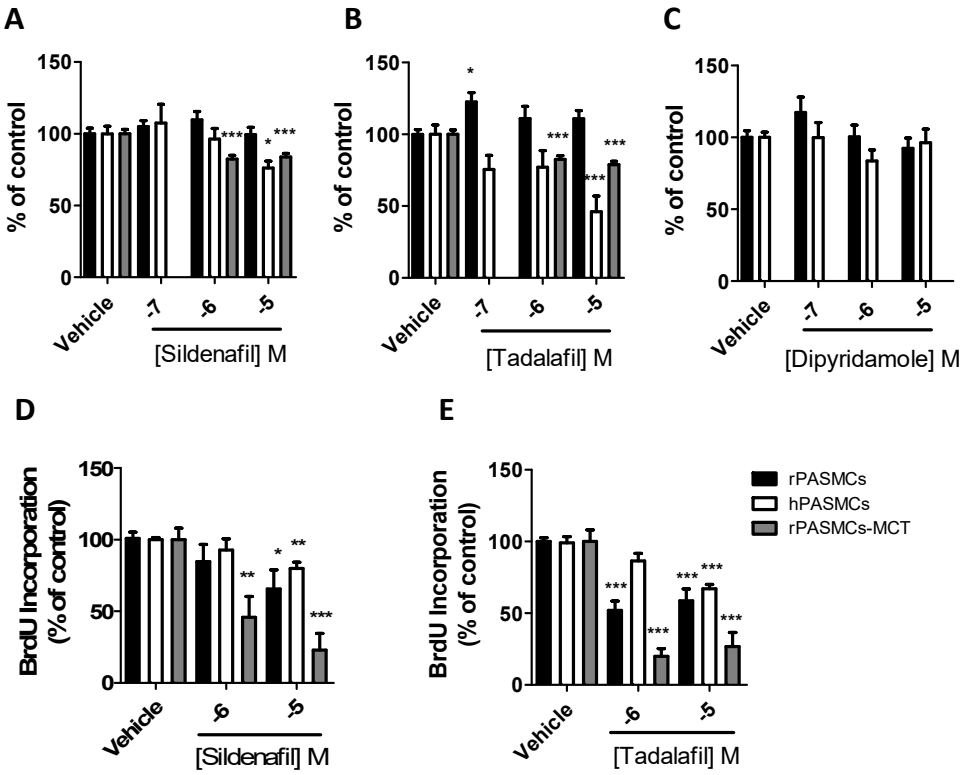

***Figure R15**: **Antiproliferative effects of PDE5 inhibitors in PASMCs**. Concentration-dependent inhibition of cell viability induced by sildenafil (A), tadalafil (B) and dipyridamole (C) in rPASMCs (black bars), rPASMCs-MCT (grey bars) and hPASMCs cells (white bars) for 48 hours. Concentration-dependent inhibition of BrdU incorporation induced by sildenafil (D), tadalafil (E) in rPASMCs (black bars), rPASMCs-MCT (grey bars) and hPASMCs cells (white bars) for 48 hours. Data represent mean ± SEM of 3-6 experiments performed in triplicate. Results are expressed as % of vehicle (DMSO 0.1%+VC). Drug-induced responses were compared with vehicle using one-way ANOVA followed by Dunnett´s post hoc test. *, ** and *** indicate P<0.05, P< 0.01 and P<0.001, respectively.*

1.3.3. Effects of sGCs stimulators.

As shown in figure R16, BAY 41-2272 (Figure R16-B) significantly inhibited cell viability in a concentration-dependent manner in rPASMCs from healthy animals, rPASMCs-MCT and hPASMCs. In contrast, YC-1 (Figure R16-A) and riociguat (Figure R16-C) had no effect in rPASMCs and hPASMCs. It should be noted that riociguat induced a significant reduction of cell viability in rPASMCs-MCT.

Both BAY 41-2272 (Figure R16-D) and specially riociguat (Figure R16-E) inhibited the BrdU incorporation. In addition, riociguat was more effective in rPASMCs-MCT than in rPASMCs and hPASMCs.

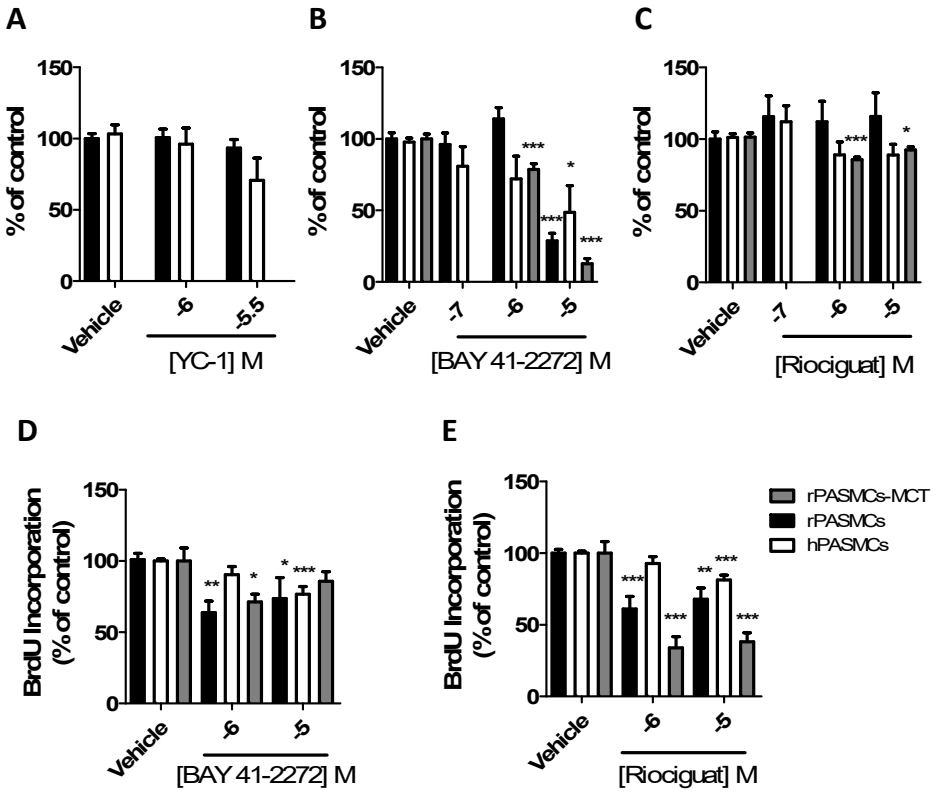

***Figure R16**: **Antiproliferative effects of sGC stimulators in PASMCs.** Concentration-dependent inhibition of cell viability induced by YC-1 (A), BAY 41-2272 (B) and riociguat (C) in rPASMCs (black bars), rPASMCs-MCT (grey bars) and hPASMCs cells (white bars) for 48 hours. Inhibition of BrdU incorporation induced by BAY 41-2272 (D) and riociguat (E) in rPASMCs (black bars), rPASMCs-MCT (grey bars) and hPASMCs cells (white bars) for 48 hours. Data represent mean ± SEM of 3-6 experiments performed in triplicate. Results are expressed as % of vehicle (DMSO 0.1%+VC). Drug-induced responses were compared with vehicle using one-way ANOVA followed by Dunnett´s post hoc test. *, ** and *** indicate P<0.05, P< 0.01 and P<0.001, respectively.*

1.3.4. Effects of drugs targeting ion channels.

As show in the figure R17, the voltage-dependent Ca^{2+} channel blocker nifedipine (Figure R17-A) inhibited cell viability in a concentration-dependent manner in hPASMCs and rPASMCs-MCT. It should be noted that hPASMCs were more sensitive to nifedipine than the other cell types.

The ATP-sensitive potassium channel activator pinacidil (Figure R17-B) significantly reduced the viability in hPASMCs but not in rPASMCs. Treatment with retigabine (Figure R17-D), but not with the other Kv7 channel activator flupirtine (Figure R17-C), significantly reduced cell viability in all cell lines. Similar results were obtained in BrdU incorporation assay. Nifedipine (Figure R17-E) inhibited the BrdU incorporation in all

cell types, whereas retigabine (Figure R17-F) only showed significant inhibitory effect in rPASMCs and rPASMCs-MCT rats.

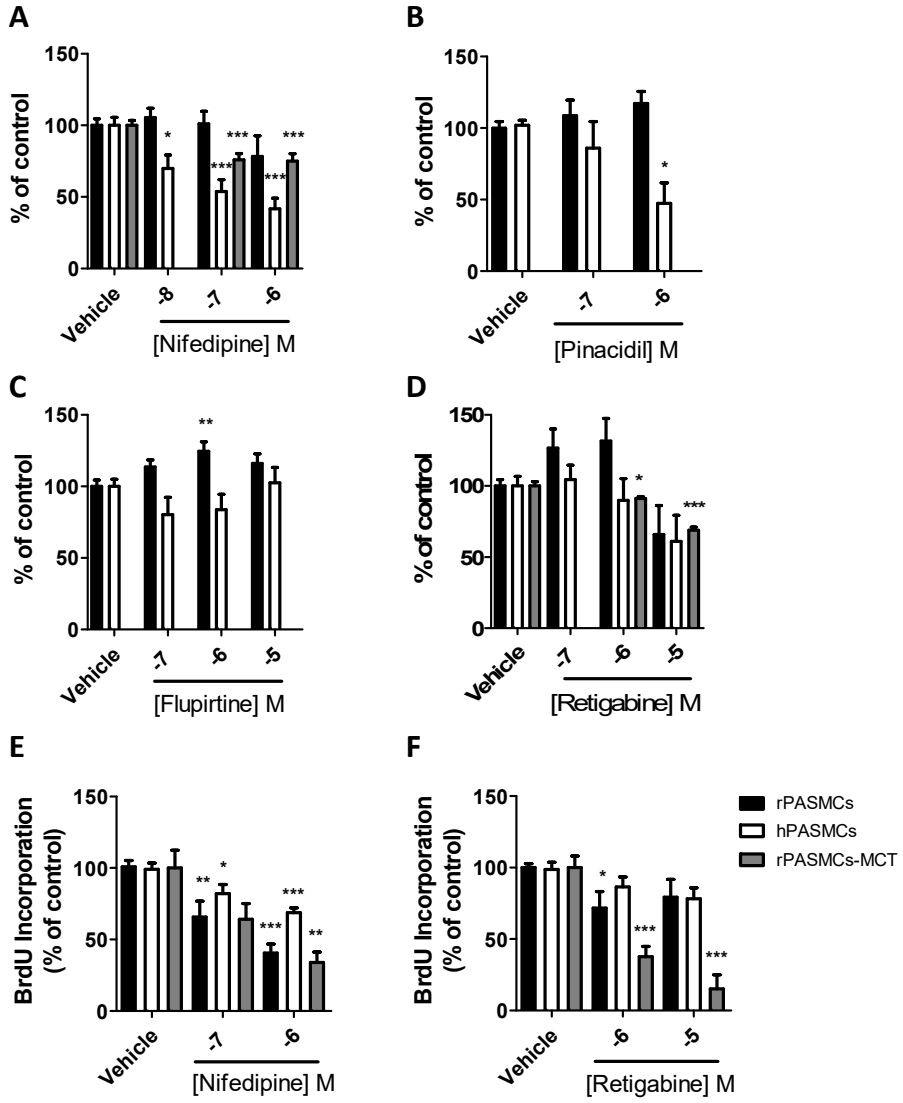

Figure R17: Antiproliferative effects of drugs targeting ion channels in PASMCs. *Concentration-dependent inhibition of cell viability induced by the voltage-dependent Ca^{2+} channel blocker nifedipine (A), the ATP-sensitive potassium channel activator pinacidil (B) and the Kv7 channel agonists flupirtine (C) and retigabine (D) in rPASMCs (black bars), rPASMCs-MCT (grey bars) and hPASMCs cells (white bars) for 48 hours. Concentration-dependent inhibition of BrdU incorporation induced by the voltage-dependent Ca^{2+} channel blocker nifedipine (E) and the Kv7 channels agonist retigabine (F) in rPASMCs (black bars), rPASMCs-MCT (grey bars) and hPASMCs cells (white bars) for 48 hours. Data represent mean ± SEM of 3-6 experiments performed in triplicate. Results are expressed as % of vehicle (DMSO 0.1%+VC). Drug-induced responses were compared with vehicle using one-way ANOVA followed by Dunnett´s post hoc test. *, ** and *** indicate P<0.05, P< 0.01 and P<0.001, respectively.*

1.3.5. Effects of adenylate cyclase activators

As shown in figure R18, we examined the effect of drugs that increase AC activity and cAMP levels. Forskolin significantly inhibited cell viability (Figure R18-A) and BrdU incorporation (Figure R18-C in hPASMCs). In contrast, this drug induced a significant increase on BrdU incorporation in rPASMCs and rPASMCs-MCT.

The PGI_2 mimetic treprostinil (Figure R18-B) showed weak effects on cell proliferation. It inhibited cell viability in rPASMCs at the highest concentration and caused a modest reduction of BrdU incorporation (Figure R18-D) in hPASMCs.

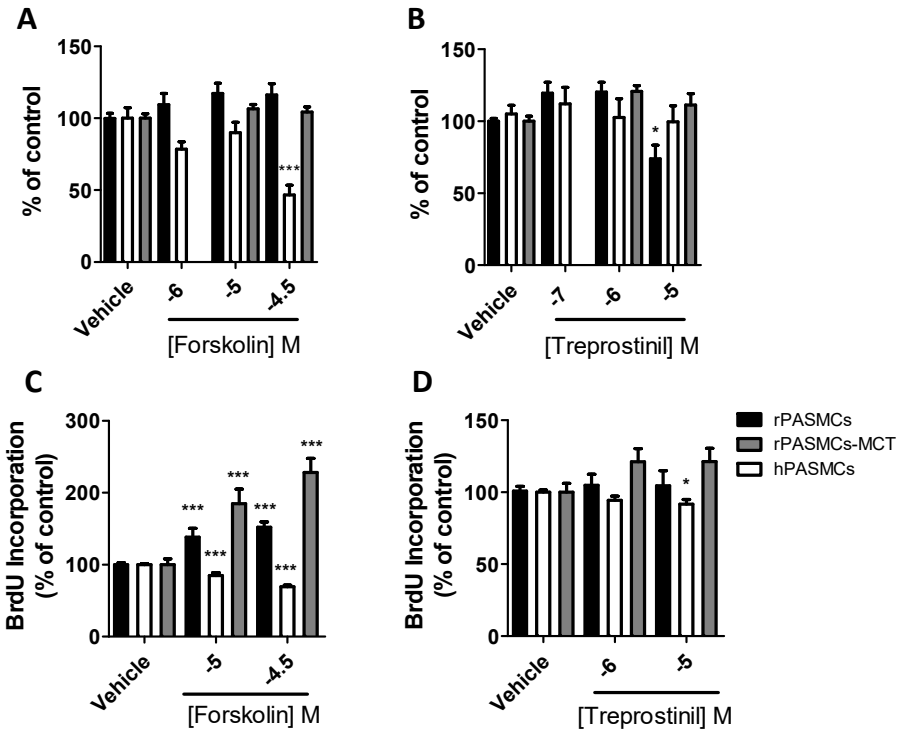

Figure R18: Antiproliferative effects of adenylate cyclase activators in PASMCs. *Concentration-dependent inhibition of cell viability induced by the AC activator forskolin (A), and the PGI_2 mimetic treprostinil (B) in rPASMCs (black bars), rPASMCs-MCT (grey bars) and hPASMCs cells (white bars) for 48 hours. Concentration-dependent inhibition of BrdU incorporation induced by the AC activator forskolin (C) and the PGI_2 mimetic treprostinil (D) in rPASMCs (black bars), rPASMCs-MCT (grey bars) and hPASMCs cells (white bars) for 48 hours. Data represent mean ± SEM of 3-6 experiments performed in triplicate. Results are expressed as % of vehicle (DMSO 0.1%+VC). Drug-induced responses were compared with vehicle using one-way ANOVA followed by Dunnett´s post hoc test. *, ** and *** indicate P<0.05, P< 0.01 and P<0.001, respectively.*

1.3.6. Effects of PPAR agonists

The PPARβ/δ agonist GW0742 (Figure R19-A) significantly inhibited cell viability in a concentration-dependent manner in hPASMCs and rPASMCs-MCT, although this effect only was observed at the highest concentration tested. In contrast, the other PPARβ/δ agonist, L165041 (Figure R19-B) did not reduce cell viability in rPASMCs and hPASMCs. The PPARγ agonist rosiglitazone (Figure R19-C) significantly inhibited cell viability in a concentration-dependent manner in hPASMCs, while it did not show effect in rPASMCs and rPASMCs-MCT.

As shown in figure R19-D, GW0742 inhibited the BrdU incorporation in a concentration-dependent manner in rPASMCs and rPASMCs-MCT but not in hPASMCs. Likewise, rosiglitazone (Figure R19-E) significantly reduced BrdU incorporation in a concentration-dependent manner in all cell types, although its effect was weaker in hPASMCs than in rPASMCs and rPASMCs-MCT.

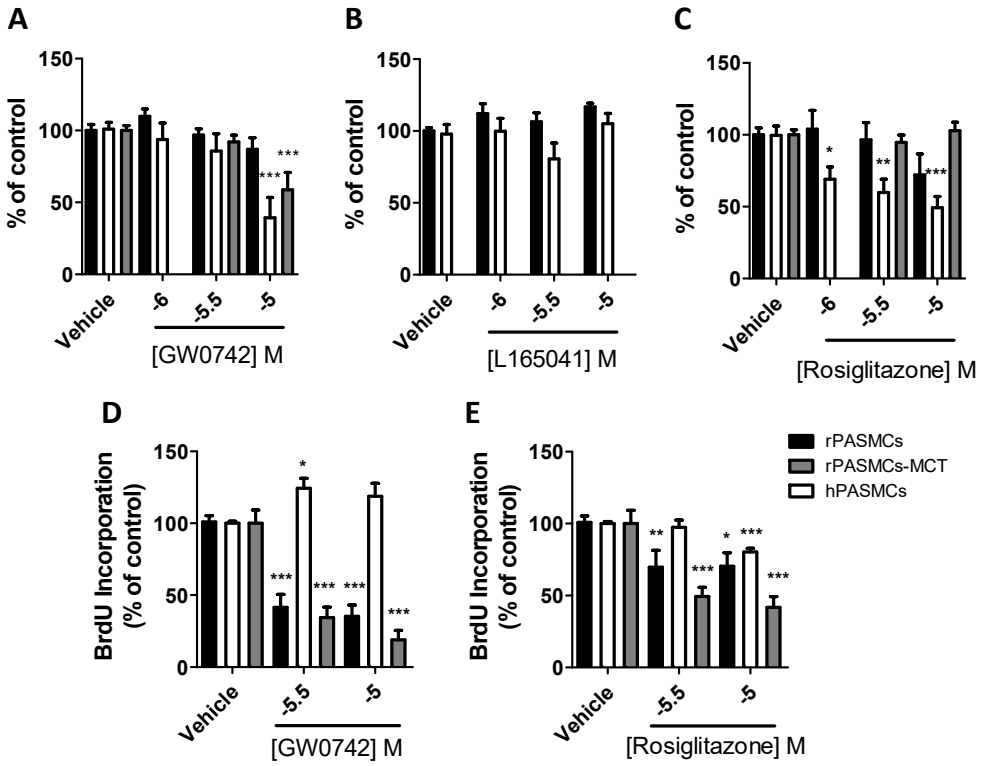

Figure R19. Antiproliferative effects of PPAR agonists in PASMCs*. Concentration-dependent inhibition of cell viability induced by the PPARβ/δ agonists GW0742 (A), and L165041 (B) and the PPARγ agonist rosiglitazone (C) in rPASMCs (black bars), rPASMCs-MCT (grey bars) and hPASMCs cells (white bars) for 48 hours. Concentration-dependent inhibition of BrdU incorporation induced by the PPARβ/δ agonists GW0742 (D) and the PPARγ agonist rosiglitazone (E) in rPASMCs (black bars), rPASMCs-MCT (grey bars) and hPASMCs cells (white bars) for 48 hours. Data represent mean ± SEM of 3-6 experiments performed in triplicate. Results are expressed as % of vehicle (DMSO 0.1%+VC). Drug-induced responses were compared with vehicle using one-way ANOVA followed by Dunnett´s post hoc test. *, ** and *** indicates P<0.05, P< 0.01 and P<0.001, respectively*.

1.3.7. Effects of kinase inhibitors

The ROCK1/2 inhibitor hydroxyfasudil (Figure R20-A) significantly inhibited cell viability, at the highest concentration tested ($3x10^{-5}$ M) in hPASMCs and rPASMCs-MCT. Similarly, this drug inhibited the BrdU incorporation in hPASMCs, whereas, surprisingly, increased their BrdU incorporation in rPASMCs and rPASMCs-MCT (Figure R20-B) at their highest concentration tested. The flavonoid quercetin (Figure R20-C), caused a potent and significant inhibition of the cell viability in a concentration-dependent manner in all cell types. It should be noted that rPASMCs were more sensitive to quercetin than hPASMCs and rPASMCs-MCT. In fact, cell viability was

reduced below baseline values. This flavonoid also inhibited BrdU incorporation in a concentration-dependent manner in all cell types (Figure R19-D). Again, rPASMCs were more sensitive to quercetin than hPASMCs and rPASMCs-MCT.

The TAK-1 inhibitor, 5z-7-oxozeaenol markedly inhibited cell viability (Figure R20-E) and BrdU incorporation (Figure R20-F) in a concentration-dependent manner in all cells tested. Finally, the tyrosine kinase inhibitor imatinib caused a potent inhibition of cell viability (Figure R20-G) in all cell types butin rPASMCs-MCT the highest concentration of the drug was not tested. Imatinib also inhibited BrdU incorporation (Figure R20-H) in all the cell types, hPASMCs being the least sensitive to the drug.

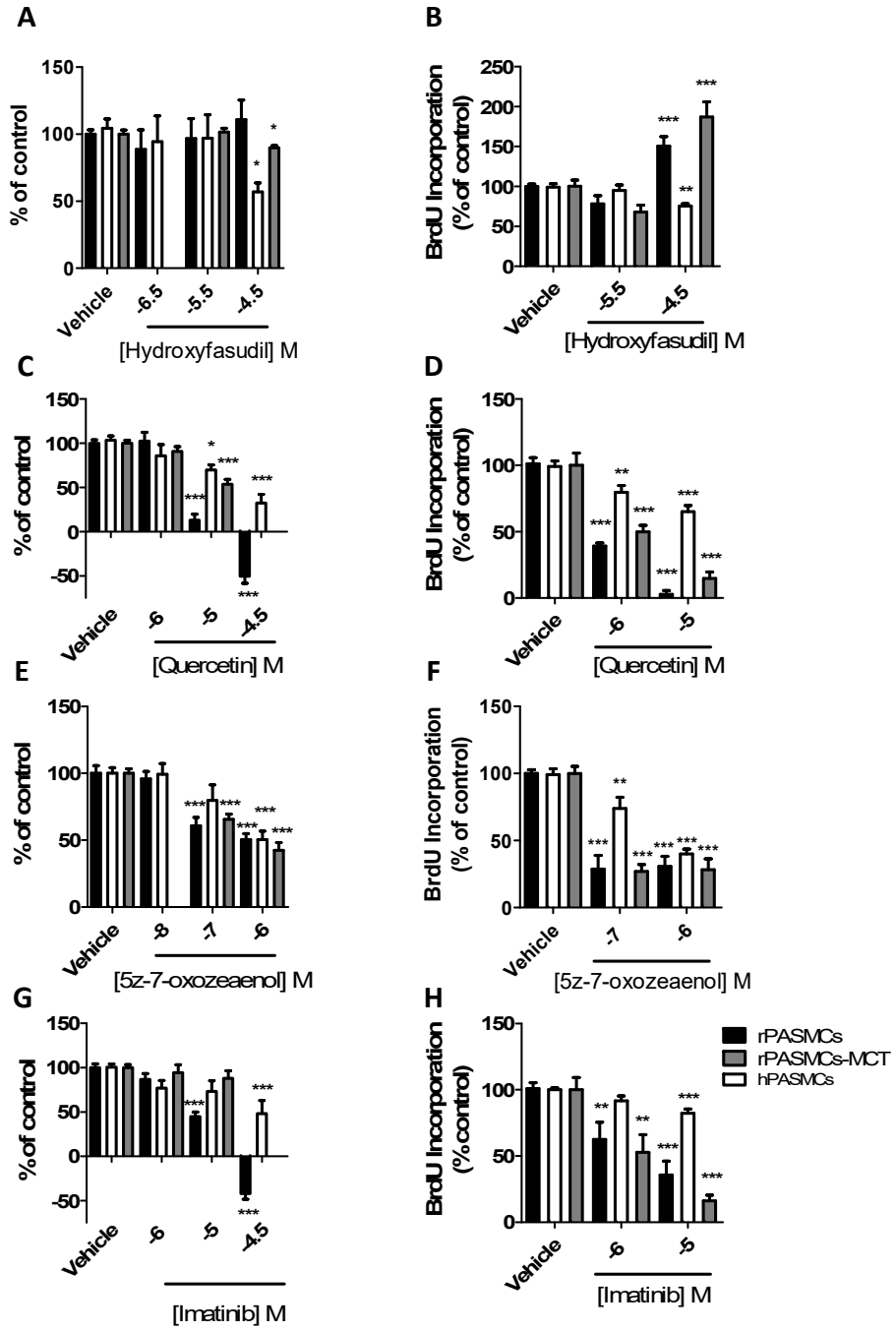

Figure R20: Antiproliferative effects of kinase inhibitors in PASMCs*. Concentration-dependent inhibition of cell viability induced by the ROCK inhibitor hydroxyfasudil (A), the flavonoid quercetin (C) the TAK-1 inhibitor 5z-7-oxozeaenol (E) and the tyr-kinase inhibitor imatinib (G) in rPASMCs (black bars), rPASMCs-MCT (grey bars) and hPASMCs cells (white bars) for 48 hours. Concentration-dependent inhibition of BrdU incorporation induced by the ROCK inhibitor hydroxyfasudil (B), the flavoniod quercetin (D) the TAK-1 inhibitor 5z-7-oxozeaenol (F) and the tyr-kinase inhibitor imatinib (H) in rPASMCs (black bars), rPASMCs-MCT (grey bars) and hPASMCs cells (white bars) for 48 hours. Data represent mean ± SEM of 3-6 experiments performed in triplicate. Results are expressed as % of vehicle (DMSO 0.1%+VC). Drug-induced responses were compared with vehicle using one-way ANOVA followed by Dunnett´s post hoc test. *, ** and *** indicate P<0.05, P< 0.01 and P<0.001, respectively.*

1.3.8. Effects of drugs used for other indications

The calcineurin inhibitor tacrolimus, at the highest concentration tested reduced cell viability (Figure R21-A) and increased BrdU incorporation in rPASMCs (Figure R21-D). In addition, treatment with tacrolimus significantly reduced BrdU incorporation in hPASMCs and rPASMCs-MCT (Figure R21-D), but the effect in rPASMCs-MCT was only observed at the lowest concentration tested. The calcium sentitizer levosimendan (Figure R21-B) significantly inhibited cell viability in a concentration-dependent manner in rPASMCs and rPASMCs-MCT, while the effect in hPAMCs did not reach statistical significance (P=0.08). Treatment with levosimendan (Figure R21-E) only significantly reduced BrdU incorporation in hPASMCs at the highest concentration ($3x10^{-5}$ M), whereas in rPASMCs-MCT, levosimendan significantly increased the BrdU incorporation.

Finally, the $P2Y_1$ receptor agonist 2-MeSADP (Figure R21-C) did not show any effect on cell viability in rPASMCs and hPASMCs.

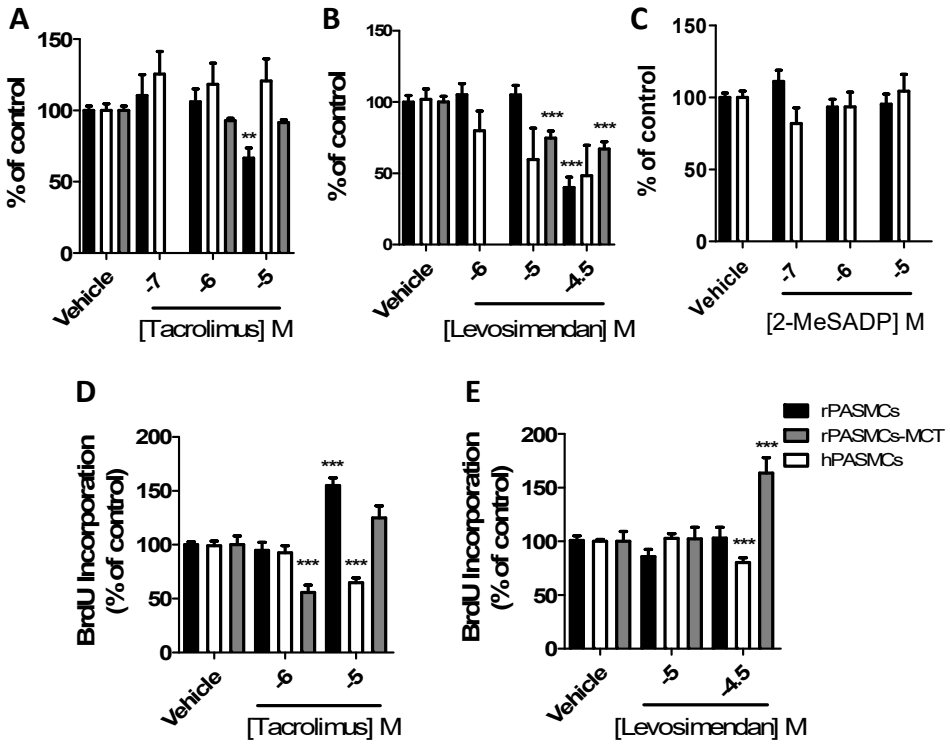

Figure R21: Antiproliferative effects of drugs used for other indications in PASMCs. *Concentration-dependent inhibition of cell viability induced by the calcineurin inhibitor tacrolimus (A), the calcium sentitizer levosimendan (B) and the P2Y1 receptor agonist 2-MeSADP (C) in rPASMCs (black bars), rPASMCs-MCT (grey bars) and hPASMCs cells (white bars) for 48 hours. Concentration-dependent inhibition of BrdU incorporation induced by tacrolimus (D) and levosimendam (E) in rPASMCs (black bars), rPASMCs-MCT (grey bars) and hPASMCs cells (white bars) for 48 hours. Data represent mean ± SEM of 3-6 experiments performed in triplicate. Results are expressed as % of vehicle (DMSO 0.1%+VC). Drug-induced responses were compared with vehicle using one-way ANOVA followed by Dunnett´s post hoc test. *, ** and *** indicate P<0.05, P< 0.01 and P<0.001, respectively.*

In order to compare the relative sensitivity of the drugs tested on cell proliferation we have plotted the effects on cell viability or BrdU incorporation in rat and human cells. (Figures R22 and R23, respectively).

When comparing the effects of the maximum concentration tested for each drug on cell viability in rPASMCs versus hPASMCs it is observed that hPASMCs were more sensitive to the effects of the drugs tested (Figure R22-A); except imatinib (pink diamond), quercetin (pink square), BAY 41-2272 (red triangle), tacrolimus (brown square) and treprostinil (orange diamond) which showed an antiproliferative effects mainly in rPASMCs. In contrast, levosimendan (brown inverted triangle), 5z-7-

oxozeaenol (pink triangle), dipyridamole (blue diamond) and 2-MeSADP (brown triangle) showed similar effects in both cell types. However, when we compared their effects on cell viability in rPASMCs versus rPASMCs-MCT (Figure R22-B), we observed that imatinib, quercetin, tacrolimus and treprostinil showed again higher effects in rPASMCs, while BAY 41-2272, GW0742 (yellow diamond), sildenafil (blue diamond) and tadalafil (blue triengle) exhibited higher effects in rPASMCs-MCT.

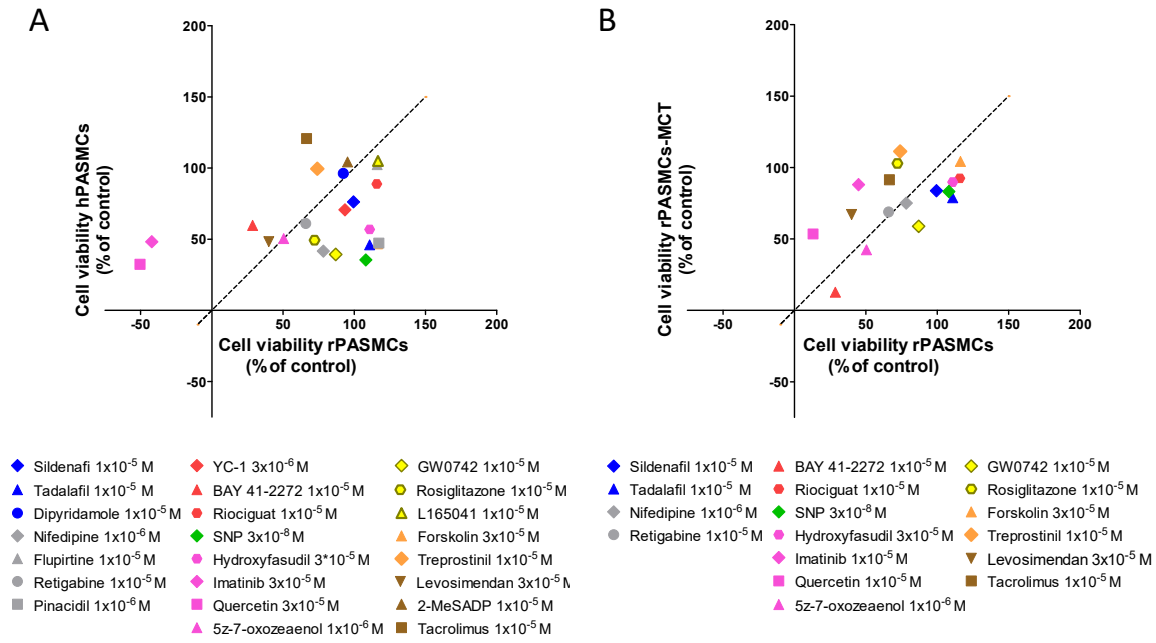

Figure R22: Antiproliferative effects of drugs used measured by MTT. *Comparison of the effects of several vasodilator drugs on cell viability in rPASMCs versus hPASMCs (A) and in rPASMCs versus rPASMCs-MCT (B). Abcissa, % cell viability rPASMCs for or panel A and B; ordinate, % cell viability in hPASMCs (A) and rPASMCs-MCT (B).*

When we examined the effects on BrdU incorporation (Figure R23), most of the drugs showed higher effects in rPASMCs than in hPASMCs (Figure R23-A). However tacrolimus (brown inverted triangle), forskolin (orange triangle) and hydroxyfasudil (pink circle) increased the BrdU incorporation in rPASMCs.

However, when we compared their effects on BrdU incorporation in rPASMCs versus rPASMCs-MCT (Figure R23-B), we observed that, in general, all drugs were more effective in rPASMCs-MCT but again, tacrolimus, forkolin and hydroxyfasudil increased the BrdU incorparion in both cells. Nevertheless, their effects in rPASMCs-MCT were more marked than in rPASMCs.

Therefore, our data on BrdU incorporation suggest that drugs tested were more effective in rPASMCs than in hPASMCs, although, in general, they were more effective in rPASMCs-MCT.

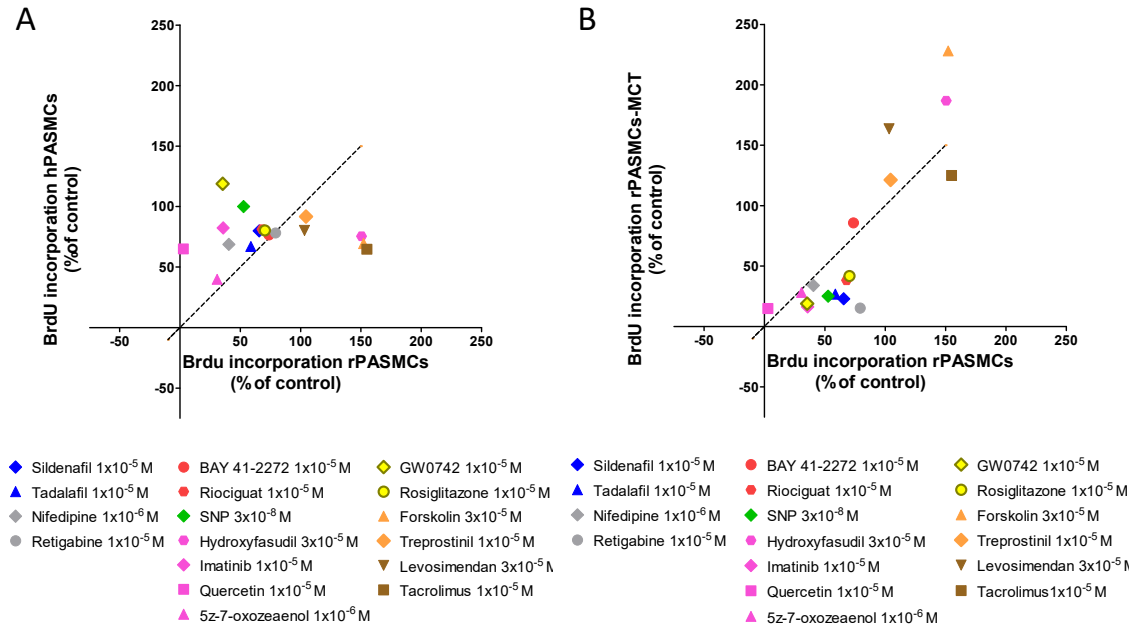

***Figure R23**: **Antiproliferative effects of drugs used measured by BrdU incorporation**. Comparison of the effects of several vasodilator drugs on BrdU incorporation in rPASMCs versus hPASMCs (A) and in rPASMCs versus rPASMCs-MCT (B). Abcissa, % BrdU incorporation in rPASMCs for or panel A and B; ordinate, % BrdU incorporation in hPASMCs (A) and rPASMCs-MCT (B).*

2. Vasodilator versus anti-proliferative effects.

In order to compare the relative potency of the drugs on vasodilation and proliferation we have plotted the vasodilator effects (abscissa axis) versus cell viability or BrdU incorporation (ordinate axis) in rat and human cells and tissues (Figures R24 and R25, respectively). A dotted line was drawn from 0 to 100%. Thus, drugs appearing below the line act mainly as are vasodilators, while drugs appearing above the line are essentially antiproliferative. Drugs within the same class are depicted with the same color.

When comparing the effects of the maximum concentration tested for each drug on vascular reactivity versus cell viability in rat arteries and cells it is observed that most

of the drugs tested act as vasodilators (Figure R24-A); except imatinib (pink diamond), quercetin (pink square) and 5z-7-oxozeaenol (pink triangle), rosiglitazone (yellow circle) and the retigabine (grey circle) which showed an antiproliferative profile. In contrast, levosimendan (brown inverted triangle) showed a similar profile as vasodilator and antiproliferative drug. However, when we compared their effects on vascular reactivity versus BrdU incorporation (Figure R24-B), we observed that the kinase inhibitors imatinib, quercetin and 5z-7-oxozeaenol showed again a behavior as antiproliferative, while nifedipine (grey diamond), GW0742 (yellow diamond), sildenafil (blue diamond) and SNP (green diamond) exhibited a similar profile as vasodilator and antiproliferative drug.

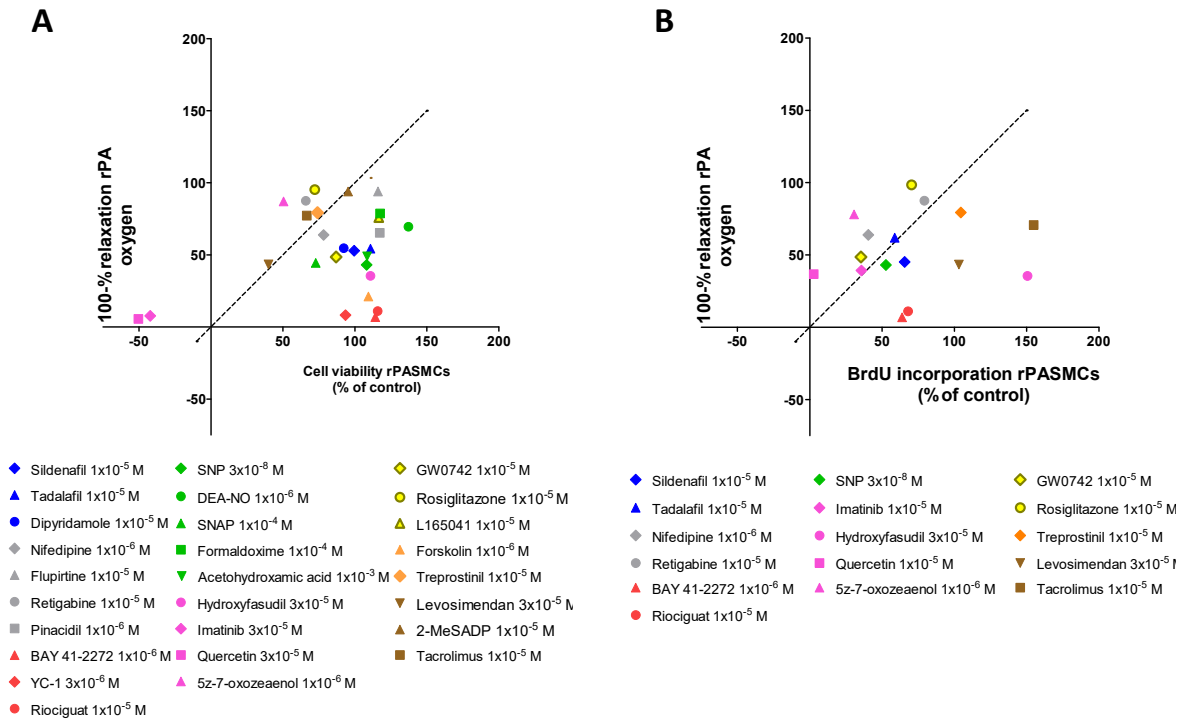

Figure R24. Vasodilator versus antiproliferative effects*. Comparison of the effects of several vasodilator drugs on contractile tone in rat pulmonary arteries bubbled with 95% O_2-5% CO_2 (PA oxygen) versus cell viability (A) and BrdU incorporation (B) in rPASMCs. Abcissa, % cell viability or % BrdU incorporation ordinate, vasodilatation on PA (100 -% relaxation).*

Figure R25 shows that in human arteries and cells, most of the drugs also behave mainly as vasodilators, either comparing their effects on vascular reactivity versus cell viability (Figure R25-A) or BrdU incorporation (Figure R25-B). Similar to in the rat

tissues, the kinase inhibitors imatinib and quercetin showed a behavior as antiproliferative drugs.

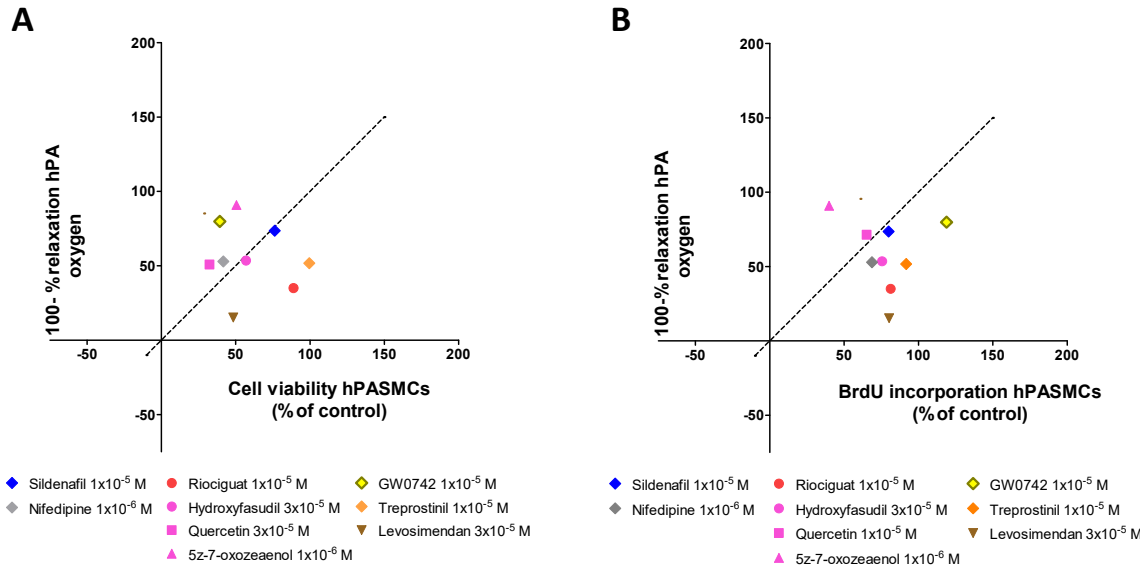

Figure R25. Vasodilator versus antiproliferative effects*. Comparison of the effects of several vasodilator drugs on contractile tone in human pulmonary arteries bubbled with 95% O_2-5% CO_2 (PA oxygen) versus cell viability (A) and BrdU incorporation (B) in hPASMCs. Abcissa, % cell viability or % BrdU incorporation ordinate, vasodilatation on PA (100 -% relaxation).*

The vasodilator/antiproliferative profile for each family of drugs separately is shown in figures R26 and R27. The comparison of the effects of several concentrations of each drug on vascular reactivity versus cell viability revealed a similar profile among their different members (Figure R26). PDE5 inhibitors (Figure R26-A), sGC stimulators (Figure R26-B), drugs targeting ion channels (Figure R26-C), NO donors (Figure R26-D), the PPARβ/δ agonist GW0742 (Figure R26-E), the ROCK1/2 inhibitor hydroxyfasudil (Figure R26-F), the adenylate cyclase activators (Figure R26-G) forskolin and the calcium sentitizer levosimendan (Figure R26-H) showed a preferential vasodilator profile. In contrat, the kinase inhibitors imatinib, quercetin and 5z-7-oxozeaenol (Figure R26-F), the PPARγ agonist rosiglitazone (Figure R26-E) and the Kv7channels agonist retibabine (Figure R26-C) showed essentially an antiproliferative profile.

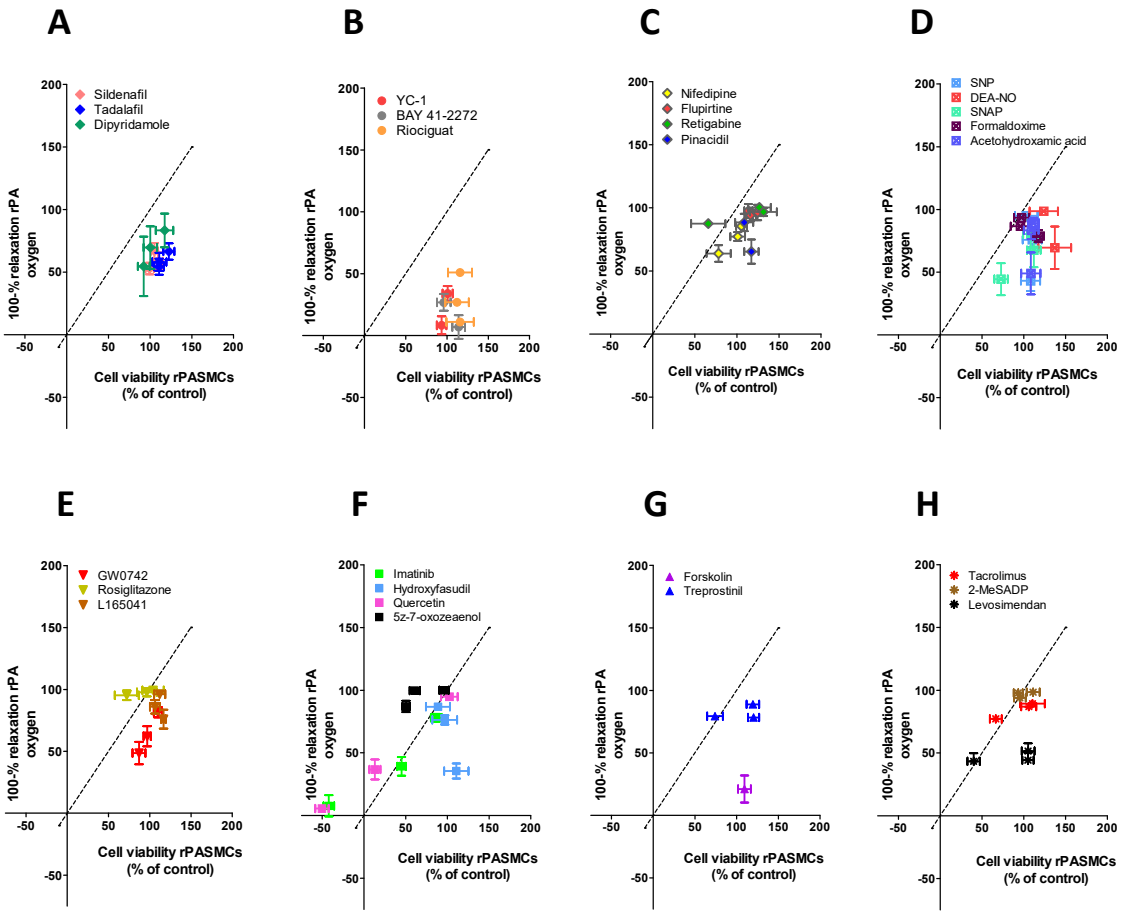

Figure R26: Vasodilator versus antiproliferative effects*. Comparison of the effects of PDE5 inhibitors (A), sGC stimulators (B), drugs targeting ion channels (C), NO donors (D), PPAR agonists (E), kinases inhibitors (F), adenylate cyclase activators (G) and drugs used for other indications (H) on contractile tone in rat pulmonary arteries under high oxygen (PA oxygen) versus cell viability in rPASMCs. Abcissa, % cell viability, ordinate, vasodilatation on rPA (100 -% relaxation).*

When we examined the effects on vascular reactivity versus BrdU incorporation (Figure R27), most of the drug classes showed again a vasodilator profile. In general, all drugs were more effective on BrdU incorporation than on the MTT test. Therefore, drugs classified as preferential vasodilators based on the MTT test such as PDE5 inhibitors (Figure R27-A), drugs targeting ion channels (Figure R27-C), NO donors (Figure R27-D) and PPAR agonists (Figure R27-E) should be considered equally vasodilators and antiproliferative agents.

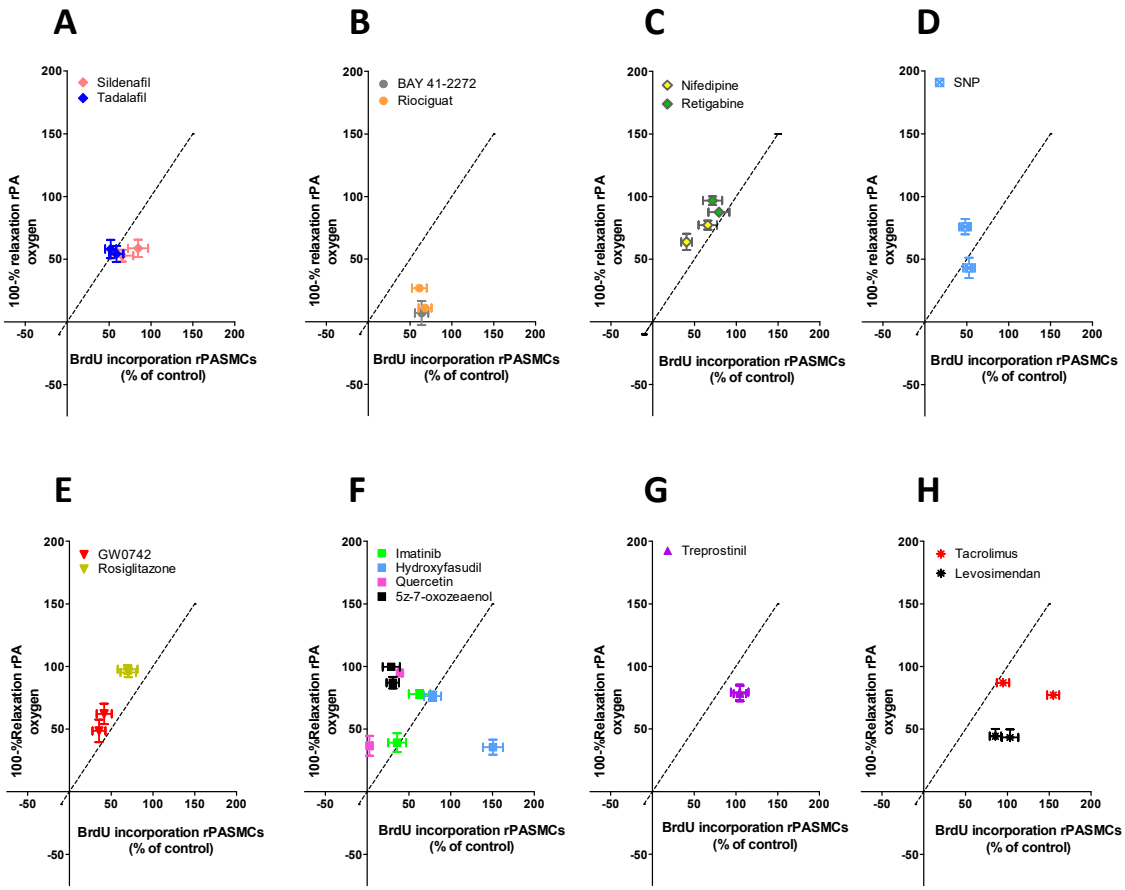

Figure R27: Vasodilator versus antiproliferative effect*. Comparison of the effects of PDE5 inhibitors (A), sGC stimulators (B), drugs targeting ion channels (C), NO donors (D), PPAR agonists (E), kinases inhibitors (F), adenylate cyclase activators (G) and drugs used for other indications (H) on contractile tone in rat pulmonary arteries under high oxygen (PA oxygen) versus BrdU incorporation in rPASMCs. Abcissa, % BrdU incorporation, ordinate, vasodilatation on rPA (100 -% relaxation).*

CHAPTER 2

3. Effects of riociguat and sildenafil on ventilation-perfusion coupling in rat lungs

3.1. Sildenafil and riociguat inhibited the vasoconstriction induced by hypoxia and U46619 in isolated PA

Intrapulmonary artery rings from rats were bubbled with 21%O_2, 74%N_2 and 5% CO_2 and firstly stimulated with KCl (80 mM) to determine the maximum response of the artery rings. After a period of stabilization, PAs were exposed to acute hypoxia (95% N_2 and 5% CO_2, yielding approx. 2-4% O_2 in the buffer due to contact with room air) for 15 minutes leading to a contractile response. Following this first hypoxic challenge, PAs were returned to normoxia and treated in the absence (vehicle) or in the presence of the PDE5 inhibitor sildenafil (10^{-7} M) or the sGC stimulator riociguat (10^{-7} M) and exposed to hypoxia again. Both treatments reduced the hypoxic pulmonary vasoconstriction (HPV, Figure R28-A and B) compared to the vehicle. After returning to normoxia, PAs were exposed to the thromboxane A_2 mimetic U46619 (10^{-7} M). Similar to HPV, the contraction induced by U46619 was inhibited by riociguat and sildenafil (Figure 28-C).

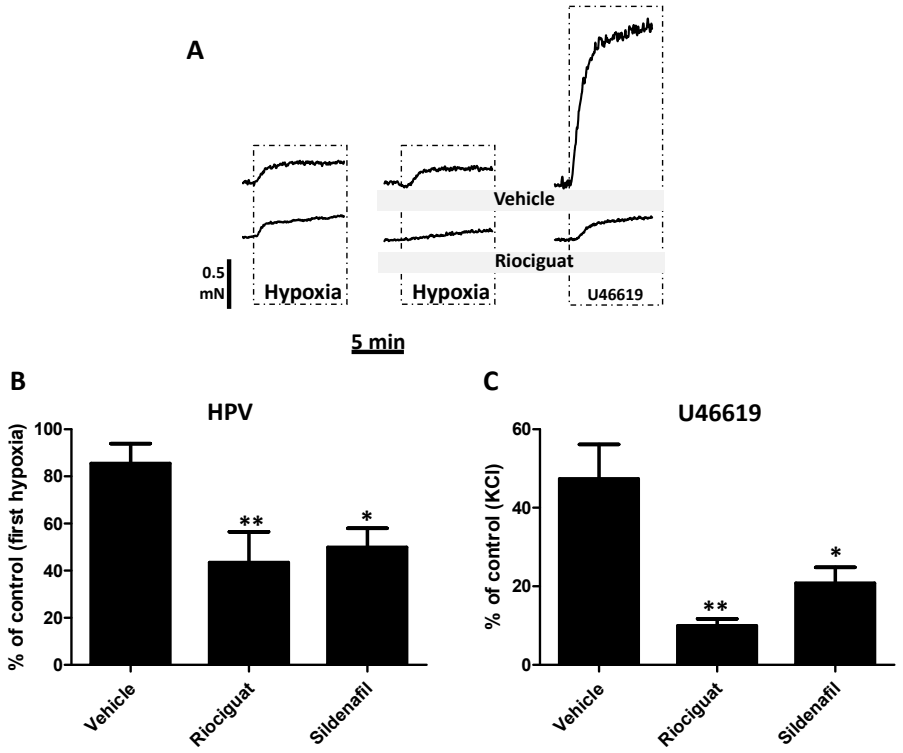

Figure 28: Effect of riociguat and sildenafil on HPV and on U46619-induced vasoconstriction in isolated rat PA. *Representative traces (A) and average values of (B) HPV and (C) U46619 responses in the absence (vehicle) or in the presence of either riociguat or sildenafil. Data are expressed as a percentage of an initial response to the first hypoxia or KCl and shown as means ± SEM (n = 8-12). Data were analyzed using a one-way ANOVA followed by Bonferroni post hoc tests. *P<0.05 and **P < 0.01 versus vehicle*.

3.2. Response of riociguat and sildenafil on systemic and pulmonary arterial pressure and oxygen saturation in response to global and unilateral hypoxia and U46619.

In another set of experiments we assessed the *in vivo* effects of sildenafil and riociguat. Animals were initially switched from normoxia (21% O_2) to global hypoxia (10% O_2, I, GH) for 5 minutes, which caused a characteristic increase in mean PAP as a result of a HPV response (Figure R29-D). This was accompanied by a decrease in mean SAP (Figure R29-C) and in SO_2 (Figure R29-B), whereas no changes were observed in HR (Figure R29-A). These responses were reversed when returning to normoxia. After a 20 minutes stabilization period, rats were exposed to unilateral hypoxia by obstruction of the left bronchi for 5 minutes (II, UH), which caused a similar effect that GH, with an increase in mean PAP, a decrease in mean SAP and a decrease in the SO_2. Following

another 20 minutes stabilization period, animals were treated with vehicle (DMSO 500 µL), sildenafil (0.5 mg/kg) or riociguat (0.1 mg/kg) for 15 minutes before an additional exposure to GH and UH. Vehicle had no significant effects on mean PAP or mean SAP and did not modify either the global or unilateral hypoxic response (Figure R29-C-D and R30A-B). Administration of riociguat and sildenafil produced minimal changes in mean PAP (Figure R29-D) but riociguat significantly reduced mean SAP (Figure R29-C).

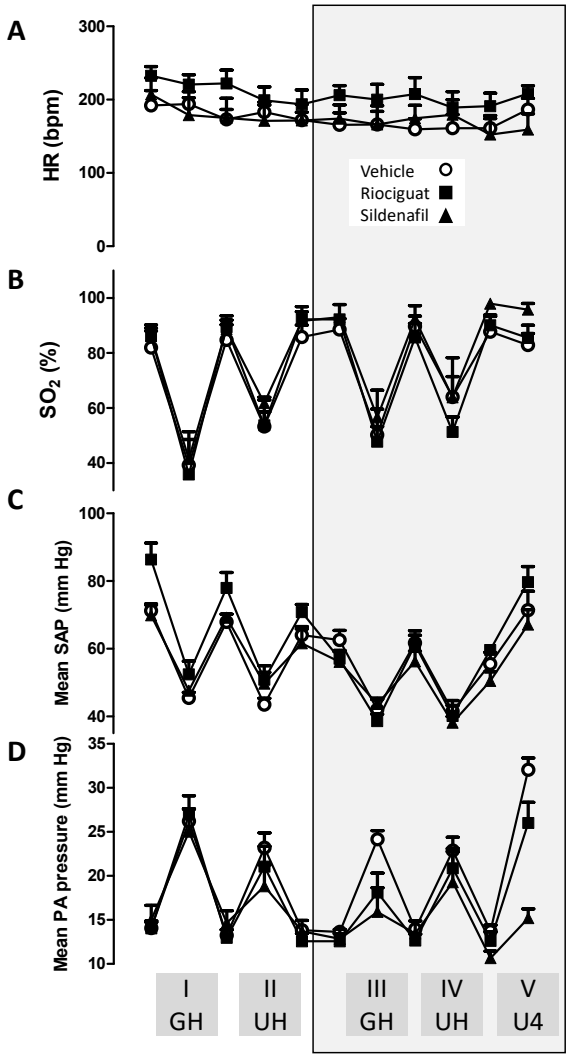

Figure R29: Hemodynamic changes in response to global, unilateral hypoxia and U46619 in anesthetized rats*. Changes in (A) heart rate (HR), (B) oxygen saturation (SO_2), (C) mean systemic arterial pressure (mSAP) and (D) mean pulmonary arterial pressure (mPAP) during the course of the different experimental groups (vehicle, riociguat (0.1 mg/kg) or sildenafil (0.5 mg/kg)). Data are shown after each exposure to global hypoxia (GH) and by unilateral hypoxia (UH) induced by obstruction of the left bronchi and, finally the thromboxane A_2 mimetic U46619 (U4) administration. The grey box indicates the protocols performed in the presence of vehicle or drugs.*

Both drugs significantly inhibited the increase in mean PAP induced by GH, whereas the response to UH was preserved (Figure R30-A). In addition, the drugs did not affect the changes in SO_2 induced by GH or UH (Figure R30-B). As expected, both riociguat and sildenafil induced a reduction on mean SAP (Figure R30-C), although only the effect of riociguat reached statistical significance. Interestingly, both drugs showed a pulmonary selective inhibition of U46619-induced responses, which was stronger for sildenafil than for riociguat (Figure R30-D). The drugs had no significant effect on the systemic hypotension induced by either global or unilateral hypoxia or on heart rate (Figure R29).

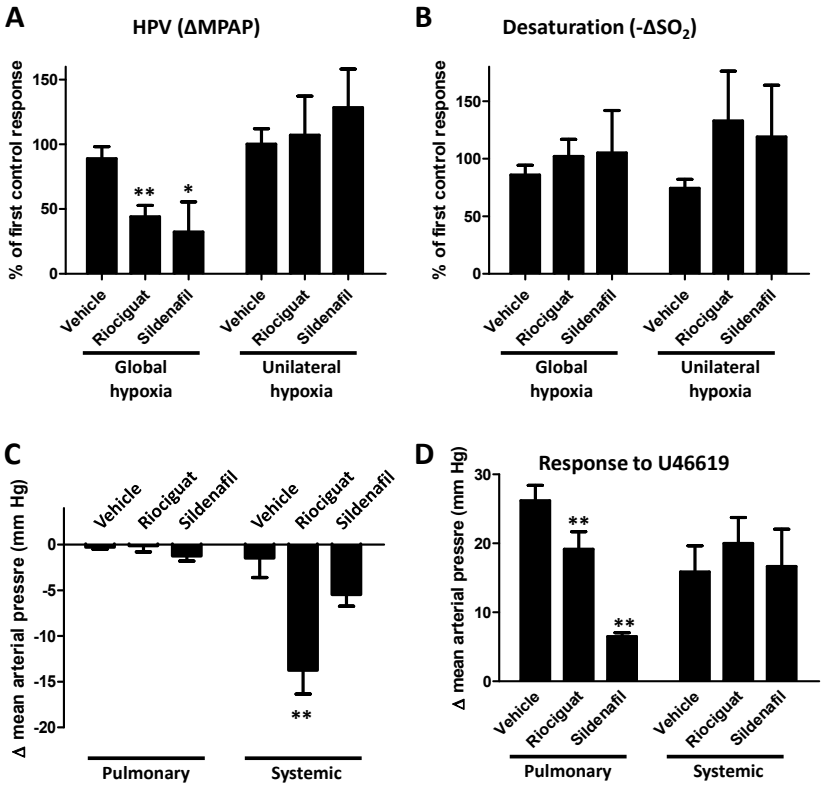

Figure R30. Effects of riociguat and sildenafil on the responses induced by global and unilateral hypoxia, and U46619 in anesthetized rats. *Average values of the (A) hypoxic pulmonary vasoconstriction (HPV) and (B) oxygen saturation (SO_2) in response to either global (left columns) or unilateral (right columns) hypoxia in the presence of vehicle (DMSO), riociguat (0.1 mg/kg) or sildenafil (0.5 mg/kg). Results are expressed as a percentage of the first exposition. Effects of vehicle (DMSO), riociguat (0.1 mg/kg) or sildenafil (0.5 mg/kg) on basal (C) or U46619-induced responses (D) in mean pulmonary and systemic pressures. Results are means ± SEM (n = 4-6). Data were analyzed using a one-way ANOVA followed by Bonferroni post hoc tests. *P<0.05 and **P < 0.01 versus vehicle.*

3.3. Effects on ventilation-perfusion mismatch in fibrotic rats

In order to analyze the effects of the drugs on ventilation and perfusion (V/Q) rats were given saline (control) or bleomycin (to induce pulmonary fibrosis and PH) intratracheally. Three weeks after bleomycin or vehicle administration, ventilation and perfusion were analyzed by SPECT imaging. Ventilation images were taken after breathing DTPA-^{99m}Tc, and perfusion images were taken after perfusing MAA-^{99m}Tc. As expected, ventilation, perfusion and the V/Q ratio was clearly impaired in the lungs of bleomycin-treated rats as compared to control animals (Figure R31). Acute administration of riociguat (0.1 mg/kg) or sildenafil (0.5 mg/kg) in control animals did not show significant effects on ventilation, perfusion or the V/Q ratio (Figure 31-A, B and C). In addition, acute administration of riociguat or sildenafil on bleomycin-treated rats did not modify the ventilation, perfusion and the V/Q ratio (Figure R31-A, B and C).

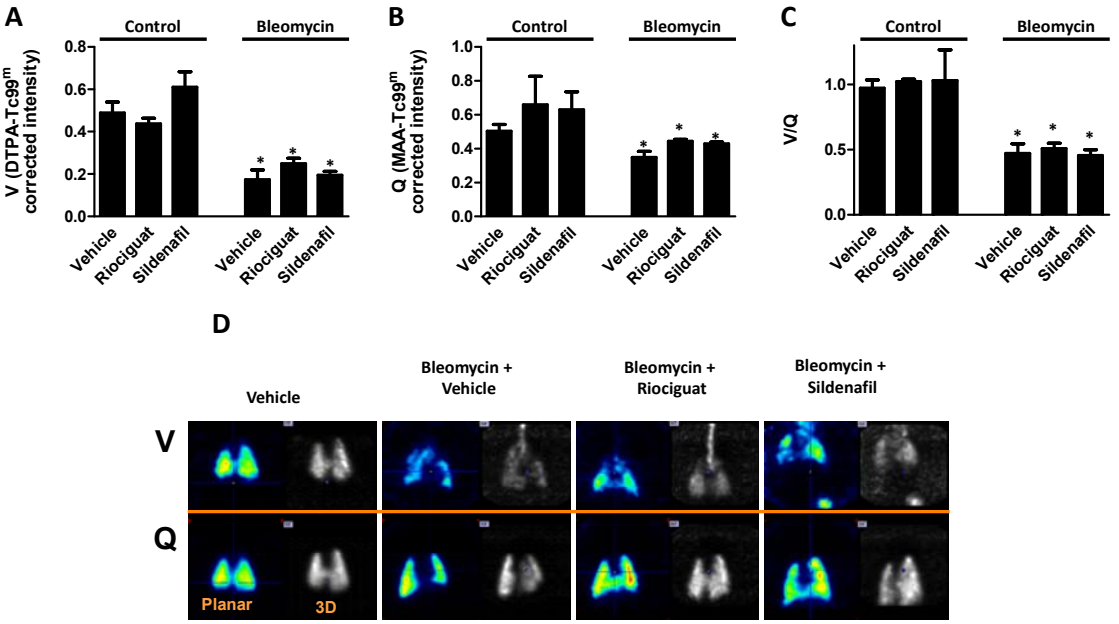

Figure R31. Effects of riociguat (0.1 mg/kg) and sildenafil (0.5 mg/kg) on ventilation, perfusion and ventilation-perfusion coupling in a rat model of pulmonary fibrosis-associated with bleomycin-induced pulmonary hypertension. *Average values of radiation intensity of (A) ventilation signal, (B) perfusion signal and the (C) ventilation-perfusion ratio. (D) Representative images of ventilation and perfusion were obtained by micro-CT-SPECT. Results are means ± SEM (n = 8). Data were analyzed using a one-way ANOVA followed by Bonferroni post hoc tests. *P<0.05 and #P < 0.05 versus vehicle.*

CHAPTER 3

4. The flavonoid quercetin reverses monocrotaline-induced pulmonary hypertension in rats.

4.1. Survival, pulmonary artery pressure and right ventricular hypertrophy

All animals were healthy at baseline. Four out of 35 rats treated with MCT died within the first three weeks, i.e. before randomization to quercetin-vehicle (Figure R32-A). Only 8 of the 18 MCT-treated rats assigned to vehicle treatment survived until the end of the experiment and PAP could only be recorded in 4 of them because the rest died during the anesthesia or surgery. These latter rats were not included in the mortality analysis but their organs and tissues were immediately dissected for further use. Four out of 13 monocrotaline treated rats died during the treatment with quercetin. The Kaplan-Meier analysis (Figure R32-B) shows that quercetin produced a significant increase in survival.

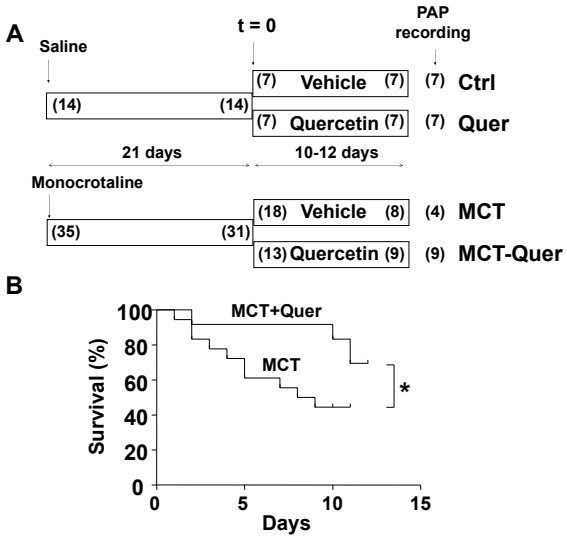

Figure R32. Quercetin increases survival. *(A) Study protocol. Numbers in parenthesis indicate the number of rats which started and finished each period. The numbers at the far right indicate the number of rats in which pulmonary arterial pressure could be recorded; the missing animals in the monocrotaline (MCT) group died during the anesthesia or surgery. (B) Kaplan-Meier analysis of survival in rats treated with monocrotaline and monocrotaline plus quercetin (Quer). * indicates P<0.05.*

Monocrotaline produced significant increases in RVSP, RVDP, SPAP, DPAP and MPAP (Figure R33). Therefore, as expected, monocrotaline treated rats developed pulmonary hypertension, with mean PAP values of 45.2±7.1 mmHg (vs. 13.6±0.6 mmHg in controls). An oral daily dose of quercetin starting three weeks after monocrotaline significantly reduced these parameters (except for RVDP) with mean PAP values of 29.7±5.9 mmHg, which were still significantly above control values. The HR was similar in all experimental groups.

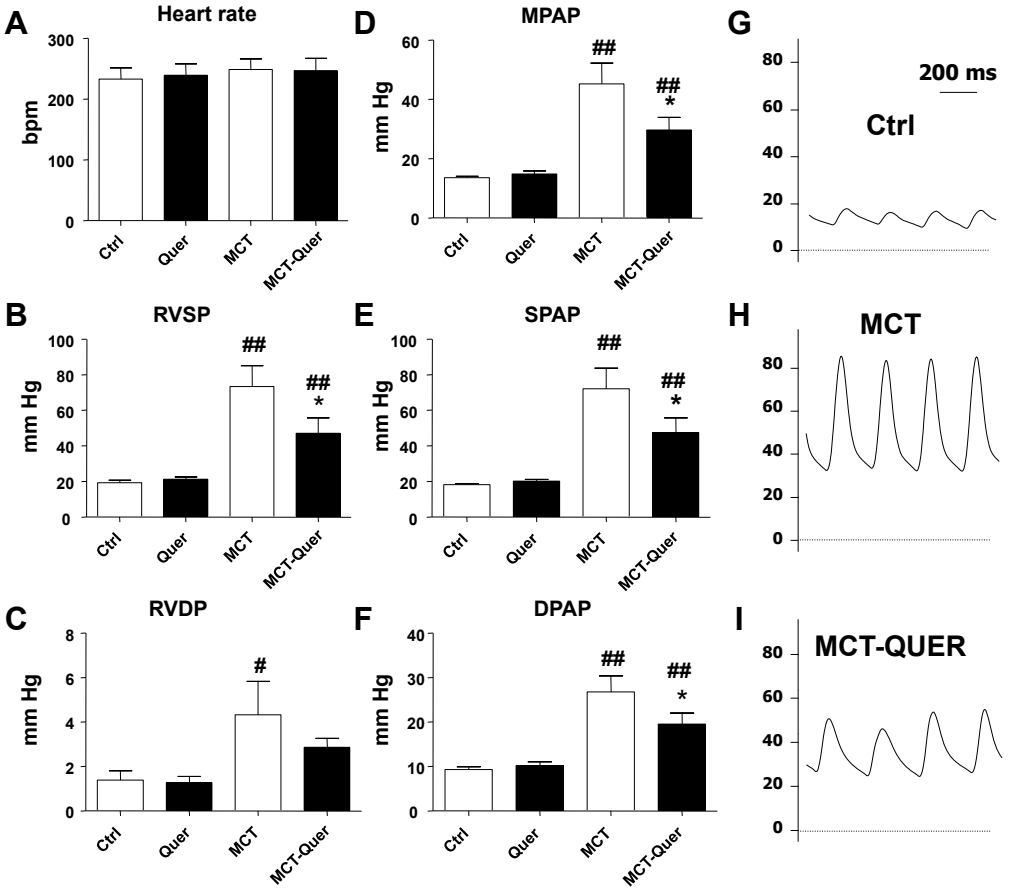

Figure R33. Quercetin reduces pulmonary artery pressure. *Heart rate (A), right systolic (B) and diastolic (C) ventricular pressure, mean (D), systolic (E) and diastolic (F) pulmonary arterial pressure. Panels G, H, I show pulmonary artery pressure recordings in the control (Ctrl), monocrotaline (MCT) and monocrotaline plus quercetin (Quer) group, respectively. Results are means ± SEM of 4-9 animals, * indicates P<0.05 versus MCT and $^{\#}$P<0.05, $^{\#\#}$ P<0.01 versus Ctrl.*

Accordingly with hemodynamic changes observed, rats treated with monocrotaline developed a marked right ventricular hypertrophy as shown by the increased RV weight referred either to the LV+S weight or to BW (Figure R34-A and B). Quercetin significantly reduced both parameters but again they were still significantly above controls.

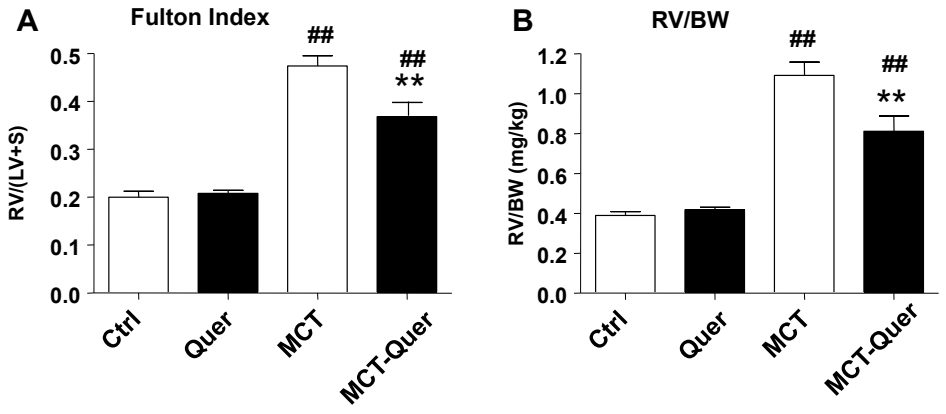

Figure R34. Quercetin reduces right ventricular hypertrophy. *(A) Fulton index [RV/(LV + S) ratio]. (B) Right ventricular weight relative to body weight (RV/BW). Panels A and B each column represents the mean ± SEM of 7-9 animals. ** indicates P < 0.01 versus monocrotaline (MCT) and ## indicates P<0.01 versus control (Ctrl).*

4.2. Histological changes

We investigated the wall thickness in small PA (25–100 μm) observed in lung sections, which were classified as muscular, partially muscular and non-muscular arteries (Figures R35-A and B). The histological studies showed that MCT increased the percentage of muscular arteries, with a corresponding decrease in partially muscular and non-muscular arteries. The treatment with quercetin resulted in a partial prevention of MCT-induced vascular remodelling ($P < 0.01$).

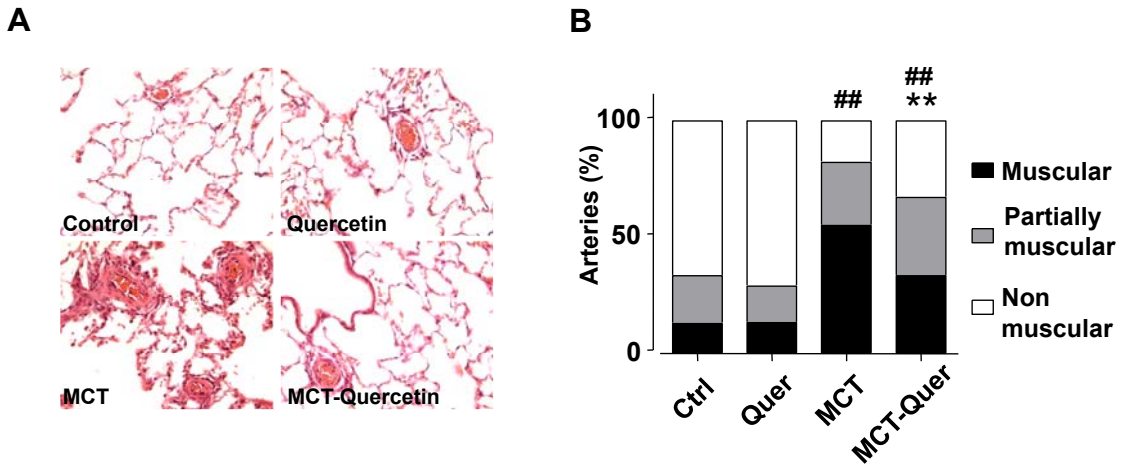

Figure R35. Quercetin reduces vascular remodelling. *(A) Representative images of lung histology. (B) Percentage of muscular, partially muscular and non-muscular arteries in different groups. For panel B, between 26 and 110 arteries (25–100 µm) were analyzed in cross-sections of lungs (stained with haematoxylin and eosin) from at least four animals in each group. ** indicates P < 0.01 versus monocrotaline (MCT) and ## indicates P<0.01 versus control (Ctrl).*

4.3. K_V currents and membrane potential

In freshly isolated PASMC, membrane capacitance, an estimate of membrane surface, was significantly increased in MCT treated rats compared with control animals. Quercetin was not able to restore this increase (Figure R36-A). Furthermore, MCT also induced a significant decrease in the amplitude of the K_V currents and membrane depolarization. In this case, quercetin significantly reversed the inhibition of the K_V currents but it had no significant effect on membrane potential (Figure R36-B and R36-C).

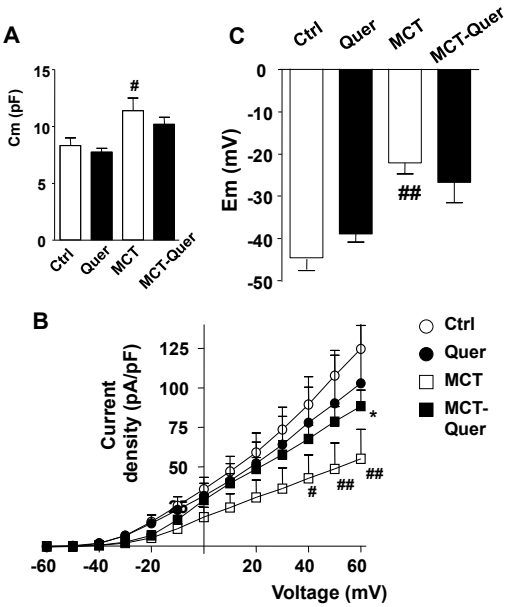

Figure R36. Quercetin prevents the inhibition of Kv currents*. (A) Cell capacitance (Cm). (B) Current–voltage relationships measured at the end of the pulse. (C) Membrane potential (Em). * indicates P<0.05 versus monocrotaline (MCT). # and ## indicate P<0.05 and P< 0.01 versus control (Ctrl). Each column or symbol represents the mean value ± SEM (n = 4–6).*

4.4. BMPR2, survivin, $5HT_{2A}$ receptor, iNOS, and Kv channels expression.

We examined the gene expression in whole lung homogenates of key proteins involved in PAH. BMPR2, Kv1.5 and Kv2.1 were strongly downregulated by monocrotaline (Figure R37). The difference in expression of these genes in the monocrotaline plus quercetin vs monocrotaline group was not statistically significant. The expression of survivin and $5HT_{2A}$ mRNA was significantly increased by monocrotaline, and quercetin was able to reverse the latter change. However, changes in survivin protein expression (Figure R38) were smaller and not significant among groups. The mRNA expression of iNOS in whole lung was highly variable in the monocrotaline group; despite a trend for increased expression in the monocrotaline group the ANOVA did not yield significant differences. Thus, we analyzed the mRNA expression of iNOS in homogenates from isolated pulmonary arteries. In this tissue, iNOS mRNA was significantly increased by monocrotaline (2.4 ±0.7 fold) and this effect was inhibited by quercetin (1.02 ±0.6).

Despite a positive trend, the changes in expression of Kv7.1 and Kv7.5 in whole lung were not statistically different among groups.

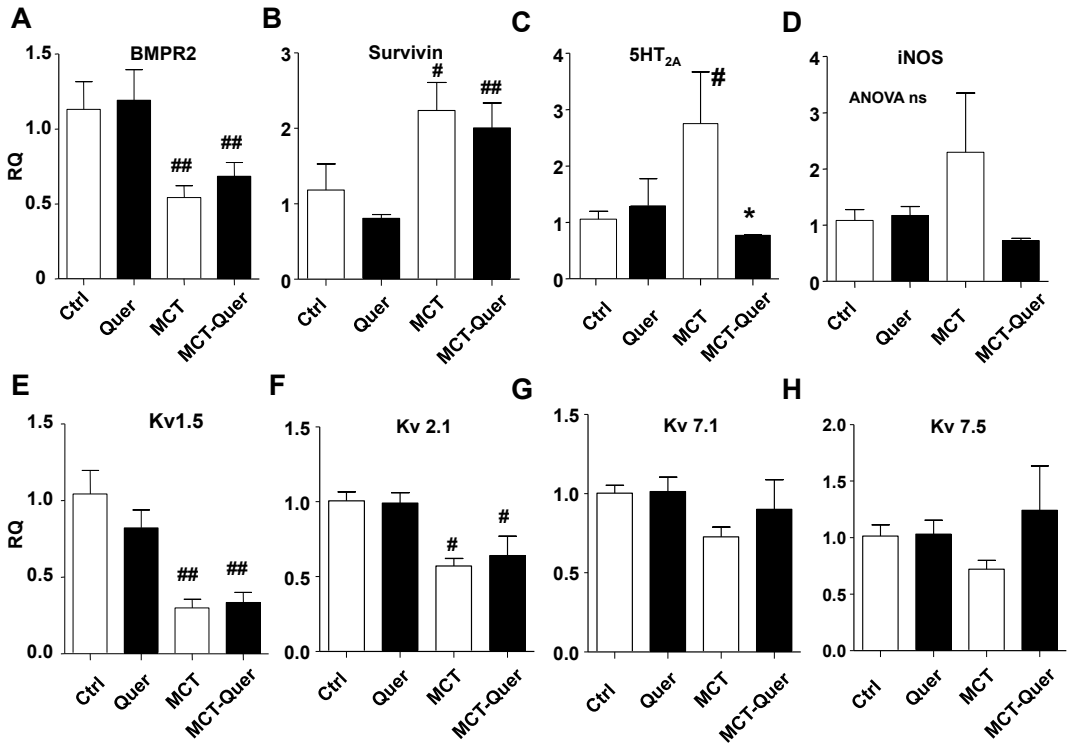

Figure R37: Changes in lung expression of (A) BMPRII, (B) Survivin, (C) 5HT2A, (D) iNOS, (E) Kv1.5, (F) Kv2.1, (G) Kv7.1 and (H) Kv7.5 mRNA by RT-PCR. *Results are means ± SEM of 4-8 animals normalized by the expression of β-actin. * indicates P<0.05 versus monocrotaline (MCT), # and ## P<0.05 and P< 0.01 versus control (Ctrl).*

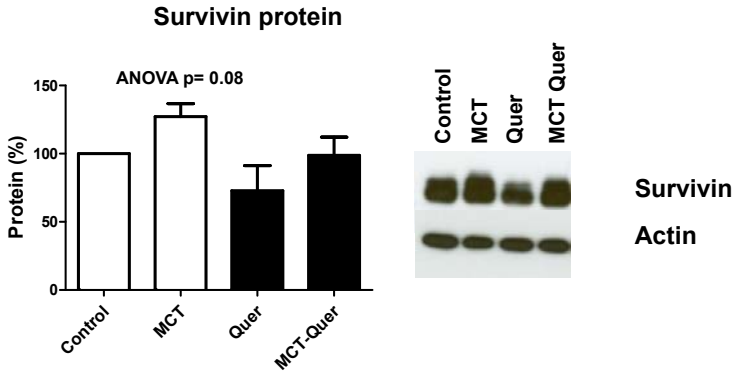

Figure R38: Changes in the expression of survivin at the protein level . *Lung homogenates were analyzed by Western blot. Results are means ± SEM of 5-8 animals. Protein levels were normalized by the expression of β-actin.*

4.5. Vascular dysfunction

Monocrotaline significantly decreased the maximal relaxation evoked by acetylcholine in isolated rat pulmonary arteries (Figure R39-A) and no changes were found in rats treated with quercetin. The endothelial dysfunction was accompanied by a reduction in the expression of eNOS which again was not reverted by quercetin (Figure R39-B). Monocrotaline also produced a significant hyperresponsiveness of pulmonary arteries to 5-HT (E_{max} values of 102 ± 3% of the response to KCl vs 35 ± 1% in control) and quercetin again was not able to prevent it (98 ± 1%) (Figure R39-C).

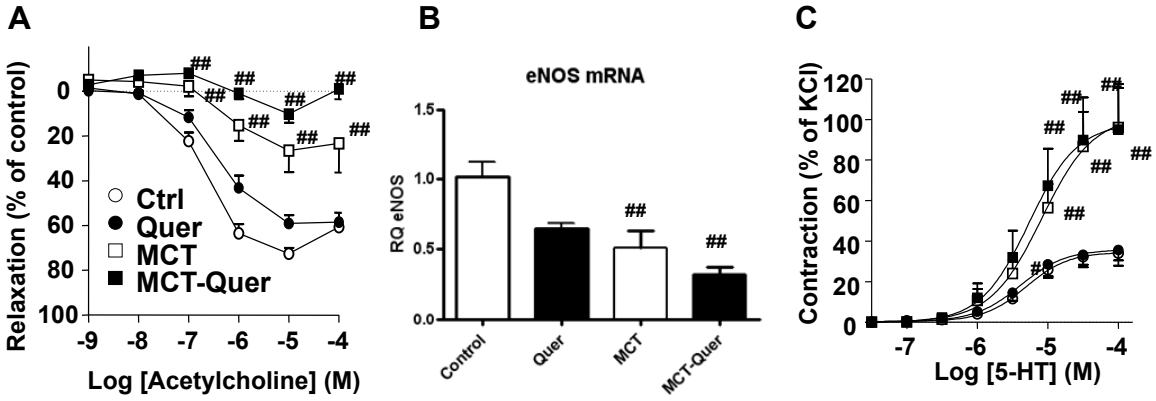

Figure R39: Quercetin (Quer) does not prevent vascular dysfunction*. (A) Relaxant effects of pulmonary arteries to the endothelium-dependent vasodilator acetylcholine in pulmonary arteries stimulated with phenylephrine. (B) Expression of eNOS in pulmonary arteries homogenates analyzed by RT-PCR. (C) Contractile responses to 5-HT in pulmonary arteries expressed as a percent of a previous response to KCl. Results are means ± SEM of 4-9 experiments. Results are means ± SEM of 4-8 animals normalized by the expression of β-actin. * indicates P<0.05 versus monocrotaline (MCT), # and ## P<0.05 and P< 0.01 versus control (Ctrl).*

4.6. Vasodilator effects

In isolated PA from control rats mounted in a myograph, exposure to U46619 induced a sustained contraction which was fully relaxed by quercetin in a concentration-dependent manner ($LogIC_{50}$ = -5.26±0.06, E_{max}= 106±3%, Figure R40-A). In PA from monocrotaline-treated rats stimulated with U46619, quercetin induced a similar vasodilator effect ($LogIC_{50}$ = -5.12±0.17, E_{max}= 111±4%, Figure R40-A) which was not modified by exposing the arteries to hypoxia ($LogIC_{50}$ = -5.36±0.11, E_{max}= 120±9%, Figure R40-B).

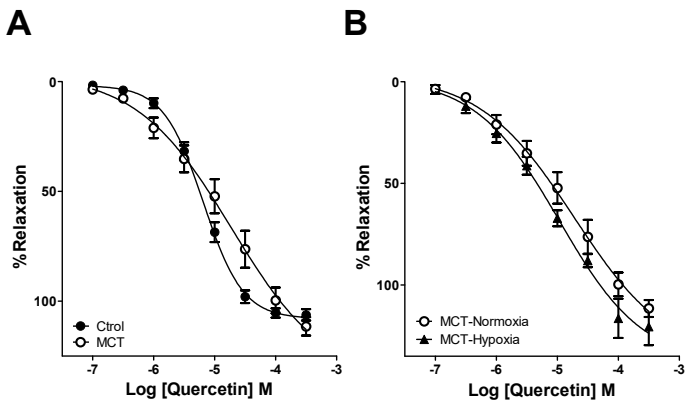

Figure R40. Quercetin induces vasodilator effects in isolated pulmonary arteries*. PA from (A) control and (A and B) monocrotaline-treated rats were mounted in a wire myograph, stimulated by U46619 (100 nM) and were relaxed by cumulative addition of quercetin. Panel A shows experiments performed in normoxic conditions in the control and monocrotaline-treated rats. In panel B arteries from monocrotaline-treated animals were bubbled with 21% O_2-5%CO_2 (normoxia) or 95% N_2-5%CO_2 (hypoxia).*

4.7. Expression of MAPK and Akt pathways

Despite an apparent increase in phosphoERK1/2 in some monocrotaline-treated rats, on average, the phosphorylation of MAP kinases ERK1/2 and p38 was not significantly different (Figures R41-A and B). Pulmonary hypertensive animals showed increased phosphorylation of Akt (p-Akt to total-Akt ratio), and this effect was not evident in monocrotaline-quercetin treated animals (Figure R42-A). However, it should be noted that the increased p-Akt/total-Akt ratio was accompanied by a strong downregulation of Akt, and therefore, when normalized by β-actin phosphorylated Akt was lower in the hypertensive animals when compared to controls. Phosphorylation of S6 at residues 240-244 was significantly increased by monocrotaline and this effect was prevented by quercetin (Figure R42-B).

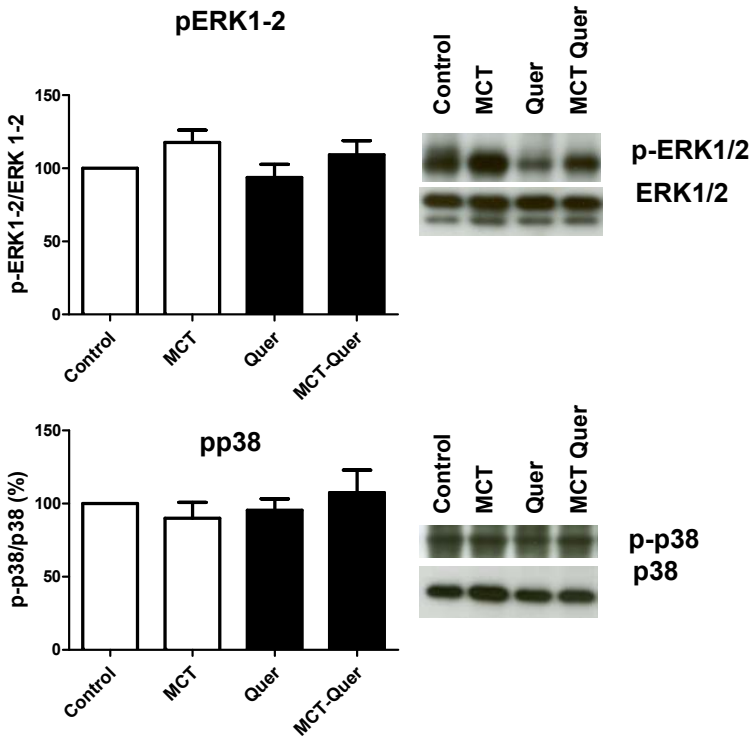

Figure R41: Lack of changes in the activation of MAPKs: ERK1/2 and p38-MAPK. *Lung homogenates were analyzed by Western blot and probed with the anti-phospho MAPK or the anti-total MAPK antibodies. Results expressed as phosphorylated forms normalized by the total protein, are means ± SEM of 5-8 animals.*

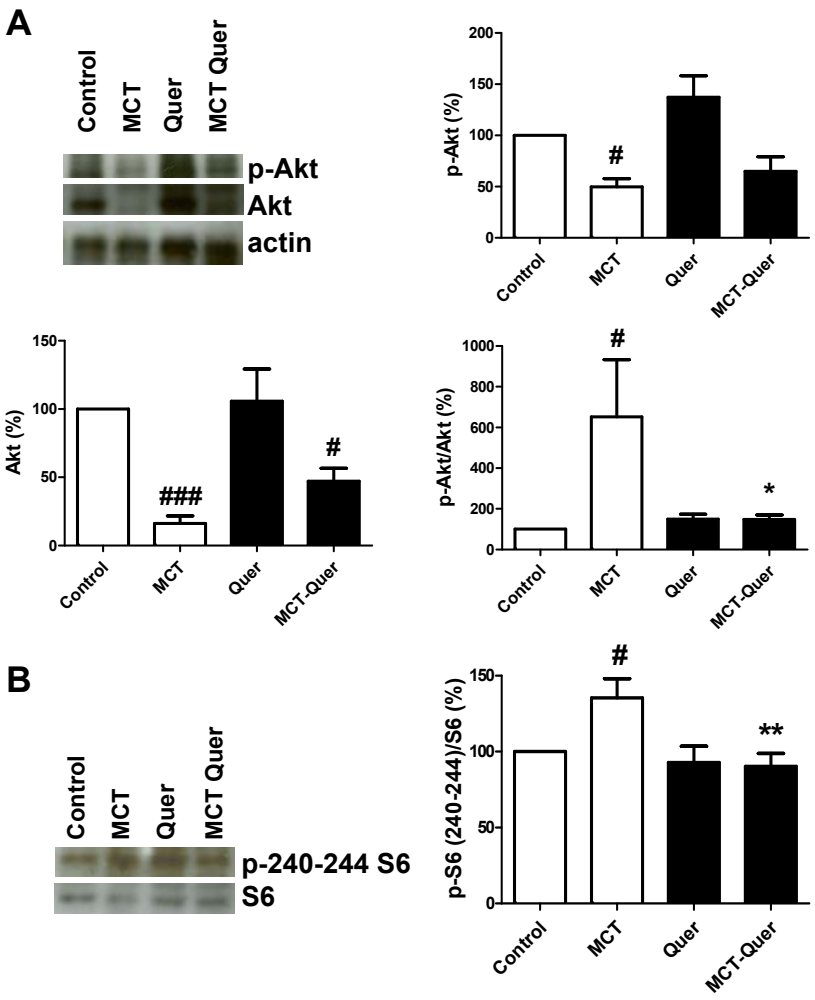

Figure R42. Changes in the PI3K/Akt/mTOR/S6 signalling pathway*. Lung homogenates were analyzed by Western blot and probed with the anti-phospho Akt, the anti-total Akt or anti-β actin (A) or antiphospho S6 ribosomal protein (serines 240, 244) or total S6 (B) antibodies. Results expressed as phosphorylated forms normalized by the total protein, are means ± SEM of 5-8 animals. * indicates P<0.05 versus monocrotaline (MCT), #, and ### indicate P<0.05, and P <0.0001 versus control (Ctrl).*

4.8. Antiproliferative and pro-apoptotic effect *in vitro*

Having demonstrated the effect of quercetin in the MCT-treated rats *in vivo* model. We next investigated their effect in PASMC and fibroblasts from MCT-treated rats cultured in the presence of 10% FBS and grown at an exponential rate for 48 h. Addition of quercetin produced a concentration- and time-dependent decrease in the number of viable cells estimated by the MTT assay in both cell types (Figures R43-A and R43-B). We analyzed whether quercetin was reducing cell proliferation in PASMC from

monocrotaline-treated rats by the analysis of BrdU incorporation. Quercetin produced significant inhibitory effects on BrdU incorporation at 24 h (Figure R43-C).

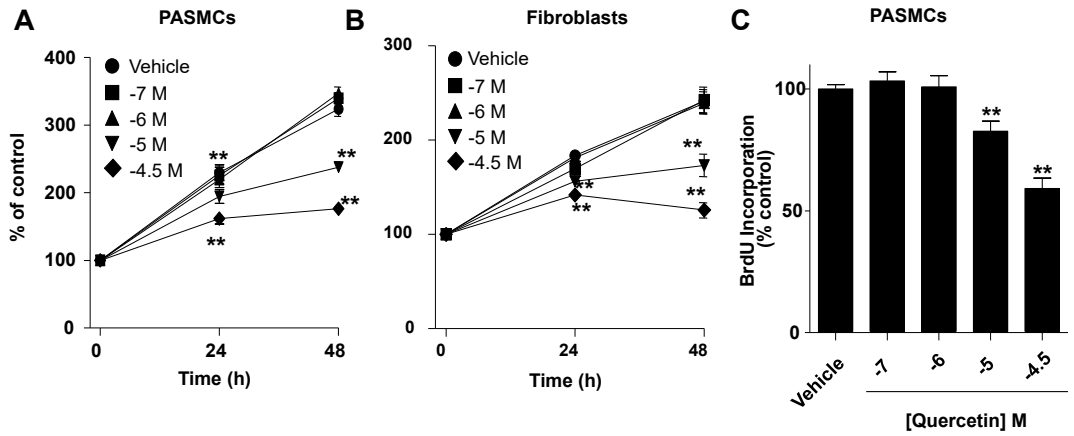

Figure R43: Quercetin decreases PASMC and fibroblast proliferation*. (A) PASMC and (B) fibroblasts were isolated from monocrotaline-treated rats and grown in culture. Viable cells were estimated by the MTT test exposed to quercetin in culture for 24 or 48 h. (C) PASMC proliferation was analyzed by the BrdU incorporation after 24 h of treatment with increasing concentrations of quercetin. Results are means ± SEM of 3-4 experiments performed in triplicate. ** indicates P<0.01 versus vehicle (DMSO).*

In PASMC from control rats, proliferation, measured by the BrdU incorporation was also inhibited (Figure R44). It also strongly reduced the total number of cells (positive for the membrane permeable dye Hoescht 33258) and produced an increase in non-viable cells (positive for the membrane impermeable dye propidium iodide, Figure R44-B and R44-C). Non-viable cells showed chromatin condensation and nuclear fragmentation characteristic of apoptotic cells.

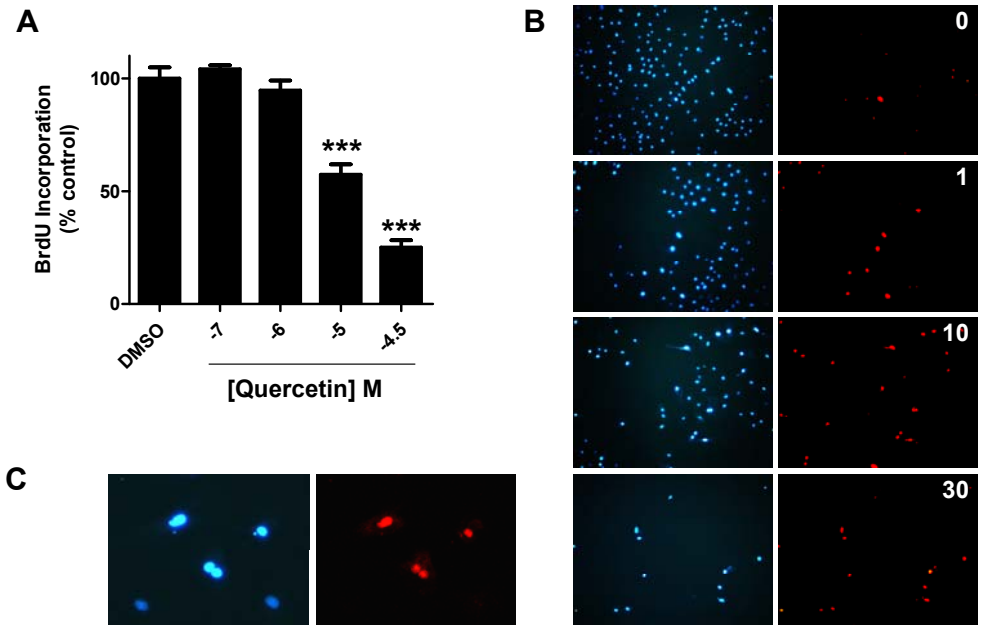

Figure R44. Quercetin decreases proliferation (A) and induces apoptosis (B) in cultured PASMC from control rats. *(A) PASMC proliferation was analyzed by the BrdU incorporation after 24 h of treatment with increasing concentrations of quercetin. Results are means ± SEM of 4-5 experiments. (B) Photographs of PASMC after 48 h treatment with quercetin in culture stained with the membrane permeable blue dye Hoescht 33258 (left, viable and non-viable cells) and with the membrane impermeable red dye propidium iodide (right, non-viable cells). (C) Magnified photographs of cells treated with $1x10^{-5}$ M quercetin showing three apoptotic cells (top and middle cells) with chromatin condensation and nuclear fragmentation and two healthy cells (bottom).*

DISCUSSION

1. Drug Screening

The current treatment of PH, based mainly on vasodilator drugs, is limited by several factors. First, all these drugs lack of pulmonary vascular selectivity. Thus, when the pulmonary vasculature is relatively unresponsive, the use of high doses is accompanied by systemic vasodilatation leading to side effects, including systemic hypotension (Young et al., 1983). Second, currently used vasodilators may exert their effects preferentially on poorly oxygenated and ventilated vessels. This may lead to ventilation-perfusion mismatch and detrimental effects on gas exchange. Third, the constriction of pulmonary vessels is often resistant to vasodilators. Finally, the available drugs have focused mainly on vasodilatation, despite the fact that the more severe forms of PH are accompanied by vascular remodelling. For these reasons, we have characterized a wide range of existing vasodilators in order to compare their efficacy to relax pulmonary vessels, their selectivity for the pulmonary circulation, whether their vasodilator effects are modified by the oxygen levels (oxygen selectivity) and their anti-proliferative vs their vasodilator potency.

Because the results of the present *in vitro* study may be strongly influenced by the experimental conditions, we must raise several methodological considerations. We have studied the effects of several vasodilators under conditions of high vascular tone, i.e. after inducing near maximal contraction, which presumably reflects what happens in PH. A mixture of the vasoconstrictors ET-1, 5-HT and TXA_2 mimetic U46619 was chosen as contractile and proliferative stimulus since all of these factors have been associated with PH (Selej et al., 2015; Morrell el al., 2009; Christman et al., 1992). Mesenteric arteries of a similar diameter than pulmonary arteries were chosen as representative systemic arteries. Drugs were initially screened in control rat cells and tissues and selected drugs were further analyzed in human samples and in cells from a PH rat model. For the studies on oxygen selectivity, we used 0% oxygen to bubble the buffer leading to oxygen concentrations of approx. 4% in the bath solution and 95% oxygen. We chose these two extreme conditions in order to maximize the differences even when none of them may strictly reflect physiological conditions. Moreover, both hypoxia and hyperoxia are known to induce oxidative stress. Thus, the comparison of

the effects in these two conditions would reveal true oxygen selectivity, independent of oxidative stress.

1.1. NO donors

PH is associated to decreased NO availability (Rabinovitch et al., 2012) and, therefore, it seems reasonable to treat PH patients with NO. Because of the short half-life of NO gas *in vivo*, NO has to be administered by inhalation. The direct access of NO to the best ventilated alveoli induces a pulmonary selective effect and vasodilates preferentially the arteries irrigating the best oxygenated lung areas, i.e. it shows also oxygen selectivity. However, inhaled NO requires a complex technology, normally restricted to intensive care units, which makes it inadequate for chronic therapy. Several NO donors have been used in order to deliver NO (Cogolludo et al., 2001, Ignarro et al., 2002). In the current study, we compared NO donors belonging to different chemical classes and with different mechanisms of NO release, potentially influenced by the oxygen levels and the cell type (Wang et al., 2002) in the search for the best profile. Furthermore, differences in their relaxant effects could be related with their chemical and pharmacological properties. Thus, SNP is relatively stable and does not release NO spontaneously; instead, SNP requires either light or cellular metabolism to produce NO (Miller et al., 2007, López-López et al., 2001). SNAP belongs to a class of NO-donating compounds that spontaneously release NO, which transport this NO across the plasma membrane to the intracellular compartment by the catalytic action of plasma membrane bound protein disulphide isomerase (Miller et al., 2007, Ignarro et al., 2002). DEA-NO, in contrast, it decomposes spontaneously in solution at physiological pH and temperature, their decomposition is not catalyzed by thiols or biological tissue. DEA-NO releases NO within minutes, and due to it short half-life, generates short and transient NO peaks (Miller et al., 2007; Krawutschke et al., 2015). The oxime derivatives do not release spontaneously NO into the bathing solutions; instead, require their metabolic formation in SMC by hemoproteins like horseradish peroxidase, rat liver microsomal cytochrome P450, hemoglobin, and catalase (Dantas et al., 2014; Chalupsky et al., 2004; King et al., 2004). Therefore, the activity of oximes is potentially influenced by oxygen levels.

SNP, SNAP and DEA-NO induced a relaxant response in a concentration-dependent manner in pulmonary and mesenteric arteries. The effects of SNP were similar in both arteries, but the other NO donors exerted inverse pulmonary selectivity, i.e. they were more potent in mesenteric than in pulmonary arteries. A similar order of potency for the different classes of NO donors is observed by other authors (Salom *et al* 1999; López-López et al., 2001). The oxime derivatives, acetohydroxamic acid and formaldoxime, showed very weak relaxant effects in pulmonary arteries and again their relaxant effects were greater in mesenteric vessels.

Therefore, our data suggests that, in general, the vasodilator effects of NO donors were selective for mesenteric over pulmonary arteries. In previous results obtained by our group, the NO donor SNP induced more potent relaxant effects in endothelium-denuded porcine mesenteric arteries than in pulmonary arteries pre-contracted with U46619 (Cogolludo et al., 2001, Pérez-Vizcaíno et al., 1996). These results of low pulmonary selectivity are also consistent with findings from other groups in animal models (Kadowitz et al., 1981; De Witt et al., 2001) and humans (Cockrill et al., 2001) using NO donors.

In addition, NO donors were similarly effective in pulmonary arteries in the presence of high and low oxygen. This suggests that the oxygen levels do not influence NO release in any drug class. The lack of oxygen selectivity for SNP is consistent with the inhibition of HPV and its detrimental effects on ventilation perfusion matching (Adnot et al., 1991).

NO is a physiological mediator of numerous cellular and organ functions including inhibition of cell proliferation (Ignarro et al., 2001). The antiproliferative effects of NO have been attributed to specific alterations in cell cycle regulation by inducing the G_1 phase cycle arrest which is mediated by decrease of both cyclin-dependent kinase 2 (cdk2) and cyclin A levels as well as by an increase of the cyclin-dependent kinase inhibitor (CKI) p21 protein (Tanner et al., 2000). SNP reduced the cell viability in hPASMCs and rPASMCs-MCT, whereas, surprisingly, the BrdU incorporation was only inhibited in rPASMCs and rPASMCs-MCT. On the other hand, SNAP only was able to reduce the cell viability at the highest concentration tested. In contrast, the least

potent NO donors DEA-NO, formaldoxime and acetohydroxamic acid did not show effects on cell viability. Our results are in a good agreement with findings from other groups. SNP and SNAP are able to induce apoptosis in rat carotid arterial smooth muscle cells stimulated with FBS (1%) (Lau et al., 2003). In addition, this apoptotic effect has been observed by Nishio *et.at*. (1996) in serum deprived rabbit aortic smooth muscle cells serum treated with different concentrations of SNAP. Moreover, the NO donor diethylenetriamineNONOate (DETA-NO), which belongs to the same chemical class as DEA-NO, although with a higher half-life (De Witt et al., 2001) (DEA-NO $t_{1/2}$=2 minutes and DETA-NO, $t_{1/2}$=20 hours) inhibits proliferation of human aortic smooth muscle cells stimulated by either 10% FBS or PDFG (Tanner et al., 2000). Therefore, our data suggest that NO released by SNP and SNAP were able to reduce the proliferation induced by the mixture of vasoconstrictors, and rPASMCs-MCT was more sensitive to SNP. Nevertheless, the inhibitory effects on cell proliferation were achieved at concentrations much higher than those inducing pulmonary vasodilation.

1.2. PDE5 inhibitors.

The main PDE that degrades cGMP within the lungs is PDE5 and its inhibition causes smooth muscle relaxation and decreased vasomotor tone (Agarwal et al., 2011; Wilkins et al., 2008). We observed that addition of the PDE5 inhibitors sildenafil, tadalafil and dipirydamole induced a relaxation in a concentration-dependent manner, although they did not reach full relaxation. The effects of the three PDE5s inhibitors were similar under high oxygen and hypoxia in pulmonary arteries and, there were no significantly differences with mesenteric arteries. In previous studies sildenafil, tadalafil and dipyridamole showed a different effect accordingly to the vasoconstrictor agent. Thus, in rabbit pulmonary arteries pre-contracted with phenylephrine, both sildenafil and tadalafil, show a significant concentration dependent vasorelaxation (Toque et al., 2008), while in PA harvested from patients undergoing thoracic surgical lobectomy and pre-contracted with norepinephrine, sildenafil shows a weak vasodilator effect (Ried et al., 2014). In line with this, in several human (Medina et al., 2000) or newborn piglets (Moreno et al., 2004) vessels pre-contracted with U46619, sildenafil shows weak vasodilator effects. Furthermore, in human pulmonary arteries, sildenafil produced a concentration-dependent relaxation which was more potent under hypoxic conditions.

This is well in line with previous findings from other authors either in animal models or patients. Thus, sildenafil inhibits the rise of PAP induced by a hypoxic stimulus on patients and mice, and this is also reproduced in isolated perfused mouse lungs (Zhao et al., 2001). Sildenafil and tadalafil have been proposed to act mainly as pulmonary vasodilators since they reduce mPAP in patients with PAH, and lack of significant systemic vasodilation (Ghofrani et al., 2004). However, our results suggest that PDE5 inhibitors are able to induce a similar vasodilatation in pulmonary and mesenteric arteries, and even tadalafil was more selective for mesenteric arteries. In general, the low efficacy of PDE5 inhibitors, which contrasts with higher effects of NO donors and sGC stimulators, is likely to reflect a low basal activity of sGC.

All PDE5 inhibitors produced similar effect under high or low oxygen conditions which implies that hypoxia, at least acutely, does not modify PDE5 or sGC activity. These results contrast with the increase in PDE5 activity induced by brief hyperoxia (Farrow et al., 2012). Moreover, downregulation of PDE5 expression has been associated with hypoxia in the corpus cavernosus (Lin et al., 2009).

Besides their effect on vascular contractility, cGMP has an antiproliferative effect on SMC (Zhuplatov et al., 2006). We observed that sildenafil and tadalafil reduced the cell viability and BrdU incorporation, although these effects were more significant in PASMCs-MCT and hPASMCs. However, dipyridamole had no effect on cell viability. These differences observed among these compounds could be explained because dipyridamole is a less potent PDE5 inhibitor than sildenafil and tadalafil (Blount et al., 2004; Mancina et al., 2005). Our results are consistent with findings from other groups in several cell types and animal model with these PDE5 inhibitors. Sildenafil inhibits cell proliferation in rPASMCs stimulated with 5-HT (Li et al., 2009), in hPASMCs (Tantini et al, 2005) and porcine PASMC (Li et al., 2007) stimulated with PDGF. Likewise, dipyridamole inhibits serum-stimulated human arterial smooth muscle cells proliferation (Zhuplatov et al., 2006) and both human aortic smooth muscle cells (Himmelfarb et al., 1997) and human peritoneal mesothelial cells (Hung et al., 2001) stimulated with PDGF. Moreover, studies in experimental animals have also demonstrated their antiproliferative effects. Thus, sildenafil was able to reduce the vascular remodelling in both hypoxia and MCT models of PH (Wharton et al., 2005) and

tadalafil attenuates the right ventricular hypertrophy and vascular remodelling in rats with MCT-induced PH (Zhang et al., 2012). Therefore, our results suggest that sildenafil and tadalafil were able to reduce the proliferation induced by the mixture of vasoconstrictors, and both hPASMCs and rPASMCs-MCT were more sensitive to these PDE5 inhibitors.

1.3. sGC stimulators

As mentioned above, the sGC stimulators are able to stimulate directly the sGC enzyme in a NO-independent fashion and produce their sensitization to low endogenous NO levels. As a result, these drugs augment cGMP biosynthesis, which in turn leads to vascular relaxation (Cogolludo et al., 2007). In the present study, we observed that the sGC stimulators YC-1, BAY 41-2272 and riociguat caused a profound relaxation, reaching a full relaxation in rat mesenteric and pulmonary arteries, independently of the oxygen level. Furthermore, in human pulmonary arteries, riociguat produced a similar relaxation than in rat pulmonary arteries, although, their potency was lower than in rat, as showed by a lower pIC_{50} .

As expected, we observed that the pIC_{50} of YC-1 was lower than the other sGC stimulators, whereas they did not show differences in their E_{max}. These data are in good agreement with the effects observed by other authors. Thus, Teixeira *et al*, (2006), found that BAY 41-2272 is more potent than YC-1 to induce vasorelaxation in mesenteric arteries contracted with phenylephrine. The vasorelaxant effects of these drugs have been tested in several vessels such as ovine pulmonary arteries (Bawankule et al., 2005), rat mesenteric arteries (Teixeira et al., 2006) and piglet pulmonary arteries (Moreno et al., 2005), contracted with serotonin, phenylephrine and with the thromboxane A_2 mimetic U46619, respectively. In all of these preparations, the sGC stimulator used, induces a concentration-dependent relaxation. In addition, the poor pulmonary selectivity observed by the three sGC stimulators in our study were comparable with results observed in several animal models and patients. Rothermund *et al*, (2011) showed that *i.v.* injection of 5 mg/kg YC-1 caused a transient decrease in the mean SAP in rats. Likewise, Evgenov *et al* (2004) found that in lambs with acute pulmonary hypertension induced by *i.v.* administration of U46619, BAY 41-2272

caused dose-dependent reductions of mean PAP, but it also induced systemic vasodilatation and a drop in SAP. Furthermore, in patients with PAH, distal chronic thromboembolic PH or PH associated with mild to moderate interstitial lung disease (Grimminger et al., 2009) and in patients with PH associated with COPD (Ghofrani et al., 2015) riociguat reduces systemic blood pressure and systemic vascular resistance. Therefore, this family of compounds did not demonstrated pulmonary selectivity. Unfortunately, the sGC stimulators produced similar effect under high or low oxygen conditions.

We observed that BAY 41-2272 reduced the cell viability and BrdU incorporation, although its effects on cell viability were stronger than on BrdU incorporation. Surprisingly, YC-1 and riociguat showed a slight effect on cell viability, but riociguat caused a significant reduction on BrdU incorporation. These differences could be explained by the direct effect that these compounds exert on the sGC activity. Thus, YC-1 increases 10-fold, BAY 41-2272 200-fold and riociguat 73-fold the enzyme activity (Hambly et al., 2015). Therefore, these data suggest that direct stimulation of sGC plays a critical role in inhibition of PASMC proliferation. These antiproliferative effects are consistent with findings from other groups. Pretreatment with YC-1 inhibits cell proliferation in hPASMCs induced by hypoxia (1% O_2) (Huh et al., 2011). In the same study, authors also demonstrated that YC-1 prevents and attenuates, respectively, vascular remodelling and right ventricular hypertrophy in chronic hypoxia-induced PH model in mice. Likewise, BAY 41-2272 inhibits serum-induced growth in rat A7R5 VSM cells (Mendelev et al., 2009) and rat aortic smooth muscle cells (Joshi et al., 2011). These antiproliferative effects of BAY 41-2272 have been confirmed in several animal models. Joshi *et al*. (2011) demonstrated that BAY 41-2272 inhibits neointimal growth in the rat carotid artery balloon injury model by reducing VSMC proliferation and migration. Deruelle *et al*. (2006) found that BAY 41-2272 prevents pulmonary vascular remodelling induced by chronic PH in neonatal rats, whereas Dumitrascu *et al*. (2006) found that it significantly reverses the degree of pulmonary hypertension in chronic hypoxia mice and MCT-induced PAH rats. However, Thorsen *et al*. (2010) found that BAY 41-2272 did not alter muscularization of pulmonary arteries in a rat model of chronic hypoxia. A recent study have found that riociguat is able to prevent further

progression of pulmonary vascular remodelling and formation of occlusive lesion in a rat model of severe angioproliferative PAH induced by combined exposure to the VEGF receptor antagonist SU5416 and chronic hypoxia (Lang et al., 2010). Therefore, the present study suggests that differences in susceptibility toward sGC stimulators may be caused by their direct effect on sGC and by the cell type.

1.4. Drugs targeting ion channels

In the present study, both Kv7 channels activators flupirtine and retigabine relaxed mesenteric arteries but had no effect on pulmonary arteries, Our results in systemic arteries are thus in good agreement with those found after *in vivo* or *in vitro* administration of flupirtine (Mackie et al., 2008; Morales-Cano et al., 2015). The differences in the relaxation induced by both kv7 activators in mesenteric and pulmonary arteries might be attributed to the different expression of the Kv7 isoforms in the two vascular beds. Kv7.4 is the most expressed isoform in pulmonary and mesenteric arteries followed by Kv7.1 while Kv7.5 was very low (Joshi *et al.*, 2009). However, a more prominent role of Kv7 channels in mesenteric arteries is not supported by the higher expression of both Kv7.4 and Kv7.1 (10-fold) in PA when compared to mesenteric arteries. Alternatively, the assembly of homomeric or heteromeric complexes, the expression of KCNE regulatory subunits or the trafficking of the channel proteins might be different in the two vascular beds. Oliveras *et al*. (2014) found that Kv7.1 could form heterotetramers with Kv7.5 and, as a consequence of this association, the channel is retained in the endoplasmic reticulum leading to a reduced response to Kv7 activators such as retigabine. Therefore, the different regulation rather than the expression of Kv7 channels might explain the higher sensitivity of mesenteric arteries. An additional explanation is that, as described below, the contraction induced by the mixture of vasoconstrictors is much more resistant to calcium lowering drugs (K^+ channel openers and Calcium antagonists) in pulmonary than in systemic vessels.

The ATP-sensitive potassium channel activator pinacidil relaxed both vessels, although its relaxant response was more potent in mesenteric than in pulmonary arteries. It should be noted that pinacidil was the only drug targeting ion channels that was able

to cause a 50% relaxation of pulmonary arteries. These results are consistent with an effective relaxant response in rat endothelium-denuded small mesenteric arteries (Tsang et al*.,* 2003), rat aorta and main pulmonary arteries (Wanstall et al., 1992; Wanstall et al., 1994) and in lamb pulmonary arteries (de Buys Roessingh et al., 2006). This lack of pulmonary selectivity has previously been reported (Wanstall *et al*. 1992; 1994). However, in preparations from two rat models of pulmonary hypertension (MCT and chronic hypoxia for two weeks), pinacidil was significantly more effective for pulmonary arteries.

Finally, in our experiments the relaxant response to the calcium antagonist nifedipine was very poor in rat pulmonary arteries while it was highly effective in mesenteric arteries. This poor pulmonary selectivity is in good agreement with results previously presented by our group in piglet mesenteric and pulmonary arteries, where nifedipine induces a stronger relaxant responses in mesenteric than in pulmonary arteries pre-contracted either with noradrenaline or U46619 (Pérez-Vizcaíno et al., 1996). Notably, human pulmonary arteries were more sensitive than those of the rat. However, in patients with pulmonary hypertension secondary to advanced COPD and patients with IPAH, administration of nifedipine induces preferential systemic vasodilation with no significant changes in pulmonary arterial pressures (Melot et al., 1983; Melot et al., 1984). Similar results were observed by Young *et al.* (1983) in two models of acute pulmonary vasoconstriction induced by hypoxia (12% FIO_2) and $PGF_{2\alpha}$ in dogs.

Taken together the low efficacy of vasodilators modulating Ca^{2+} channel activity, either directly (Ca^{2+} channel blockade with nifedipine) or indirectly (via K^+ channel opening induced hyperpolarization with pinacidil, retigabine or flupirtine), indicates that the vasoconstriction of pulmonary arteries, at least under our experimental conditions, is not mainly mediated by Ca^{2+} entry through Ca_L. Moreover, the vasodilator effects of drugs modulating ion channels were not significantly different under high vs low oxygen concentrations. This is consistent with the poor effects of calcium antagonist on gas exchange (Ballester et al, 1986).

Elevated i[Ca2+] is also implicated in stimulation of cell proliferation besides triggering vasoconstriction. Furthermore, apoptosis is inhibited when K^+ efflux is prevented,

either by raising the extracellular K^+ concentration (that is, decreasing the driving force on K^+ efflux) or by pharmacologically blocking K^+ channels (Burg et al., 2008). Nifedipine was able to reduce the cell viability and BrdU incorporation in our experiments. These results are agree with those found with nifedipine in rat aortic SMC stimulated either with PDGF (Nilsson et al., 1985) or serum (Nilsson et al, 1985; Sung et al., 2012) and with studies carried out in animal models of PH, such as MCT (Inoue et al., 1993) and 1 month exposure to intermittent hypoxia (Stanbrook et al., 1984), where nifedipine reduced the vascular remodelling. However, nifedipine induced lower antiproliferative than vasodilator effects at a given concentration.

On the other hand, the K_{ATP} channel opener pinacidil significantly reduced cell viability in hPASMCs at the highest concentration tested, whereas it had no effect in rPASMCs. The antiproliferative responses of pinacidil have been also shown by other authors in hPASMCs (Zhu et al., 2008) and rabbit PASMCs (Xie et al., 2005) stimulated with ET-1. Moreover, the study conducted by Jiang *et al.* (2012) found that pinacidil reduces the pulmonary remodelling caused in the MCT-induced PAH rat model.

The Kv7 activator retigabine was able to reduce the cell viability in the three cell lines, although its effect on BrdU incorporation was more accused in rPASMCs-MCT. In contrast, flupirtine did not reduce the cell viability of rPASMCs and hPASMCs. These differences observed between both Kv7 activators could be explained because retigabine is a more potent analog of flupirtine (Morecroft et al., 2009). To our knowledge, this is the first study showing the antiproliferative effect of Kv7 activators in PASMCs. Interestingly, a significant inhibition of cell proliferation was observed at concentrations at which it had no apparent vasodilator effect. Other authors have studied the regulation of proliferation induced by Kv7 modulators in skeletal muscle cells, but with different results. Roura-Ferrer *et al.* (2008) found that the Kv7 channel blocker linopirdine inhibits proliferation of rat muscle-derived L6E9 cell line stimulated with serum, whereas Iannotti *et al*. (2010) found that retigabine is able to reduce cell viability in murine C2C12 myoblasts stimulated with serum. The antiproliferative effects of flupirtine have also been reported in a chronic hypoxic mice model of PH, where flupirtine reduces the percentage of remodeled arteries (Morecroft *et al*. (2009).

Therefore, our results suggest that activation of Kv7 channels by retigabine or inhibition of the Ca_L channels reduced the proliferation induced by the mixture of vasoconstrictors. Notably, while nifedipine was significantly more effective as a vasodilator, retigabine produced stronger antiproliferative effects, suggesting that Kv7 activation might have effects beyond its indirect Ca^{2+} channel blockade.

1.5. Adenylate cyclase activators

Treprostinil is an agonist of the IP which is coupled to AC and forskolin is a direct activator of the AC. Both drugs induced vasodilatation. Their relaxant responses were more potent in mesenteric than in pulmonary arteries and similar under high or low oxygen levels. Our results with forskolin are similar to those reported by several authors in canine pulmonary arteries (Mathew et al., 1993), lamb pulmonary arteries (Lakshminrusimha et al., 2009) and rat mesenteric arteries (Matsumoto et al., 2003). In contrast, addition of treprostinil caused only a weak relaxant effect in pulmonary arteries but relaxed mesenteric arteries. However, in human pulmonary arteries treprostinil induced a stronger relaxant effect than in rat pulmonary arteries. In previous studies treprostinil have showed different relaxant effects in rat (Orie et al., 2013), and in human (Benyahia et al., 2013) pulmonary arteries and veins. Very recently, it has been reported by Benyahia et al, (2015), that the *ex vivo* relaxation or sensitivity of pulmonary arteries to PGI_2 mimetics depends on the contractile agent (PE, U46619 and ET-1) and the specie used (rat or human vessels). Our results are consistent with this view since treprostinil relaxed better human than rat pulmonary arteries. Furthermore, in line with our data, intravenous administration of treprostinil in a sheep model of acute PH induced by infusion of U46619 caused a higher decrease in systemic than in pulmonary pressure (Sandifer et al., 2005). Therefore, these data suggest that the direct activation of AC with forskolin showed higher efficacy than activation of IP by treprostinil, which is upstream of AC.

Besides their effect on vascular tone, cAMP acts as a gate to prevent SMC mitogenic in response to growth factors (Stork et al., 2002) via activation of PKA, and the subsequent phosphorylation of its substrates as MAPK and finally arrest cells in G_1 phase of the cell cycle (Hewer et al., 2010; Stork et al., 2002; Li et al., 2004).

Surprisingly, forskolin stimulated BrdU incorporation in rat cells and a similar trend was observed for the MTT assay. In hPASMC forskolin inhibited proliferation measured by both assays but only at the highest concentration, indicating species variations. Our findings are consistent with those found by Hayashi *et al*. (2000), which reported that forskolin is able to inhibit the proliferation of human aortic VSMC stimulated with PDGF. Likewise, Wharton *et al.* (2000) found that forskolin inhibit DNA synthesis and proliferation of distal hPASMCs maintained in 0.1% FBS and stimulated with PDGF-BB. In addition, the dual effect of forskolin on cell proliferation has been described previously by Guldemeester *el al.* (1999), where both, forskolin and 8-bromo-cAMP (a cAMP mimetic) induce an increase in [^{3}H]-thymidine incorporation in neonatal calves PASMCs, but not in adult cows PASMCs. This was attributed to differences in PKC activation by cAMP in neonatal versus adult PASMCs. Therefore, these differences suggest that direct activation of AC could account for positive or negative regulation of cell proliferation (Stork et al., 2002).

The PGI_2 mimetic treprostinil, inhibited cell viability in rPASMCs at the highest concentration tested, and induced a weak reduction of BrdU incorporation in hPASMCs. However, treprostinil showed a trend to increase the BrdU incorporation in rPASMCs and rPASMCs-MCT. Our results are consistent with those found with treprostinil and other IP agonists in several cell lines and animal models. Thus, treprostinil inhibits cell proliferation in normal and IPAH PASMCs (Falcetti et al., 2010) and in human and mice lung fibroblasts (Ali et al., 2005) stimulated with FBS, although in this study authors showed that treprostinil had no effect on cell viability at concentrations up to 10^{-4} M, measured by MTT. In addition, other IP agonists such as cicaprost and iloprost abolish the proliferation of rat aortic VSMC induced both by bFGF or ET-1 (Li et al., 2004) and in hPASMC stimulated with either PDGF-BB (Wharton et al., 2000) or serum (Clapp et al., 2002). Furthermore, our results are in good agreement with studies in animal models of PH where treprostinil could not demonstrate improvement on vascular remodelling in both chronic hypoxic mice model (Nikam et al., 2010) and in a rat model of PAH induced by MCT followed by the creation of an abdominal aortocaval shunt (van Albada et al., 2006). Therefore, our results suggest that both direct and indirect stimulation of cAMP production were able

to reduce the proliferation induced by the mixture of vasoconstrictors in hPASMCs, while rPASMCs and rPASMCs-MCT were more resistant.

1.6. PPAR agonists

In the present study, these drugs were used in the range of therapeutic concentrations (i.e., micromolar) at which they are selective activators of their expected targets, PPARβ/δ (GW0742 and L165041) and PPARγ (rosiglitazone) (Jiménez et al, 2010; Harrington et al., 2010). As expected (Harrington et al., 2010), addition of the selective PPARβ/δ agonist GW0742 relaxed rPA. Interestingly, this effect was significantly more potent when arteries where exposed to high oxygen. In fact, this is the only drug that showed a clear oxygen selectivity in rat arteries. Unfortunately, this selectivity is absent in hPA, where GW0742 caused a similar effect under high oxygen and hypoxic conditions. In contrast, the relaxant response induced by the weak nonselective PPARβ/δ agonist L165041 was poor, specially in pulmonary arteries, and independent of the oxygen level. Similar effects were observed with the the selective PPARγ agonist rosiglitazone. Thus, our findings are consistent with previous studies showing vasodilator effects of these three PPAR agonists (Jiménez et al., 2010; Harrington *et al.,* 2010). Furthermore, in agreement with these studies we found that the PPARβ/δ agonists GW0742 and L165041 were more potent vasodilators than the PPARγ agonist rosiglitazone. In contrast to our results, rosiglitazone caused a full relaxation in endothelium-intact human pulmonary arteries pre-contracted with U46619 (Kozłowska et al., 2013), and in carotid arteries from hypertensive mice, but this effect was reached using concentrations higher than $1x10^{-4}$ M (Ryan et al., 2004). All these data indicate that PPAR agonists are vasodilators but lack of selectivity for the pulmonary vasculature. While the oxygen dependent pulmonary vasodilation elicited by GW0742 is a very interesting finding, this could not be confirmed in hPA.

A large number of proteins are modulated by PPARs and may be involved in the regulation of metabolism, inflammation, cell differentiation, cell growth and angiogenesis (Chu et al., 2015; Quintela et al., 2012; Nisbet et al., 2007; Han et al., 2015). The antiproliferative effects of stimulation of PPARβ/δ and PPARγ isoforms have been attributed to suppressing the cell cycle progression by cell cycle arrest on G_1

phase mediated by increased levels of p27 and p21 CKIs (Lim et al., 2009; Li et al., 2010). In the present study, the PPARβ/δ agonist GW0742 reduced the cell viability in hPASMCs and rPASMCs-MCT, whereas it reduced the BrdU incorporation in rPASMCs and rPASMCs-MCT. In contrast, the other PPARβ/δ agonist, L165041, which was also less effective as vasodilator than GW0742 (see above), did not reduce the cell viability in rPASMCs and hPASMCs. Of direct relevance to our work, other authors have shown that activation of PPARβ/δ using GW501516 diminish the proliferation of hPASMCs stimulated with PDGF (Liu et al., 2013), reduce cardiac fibroblast proliferation (Teunissen et al., 2007) and attenuated the proliferation of rat aortic VSMC stimulated with IL-1β (Kim et al., 2010). However, in contrast with our results, Lim *et al.* (2009) found that L165041 was able to decrease the proliferation induced by PDGF in rat aortic VSMCs and to reduce the neointima formation in a rat model of carotid artery balloon injury model. Moreover, in the study carried out by Harrington *et al.* (2010), administration of GW0742 had no effect on the vascular remodelling observed in the chronic hypoxia-induced PH rat model.

The PPARγ agonist rosiglitazone only was able to reduce the cell viability in hPASMCs. In contrast, BrdU incorporation was diminished in the three cell types treated with rosiglitazone. Activation of PPARγ by pharmacological ligands has also been shown to exert antiproliferative effects on a variety of cell types. Thus, rosiglitazone inhibits hPASMCs proliferation stimulated by 5-HT (Han et al., 2015) and hypoxia-induced human PAEC proliferation (Kang et al., 2011). In addition, studies in experimental animal models have also demonstrated their antiproliferative effects. Rosiglitazone was able to reduce and prevent the vascular remodelling induced by chronic hypoxia in rats (Crossno et al., 2007) and in mice (Nisbet et al., 2010), as well as in MCT treated rats (Zhang et al., 2014).

Therefore, our data suggests that both GW0742 and rosiglitazone were able to reduce the proliferation induced by the mixture of vasoconstrictors, and both rPASMCs and rPASMCs-MCT were more sensitive to these PPAR agonists. However, the PPARβ/δ agonist was more effective as vasodilator than as antiproliferative while the opposite profile was observed for the PPARγ agonist.

1.7. Kinase inhibitors

As mentioned previously, ROCK produces vasoconstriction by phosphorylation of MLC via Ca^{2+}-independent phosphorylation of MLCP. This leads to Ca^{2+} sensitization, which referes to an increase in vascular tone under constant or even declining levels of cytosolic Ca^{2+}(McMurtry et al., 2010). In the present study, the ROCK1/2 inhibitor hydroxyfasudil, which is the major active metabolite of fasudil after oral administration (Shimokawa et al., 2007), induced relaxant responses in mesenteric and pulmonary arteries, but this effect was more potent in mesenteric than in pulmonary arteries. However, pulmonary arteries under hypoxia were significantly more sensitive to hydroxyfasudil than under high oxygen level. This is consistent with the activation of ROCK1/2 by hypoxia in pulmonary arteries as previously described (Do et al., 2009) However, hydroxyfasudil induced a less potent relaxation of human pulmonary arteries and independently of the oxygen levels. Conflicting results have been reported regarding the pulmonary selectivity of ROCK inhibitors in several animal models and humans. Fasudil shows pulmonary selectivity in rats with MCT-induced PAH (Jiang et al., 2007) and in patients with severe PH (Fukumoto et al., 2005). On the other hand, acute oral administration of Y-27632 (30 mg/kg) decreases both mean PAP and SAP in chronic hypoxic PH rats (Nagaoka et al., 2005). The reason for this discrepancy among these studies (including ours) remains unkown but might be related to the need of metabolic activation of fasudil into the active form hydroxyfasudil.

A number of studies have shown the relaxant effects of the prototypical flavonoid quercetin (Duarte et al., 1993; Perez-Vizcaino et al., 2010; Cogolludo et al., 2007; Perez et al., 2014). We found that quercetin caused a full relaxation in mesenteric and pulmonary arteries from rats, which was more potent under hypoxic conditions.In human PA quercetin was less potent than in rPA, and not affected by oxygen level. Therefore, our results suggest that quercetin exerts inverse pulmonary and inverse oxygen selectivity in rat but not in human arteries

In the present study, the TAK-1 inhibitor 5z-7-oxozeaenol (Ninomiya-Tsuji et al., 2003; Zippel et al., 2013) had no effect either in rat or human pulmonary arteries under high and low oxygen levels, which suggest that TAK-1 is not implicated in the maintenance

of contraction induced by the mixture of vasoconstrictors. To our knowledge, this is the first study on the direct vasodilator effect of 5z-7-oxozeaenol in PA.

Tyrosine kinase inhibitors also induce VSMC relaxation and vasodilation because cell growth–related kinases may be involved in cell contraction. The vasoactive effects of imatinib have been attributed to the inhibition of its main targets PDGFR, c-Abelson tyrosine kinase (c-Abl), and c-kit at low concentrations (<1 μM). In addition, it may inhibit other kinases, such as EGFR, Src family kinases, and PKC, at higher concentrations (Abe et al., 2011). The present results shows that imatinib induced relaxation in mesenteric and pulmonary arteries, being the former more sensitive than the latter and with no oxygen selectivity. The observation that imatinib relaxes mesenteric and pulmonary arteries is in good agreement with previous reports obtained in several vascular tissues such as guinea pig bladder, rabbit and human corpora cavernosa, human prostate gland, rabbit and human myometrium, and isolated pulmonary and penile arteries from rat (Pankey et al., 2013). In contrast, Abe *et al*. (2011) reported that high doses (> 20 mg/Kg) of imatinib present pulmonary selectivity activity in anesthetized SU5416/hypoxia/normoxia-exposed severe pulmonary hypertensive rats. Therefore, these data suggest that imatinib has a marked vasodilator activity both in the pulmonary and mesenteric arteries, but might reveal pulmonary selectivity under exaggerated pulmonary vascular tone.

RhoA-ROCK pathway besides their role on VSMC contraction, it is found to induce proliferation of VSMC (Duong-Quy et al., 2013). Hence, the antiproliferative effects of ROCK inhibitors have been attributed to the upregulation of p27 protein and inhibition of ERK1/2 translocation. In the current study, we have found that hydroxyfasudil reduced the cell viability of hPASMCs and rPASMCs-MCT at the higher concentration ($3x10^{-5}$ M), whereas it had no effect in rPASMCs. However, hydroxyfasudil reduced the BrdU incorporation in hPASMCs, whereas in both rPASMCs and rPASMCs-MCT, BrdU was increased. These differences could be explained because BrdU despite is incorporated into nuclear DNA during the S phase of the cell cycle, it may be incorporated during DNA synthesis not related with cell proliferation, such as DNA repair or DNA turnover. This effect has been described in cells that incorporate BrdU as part of an apoptotic process, with is apparently triggered by the DNA damage response

(Bauer et al., 2005). Previous studies on the effects of ROCK inhibitors on cell viability and proliferation are in line with our finding. Thus, fasudil (Chen et al., 2009) and Y-27632 (Xu et al., 2010) inhibit the proliferation induced by 5-HT and serum, respectively in rPASMCs. Moreover, studies in animal models have demonstrated their antiproliferative effects. Thus, fasudil is able to prevent and reduce the muscularization and medial thickness within the PA in the prevention and treatment protocol, respectively in a MCT-induced PAH in rats (Abe et al., 2003; Mouchaers et al., 2010). Likewise, fasudil decreases hypoxia-induced muscularization of pulmonary arterioles in wild-type and eNOS-deficient (eNOS $^{-/-}$) mice (Abe et al., 2006). Therefore, our results suggest that hydroxyfasudil reduces the proliferation induced by the mixture of vasoconstrictors, and hPASMCs was more sensitive to this compound.

In addition to their vasodilator and anti-hypertensive effects in spontaneously hypertensive rats, quercetin exhibits a range of biological activities, including antioxidative, antiproliferative, antimigratory, and platelet inhibitor properties. These antiproliferative effects have been related to the interaction of quercetin with members of the MAPK family, such as ERK1/2, JNK and p38 (Perez-Vizcaino et al., 2010; Perez-Vizcaino et al., 2006). In the present study we found that quercetin was able to reduce both cell viability and BrdU incorporation. However, it should be noted that these effects were more accused in rPASMCs. This is well in line with previous findings in with antiproliferative properties of quercetin were observed in human (Khandelwal et al., 2012) and rat VSMC (Perez-Vizcaino et al., 2006) stimulated with PDGF and serum, respectively, and in rPASMCs stimulated by hypoxia (1%O_2) (He Y, 2015). Furthermore, studies in animal models have supported their antiproliferative effects. Thus, quercetin was able to reduce the vascular remodelling observed either in the MCT-induced PAH rat model as a preventive treatment (see chapter 3), Gao et al., 2012) and in the chronic hypoxia- induced PH rat model (He et al., 2015). Therefore, our results suggest that quercetin was able to reduce the proliferation induced by the mixture of vasoconstrictors.

TAK-1 as a member of the mitogen-activated protein kinase kinase kinase (MAPKKK), is an important regulator of the cell cycle and apoptosis, and its activity is regulated by various cytokines, including IL-1β and TGF-β (Zippel et al., 2013, Mihaly et al., 2014).

Hence, their antiproliferative properties observed by inhibition of TAK-1 have been attributed to the inhibition of JNK, p38, IKK and subsequent release of NF-κB (Zippel et al., 2013, Mihaly et al., 2014). We observed that 5z-7-oxozeaenol reduced both cell viability and BrdU incorporation. Our results are consistent with findings from other groups in several cell types with down-regulation or TAK-1 inhibition. Thus, Zippel *et al*. (2013) found that either silencing of TAK-1 or inhibition of TAK-1 with 5z-7-oxozeaenol inhibits cell proliferation, migration and sprouting of EC stimulated with serum or VEGF. Likewise, 5z-7-oxozeaenol is able to inhibits proliferation in mutant *bmpr2* $^{R899X\ -/+}$ PASMCs stimulated either with serum or TGF-β (Nasim et al., 2012). Furthermore, LYTAK1 (other TAK-1 inhibitor) inhibits the proliferation of ARPE-19 human RPE cells (retinal pigment epithelium) stimulated with TGF-β (Chen et al., 2016).

In our study, we found that imatinib caused a reduction in cell viability and BrdU incorporation; although in rPASMCs-MCT their effect on cell viability was not significant. In line with results obtained with quercetin, rPASMCs were more sensitive to the antiproliferative effects of these compounds. These results agree with those found with imatinib in PASMCs isolated from IPAH patients stimulated with PDGF-BB (Nakamura et al., 2012) and in rPASMCs stimulated either with serum, PDGF-AA, PDGF-BB or PDFG-AB (Schermuly et al., 2005; Pankey et al., 2013). In addition, these antiproliferative effects are supported by studies carried out in animal models in rats with MCT-induced PAH and in mice with chronic hypoxia-induced PH with imatinib used as treatment (Schermuly et al., 2005) and in MCT-induced PAH rat model as a preventive study (Pankey et al., 2013), where imatinib is able to reduce the pulmonary arterial remodelling, as well as the media wall thickness observed in these models. Therefore, our results suggest that imatinib is able to reduce the proliferation induced by the mixture of vasoconstrictors, and both rPASMCs and rPASMCs-MCT were more sensitive to imatinib.

1.8. Drugs used for other indications

Tacrolimus or FK506, is an immunosuppressant widely used in organ transplantations. Tacrolumus binds to its cytosolic receptor, tacrolimus binding protein (FKBP12) 12, and the resulting complex inhibit the type 2B Ca^{2+}-calmodulin-dependent protein

phosphatase, calcineurin (Yasutsune et al., 1999). This inhibition of calcineurin prevents the calcineurin-induced dephosphorylation of the cytoplasmic NFATc, and its translocation to the cell nucleus (Hoorn et al., 2012). In the present study, addition of the calcineurin inhibitor tacrolimus produced a weak relaxant effect in pulmonary and mesenteric arteries. Thus, the order of sensitivity for inhibition of responses observed by tacrolimus was MA oxygen > PA hypoxia >PA oxygen. These results are consistent with previous findings *in vitro* by other groups in several vascular tissues such as in porcine endothelium removed mesenteric and coronary artery strips (Akiyoshi et al., 2009; Yasutsune et al., 1999) where tacrolimus induces vasodilation. It should be noted that the concentration of tacrolimus used in both studies was much higher than the concentrations used in our study.

In the present study, we observed that addition of the calcium sensitizer levosimendan relaxed rat mesenteric and pulmonary arteries, although the former were more sensitive than the latter. We also showed that human pulmonary arteries were more sensitive than rat pulmonary arteries to the relaxant effects of levosimendan. Nevertheless, in both species, the relaxant effects of levosimendan in pulmonary arteries were similar under oxygen and hypoxic conditions. These results are consistent with findings from other groups in several vascular tissues and animal models since levosimendan reduces both pulmonary and systemic pressure. The vasodilator effects of levosimendan have been demonstrated in coronary, pulmonary and systemic arteries and saphenous veins (Antoniades et al., 2007). Furthermore, the pulmonary vasodilator effects have been tested in cat (De Witt et al*.;* 2002), dog, porcine (Wiklund et al., 2012), and rat (Vildbrad et al., 2014) models of PH. In addition, because levosimendan is a potent vasodilator also decreases systemic vascular resistance in animal models (Banfor et al., 2008; Vildbrad et al., 2014) and humans (Wiklund et al., 2012; Antoniades et al., 2007). Therefore, these data suggest that the vasodilator effects of levosimendan are not pulmonary selective.

Nucleotides play important roles not only in intracellular nucleic acid synthesis and energy supply but also, once released into the extracellular space, can interact with cell surface P2 receptors and produce various biological responses involved in the control of cellular functions (Ishida et al., 2013). In this context, the selective $P2Y_1$

agonist 2-MeSADP (von Kügelgen et al.; 2006) had a minimal effect in mesenteric arteries and in pulmonary arteries under hypoxia, whereas in pulmonary arteries under high oxygen 2-MeSADP did not show effect. The vasodilator effects of 2-MeSADP have been reported in rat mesenteric arteries (Ishida et al., 2013) and in dog coronary arteries (Bender et al., 2011) among others. In contrast, a recent study of Kylhammar *et al.* (2014) have found that infusion of ADP in the right atrium of pigs causes immediate increases in mPAP and PVR, which are fully reversible immediately when ADP-infusion is stopped. This full and quick reversibility indicates that it was caused by vasoconstriction. In addition, Mitchell *et al*. (2012) found that $P2Y_1$ activation elicits a small pulmonary vasoconstriction *in vitro* in rat endothelium denuded pulmonary arteries. Altogether, these data suggest that 2-MeSADP behave, at best, as a poor vasodilator both in pulmonary and systemic vessels

Structurally, tacrolimus has two domains, a domain bound by FKBP12 and an effector domain that, together with FKBP12, interact with calcineurin, thereby inhibiting its phosphatase activity, that finally prevents NFATc translocation into the cell nucleus (Hoorn et al.; 2012; Yasutsune et al., 1999; Giordano et al., 2008). Thus, the antiproliferative effect of tacrolimus has been attributed to the inhibition of NFATc translocation into the nucleus and inhibition of multiple cytokine expression. We found that tacrolimus reduced cell viability only in rPASMCs and at the higher concentration tested. However, tacrolimus showed conflicting results on BrdU incorporation depending on the concentration used and the cell type. These findings are in accordance with previous studies demonstrating stimulation, inhibition or no effect on proliferation, by this drug. Thus, tacrolimus inhibits DNA synthesis and proliferation in rat PASMCs and in human VSMC and EC stimulated with PDGF (Matter et al., 2006), whereas in human aortic VSMC, tacrolimus promotes cell growth by stimulation of TGF-β receptor enhancing proliferation and ECM production (Giordano et al., 2008). Finally, tacrolimus and other immunosuppressants did not show antiproliferative effects on PASMC isolated from patients with IPAH and stimulated with PDGF (Ogawa et al., 2005). Interestingly, tacrolimus reduces vascular remodelling in several PH animal models (Spiekerkoetter et al., 2013). Therefore, there are discrepancies

regarding the effect of tacrolimus among the different cell lines, stimulus and concentration of tacrolimus used.

The calcium sensitizer levosimendan, besides its positive inotropic effect by stabilizing Ca^{2+}-troponin C-complex in cardiomyocytes, and its vasodilator effect via opening K_{ATP} channels in VSMC, inhibits apoptosis and hypertrophy of cardiomyocytes (Okada et al., 2013). Thus, in the present study we observed that levosimendan was able to reduce the cell viability in all cell types studied. However, levosimendan only was able to reduce the BrdU incorporation in hPASMCs, whereas in rPASMCs-MCT, levosimendan significantly increased the BrdU values. Previous studies have shown that levosimendan attenuates the MCT-induced pulmonary vascular remodelling and proliferation of PASMCs by BrdU labeling *in vivo*. In addition, in cultured PASMC, high concentrations of levosimendan exhibit a direct inhibitory effect on PDGF-induced proliferation (Revermann et al., 2011). These effects are in good agreement with our results, as in our conditions, we need high concentrations of levosimendan to see an effect.

Besides their short-term effects as vasodilator, nucleotides also show long-term actions on cell proliferation and death (Burnstock et al., 2009; Ishida et al., 2013). We have focused on $P2Y_1$ receptor because cells with a proliferative phenotype express a higher levels of this receptor compared with cell with contractile phenotype (Burnstock et al., 2009). Our study revealed that the $P2Y_1$ receptor agonist 2-MeSADP did not affect cell viability in both rPASMCs and hPASMCs, which suggests a lack of involvement of this pathway in the proliferation of these cells.

1.9. Vasodilator and antiproliferative profile

Since the current PH treatments have been focused mainly on vasodilatation, despite the fact that the more severe forms of PH are accompanied by vascular remodelling, a search for drugs targeting both conditions is crucial to improve the treatment. Hence, we compared the vasodilator effects vs cell viability and BrdU incorporation in PA and PASMC, respectively, from humans and rats. To our knowledge, this is the first study comparings both effects in such a large number of drugs with different mechanism of actions. The main findings can be summarized as follows: 1) Drugs belonging to pharmacological groups currently approved for PH treatment (PDE5 inhibitors, sGC

stimulators and PGI_2 agonists) are preferentially vasodilators. 2) Kinase inhibitors, specially quercetin, share a dual vasodilator/antiproliferative profile which could offer additional benefit in the context of PH. 3) Drugs targeting ion channels show poor vasodilator and antipoliferative effects. 4) None of the 27 drugs tested showed pulmonary selectivity. 5) None of the 27 drugs tested showed improved relaxation under increased oxygen conditions in human pulmonary arteries.

In summary, the results from the present study indicate that the majority, if not all, of the currently approved or potentially useful drugs for PH exhibit poor pulmonary and oxygen selectivity. Thus side effects such as hypotension and ventilation-perfusion mismatch followed with detrimental effects on gas exchange, respectively, can be expected following their use. Furthermore, since most of the currently drugs used in PH are essentially vasodilators their combination with antiproliferative drugs may offer an additional benefit in these patients.

1.10. Study limitations

Several limitations should be mentioned in our study.

Our study represents an extensive comparison of the vasodilator and antiproliferative effects of 27 drugs from 8 pharmacological groups that has several limitations. First, a study like this, with such as screening approach precludes a detailed characterization of both vasodilator and antiproliferative effects and mechanisms involved. Second, while we used PASMC from MCT-induced PAH model, vasodilator analysis was performed in arteries from healthy rats and from patients that did not have any clinical evidence of PH. However, we have studied the effects of vasodilators under conditions of high vascular tone, which presumably reflect what happens in PH. Third, proliferation were studied using MTT and BrdU assays, two indirect indicators of cell viability and DNA synthesis, respectively, and both with several limitations. We are aware that direct cell counting could be useful to assess really the effect on proliferation, but this represents a really hard task due to the number of drugs, concentrations and cell types used it is difficult perform this assay.

Results derived from this thesis demonstrated that the responses of isolated arteries to vasodilator drugs may vary depending on the species, vascular bed, and oxygen levels among other factors. Likewise, our results also demonstrated that under the same stimuli and culture conditions, the effects of a given drug may dramatically change depending on the cell line. In addition, we have also demonstrated that the vasodilator or antiproliferative profile exhibited is relatively well conserved among drugs belonging to a same pharmacological group.

2. Effects of riociguat and sildenafil on ventilation-perfusion coupling in rat lungs

Mild, moderate or severe hypoxemia is a common feature of pulmonary hypertension (PH) associated to pulmonary diseases such as COPD, idiopathic pulmonary fibrosis (IPF) or sleep obstructive apnea syndrome. The obstruction and inflammation of the airways is the primary mechanism leading to reduced gas exchange. In this scenario, HPV represents a life-saving physiological mechanism which redistributes blood flow away from diseased lung tissue, where ventilation is impaired, to the best ventilated alveoli to couple ventilation and perfusion (V/Q) and optimize SO_2 (Weir et al., 2006; Kuhr et al., 2012). According to recent guidelines, vasodilators approved for PAH are not recommended for patients with PH due to lung diseases (Galiè et al., 2015). In fact, at present there is no specific antihypertensive therapy for these classes of patients. Systemic administration of vasodilators may increase blood flow to poorly-ventilated or non-ventilated areas of the lung by interfering with the physiological mechanism of HPV, thereby worsening preexistent V/Q mismatch and shunt flow. This effect causes a fall in concentration of arterial oxygen, reducing the small ventilatory reserve of these patients.

Stimulation of sGC with riociguat may have a theoretical advantage over PDE5 inhibition with sildenafil because of its NO-independent mode of action. Therefore, sGC stimulators could be effective even when NO production is impaired as occurs in PH. We have compared the vasodilator effects of the standard drug sildenafil with the

novel drug riociguat in *in vitro* studies in rat and human arteries and how these effects are modulated by hypoxia. We have also studied their effects on ventilation perfusion matching and SO_2 in healthy rats and in a model of IPF. We found that riociguat was a more effective vasodilator in isolated PA than sildenafil. The potency of both drugs was similar under conditions of high oxygen (95%) or hypoxia. Both drugs inhibited HPV *in vitro* and the vasoconstrictor response to U46619. *In vivo* the two drugs were more effective in inhibiting the increase in PA pressure induced by global hypoxia or by U46619 than in inhibiting the unilateral hypoxia induced by bronchial obstruction but this was not associated to worsened oxygen saturation. Pulmonary fibrosis was associated with ventilation-perfusion uncoupling. Both drugs increased lung perfusion but did not affect the ventilation-perfusion ratio. Therefore, despite the inhibitory effect on HPV, the two drugs did not worsen ventilation perfusion coupling.

2.1. Pulmonary selectivity

In isolated rat arteries, the pulmonary selectivity was similar for sildenafil and riociguat, i.e. both showed a trend for higher systemic than pulmonary effects *in vitro*. *In vivo,* the effects of both drugs on basal pulmonary pressure were weak while riociguat, but not sildenafil, produced a significant systemic effect confirming its low (or inverse) pulmonary selectivity. Further comparisons can also be made for the response induced by U46619 *in vivo*. Both drugs inhibited these responses in PA, sildenafil being more effective, and none of them affected the systemic pressures at the dose tested. These data are in line with previous studies in lambs and rabbits with U46619-induced acute PH (Weimann et al., 2000; Schermuly et al., 2008). In summary, pulmonary selectivity is strongly dependent on the experimental conditions, the two drugs were selective *in vitro* for systemic vessels, riociguat was also selective systemic vasodilator *in vivo* while both drugs were selective for the pulmonary circulation when challenged by the TXA_2 analog. These data reflect a different role of the NO-cGMP-PDE5 signalling pathway in the systemic and pulmonary circulation and a different regulation by U46619 in both vascular beds. Moreover, the differences between the two drugs are a consequence of their different mode of regulating this pathway; riociguat increases the cGMP levels by stimulation of sGC while sildenafil inhibits specifically PDE5, which is highly expressed within lungs.

2.2. Sildenafil and riociguat inhibited the vasoconstriction induced by hypoxia and U46619 in isolated PA

Vasodilators that inhibit HPV, such as calcium channel blockers, may lead to worsen arterial oxygenation (Galiè et al., 2015, Ballester et al., 1986). In this study, we observed that sildenafil and riociguat prevented the vasoconstrictor response induced by hypoxia and by the TXA_2 mimetic U46619 in isolated rat PA. However, it should be noted that at concentrations of riociguat and sildenafil (i.e. 10^{-7}M), which were equally effective in inhibiting hypoxia-induced vasoconstriction, the former produced a much stronger inhibitory effect on U46619-induced contraction than the later. This is consistent with the higher efficacy of riociguat as vasodilator that we reported in the previous chapter in both rat and human PAs *in vitro*. This could be attributed to a low basal sGC activity in isolated arteries which contrasts with the higher efficacy of sildenafil to inhibit U46619 induced responses *in vivo*, possibly due to higher NO and cGMP levels in these conditions.

In contrast with our results, Tsai *et al.* (2006) found that sildenafil exposure for 20 minutes had no effect on HPV. This difference with our results could be explained because these authors used the main branch of PA and exposed to 1 h of hypoxia, while we have used third-order branches of the PA, which are known respond better to HPV than main branches of the PA (Michelakis et al., 2004; Ward et al.; 2009).

2.3. Response of riociguat and sildenafil on systemic and pulmonary arterial pressure and oxygen saturation in response to global and unilateral hypoxia and U46619

Global hypoxia produces an increase in mPAP due to homogeneous (global) pulmonary vasoconstriction and hypoxemia. Unilateral hypoxia increases mPAP due to vasoconstriction only in the affected (left) lung leading to increased blood flow to the well ventilated (right) lung. This redistribution of blood flow partially compensates the reduced gas exchange and hence the desaturation. Using this protocol, vasodilators

inhibiting HPV are expected to reduce pulmonary pressure induced by global hypoxia but as vasodilation is homogeneous no effect is expected on the hypoxemia. In fact, both drugs inhibited significantly the increase in mPAP induced by global hypoxia, without affecting the desaturation. These results are consistent with findings from other groups. Thus, in healthy human volunteers and mice (Zhao et al., 2001) and in dogs (Fesler et al., 2006) pretreatment with sildenafil almost abolished hypoxia-induced increase of pulmonary pressure and it did not modify the fall of oxygen saturation induced by hypoxia. This effect has been observed also with riociguat, which reversed acute pulmonary vasoconstriction in isolated lungs from mice (Schermuly et al., 2008).

When the animals are challenged with unilateral hypoxia in the presence of vasodilators inhibiting HPV, the pressure response and hence the blood redistribution is expected to be decreased leading to increased blood desaturation (Becker *et al.* 2013). Surprisingly, despite the drugs inhibited by > 50% the pressor response to global hypoxia, neither sildenafil nor riociguat were able to inhibit the increase in pulmonary pressure induced by unilateral hypoxia. Accordingly, they did not modify the oxygen saturation suggesting that blood distribution is also unaffected, however, we did not measure global or local blood flow to test this possibility.

2.4. Effects on ventilation-perfusion mismatch in fibrotic rats

Chronic pulmonary hypoxic diseases such as COPD or IPF have an impaired ventilation and perfusion of the lung units and can be monitored by the analysis of the inhaled DTPA-^{99m} Tc signal and perfused MAA-^{99m} Tc (Milara et al, 2016). V/Q SPECT imaging is a well-established nuclear medicine technique that provides spatial information of respiratory gas exchange, ventilation of alveolar units and perfusion of the pulmonary capillary beds (Amen et al., 2011).

Acute administration of sildenafil and riociguat in the bleomycin-induced pulmonary fibrosis model associated with PH induced an increase in lung perfusion without changes in V/Q ratio. These results are consistent with findings of other groups in humans. Acute administration of sildenafil (Ghofrani et al., 2002) and riociguat

(Grimminger et al., 2009) in patients with PH associated to interstitial lung disease, exerted pulmonary vasodilatory effects whereas they did not produce any deterioration in gas exchange or V/Q matching.

2.5. Study limitations

Several limitations should be mentioned in our study. First, unilateral lung ventilation, although an inducer of hypoxemia, is not an exact model of the heterogeneous ventilation that is observed in parenchymal lung disease (e.g. pulmonary fibrosis, or COPD) as the pathology affects the lobe evenly and is not related to inflammatory or fibrotic changes. Second, this study was conducted under anesthesia and mechanical ventilation so we could not evaluate any influence of spontaneous breathing. Third, in our acute *in vivo* model, we only tested a single drug dose.

3. The flavonoid quercetin reverses monocrotaline-induced pulmonary hypertension in rats.

PAH is characterized by increased pulmonary artery pressure as a result of increased pulmonary vascular resistance due to pulmonary vascular vasoconstriction, increased smooth muscle cell proliferation/apoptosis ratio and *in situ* thrombosis (Rabinovitch et al., 2012). Quercetin has shown a number of vascular effects including vasodilator, antiplatelet, smooth muscle antiproliferative and proapoptotic effects in the systemic and coronary circulation. Herein we show that quercetin is also partially protective in a model of PAH by lowering PAP, RVH and vascular remodelling. In addition, *in vitro* quercetin exerted pulmonary vasodilator effects and inhibited cell proliferation in PASMCs.

PAH develops progressively and most PAH patients with earlier-stage disease such as NYHA class I or II are asymptomatic and the condition is not identified until symptoms become severe (Simonneau et al., 2009). Therefore, treatments for PAH must be effective once the symptoms have developed. Gao et al. have recently reported that a high dose of quercetin (10 fold the one we used) from day 2 to day 21 after monocrotaline and analyzing the results at day 41st, i.e. a preventive strategy, produced a reduction of PAP and RVH but they did not attempt to analyze the mechanisms involved (Gao et al.,2012) We chose to start treatment with quercetin 21 days after monocrotaline, in order to mimic the clinical situation. At this stage, the animals develop marked increases in PAP and the severity of the disease in our study was evidenced by 11% mortality. The final mortality in untreated animals was 56% (78% including animals which died during anesthesia or surgery). Moreover, surviving rats were in better hemodynamic conditions when treated by quercetin.

As expected by the reduced right ventricular afterload, quercetin also decreased the right ventricular hypertrophy. The effectiveness of quercetin in this experiment with a very aggressive form of PAH suggests that it might prevent premature death in humans with PAH. It should be noted, however, that although all clinically useful drugs for PAH are effective in this animal model, not all drugs reversing monocrotaline-induced

increased PAP are effective in clinical PAH (Stenmark et al., 2009). Despite the increased survival and the hemodynamic, anatomical and histological improvement, most of the conventional markers of PAH such as membrane depolarization, endothelial dysfunction and downregulation of BMPR2 and Kv1.5, were unaffected or modestly affected by quercetin. Endothelial dysfunction was accompanied by a reduced the expression of eNOS. This is consistent with previous studies showing that eNOS and other endothelial cell markers, such as caveolin-1 or CD31, are downregulated, suggesting that monocrotaline causes disruption of the integrity of the EC (Mathew et al., 2004; Sahara et al., 2012). Quercetin has demonstrated to improve endothelial function in several models of cardiovascular disease via decreased expression of NADPH oxidase subunits, restoring eNOS uncoupling, eNOS phosphorylation or scavenging superoxide (Perez-Vizcaino et al., 2006). However, quercetin was unable to restore eNOS downregulation which appears to be a major contributor to endothelial dysfunction in this model. In fact, a trend for reduced eNOS expression was found in quercetin-treated animals which are in agreement with *in vitro* data in human umbilical endothelial cells or in spontaneously hypertensive rats (Tribolo et al., 2013; Sánchez et al., 2006). Notably, quercetin inhibited the decrease in Kv currents and the overexpression of 5-HT_{2A} and iNOS induced by monocrotaline. Downregulated 5-HT_{2A} receptors might contribute to reduce arterial remodelling (Liu et al., 2013) but it was not sufficient to decrease the vascular hyperresponsiveness to 5-HT. This later effect is probably related to changes in ROS and COX activity as observed in other models of PAH as it can be normalized by cyclooxygenase inhibitors and antioxidants (Thomas et al., 2003; Sato et al., 2000; Lopez-Lopez et al., 2011). The fact that quercetin inhibits the changes in specific genes but does not affect other genes may reflect that changes in gene expression in this model of PAH operate through quercetin-sensitive and -insensitive signalling pathways.

Proliferation of PASMC leading to increased muscularization of small PA and reduced vascular lumen is considered the hallmark of the most advanced and aggressive forms of PAH. Quercetin reduced the number of muscular arteries, an effect that is likely to contribute to the decrease in PAP. In order to confirm the *in vivo* findings, we tested the effects of quercetin on PASMC *in vitro*. We found that quercetin produced a

concentration-dependent decrease in cell number of PASMC and fibroblasts, related to the inhibition of proliferation, as measured by the BrdU incorporation. However, quercetin also induces apoptosis in vascular smooth muscle (Perez-Vizcaino et al., 2006) which may also marginally contribute to reduce cell viability in these in vitro experiments.

A large number of cell signalling pathways may be affected by quercetin. In fact, quercetin is a broad-spectrum protein kinase inhibitor being a competitive and reversible ligand for the ATP binding site (Walker et al., 2000). However, few studies have confirmed it in its *in vivo* effects. Therefore, we analyzed in the rat lungs from the *in vivo* study the signalling pathways reported to be involved in the pathophysiology of PAH which could be potentially targeted by quercetin. These include those activated by PDGF and TGF-β, MAPKs, the PI3K/Akt/mTOR pathway, and the antiapoptotic protein survivin. Quercetin is a canonical pan-inhibitor of MAPKs and the TGF-β pathway (Nakamura et al., 2011) and previous studies on the effects of quercetin on VSMC viability, migration, and proliferation have related their findings to interactions with MAPKs (Perez-Vizcaino et al., 2006; Moon et al., 2003; Yoshizumi et al., 2002). MAPKs (e.g. ERK1/2, p38-MAPK and JNK) play a key role in cell proliferation and this axis has been suggested as a potential therapeutic target in PAH (Nasim et al., 2012). However, their role in PAH induced by monocrotaline is controversial. In fact, increased (Henriques-Coelho et al., 2008), unchanged (Morty et al., 2007) or decreased (Ramos et al., 2007) phosphorylation of p38-MAPK and unchanged (Henriques-Coelho et al., 2008; Morty et al., 2007) or increased (Nasim et al., 2012) phosphorylation of ERK1/2 have been reported. We found no significant changes among groups in p38-MAPK and ERK1/2 phosphorylation suggesting that MAPKs play little role in the PAH and in the effects of quercetin in this model.

Another potential pathway for PASMC muscularization in PAH is via overexpression of the antiapoptotic protein survivin. In fact, genetic targeting of survivin has been shown to reduce PAH in the monocrotaline-treated rats (McMurtry et al., 2005). We found that survivin mRNA was significantly overexpressed in the lungs of monocrotaline-treated rats but the protein increase did not achieve statistical significance. This difference might be due to post-transductional changes. Interestingly, quercetin has

been shown to induce survivin downregulation in several cancer cells, via decreasing the survivin promoter activity (Kim et al., 2008). Herein we show that chronic quercetin had no clear effect on survivin expression, suggesting that *in vivo* the downregulation of survivin is not a major mechanism for the antiproliferative effect. This is consistent with the high concentrations (50 mM) of quercetin required to downregulate survivin (Kim et al., 2008). The intracellular signalling pathway involving the PI3K/Akt/mTOR/S6 plays an important role in cell proliferation in PAH and it is thought to be a promising therapeutic target for this syndrome (Goncharova et al., 2013; Houssaini et al., 2013; Goncharov et al., 2014). Quercetin may interfere with the activity of both PI3K and mTOR (Bruning et al., 2012; Pratheeshkumar et al., 2012). We found that Akt phosphorylation was increased by monocrotaline which was associated by a strong downregulation of Akt expression. As previously reported in other cell types (Pratheeshkumar et al., 2012; Yuan et al., 2012), the Akt phosphorylation was diminished by quercetin, suggesting that inhibition of this pathway may be involved in the decreased PA muscularization. This is consistent with the high potency of quercetin to inhibit PI3K (KD at submicromolar concentrations) (Walker et al., 2000). Furthermore, we also found that phosphorylation of S6, the downstream target of mTOR, was higher in the group treated with monocrotaline and this increase was inhibited by quercetin. Quercetin is also a well-known vasodilator (Duarte et al., 1993; Cogolludo et al., 2007). We also found that quercetin was similarly effective in isolated PA both from control and monocrotaline-treated rats stimulated by the thromboxane A_2 mimetic U46619 ($logIC_{50}$ of 5.3 and 5.1, respectively, not shown). Thus, this vasodilator effect may be an additional contributor to the reduction in PA pressure in this model.

The pharmacokinetics of quercetin is complex. It is not present in the blood in its free form but circulates conjugated with glucuronide which is released in the tissues after deconjugation (Menendez et al., 2012). Because quercetin was not administered the day of the end-point measurements, it is likely that the effects observed reflect the chronic rather than the acute actions of quercetin and the reduction in PA pressure may be underestimated.

In conclusion, quercetin is partially protective in this rat model of PAH. It delayed mortality by lowering PAP, RVH and vascular remodelling. Quercetin exerted effective vasodilator effects in isolated PA, inhibited cell proliferation and induced apoptosis in PASMCs. These effects were associated with decreased 5-HT_{2A} receptor expression and Akt and S6 phosphorylation and partially restored Kv currents. Therefore, quercetin could be useful in the treatment of PAH.

CONCLUSIONS

1. The drugs studied in this thesis showed low pulmonary selectivity, being equally or more effective as vasodilators in systemic (i.e. mesenteric) than in pulmonary arteries.

2. The drugs studied, with the exception of GW0742 in rat arteries, showed no oxygen selectivity, being equally or more effective as vasodilators under conditions of low oxygen as compared to high oxygen levels in rat or human pulmonary arteries.

3. The comparison of the vasodilator versus antiproliferative effects indicates that most of the drugs tested, including NO donors, PDE5 inhibitors, sGC activators, adenylate cyclase activator forskolin, the PPARβ/δ agonist GW0742 and the ROCK1/2 inhibitor hydroxyfasudil exert preferential vasodilator effects. Some drugs including the calcium sentitizer levosimendan and drugs targeting ion channels were similarly effective to exert both effects.

4. The TAK-1 inhibitor 5-z-7-oxozeaenol produced strong and specific antiproliferative effects in pulmonary vascular smooth muscle cells without any effect on vascular tone. Thus, our data suggest that TAK-1 may represent a novel target for the treatment of PAH.

5. Riociguat was a more effective vasodilator in isolated PA than sildenafil. The potency of both drugs was similar under conditions of high oxygen vs hypoxia. Both drugs inhibited *in vitro* the vasoconstrictor response to hypoxia and U46619. *In vivo,* the two drugs were more effective in inhibiting the increase in PA pressure induced by global hypoxia or by U46619 than in inhibiting the response to unilateral hypoxia induced by bronchial obstruction. Furthermore, pulmonary fibrosis was associated with ventilation-perfusion uncoupling and although both drugs increased lung perfusion, they did not affect the ventilation-perfusion coupling.

6. Quercetin induced a strong vasodilator and antiproliferative effect in rat and human pulmonary smooth muscle *in vitro*. In the rat model of PAH, quercetin increased the survival by lowering PAP, RVH and vascular remodeling. Even when some classic biomarkers of pulmonary arterial hypertension were unaffected by quercetin, it restored the decrease in Kv current and reduced the increase in Akt and S6 phosphorylation induced by monocrotaline. Therefore, quercetin could be useful in the treatment of PAH.

REFERENCES

Abe K, Shimokawa H, Morikawa K, Uwatoku T, Oi K, Matsumoto Y, Hattori T, Nakashima Y, Kaibuchi K, Sueishi K, Takeshit A. Long-term treatment with a Rho-kinase inhibitor improves monocrotaline-induced fatal pulmonary hypertension in rats. Circ Res. 2004 Feb 20;94(3):385-93. Epub 2003 Dec 11.

Abe K, Tawara S, Oi K, Hizume T, Uwatoku T, Fukumoto Y, Kaibuchi K, Shimokawa H. Long-term inhibition of Rho-kinase ameliorates hypoxia-induced pulmonary hypertension in mice. J Cardiovasc Pharmacol. 2006 Dec;48(6):280-5.

Abe K, Toba M, Alzoubi A, Koubsky K, Ito M, Ota H, Gairhe S, Gerthoffer WT, Fagan KA, McMurtry IF, Oka M. Tyrosine kinase inhibitors are potent acute pulmonary vasodilators in rats. Am J Respir Cell Mol Biol. 2011 Oct;45(4):804-8. doi: 10.1165/rcmb.2010-0371OC. Epub 2011 Mar 4.

Adnot S, Radermacher P, Andrivet P, Dubois-Rande JL, Dupeyrat A, Lemaire F. Effects of sodium-nitroprusside and urapidil on gas exchange and ventilation-perfusion relationships in patients with congestive heart failure. Eur Respir J. 1991 Jan;4(1):69-75.

Agarwal R, Gomberg-Maitland M. Current therapeutics and practical management strategies for pulmonary arterial hypertension. Am Heart J. 2011 Aug;162(2):201-13. doi: 10.1016/j.ahj.2011.05.012. Epub 2011 Jul 13.

Aggarwal S, Gross CM, Sharma S, Fineman JR, Black SM. Reactive oxygen species in pulmonary vascular remodeling. Compr Physiol. 2013 Jul;3(3):1011-34. doi: 10.1002/cphy.c120024.

Akiyoshi J, Ieiri S, Nakatsuji T, Taguchi T. Direct vasodilative effect of FK506 on porcine mesenteric artery in small bowel transplantation. J Pediatr Surg. 2009 Dec;44(12):2322-6. doi: 10.1016/j.jpedsurg.2009.07.060.

Ali FY, Egan K, FitzGerald GA, Desvergne B, Wahli W, Bishop-Bailey D, Warner TD, Mitchell JA. Role of prostacyclin versus peroxisome proliferator-activated receptor beta receptors in prostacyclin sensing by lung fibroblasts. Am J Respir Cell Mol Biol. 2006 Feb;34(2):242-6. Epub 2005 Oct 20.

Almudéver P, Milara J, De Diego A, Serrano-Mollar A, Xaubet A, Perez-Vizcaino F, Cogolludo A, Cortijo J. Role of tetrahydrobiopterin in pulmonary vascular remodelling associated with pulmonary fibrosis. Thorax. 2013 Oct;68(10):938-48. doi: 10.1136/thoraxjnl-2013-203408. Epub 2013 Jun 5

Amen EM, Becker EM, Truebel H. Analysis of V/Q-matching--a safety "biomarker" in pulmonary drug development? Biomarkers. 2011 Jul;16 Suppl 1:S5-10. doi: 10.3109/1354750X.2011.585243.

Ameshima S, Golpon H, Cool CD, Chan D, Vandivier RW, Gardai SJ, Wick M, Nemenoff RA, Geraci MW, Voelkel NF. Peroxisome proliferator-activated receptor gamma (PPARgamma) expression is decreased in pulmonary hypertension and affects endothelial cell growth. Circ Res. 2003 May 30;92(10):1162-9. Epub 2003 Apr 24.

Antoniades C, Tousoulis D, Koumallos N, Marinou K, Stefanadis C. Levosimendan: beyond its simple inotropic effect in heart failure. Pharmacol Ther. 2007 May;114(2):184-97. Epub 2007 Feb 16.

Ballester E, Roca J, Rodriguez-Roisin R, Agusti-Vidal A. Effect of nifedipine on arterial hypoxaemia occurring after methacholine challenge in asthma. Thorax. 1986 Jun;41(6):468-72.

Banfor PN, Preusser LC, Campbell TJ, Marsh KC, Polakowski JS, Reinhart GA, Cox BF, Fryer RM. Comparative effects of levosimendan, OR-1896, OR-1855, dobutamine, and milrinone on vascular resistance, indexes of cardiac function, and O2 consumption in dogs. Am J Physiol Heart Circ Physiol. 2008 Jan;294(1):H238-48. Epub 2007 Nov 2.

Bauer S, Patterson PH. The cell cycle-apoptosis connection revisited in the adult brain. J Cell Biol. 2005 Nov 21;171(4):641-50. Epub 2005 Nov 15.

Bawankule DU, Sathishkumar K, Sardar KK, Chanda D, Krishna AV, Prakash VR, Mishra SK. BAY 41-2272 [5-cyclopropyl-2-[1-(2-fluoro-benzyl)-1H-pyrazolo[3,4-b]pyridine-3-yl]pyrimidin-4-ylamine]-induced dilation in ovine pulmonary artery: role of sodium pump. J Pharmacol Exp Ther. 2005 Jul;314(1):207-13. Epub 2005 Mar 25.

Becker EM, Stasch JP, Bechem M, Keldenich J, Klipp A, Schaefer K, Ulbrich HF, Truebel H. Effects of different pulmonary vasodilators on arterial saturation in a model of pulmonary hypertension. PLoS One. 2013 Aug 28;8(8):e73502. doi: 10.1371/journal.pone.0073502. eCollection 2013.

Bender SB, Berwick ZC, Laughlin MH, Tune JD. Functional contribution of P2Y1 receptors to the control of coronary blood flow. J Appl Physiol (1985). 2011 Dec;111(6):1744-50. doi: 10.1152/japplphysiol.00946.2011. Epub 2011 Sep 22.

Benyahia C, Boukais K, Gomez I, Silverstein A, Clapp L, Fabre A, Danel C, Leséche G, Longrois D, Norel X. A comparative study of PGI_2 mimetics used clinically on the vasorelaxation of human pulmonary arteries and veins, role of the DP-receptor. Prostaglandins Other Lipid Mediat. 2013 Dec;107:48-55. doi: 10.1016/j.prostaglandins.2013.07.001. Epub 2013 Jul 12.

Benyahia C, Ozen G, Orie N, Ledwozyw A, Louedec L, Li F, Senbel AM, Silverstein A, Danel C, Longrois D, Clapp LH, Norel X, Topal G. Ex vivo relaxations of pulmonary arteries induced by prostacyclin mimetics are highly dependent of the precontractile agents. Prostaglandins Other Lipid Mediat. 2015 Sep;121(Pt A):46-52. doi: 10.1016/j.prostaglandins.2015.09.002. Epub 2015 Sep 8.

Berger G, Azzam ZS, Hoffman R, Yigla M. Coagulation and anticoagulation in pulmonary arterial hypertension. Isr Med Assoc J. 2009 Jun;11(6):376-9.

Biasin V, Chwalek K, Wilhelm J, Best J, Marsh LM, Ghanim B, Klepetko W, Fink L, Schermuly RT, Weissmann N, Olschewski A, Kwapiszewska G. Endothelin-1 driven proliferation of pulmonary arterial smooth muscle cells is c-fos dependent. Int J Biochem Cell Biol. 2014 Sep;54:137-48. doi: 10.1016/j.biocel.2014.06.020. Epub 2014 Jul 10.

Blanco I, Gimeno E, Munoz PA, Pizarro S, Gistau C, Rodriguez-Roisin R, Roca J, Barberà JA. Hemodynamic and gas exchange effects of sildenafil in patients with chronic obstructive pulmonary disease and pulmonary hypertension. Am J Respir Crit Care Med. 2010 Feb 1;181(3):270-8. doi: 10.1164/rccm.200907-0988OC. Epub 2009 Oct 29.

Blount MA, Beasley A, Zoraghi R, Sekhar KR, Bessay EP, Francis SH, Corbin JD. Binding of tritiated sildenafil, tadalafil, or vardenafil to the phosphodiesterase-5 catalytic site displays potency, specificity, heterogeneity, and cGMP stimulation. Mol Pharmacol. 2004 Jul;66(1):144-52.

Bonnet S, Archer SL. Potassium channel diversity in the pulmonary arteries and pulmonary veins: implications for regulation of the pulmonary vasculature in health and during pulmonary hypertension. Pharmacol Ther. 2007 Jul;115(1):56-69. Epub 2007 Apr 21.

Bonnet S, Rochefort G, Sutendra G, Archer SL, Haromy A, Webster L, Hashimoto K, Bonnet SN, Michelakis ED. The nuclear factor of activated T cells in pulmonary arterial hypertension can be therapeutically targeted. PNAS 104: 11418–11423, 2007.

Boucherat O, Chabot S, Antigny F, Perros F, Provencher S, Bonnet S. Potassium channels in pulmonary arterial hypertension. Eur Respir J. 2015 Oct;46(4):1167-77. doi: 10.1183/13993003.00798-2015. Epub 2015 Sep 4.

Braissant O, Foufelle F, Scotto C, Dauça M, Wahli W. Differential expression of peroxisome proliferator-activated receptors (PPARs): tissue distribution of PPAR-alpha, -beta, and -gamma in the adult rat. Endocrinology. 1996 Jan;137(1):354-66.

Bruning A. Inhibition of mTOR signaling by quercetin in cancer treatment and prevention. Anticancer Agents Med Chem. 2013 Sep;13(7):1025-31.

Burg ED, Remillard CV, Yuan JX. Potassium channels in the regulation of pulmonary artery smooth muscle cell proliferation and apoptosis: pharmacotherapeutic implications. Br J Pharmacol. 2008 Mar;153 Suppl 1:S99-S111. Epub 2007 Dec 17.

Burnstock G. Purinergic regulation of vascular tone and remodelling. Auton Autacoid Pharmacol. 2009 Jul;29(3):63-72. doi: 10.1111/j.1474-8673.2009.00435.x.

Cai J, Pardali E, Sánchez-Duffhues G, ten Dijke P. BMP signaling in vascular diseases. FEBS Lett. 2012 Jul 4;586(14):1993-2002. doi: 10.1016/j.febslet.2012.04.030. Epub 2012 May 3

Capra V, Bäck M, Angiolillo DJ, Cattaneo M, Sakariassen KS. Impact of vascular thromboxane prostanoid receptor activation on hemostasis, thrombosis, oxidative stress, and inflammation. J Thromb Haemost. 2014 Feb;12(2):126-37. doi: 10.1111/jth.12472.

Chalupsky K, Lobysheva I, Nepveu F, Gadea I, Beranova P, Entlicher G, Stoclet JC, Muller B. Relaxant effect of oxime derivatives in isolated rat aorta: role of nitric oxide (NO) formation in smooth muscle. Biochem Pharmacol. 2004 Mar 15;67(6):1203-14.

Chen XY, Dun JN, Miao QF, Zhang YJ. Fasudil hydrochloride hydrate, a Rho-kinase inhibitor, suppresses 5-hydroxytryptamine-induced pulmonary artery smooth muscle cell proliferation via JNK and ERK1/2 pathway. Pharmacology. 2009;83(2):67-79. doi: 10.1159/000178814. Epub 2008 Dec 4.

Chen Z, Mei Y, Lei H, Tian R, Ni N, Han F, Gan S, Sun S. LYTAK1, a TAK1 inhibitor, suppresses proliferation and epithelial‑mesenchymal transition in retinal pigment epithelium cells. Mol Med Rep. 2016 Jul;14(1):145-50. doi: 10.3892/mmr.2016.5275. Epub 2016 May 13.

Chester AH, Yacoub MH. The role of endothelin-1 in pulmonary arterial hypertension. Glob Cardiol Sci Pract. 2014 Jun 18;2014(2):62-78. doi: 10.5339/gcsp.2014.29.

Christman BW, McPherson CD, Newman JH, King GA, Bernard GR, Groves BM, Loyd JE. An imbalance between the excretion of thromboxane and prostacyclin metabolites in pulmonary hypertension. N Engl J Med. 1992 Jul 9;327(2):70-5.

Chu LY, Liou JY, Wu KK. Prostacyclin protects vascular integrity via PPAR/14-3-3 pathway. Prostaglandins Other Lipid Mediat. 2015 Apr-Jun;118-119:19-27. doi: 10.1016/j.prostaglandins.2015.04.006. Epub 2015 Apr 21.

Clapp LH, Finney P, Turcato S, Tran S, Rubin LJ, Tinker A. Differential effects of stable prostacyclin analogs on smooth muscle proliferation and cyclic AMP generation in human pulmonary artery. Am J Respir Cell Mol Biol. 2002 Feb;26(2):194-201.

Clapp LH, Gurung R. The mechanistic basis of prostacyclin and its stable analogues in pulmonary arterial hypertension: Role of membrane versus nuclear receptors. Prostaglandins Other Lipid Mediat. 2015 Jul;120:56-71. doi: 10.1016/j.prostaglandins.2015.04.007. Epub 2015 Apr 23.

Cockrill BA, Kacmarek RM, Fifer MA, Bigatello LM, Ginns LC, Zapol WM, Semigran MJ. Comparison of the effects of nitric oxide, nitroprusside, and nifedipine on hemodynamics and right ventricular contractility in patients with chronic pulmonary hypertension. Chest. 2001 Jan;119(1):128-36.

Cogolludo A, Frazziano G, Briones AM, Cobeno L, Moreno L, Lodi F, Salaices M, Tamargo J, Perez-Vizcaino F. The dietary flavonoid quercetin activates BKCa currents in coronary arteries via production of H2O2. Role in vasodilatation. Cardiovascular Research 2007;73:424-431.

Cogolludo A, Moreno L, Bosca L, Tamargo J, Perez-Vizcaino F. Thromboxane A2-induced inhibition of voltage-gated K+ channels and pulmonary vasoconstriction: role of protein kinase Czeta. Circ Res. 2003 Oct 3;93(7):656-63. Epub 2003 Sep 11.

Cogolludo A, Moreno L, Frazziano G, Moral-Sanz J, Menendez C, Castañeda J, González C, Villamor E, Perez-Vizcaino F. Activation of neutral sphingomyelinase is involved in acute hypoxic pulmonary vasoconstriction. Cardiovasc Res. 2009 May 1;82(2):296-302. doi: 10.1093/cvr/cvn349. Epub 2008 Dec 16.

Cogolludo A, Moreno L, Lodi F, Frazziano G, Cobeño L, Tamargo J, Perez-Vizcaino F. Serotonin inhibits voltage-gated K+ currents in pulmonary artery smooth muscle cells: role of 5-HT2A receptors, caveolin-1, and KV1.5 channel internalization. Circ Res. 2006 Apr 14;98(7):931-8. Epub 2006 Mar 9.

Cogolludo A, Moreno L, Villamor E. Mechanisms controlling vascular tone in pulmonary arterial hypertension: implications for vasodilator therapy. Pharmacology. 2007;79(2):65-75. Epub 2006 Dec 5.

Cogolludo AL, Moral-Sanz J, van der Sterren S, Frazziano G, van Cleef AN, Menéndez C, Zoer B, Moreno E, Roman A, Pérez-Vizcaino F, Villamor E. Maturation of O2 sensing and signaling in the chicken ductus arteriosus. Am J Physiol Lung Cell Mol Physiol. 2009 Oct;297(4):L619-30. doi: 10.1152/ajplung.00092.2009. Epub 2009 Jul 17.

Cogolludo AL, Pérez-Vizcaíno F, Zaragozá-Arnáez F, Ibarra M, López-López G, López-Miranda V, Tamargo J. Mechanisms involved in SNP-induced relaxation and [Ca+]i reduction in piglet pulmonary and systemic arteries. Br J Pharmacol. 2001 Feb;132(4):959-67.

Connolly MJ, Aaronson PI. Cell redox state and hypoxic pulmonary vasoconstriction: recent evidence and possible mechanisms. Respir Physiol Neurobiol. 2010 Dec 31;174(3):165-74. doi: 10.1016/j.resp.2010.08.016. Epub 2010 Aug 27.

Cottrill KA, Chan SY. Metabolic dysfunction in pulmonary hypertension: the expanding relevance of the Warburg effect. Eur J Clin Invest. 2013 Aug;43(8):855-65. doi: 10.1111/eci.12104. Epub 2013 Apr 26.

Crossno JT Jr, Garat CV, Reusch JE, Morris KG, Dempsey EC, McMurtry IF, Stenmark KR, Klemm DJ. Rosiglitazone attenuates hypoxia-induced pulmonary arterial remodeling. Am J Physiol Lung Cell Mol Physiol. 2007 Apr;292(4):L885-97. Epub 2006 Dec 22.

Dantas BP, Ribeiro TP, Assis VL, Furtado FF, Assis KS, Alves JS, Silva TM, Camara CA, França-Silva MS, Veras RC, Medeiros IA, Alencar JL, Braga VA. Vasorelaxation induced by a new naphthoquinone-oxime is mediated by NO-sGC-cGMP pathway. Molecules. 2014 Jul 8;19(7):9773-85. doi: 10.3390/molecules19079773.

Dasgupta A, Bowman L, D'Arsigny CL, Archer SL. Soluble guanylate cyclase: a new therapeutic target for pulmonary arterial hypertension and chronic thromboembolic pulmonary hypertension. Clin Pharmacol Ther. 2015 Jan;97(1):88-102. doi: 10.1002/cpt.10. Epub 2014 Nov 28.

de Buys Roessingh AS, de Lagausie P, Barbet JP, Mercier JC, Aigrain Y, Dinh-Xuan AT. Role of ATP-dependent potassium channels in pulmonary vascular tone of fetal lambs with congenital diaphragmatic hernia. Pediatr Res. 2006 Nov;60(5):537-42. Epub 2006 Sep 20.

de Frutos S, Spangler R, Alò D, Bosc LV. NFATc3 mediates chronic hypoxia-induced pulmonary arterial remodeling with alpha-actin up-regulation. J Biol Chem. 2007 May 18;282(20):15081-9. Epub 2007 Apr 2.

De Witt BJ, Ibrahim IN, Bayer E, Fields AM, Richards TA, Banister RE, Kaye AD. An analysis of responses to levosimendan in the pulmonary vascular bed of the cat. Anesth Analg. 2002 Jun;94(6):1427-33, table of contents.

De Witt BJ, Marrone JR, Kaye AD, Keefer LK, Kadowitz PJ. Comparison of responses to novel nitric oxide donors in the feline pulmonary vascular bed. Eur J Pharmacol. 2001 Nov 2;430(2-3):311-5.

Delannoy E, Courtois A, Freund-Michel V, Leblais V, Marthan R, Muller B. Hypoxia-induced hyperreactivity of pulmonary arteries: role of cyclooxygenase-2, isoprostanes, and thromboxane receptors. Cardiovasc Res. 2010 Feb 1;85(3):582-92. doi: 10.1093/cvr/cvp292. Epub 2009 Aug 26.

Dempsie Y, MacLean MR. Pulmonary hypertension: therapeutic targets within the serotonin system. Br J Pharmacol. 2008 Oct;155(4):455-62. doi: 10.1038/bjp.2008.241. Epub 2008 Jun 9.

Deruelle P, Balasubramaniam V, Kunig AM, Seedorf GJ, Markham NE, Abman SH. BAY 41-2272, a direct activator of soluble guanylate cyclase, reduces right ventricular hypertrophy and prevents pulmonary vascular remodeling during chronic hypoxia in neonatal rats. Biol Neonate. 2006;90(2):135-44. Epub 2006 Mar 19.

Do e Z, Fukumoto Y, Takaki A, Tawara S, Ohashi J, Nakano M, Tada T, Saji K, Sugimura K, Fujita H, Hoshikawa Y, Nawata J, Kondo T, Shimokawa H. Evidence for Rho-kinase activation in patients with pulmonary arterial hypertension. Circ J. 2009 Sep;73(9):1731-9. Epub 2009 Jul 9.

Duarte J, Pérez-Vizcaíno F, Zarzuelo A, Jiménez J, Tamargo J. Vasodilator effects of quercetin in isolated rat vascular smooth muscle. Eur J Pharmacol. 1993 Aug 3;239(1-3):1-7.

Dumitrascu R, Weissmann N, Ghofrani HA, Dony E, Beuerlein K, Schmidt H, Stasch JP, Gnoth MJ, Seeger W, Grimminger F, Schermuly RT. Activation of soluble guanylate cyclase reverses experimental pulmonary hypertension and vascular remodeling. Circulation. 2006 Jan 17;113(2):286-95. Epub 2006 Jan 3.

Duong-Quy S, Bei Y, Liu Z, Dinh-Xuan AT. Role of Rho-kinase and its inhibitors in pulmonary hypertension. Pharmacol Ther. 2013 Mar;137(3):352-64. doi: 10.1016/j.pharmthera.2012.12.003. Epub 2012 Dec 20.

Egermayer P, Town GI, Peacock AJ. Role of serotonin in the pathogenesis of acute and chronic pulmonary hypertension. Thorax. 1999 Feb;54(2):161-8.

El Chami H, Hassoun PM. Immune and inflammatory mechanisms in pulmonary arterial hypertension. Prog Cardiovasc Dis. 2012 Sep-Oct;55(2):218-28. doi: 10.1016/j.pcad.2012.07.006.

Enderby CY, Burger C. Medical treatment update on pulmonary arterial hypertension. Ther Adv Chronic Dis. 2015 Sep;6(5):264-72. doi: 10.1177/2040622315590757.

Evgenov OV, Ichinose F, Evgenov NV, Gnoth MJ, Falkowski GE, Chang Y, Bloch KD, Zapol WM. Soluble guanylate cyclase activator reverses acute pulmonary hypertension and augments the pulmonary vasodilator response to inhaled nitric oxide in awake lambs. Circulation. 2004 Oct 12;110(15):2253-9. Epub 2004 Oct 4.

Falcetti E, Hall SM, Phillips PG, Patel J, Morrell NW, Haworth SG, Clapp LH. Smooth muscle proliferation and role of the prostacyclin (IP) receptor in idiopathic pulmonary arterial hypertension. Am J Respir Crit Care Med. 2010 Nov 1;182(9):1161-70. doi: 10.1164/rccm.201001-0011OC. Epub 2010 Jul 9.

Farrow KN, Lee KJ, Perez M, Schriewer JM, Wedgwood S, Lakshminrusimha S, Smith CL, Steinhorn RH, Schumacker PT. Brief hyperoxia increases mitochondrial oxidation and increases phosphodiesterase 5 activity in fetal pulmonary artery smooth muscle cells. Antioxid Redox Signal. 2012 Aug 1;17(3):460-70. doi: 10.1089/ars.2011.4184. Epub 2012 Mar 8.

Fesler P, Pagnamenta A, Rondelet B, Kerbaul F, Naeije R. Effects of sildenafil on hypoxic pulmonary vascular function in dogs. J Appl Physiol (1985). 2006 Oct;101(4):1085-90. Epub 2006 Jun 15.

Fidalgo S, Ivanov DK, Wood SH. Serotonin: from top to bottom. Biogerontology. 2013 Feb;14(1):21-45. doi: 10.1007/s10522-012-9406-3. Epub 2012 Oct 26.

Firth AL, Won JY, Park WS. Regulation of $Ca(^{2+})$ signaling in pulmonary hypertension. Korean J Physiol Pharmacol. 2013 Feb;17(1):1-8. doi: 10.4196/kjpp.2013.17.1.1. Epub 2013 Feb 14.

Follmann M, Griebenow N, Hahn MG, Hartung I, Mais FJ, Mittendorf J, Schäfer M, Schirok H, Stasch JP, Stoll F, Straub A. The chemistry and biology of soluble guanylate cyclase stimulators and activators. Angew Chem Int Ed Engl. 2013 Sep 2;52(36):9442-62. doi: 10.1002/anie.201302588. Epub 2013 Aug 20**.**

Foris V, Kovacs G, Tscherner M, Olschewski A, Olschewski H. Biomarkers in pulmonary hypertension: what do we know? Chest. 2013 Jul;144(1):274-83. doi: 10.1378/chest.12-1246.

Foster MN, Coetzee WA. KATP Channels in the Cardiovascular System. Physiol Rev. 2016 Jan;96(1):177-252. doi: 10.1152/physrev.00003.2015.

Francis SH, Blount MA, Corbin JD. Mammalian cyclic nucleotide phosphodiesterases: molecular mechanisms and physiological functions. Physiol Rev. 2011 Apr;91(2):651-90. doi: 10.1152/physrev.00030.2010.

Frazziano G, Moreno L, Moral-Sanz J, Menendez C, Escolano L, Gonzalez C, Villamor E, Alvarez-Sala JL, Cogolludo AL, Perez-Vizcaino F. Neutral sphingomyelinase, NADPH oxidase and reactive oxygen species. Role in acute hypoxic pulmonary vasoconstriction. J Cell Physiol. 2011 Oct;226(10):2633-40. doi: 10.1002/jcp.22611.

Freund-Michel V, Khoyrattee N, Savineau JP, Muller B, Guibert C. Mitochondria: roles in pulmonary hypertension. Int J Biochem Cell Biol. 2014 Oct;55:93-7. doi: 10.1016/j.biocel.2014.08.012. Epub 2014 Aug 20.

Fukumoto Y, Matoba T, Ito A, Tanaka H, Kishi T, Hayashidani S, Abe K, Takeshita A, Shimokawa H. Acute vasodilator effects of a Rho-kinase inhibitor, fasudil, in patients with severe pulmonary hypertension. Heart. 2005 Mar;91(3):391-2.

Galiè N, Humbert M, Vachiery JL, Gibbs S, Lang I, Torbicki A, Simonneau G, Peacock A, Vonk Noordegraaf A, Beghetti M, Ghofrani A, Gomez Sanchez MA, Hansmann G, Klepetko W, Lancellotti P, Matucci M, McDonagh T, Pierard LA, Trindade PT4, Zompatori M, Hoeper M. 2015 ESC/ERS Guidelines for the diagnosis and treatment of pulmonary hypertension: The Joint Task Force for the Diagnosis and Treatment of Pulmonary Hypertension of the European Society of Cardiology (ESC) and the European Respiratory Society (ERS): Endorsed by: Association for European Paediatric and Congenital Cardiology (AEPC), International Society for Heart and Lung Transplantation (ISHLT). Eur Respir J. 2015 Oct;46(4):903-75. doi: 10.1183/13993003.01032-2015. Epub 2015 Aug 29.

Galié N, Manes A, Branzi A. The endothelin system in pulmonary arterial hypertension. Cardiovasc Res. 2004 Feb 1;61(2):227-37.

Gangopahyay A, Oran M, Bauer EM, Wertz JW, Comhair SA, Erzurum SC, Bauer PM. Bone morphogenetic protein receptor II is a novel mediator of endothelial nitric-oxide synthase activation. J Biol Chem. 2011 Sep 23;286(38):33134-40. doi: 10.1074/jbc.M111.274100. Epub 2011 Aug 1.

Gao H, Chen C, Huang S, Li B. Quercetin attenuates the progression of monocrotaline-induced pulmonary hypertension in rats. J Biomed Res. 2012 Mar;26(2):98-102. doi: 10.1016/S1674-8301(12)60018-9.

Gao Y, Chen T, Raj JU. Endothelial and Smooth Muscle Cell Interactions in the Pathobiology of Pulmonary Hypertension. Am J Respir Cell Mol Biol. 2016 Jan 8. [Epub ahead of print]

García de Vinuesa A, Abdelilah-Seyfried S, Knaus P, Zwijsen A, Bailly S. BMP signaling in vascular biology and dysfunction. Cytokine Growth Factor Rev. 2016 Feb;27:65-79. doi: 10.1016/j.cytogfr.2015.12.005. Epub 2015 Dec 15.

Ghofrani HA, Staehler G, Grünig E, Halank M, Mitrovic V, Unger S, Mueck W, Frey R, Grimminger F, Schermuly RT, Behr J. Acute effects of riociguat in borderline or manifest pulmonary hypertension associated with chronic obstructive pulmonary disease. Pulm Circ. 2015 Jun;5(2):296-304. doi: 10.1086/680214.

Ghofrani HA, Voswinckel R, Reichenberger F, Olschewski H, Haredza P, Karadaş B, Schermuly RT, Weissmann N, Seeger W, Grimminger F. Differences in hemodynamic and oxygenation responses to three different phosphodiesterase-5 inhibitors in patients with pulmonary arterial hypertension: a randomized prospective study. J Am Coll Cardiol. 2004 Oct 6;44(7):1488-96.

Ghofrani HA, Wiedemann R, Rose F, Schermuly RT, Olschewski H, Weissmann N, Gunther A, Walmrath D, Seeger W, Grimminger F. Sildenafil for treatment of lung fibrosis and pulmonary hypertension: a randomised controlled trial. Lancet. 2002 Sep 21;360(9337):895-900.

Giordano A, Romano S, Mallardo M, D'Angelillo A, Calì G, Corcione N, Ferraro P, Romano MF. FK506 can activate transforming growth factor-beta signalling in vascular smooth

muscle cells and promote proliferation. Cardiovasc Res. 2008 Aug 1;79(3):519-26. doi: 10.1093/cvr/cvn079. Epub 2008 Mar 18.

Gomberg-Maitland M, Olschewski H. Prostacyclin therapies for the treatment of pulmonary arterial hypertension. Eur Respir J. 2008 Apr;31(4):891-901. doi: 10.1183/09031936.00097107.

Gomez-Arroyo JG, Farkas L, Alhussaini AA, Farkas D, Kraskauskas D, Voelkel NF, Bogaard HJ. The monocrotaline model of pulmonary hypertension in perspective. Am J Physiol Lung Cell Mol Physiol. 2012 Feb 15;302(4):L363-9.

Goncharov DA, Kudryashova TV, Ziai H, Ihida-Stansbury K, DeLisser H, Krymskaya VP, Tuder RM, Kawut SM, Goncharova EA. Mammalian target of rapamycin complex 2 (mTORC2) coordinates pulmonary artery smooth muscle cell metabolism, proliferation, and survival in pulmonary arterial hypertension. Circulation. 2014 Feb 25;129(8):864-74. doi: 10.1161/CIRCULATIONAHA.113.004581. Epub 2013 Nov 22.

Goncharova EA. mTOR and vascular remodeling in lung diseases: current challenges and therapeutic prospects. FASEB J. 2013 May;27(5):1796-807. doi: 10.1096/fj.12-222224. Epub 2013 Jan 25

Grassie ME, Sutherland C, Ulke-Lemée A, Chappellaz M, Kiss E, Walsh MP, MacDonald JA. Cross-talk between Rho-associated kinase and cyclic nucleotide-dependent kinase signaling pathways in the regulation of smooth muscle myosin light chain phosphatase. J Biol Chem. 2012 Oct 19;287(43):36356-69. doi: 10.1074/jbc.M112.398479. Epub 2012 Sep 4.

Green DE, Sutliff RL, Hart CM. Is peroxisome proliferator-activated receptor gamma (PPARγ) a therapeutic target for the treatment of pulmonary hypertension? Pulm Circ. 2011 Jan 1;1(1):33-47.

Grimminger F, Weimann G, Frey R, Voswinckel R, Thamm M, Bölkow D, Weissmann N, Mück W, Unger S, Wensing G, Schermuly RT, Ghofrani HA. First acute haemodynamic study of soluble guanylate cyclase stimulator riociguat in pulmonary hypertension. Eur Respir J. 2009 Apr;33(4):785-92. doi: 10.1183/09031936.00039808. Epub 2009 Jan 7.

Grizel AV, Glukhov GS, Sokolova OS. Mechanisms of activation of voltage-gated potassium channels. Acta Naturae. 2014 Oct;6(4):10-26.

Gryglewski RJ, Korbut R, Robak J, Swies J. On the mechanism of antithrombotic action of flavonoids. Biochem Pharmacol. 1987 Feb 1;36(3):317-22.

Gryglewski RJ. Prostacyclin among prostanoids. Pharmacol Rep. 2008 Jan-Feb;60(1):3-11.

Guldemeester A, Stenmark KR, Brough GH, Stevens T. Mechanisms regulating cAMP-mediated growth of bovine neonatal pulmonary artery smooth muscle cells. Am J Physiol. 1999 Jun;276(6 Pt 1):L1010-7.

Gutman GA, Chandy KG, Grissmer S, Lazdunski M, McKinnon D, Pardo LA, Robertson GA, Rudy B, Sanguinetti MC, Stühmer W, Wang X. International Union of Pharmacology. LIII. Nomenclature and molecular relationships of voltage-gated potassium channels. Pharmacol Rev. 2005 Dec;57(4):473-508.

Hambly N, Granton J. Riociguat for the treatment of pulmonary hypertension. Expert Rev Respir Med. 2015;9(6):679-95. doi: 10.1586/17476348.2015.1106316. Epub 2015 Nov 24.

Hampl V, Bíbová J, Banasová A, Uhlík J, Miková D, Hnilicková O, Lachmanová V, Herget J. Pulmonary vascular iNOS induction participates in the onset of chronic hypoxic pulmonary hypertension. Am J Physiol Lung Cell Mol Physiol. 2006 Jan;290(1):L11-20. Epub 2005 Aug 19.

Han X, Chen C, Cheng G, Liang L, Yao X, Yang G, You P, Shou X. Peroxisome proliferator-activated receptor γ attenuates serotonin-induced pulmonary artery smooth muscle cell proliferation and apoptosis inhibition involving ERK1/2 pathway. Microvasc Res. 2015 Jul;100:17-24. doi: 10.1016/j.mvr.2015.04.008. Epub 2015 Apr 30.

Hanahan D, Weinberg RA. Hallmarks of cancer: the next generation. Cell. 2011 Mar 4;144(5):646-74. doi: 10.1016/j.cell.2011.02.013.

Harrington LS, Moreno L, Reed A, Wort SJ, Desvergne B, Garland C, Zhao L, Mitchell JA. The PPARbeta/delta agonist GW0742 relaxes pulmonary vessels and limits right heart hypertrophy in rats with hypoxia-induced pulmonary hypertension. PLoS One. 2010 Mar 4;5(3):e9526. doi: 10.1371/journal.pone.0009526.

Hayashi S, Morishita R, Matsushita H, Nakagami H, Taniyama Y, Nakamura T, Aoki M, Yamamoto K, Higaki J, Ogihara T. Cyclic AMP inhibited proliferation of human aortic vascular smooth muscle cells, accompanied by induction of p53 and p21. Hypertension. 2000 Jan;35(1 Pt 2):237-43.

He Y, Cao X, Liu X, Li X, Xu Y, Liu J, Shi J. Quercetin reverses experimental pulmonary arterial hypertension by modulating the TrkA pathway. Exp Cell Res. 2015 Nov 15;339(1):122-34. doi: 10.1016/j.yexcr.2015.10.013. Epub 2015 Oct 21

Henriques-Coelho T, Oliveira SM, Moura RS, Roncon-Albuquerque R Jr, Neves AL, Santos M, Nogueira-Silva C, La Fuente Carvalho F, Brandão-Nogueira A, Correia-Pinto J, Leite-Moreira AF. Thymulin inhibits monocrotaline-induced pulmonary hypertension modulating interleukin-6 expression and suppressing p38 pathway. Endocrinology. 2008 Sep;149(9):4367-73. doi: 10.1210/en.2008-0018. Epub 2008 May 29.

Hewer RC, Sala-Newby GB, Wu YJ, Newby AC, Bond M. PKA and Epac synergistically inhibit smooth muscle cell proliferation. J Mol Cell Cardiol. 2011 Jan;50(1):87-98. doi: 10.1016/j.yjmcc.2010.10.010. Epub 2010 Oct 30.

Himmelfarb J, Couper L. Dipyridamole inhibits PDGF- and bFGF-induced vascular smooth muscle cell proliferation. Kidney Int. 1997 Dec;52(6):1671-7.

Hoeper MM, Bogaard HJ, Condliffe R, Frantz R, Khanna D, Kurzyna M, Langleben D, Manes A, Satoh T, Torres F, Wilkins MR, Badesch DB. Definitions and diagnosis of pulmonary hypertension. J Am Coll Cardiol. 2013 Dec 24;62(25 Suppl):D42-50. doi: 10.1016/j.jacc.2013.10.032

Homsi J, Daud AI. Spectrum of activity and mechanism of action of VEGF/PDGF inhibitors. Cancer Control. 2007 Jul;14(3):285-94.

Hoorn EJ, Walsh SB, McCormick JA, Zietse R, Unwin RJ, Ellison DH. Pathogenesis of calcineurin inhibitor-induced hypertension. J Nephrol. 2012 May-Jun;25(3):269-75. doi: 10.5301/jn.5000174.

Houssaini A, Abid S, Mouraret N, Wan F, Rideau D, Saker M, Marcos E, Tissot CM, Dubois-Randé JL, Amsellem V, Adnot S. Rapamycin reverses pulmonary artery smooth muscle cell proliferation in pulmonary hypertension. Am J Respir Cell Mol Biol. 2013 May;48(5):568-77. doi: 10.1165/rcmb.2012-0429OC.

Hu J, Xu Q, McTiernan C, Lai YC, Osei-Hwedieh D, Gladwin M. Novel Targets of Drug Treatment for Pulmonary Hypertension. Am J Cardiovasc Drugs. 2015 Aug;15(4):225-34. doi: 10.1007/s40256-015-0125-4.

Huang JS, Ramamurthy SK, Lin X, Le Breton GC. Cell signalling through thromboxane A2 receptors. Cell Signal. 2004 May;16(5):521-33.

Huang YY, Li Z, Cai YH, Feng LJ, Wu Y, Li X, Luo HB. The molecular basis for the selectivity of tadalafil toward phosphodiesterase 5 and 6: a modeling study. J Chem Inf Model. 2013 Nov 25;53(11):3044-53. doi: 10.1021/ci400458z. Epub 2013 Nov 12.

Huh JW, Kim SY, Lee JH, Lee YS. YC-1 attenuates hypoxia-induced pulmonary arterial hypertension in mice. Pulm Pharmacol Ther. 2011 Dec;24(6):638-46. doi: 10.1016/j.pupt.2011.09.003. Epub 2011 Sep 24.

Humbert M, Ghofrani HA. The molecular targets of approved treatments for pulmonary arterial hypertension. Thorax. 2016 Jan;71(1):73-83. doi: 10.1136/thoraxjnl-2015-207170. Epub 2015 Jul 28.

Hung KY, Chen CT, Yen CJ, Lee PH, Tsai TJ, Hsieh BS. Dipyridamole inhibits PDGF-stimulated human peritoneal mesothelial cell proliferation. Kidney Int. 2001 Sep;60(3):872-81.

Iannotti FA, Panza E, Barrese V, Viggiano D, Soldovieri MV, Taglialatela M. Expression, localization, and pharmacological role of Kv7 potassium channels in skeletal muscle proliferation, differentiation, and survival after myotoxic insults. J Pharmacol Exp Ther. 2010 Mar;332(3):811-20. doi: 10.1124/jpet.109.162800. Epub 2009 Dec 29.

Ignarro LJ, Buga GM, Wei LH, Bauer PM, Wu G, del Soldato P. Role of the arginine-nitric oxide pathway in the regulation of vascular smooth muscle cell proliferation. Proc Natl Acad Sci U S A. 2001 Mar 27;98(7):4202-8. Epub 2001 Mar 20.

Ignarro LJ, Napoli C, Loscalzo J. Nitric oxide donors and cardiovascular agents modulating the bioactivity of nitric oxide: an overview. Circ Res. 2002 Jan 11;90(1):21-8.

Inoue M, Harada Y, Watanabe K, Mori C, Tanaka O. The effect of nifedipine on monocrotaline-induced pulmonary hypertension in rats. Acta Paediatr Jpn. 1993 Aug;35(4):273-7.

Ishida K, Matsumoto T, Taguchi K, Kamata K, Kobayashi T. Mechanisms underlying reduced P2Y(1) -receptor-mediated relaxation in superior mesenteric arteries from long-term streptozotocin-induced diabetic rats. Acta Physiol (Oxf). 2013 Jan;207(1):130-41. doi: 10.1111/j.1748-1716.2012.02469.x. Epub 2012 Aug 4.

Jasińska-Stroschein M, Orszulak-Michalak D. The current approach into signaling pathways in pulmonary arterial hypertension and their implication in novel therapeutic strategies. Pharmacol Rep. 2014 Aug;66(4):552-64. doi: 10.1016/j.pharep.2014.04.001. Epub 2014 Apr 24.

Jedlitschky G, Greinacher A, Kroemer HK. Transporters in human platelets: physiologic function and impact for pharmacotherapy. Blood. 2012 Apr 12;119(15):3394-402. doi: 10.1182/blood-2011-09-336933. Epub 2012 Feb 14.

Jiang BH, Tawara S, Abe K, Takaki A, Fukumoto Y, Shimokawa H. Acute vasodilator effect of fasudil, a Rho-kinase inhibitor, in monocrotaline-induced pulmonary hypertension in rats. J Cardiovasc Pharmacol. 2007 Feb;49(2):85-9.

Jiang L, Zhou T, Liu H. Combined effects of the ATP-sensitive potassium channel opener pinacidil and simvastatin on pulmonary vascular remodeling in rats with monocrotaline-induced pulmonary arterial hypertension. Pharmazie. 2012 Jun;67(6):547-52.

Jimenez R, Lopez-Sepulveda R, Romero M, Toral M, Cogolludo A, Perez-Vizcaino F, Duarte J. Quercetin and its metabolites inhibit the membrane NADPH oxidase activity in vascular smooth muscle cells from normotensive and spontaneously hypertensive rats. Food Funct. 2015 Feb;6(2):409-14. doi: 10.1039/c4fo00818a.

Jiménez R, Sánchez M, Zarzuelo MJ, Romero M, Quintela AM, López-Sepúlveda R, Galindo P, Gómez-Guzmán M, Haro JM, Zarzuelo A, Pérez-Vizcaíno F, Duarte J. Endothelium-dependent vasodilator effects of peroxisome proliferator-activated receptor beta agonists via the phosphatidyl-inositol-3 kinase-Akt pathway. J Pharmacol Exp Ther. 2010 Feb;332(2):554-61. doi: 10.1124/jpet.109.159806. Epub 2009 Nov 11.

Jobse BN, Rhem RG, Wang IQ, Counter WB, Stämpfli MR, Labiris NR. Detection of lung dysfunction using ventilation and perfusion SPECT in a mouse model of chronic cigarette smoke exposure. J Nucl Med. 2013 Apr;54(4):616-23. doi: 10.2967/jnumed.112.111419. Epub 2013 Feb 8.

Joshi CN, Martin DN, Fox JC, Mendelev NN, Brown TA, Tulis DA. The soluble guanylate cyclase stimulator BAY 41-2272 inhibits vascular smooth muscle growth through the cAMP-dependent protein kinase and cGMP-dependent protein kinase pathways. J Pharmacol Exp Ther. 2011 Nov;339(2):394-402. doi: 10.1124/jpet.111.183400. Epub 2011 Aug 8.

Joshi S, Sedivy V, Hodyc D, Herget J, Gurney AM. KCNQ modulators reveal a key role for KCNQ potassium channels in regulating the tone of rat pulmonary artery smooth muscle. J Pharmacol Exp Ther. 2009 Apr;329(1):368-76. doi: 10.1124/jpet.108.147785. Epub 2009 Jan 16.

Kadowitz PJ, Nandiwada P, Gruetter CA, Ignarro LJ, Hyman AL. Pulmonary vasodilator responses to nitroprusside and nitroglycerin in the dog. J Clin Invest. 1981 Mar;67(3):893-902.

Kang BY, Kleinhenz JM, Murphy TC, Hart CM. The PPARγ ligand rosiglitazone attenuates hypoxia-induced endothelin signaling in vitro and in vivo. Am J Physiol Lung Cell Mol Physiol. 2011 Dec;301(6):L881-91. doi: 10.1152/ajplung.00195.2011. Epub 2011 Sep 16.

Kawabe J, Ushikubi F, Hasebe N. Prostacyclin in vascular diseases. - Recent insights and future perspectives -. Circ J. 2010 May;74(5):836-43. Epub 2010 Apr 15.

Khandelwal AR, Hebert VY, Kleinedler JJ, Rogers LK, Ullevig SL, Asmis R, Shi R, Dugas TR. Resveratrol and quercetin interact to inhibit neointimal hyperplasia in mice with a carotid injury. J Nutr. 2012 Aug;142(8):1487-94. doi: 10.3945/jn.112.162628. Epub 2012 Jun 20.

Kherbeck N, Tamby MC, Bussone G, Dib H, Perros F, Humbert M, Mouthon L. The role of inflammation and autoimmunity in the pathophysiology of pulmonary arterial hypertension. Clin Rev Allergy Immunol. 2013 Feb;44(1):31-8. doi: 10.1007/s12016-011-8265-z.

Kim HJ, Kim MY, Hwang JS, Kim HJ, Lee JH, Chang KC, Kim JH, Han CW, Kim JH, Seo HG. PPARdelta inhibits IL-1beta-stimulated proliferation and migration of vascular smooth muscle cells via up-regulation of IL-1Ra. Cell Mol Life Sci. 2010 Jun;67(12):2119-30. doi: 10.1007/s00018-010-0328-4. Epub 2010 Mar 10.

Kim JD, Lee A, Choi J, Park Y, Kang H, Chang W, Lee MS, Kim J. Epigenetic modulation as a therapeutic approach for pulmonary arterial hypertension. Exp Mol Med. 2015 Jul 31;47:e175. doi: 10.1038/emm.2015.45.

Kim YH, Lee DH, Jeong JH, Guo ZS, Lee YJ. Quercetin augments TRAIL-induced apoptotic death: involvement of the ERK signal transduction pathway. Biochem Pharmacol. 2008 May 15;75(10):1946-58. doi: 10.1016/j.bcp.2008.02.016. Epub 2008 Mar 10.

King SB. Nitric oxide production from hydroxyurea. Free Radic Biol Med. 2004 Sep 15;37(6):737-44.

Korhonen R, Lahti A, Kankaanranta H, Moilanen E. Nitric oxide production and signaling in inflammation. Curr Drug Targets Inflamm Allergy. 2005 Aug;4(4):471-9.

Kovacs G, Berghold A, Scheidl S, Olschewski H. Pulmonary arterial pressure during rest and exercise in healthy subjects: a systematic review. Eur Respir J. 2009 Oct;34(4):888-94. doi: 10.1183/09031936.00145608. Epub 2009 Mar 26.

Kozłowska H, Baranowska-Kuczko M, Schlicker E, Kozłowski M, Kloza M, Malinowska B. Relaxation of human pulmonary arteries by PPARγ agonists. Naunyn Schmiedebergs Arch Pharmacol. 2013 May;386(5):445-53. doi: 10.1007/s00210-013-0846-3. Epub 2013 Mar 13.

Krawutschke C, Koesling D, Russwurm M. Cyclic GMP in Vascular Relaxation: Export Is of Similar Importance as Degradation. Arterioscler Thromb Vasc Biol. 2015 Sep;35(9):2011-9. doi: 10.1161/ATVBAHA.115.306133. Epub 2015 Jul 23.

Kudryashova TV, Goncharov DA, Pena A, Ihida-Stansbury K, DeLisser H, Kawut SM, Goncharova EA. Profiling the role of mammalian target of rapamycin in the vascular smooth muscle metabolome in pulmonary arterial hypertension. Pulm Circ. 2015 Dec;5(4):667-80. doi: 10.1086/683810.

Kuhr FK, Smith KA, Song MY, Levitan I, Yuan JX. New mechanisms of pulmonary arterial hypertension: role of Ca^{2+} signaling. Am J Physiol Heart Circ Physiol. 2012 Apr 15;302(8):H1546-62. doi: 10.1152/ajpheart.00944.2011. Epub 2012 Jan 13.

Kylhammar D, Bune LT, Rådegran G. $P2Y_1$ and $P2Y_{12}$ receptors in hypoxia- and adenosine diphosphate-induced pulmonary vasoconstriction in vivo in the pig. Eur J Appl Physiol. 2014 Sep;114(9):1995-2006. doi: 10.1007/s00421-014-2921-y. Epub 2014 Jun 15.

Lai N, Lu W, Wang J. $Ca(^{2+})$ and ion channels in hypoxia-mediated pulmonary hypertension. Int J Clin Exp Pathol. 2015 Feb 1;8(2):1081-92. eCollection 2015.

Lakshminrusimha S, Porta NF, Farrow KN, Chen B, Gugino SF, Kumar VH, Russell JA, Steinhorn RH. Milrinone enhances relaxation to prostacyclin and iloprost in pulmonary arteries isolated from lambs with persistent pulmonary hypertension of the newborn. Pediatr Crit Care Med. 2009 Jan;10(1):106-12. doi: 10.1097/PCC.0b013e3181936aee.

Lammers AE1, Adatia I, Cerro MJ, Diaz G, Freudenthal AH, Freudenthal F, Harikrishnan S, Ivy D, Lopes AA, Raj JU, Sandoval J, Stenmark K, Haworth SG. Functional classification of pulmonary hypertension in children: Report from the PVRI pediatric taskforce, Panama 2011. Pulm Circ. 2011 Aug 2;1(2):280-285.

Lang IM, Gaine SP. Recent advances in targeting the prostacyclin pathway in pulmonary arterial hypertension. Eur Respir Rev. 2015 Dec;24(138):630-41. doi: 10.1183/16000617.0067-2015.

Lang M, Kojonazarov B, Tian X, Kalymbetov A, Weissmann N, Grimminger F, Kretschmer A, Stasch JP, Seeger W, Ghofrani HA, Schermuly RT. The soluble guanylate cyclase stimulator riociguat ameliorates pulmonary hypertension induced by hypoxia and SU5416 in rats. PLoS One. 2012;7(8):e43433. doi: 10.1371/journal.pone.0043433. Epub 2012 Aug 17.

Lau HK. Cytotoxicity of nitric oxide donors in smooth muscle cells is dependent on phenotype, and mainly due to apoptosis. Atherosclerosis. 2003 Feb;166(2):223-32.

Leung YK, Du J, Huang Y, Yao X. Cyclic nucleotide-gated channels contribute to thromboxane A2-induced contraction of rat small mesenteric arteries. PLoS One. 2010 Jun 14;5(6):e11098. doi: 10.1371/journal.pone.0011098.

Li B, Yang L, Shen J, Wang C, Jiang Z. The antiproliferative effect of sildenafil on pulmonary artery smooth muscle cells is mediated via upregulation of mitogen-activated protein kinase phosphatase-1 and degradation of extracellular signal-regulated kinase 1/2 phosphorylation. Anesth Analg. 2007 Oct;105(4):1034-41, table of contents.

Li M, Li Z, Sun X, Yang L, Fang P, Liu Y, Li W, Xu J, Lu J, Xie M, Zhang D. Heme oxygenase-1/p21WAF1 mediates peroxisome proliferator-activated receptor-gamma signaling inhibition of proliferation of rat pulmonary artery smooth muscle cells. FEBS J. 2010 Mar;277(6):1543-50. doi: 10.1111/j.1742-4658.2010.07581.x. Epub 2010 Feb 13.

Li M, Sun X, Li Z, Liu Y. Inhibition of cGMP phosphodiesterase 5 suppresses serotonin signalling in pulmonary artery smooth muscles cells. Pharmacol Res. 2009 May;59(5):312-8. doi: 10.1016/j.phrs.2009.01.007. Epub 2009 Jan 29.

Li RC, Cindrova-Davies T, Skepper JN, Sellers LA. Prostacyclin induces apoptosis of vascular smooth muscle cells by a cAMP-mediated inhibition of extracellular signal-regulated kinase activity and can counteract the mitogenic activity of endothelin-1 or basic fibroblast growth factor. Circ Res. 2004 Apr 2;94(6):759-67. Epub 2004 Feb 12.

Li Y, Connolly M, Nagaraj C, Tang B, Bálint Z, Popper H, Smolle-Juettner FM, Lindenmann J, Kwapiszewska G, Aaronson PI, Wohlkoenig C, Leithner K, Olschewski H, Olschewski A. Peroxisome proliferator-activated receptor-β/δ, the acute signaling factor in prostacyclin-induced pulmonary vasodilation. Am J Respir Cell Mol Biol. 2012 Mar;46(3):372-9. doi: 10.1165/rcmb.2010-0428OC. Epub 2011 Oct 20.

Lim HJ, Lee S, Park JH, Lee KS, Choi HE, Chung KS, Lee HH, Park HY. PPAR delta agonist L-165041 inhibits rat vascular smooth muscle cell proliferation and migration via inhibition of cell cycle. Atherosclerosis. 2009 Feb;202(2):446-54. doi: 10.1016/j.atherosclerosis.2008.05.023. Epub 2008 May 21.

Lin CS. Phosphodiesterase type 5 regulation in the penile corpora cavernosa. J Sex Med. 2009 Mar;6 Suppl 3:203-9. doi: 10.1111/j.1743-6109.2008.01179.x.

Liu G, Li X, Li Y, Tang X, Xu J, Li R, Hao P, Sun Y. PPARδ agonist GW501516 inhibits PDGF-stimulated pulmonary arterial smooth muscle cell function related to pathological vascular remodeling. Biomed Res Int. 2013;2013:903947. doi: 10.1155/2013/903947. Epub 2013 Mar 27.

Liu Y, Tian H, Yan X, Fan F, Wang W, Han J. Serotonin inhibits apoptosis of pulmonary artery smooth muscle cells through 5-HT2A receptors involved in the pulmonary artery remodeling of pulmonary artery hypertension. Exp Lung Res. 2013 Mar;39(2):70-9. doi: 10.3109/01902148.2012.758191. Epub 2013 Jan 9**.**

Long L, MacLean MR, Jeffery TK, Morecroft I, Yang X, Rudarakanchana N, Southwood M, James V, Trembath RC, Morrell NW. Serotonin increases susceptibility to pulmonary hypertension in BMPR2-deficient mice. Circ Res. 2006 Mar 31;98(6):818-27. Epub 2006 Feb 23.

Lopez-Lopez JG, Moral-Sanz J, Frazziano G, Gomez-Villalobos MJ, Moreno L, Menendez C, Flores-Hernandez J, Lorente JA, Cogolludo A, Perez-Vizcaino F. Type 1 diabetes-induced hyper-responsiveness to 5-hydroxytryptamine in rat pulmonary arteries via oxidative stress and induction of cyclooxygenase-2. J Pharmacol Exp Ther. 2011 Jul;338(1):400-7. doi: 10.1124/jpet.111.179515. Epub 2011 Apr 26.

López-López JG, Pérez-Vizcaíno F, Cogolludo AL, Ibarra M, Zaragozá-Arnáez F, Tamargo J. Nitric oxide- and nitric oxide donors-induced relaxation and its modulation by oxidative stress in piglet pulmonary arteries. Br J Pharmacol. 2001 Jul;133(5):615-24.

Lowery JW, de Caestecker MP. BMP signaling in vascular development and disease. Cytokine Growth Factor Rev. 2010 Aug;21(4):287-98. doi: 10.1016/j.cytogfr.2010.06.001. Epub 2010 Jul 31.

Luo W, Liu B, Zhou Y. The endothelial cyclooxygenase pathway: insights from mouse arteries. Eur J Pharmacol. 2016 Mar 25. pii: S0014-2999(16)30173-X. doi: 10.1016/j.ejphar.2016.03.043. [Epub ahead of print]

Ma L, Chung WK. The genetic basis of pulmonary arterial hypertension. Hum Genet. 2014 May;133(5):471-9.

Maarman G, Lecour S, Butrous G, Thienemann F, Sliwa K. A comprehensive review: the evolution of animal models in pulmonary hypertension research; are we there yet? Pulm Circ. 2013 Dec;3(4):739-56.

Machado RD, Southgate L, Eichstaedt CA, Aldred MA, Austin ED, Best DH, Chung WK, Benjamin N, Elliott CG, Eyries M, Fischer C, Gräf S, Hinderhofer K, Humbert M, Keiles SB, Loyd JE, Morrell NW, Newman JH, Soubrier F, Trembath RC, Viales RR, Grünig E. Pulmonary Arterial Hypertension: A Current Perspective on Established and Emerging Molecular Genetic Defects. Hum Mutat. 2015 Dec;36(12):1113-27. doi: 10.1002/humu.22904. Epub 2015 Oct 12.

MacKenzie AM, Peacock AJ. Medical Therapies for the Treatment of Pulmonary Arterial Hypertension: How Do We Choose? Curr Hypertens Rep. 2015 Jul;17(7):56. doi: 10.1007/s11906-015-0560-2.

Mackie AR, Brueggemann LI, Henderson KK, Shiels AJ, Cribbs LL, Scrogin KE, Byron KL. Vascular KCNQ potassium channels as novel targets for the control of mesenteric artery constriction by vasopressin, based on studies in single cells, pressurized arteries, and in vivo measurements of mesenteric vascular resistance. J Pharmacol Exp Ther. 2008 May;325(2):475-83. doi: 10.1124/jpet.107.135764. Epub 2008 Feb 13.

MacLean MR, Dempsie Y. Serotonin and pulmonary hypertension--from bench to bedside? Curr Opin Pharmacol. 2009 Jun;9(3):281-6. doi: 10.1016/j.coph.2009.02.005. Epub 2009 Mar 13.

MacLean MR, Herve P, Eddahibi S, Adnot S. 5-hydroxytryptamine and the pulmonary circulation: receptors, transporters and relevance to pulmonary arterial hypertension. Br J Pharmacol. 2000 Sep;131(2):161-8.

Mair KM, Wright AF, Duggan N, Rowlands DJ, Hussey MJ, Roberts S, Fullerton J, Nilsen M, Loughlin L, Thomas M, MacLean MR. Sex-dependent influence of endogenous estrogen in pulmonary hypertension. Am J Respir Crit Care Med. 2014 Aug 15;190(4):456-67. doi: 10.1164/rccm.201403-0483OC.

Mancina R, Filippi S, Marini M, Morelli A, Vignozzi L, Salonia A, Montorsi F, Mondaini N, Vannelli GB, Donati S, Lotti F, Forti G, Maggi M. Expression and functional activity of phosphodiesterase type 5 in human and rabbit vas deferens. Mol Hum Reprod. 2005 Feb;11(2):107-15. Epub 2005 Jan 7.

Mandegar M, Fung YC, Huang W, Remillard CV, Rubin LJ, Yuan JX. Cellular and molecular mechanisms of pulmonary vascular remodeling: role in the development of pulmonary hypertension. Microvasc Res. 2004 Sep;68(2):75-103.

Mandegar M, Yuan JX. Role of K+ channels in pulmonary hypertension. Vascul Pharmacol. 2002 Jan;38(1):25-33.

Martin-Nizard F, Furman C, Delerive P, Kandoussi A, Fruchart JC, Staels B, Duriez P. Peroxisome proliferator-activated receptor activators inhibit oxidized low-density lipoprotein-induced endothelin-1 secretion in endothelial cells. J Cardiovasc Pharmacol. 2002 Dec;40(6):822-31.

Mason NA, Springall DR, Burke M, Pollock J, Mikhail G, Yacoub MH, Polak JM. High expression of endothelial nitric oxide synthase in plexiform lesions of pulmonary hypertension. J Pathol. 1998 Jul;185(3):313-8.

Mathew R, Huang J, Shah M, Patel K, Gewitz M, Sehgal PB. Disruption of endothelial-cell caveolin-1alpha/raft scaffolding during development of monocrotaline-induced pulmonary hypertension. Circulation. 2004 Sep 14;110(11):1499-506. Epub 2004 Sep 7.

Mathew R, Wang J, Gewitz MH, Hintze TH, Wolin MS. Congestive heart failure alters receptor-dependent cAMP-mediated relaxation of canine pulmonary arteries. Circulation. 1993 May;87(5):1722-8.

Mathew R. Pulmonary hypertension and metabolic syndrome: Possible connection, PPARγ and Caveolin-1. World J Cardiol. 2014 Aug 26;6(8):692-705. doi: 10.4330/wjc.v6.i8.692.

Matsumoto T, Wakabayashi K, Kobayashi T, Kamata K. Functional changes in adenylyl cyclases and associated decreases in relaxation responses in mesenteric arteries from diabetic rats. Am J Physiol Heart Circ Physiol. 2005 Nov;289(5):H2234-43. Epub 2005 May 13.

Matter CM, Rozenberg I, Jaschko A, Greutert H, Kurz DJ, Wnendt S, Kuttler B, Joch H, Grünenfelder J, Zünd G, Tanner FC, Lüscher TF. Effects of tacrolimus or sirolimus on proliferation of vascular smooth muscle and endothelial cells. J Cardiovasc Pharmacol. 2006 Dec;48(6):286-92.

Maurice DH, Ke H, Ahmad F, Wang Y, Chung J, Manganiello VC. Advances in targeting cyclic nucleotide phosphodiesterases. Nat Rev Drug Discov. 2014 Apr;13(4):290-314. doi: 10.1038/nrd4228.

McGoon MD, Benza RL, Escribano-Subias P, Jiang X, Miller DP, Peacock AJ, Pepke-Zaba J, Pulido T, Rich S, Rosenkranz S, Suissa S, Humbert M. Pulmonary arterial hypertension: epidemiology and registries. J Am Coll Cardiol. 2013 Dec 24;62(25 Suppl):D51-9. doi: 10.1016/j.jacc.2013.10.023.

McMurtry IF, Abe K, Ota H, Fagan KA, Oka M. Rho kinase-mediated vasoconstriction in pulmonary hypertension. Adv Exp Med Biol. 2010;661:299-308. doi: 10.1007/978-1-60761-500-2_19.

McMurtry MS, Archer SL, Altieri DC, Bonnet S, Haromy A, Harry G, Bonnet S, Puttagunta L, Michelakis ED. Gene therapy targeting survivin selectively induces pulmonary vascular apoptosis and reverses pulmonary arterial hypertension. J Clin Invest. 2005 Jun;115(6):1479-91.

Medina P, Segarra G, Martínez-León JB, Vila JM, Aldasoro M, Otero E, Lluch S. Relaxation induced by cGMP phosphodiesterase inhibitors sildenafil and zaprinast in human vessels. Ann Thorac Surg. 2000 Oct;70(4):1327-31.

Melot C, Hallemans R, Naeije R, Mols P, Lejeune P. Deleterious effect of nifedipine on pulmonary gas exchange in chronic obstructive pulmonary disease. Am Rev Respir Dis. 1984 Oct;130(4):612-6.

Mélot C, Naeije R, Mols P, Vandenbossche JL, Denolin H. Effects of nifedipine on ventilation/perfusion matching in primary pulmonary hypertension. Chest. 1983 Feb;83(2):203-7.

Mendelev NN, Williams VS, Tulis DA. Antigrowth properties of BAY 41-2272 in vascular smooth muscle cells. J Cardiovasc Pharmacol. 2009 Feb;53(2):121-31. doi: 10.1097/FJC.0b013e31819715c4.

Menendez C, Dueñas M, Galindo P, González-Manzano S, Jimenez R, Moreno L, Zarzuelo MJ, Rodríguez-Gómez I, Duarte J, Santos-Buelga C, Perez-Vizcaino F. Vascular deconjugation of quercetin glucuronide: the flavonoid paradox revealed? Mol Nutr Food Res. 2011 Dec;55(12):1780-90. doi: 10.1002/mnfr.201100378.

Menendez C, Jimenez R, Moreno L, Galindo P, Cogolludo A, Duarte J, Perez-Vizcaino F. Lack of synergistic interaction between quercetin and catechin in systemic and pulmonary vascular smooth muscle. Br J Nutr. 2011 May;105(9):1287-93. doi: 10.1017/S0007114510004952. Epub 2010 Dec 10.

Meyrick B, Hislop A, Reid L.. Pulmonary arteries of thenormal rat: the thick walled oblique muscle segment. J Anat. 1978 Feb;125(Pt 2):209-21.

Michelakis ED, Thébaud B, Weir EK, Archer SL. Hypoxic pulmonary vasoconstriction: redox regulation of O2-sensitive K+ channels by a mitochondrial O2-sensor in resistance artery smooth muscle cells. J Mol Cell Cardiol. 2004 Dec;37(6):1119-36.

Mihaly SR, Ninomiya-Tsuji J, Morioka S. TAK1 control of cell death. Cell Death Differ. 2014 Nov;21(11):1667-76. doi: 10.1038/cdd.2014.123. Epub 2014 Aug 22.

Milara J, Escrivá J, Ortiz JL, Juan G, Artigues E, Morcillo E, Cortijo J. Vascular effects of sildenafil in patients with pulmonary fibrosis and pulmonary hypertension: an ex vivo/in vitro study. Eur Respir J. 2016 Jun;47(6):1737-49. doi: 10.1183/13993003.01259-2015. Epub 2016 Mar 23.

Miller MR, Megson IL. Recent developments in nitric oxide donor drugs. Br J Pharmacol. 2007 Jun;151(3):305-21. Epub 2007 Apr 2.

Mitchell C, Syed NI, Tengah A, Gurney AM, Kennedy C. Identification of contractile P2Y1, P2Y6, and P2Y12 receptors in rat intrapulmonary artery using selective ligands. J Pharmacol Exp Ther. 2012 Dec;343(3):755-62. doi: 10.1124/jpet.112.198051. Epub 2012 Sep 18.

Mitchell JA, Ahmetaj-Shala B, Kirkby NS, Wright WR, Mackenzie LS, Reed DM, Mohamed N. Role of prostacyclin in pulmonary hypertension. Glob Cardiol Sci Pract. 2014 Dec 31;2014(4):382-93. doi: 10.5339/gcsp.2014.53. eCollection 2014.

Mitchell JA, Ali F, Bailey L, Moreno L, Harrington LS. Role of nitric oxide and prostacyclin as vasoactive hormones released by the endothelium. Exp Physiol. 2008 Jan;93(1):141-7. Epub 2007 Oct 26.

Moeller A, Ask K, Warburton D, Gauldie J, Kolb K. The bleomycin animal model: a useful tool to investigate treatment options for idiopathic pulmonary fibrosis? Int J Biochem Cell Biol. 2008; 40(3): 362–382. Published online 2007 Aug 30. doi: 10.1016/j.biocel.2007.08.011

Moon SK, Cho GO, Jung SY, Gal SW, Kwon TK, Lee YC, Madamanchi NR, Kim CH. Quercetin exerts multiple inhibitory effects on vascular smooth muscle cells: role of ERK1/2, cell-cycle regulation, and matrix metalloproteinase-9. Biochem Biophys Res Commun. 2003 Feb 21;301(4):1069-78.

Morales-Cano D, Moreno L, Barreira B, Pandolfi R, Chamorro V, Jimenez R, Villamor E, Duarte J, Perez-Vizcaino F, Cogolludo A. Kv7 channels critically determine coronary artery reactivity: left-right differences and down-regulation by hyperglycaemia. Cardiovasc Res. 2015 Apr 1;106(1):98-108. doi: 10.1093/cvr/cvv020. Epub 2015 Jan 23.

Moral-Sanz J, Lopez-Lopez JG, Menendez C, Moreno E, Barreira B, Morales-Cano D, Escolano L, Fernandez-Segoviano P, Villamor E, Cogolludo A, Perez-Vizcaino F, Moreno L.. Different patterns of pulmonary vascular disease induced by type 1 diabetes and moderate hypoxia in rats. Exp Physiol. 2012 May;97(5):676-86. doi: 10.1113/expphysiol.2011.062257. Epub 2012 Jan 13.

Morecroft I, Murray A, Nilsen M, Gurney AM, MacLean MR. Treatment with the Kv7 potassium channel activator flupirtine is beneficial in two independent mouse models of pulmonary hypertension. Br J Pharmacol. 2009 Aug;157(7):1241-9. doi: 10.1111/j.1476-5381.2009.00283.x. Epub 2009 Jun 5.

Moreno L, Gonzalez-Luis G, Cogolludo A, Lodi F, Lopez-Farre A, Tamargo J, Villamor E, Perez-Vizcaino F. Soluble guanylyl cyclase during postnatal porcine pulmonary maturation. Am J Physiol Lung Cell Mol Physiol. 2005 Jan;288(1):L125-30. Epub 2004 Sep 24.

Moreno L, Losada B, Cogolludo Al, Lodi F, Lugnier C, Villamor E, Moro M, Tamargo J, Pérez-Vizcaíno F. Postnatal maturation of phosphodiesterase 5 (PDE5) in piglet pulmonary arteries: activity, expression, effects of PDE5 inhibitors, and role of the nitric oxide/cyclic GMP pathway. Pediatr Res. 2004 Oct;56(4):563-70. Epub 2004 Aug 4.

Morrell NW, Adnot S, Archer SL, Dupuis J, Jones PL, MacLean MR, McMurtry IF, Stenmark KR, Thistlethwaite PA, Weissmann N, Yuan JX, Weir EK. Cellular and molecular basis of pulmonary arterial hypertension. J Am Coll Cardiol. 2009 Jun 30;54(1 Suppl):S20-31.

Morrell NW, Archer SL, Defelice A, Evans S, Fiszman M, Martin T, Saulnier M, Rabinovitch M, Schermuly R, Stewart D, Truebel H, Walker G, Stenmark KR. Anticipated classes of new medications and molecular targets for pulmonary arterial hypertension. Pulm Circ. 2013 Jan;3(1):226-44. doi: 10.4103/2045-8932.109940.

Morty RE, Nejman B, Kwapiszewska G, Hecker M, Zakrzewicz A, Kouri FM, Peters DM, Dumitrascu R, Seeger W, Knaus P, Schermuly RT, Eickelberg O. Dysregulated bone morphogenetic protein signaling in monocrotaline-induced pulmonary arterial hypertension. Arterioscler Thromb Vasc Biol. 2007 May;27(5):1072-8. Epub 2007 Mar 8.

Mouchaers KT, Schalij I, de Boer MA, Postmus PE, van Hinsbergh VW, van Nieuw Amerongen GP, Vonk Noordegraaf A, van der Laarse WJ. Fasudil reduces monocrotaline-induced pulmonary arterial hypertension: comparison with bosentan and sildenafil. Eur Respir J. 2010 Oct;36(4):800-7. doi: 10.1183/09031936.00130209. Epub 2010 Mar 29.

Mubarak KK. A review of prostaglandin analogs in the management of patients with pulmonary arterial hypertension. Respir Med. 2010 Jan;104(1):9-21. doi: 10.1016/j.rmed.2009.07.015. Epub 2009 Aug 15.

Murray F, Patel HH, Suda RY, Zhang S, Thistlethwaite PA, Yuan JX, Insel PA. Expression and activity of cAMP phosphodiesterase isoforms in pulmonary artery smooth muscle cells from patients with pulmonary hypertension: role for PDE1. Am J Physiol Lung Cell Mol Physiol. 2007 Jan;292(1):L294-303. Epub 2006 Sep 15.

Nagaoka T, Fagan KA, Gebb SA, Morris KG, Suzuki T, Shimokawa H, McMurtry IF, Oka M. Inhaled Rho kinase inhibitors are potent and selective vasodilators in rat pulmonary hypertension. Am J Respir Crit Care Med. 2005 Mar 1;171(5):494-9. Epub 2004 Nov 24.

Nakahata N. Thromboxane A2: physiology/pathophysiology, cellular signal transduction and pharmacology. Pharmacol Ther. 2008 Apr;118(1):18-35. doi: 10.1016/j.pharmthera.2008.01.001. Epub 2008 Jan 26.

Nakamura K, Akagi S, Ogawa A, Kusano KF, Matsubara H, Miura D, Fuke S, Nishii N, Nagase S, Kohno K, Morita H, Oto T, Yamanaka R, Otsuka F, Miura A, Yutani C, Ohe T, Ito H. Pro-apoptotic effects of imatinib on PDGF-stimulated pulmonary artery smooth muscle cells from patients with idiopathic pulmonary arterial hypertension. Int J Cardiol. 2012 Aug 23;159(2):100-6. doi: 10.1016/j.ijcard.2011.02.024. Epub 2011 Mar 4.

Nakamura T, Matsushima M, Hayashi Y, Shibasaki M, Imaizumi K, Hashimoto N, Shimokata K, Hasegawa Y, Kawabe T. Attenuation of transforming growth factor-β-stimulated collagen production in fibroblasts by quercetin-induced heme oxygenase-1. Am J Respir Cell Mol Biol. 2011 May;44(5):614-20. doi: 10.1165/rcmb.2010-0338OC. Epub 2011 Jan 7.

Namkung J, Kim H, Park S. Peripheral Serotonin: a New Player in Systemic Energy Homeostasis. Mol Cells. 2015 Dec 31;38(12):1023-8. doi: 10.14348/molcells.2015.0258. Epub 2015 Dec 1

Nasim MT, Ogo T, Chowdhury HM, Zhao L, Chen CN, Rhodes C, Trembath RC. BMPR-II deficiency elicits pro-proliferative and anti-apoptotic responses through the activation of TGFβ-TAK1-MAPK pathways in PAH. Hum Mol Genet. 2012 Jun 1;21(11):2548-58. doi: 10.1093/hmg/dds073. Epub 2012 Mar 2.

Nathan C. Points of control in inflammation. Nature. 2002 Dec 19-26;420(6917):846-52.

Nikam VS, Schermuly RT, Dumitrascu R, Weissmann N, Kwapiszewska G, Morrell N, Klepetko W, Fink L, Seeger W, Voswinckel R. Treprostinil inhibits the recruitment of bone marrow-derived circulating fibrocytes in chronic hypoxic pulmonary hypertension. Eur Respir J. 2010 Dec;36(6):1302-14. doi: 10.1183/09031936.00028009. Epub 2010 Jun 4.

Nilsson J, Sjölund M, Palmberg L, Von Euler AM, Jonzon B, Thyberg J. The calcium antagonist nifedipine inhibits arterial smooth muscle cell proliferation. Atherosclerosis. 1985 Dec;58(1-3):109-22.

Ninomiya-Tsuji J, Kajino T, Ono K, Ohtomo T, Matsumoto M, Shiina M, Mihara M, Tsuchiya M, Matsumoto K. A resorcylic acid lactone, 5Z-7-oxozeaenol, prevents inflammation by inhibiting the catalytic activity of TAK1 MAPK kinase kinase. J Biol Chem. 2003 May 16;278(20):18485-90. Epub 2003 Mar 6.

Nisbet RE, Bland JM, Kleinhenz DJ, Mitchell PO, Walp ER, Sutliff RL, Hart CM. Rosiglitazone attenuates chronic hypoxia-induced pulmonary hypertension in a mouse model. Am J Respir Cell Mol Biol. 2010 Apr;42(4):482-90. doi: 10.1165/rcmb.2008-0132OC. Epub 2009 Jun 11.

Nisbet RE, Bland JM, Kleinhenz DJ, Mitchell PO, Walp ER, Sutliff RL, Hart CM. Rosiglitazone attenuates chronic hypoxia-induced pulmonary hypertension in a mouse model. Am J Respir Cell Mol Biol. 2010 Apr;42(4):482-90. doi: 10.1165/rcmb.2008-0132OC. Epub 2009 Jun 11.

Nisbet RE, Sutliff RL, Hart CM. The role of peroxisome proliferator-activated receptors in pulmonary vascular disease. PPAR Res. 2007;2007:18797.

Nishio E, Fukushima K, Shiozaki M, Watanabe Y. Nitric oxide donor SNAP induces apoptosis in smooth muscle cells through cGMP-independent mechanism. Biochem Biophys Res Commun. 1996 Apr 5;221(1):163-8.

Nogueira-Ferreira R, Ferreira R, Henriques-Coelho T. Cellular interplay in pulmonary arterial hypertension: implications for new therapies. Biochim Biophys Acta. 2014 May;1843(5):885-93. doi: 10.1016/j.bbamcr.2014.01.030. Epub 2014 Jan 31.

Nossaman BD, Kadowitz PJ. Stimulators of soluble guanylyl cyclase: future clinical indications. Ochsner J. 2013 Spring;13(1):147-56.

Ogawa A, Nakamura K, Matsubara H, Fujio H, Ikeda T, Kobayashi K, Miyazaki I, Asanuma M, Miyaji K, Miura D, Kusano KF, Date H, Ohe T. Prednisolone inhibits proliferation of cultured pulmonary artery smooth muscle cells of patients with idiopathic pulmonary arterial hypertension. Circulation. 2005 Sep 20;112(12):1806-12. Epub 2005 Sep 12

Ohya S, Kito H, Hatano N, Muraki K. Recent advances in therapeutic strategies that focus on the regulation of ion channel expression. Pharmacol Ther. 2016 Apr;160:11-43. doi: 10.1016/j.pharmthera.2016.02.001. Epub 2016 Feb 16.

Okada M, Suzuki A, Yamawaki H, Hara Y. Levosimendan inhibits interleukin-1β-induced cell migration and MMP-9 secretion in rat cardiac fibroblasts. Eur J Pharmacol. 2013 Oct 15;718(1-3):332-9. doi: 10.1016/j.ejphar.2013.08.013. Epub 2013 Sep 3.

Oliveras A, Roura-Ferrer M, Solé L, de la Cruz A, Prieto A, Etxebarria A, Manils J, Morales-Cano D, Condom E, Soler C, Cogolludo A, Valenzuela C, Villarroel A, Comes N1, Felipe A. Functional assembly of Kv7.1/Kv7.5 channels with emerging properties on vascular muscle physiology. Arterioscler Thromb Vasc Biol. 2014 Jul;34(7):1522-30. doi: 10.1161/ATVBAHA.114.303801. Epub 2014 May 22.

Olschewski A and Weir EK. Redox Regulation of Ion Channels in the Pulmonary Circulation. Antioxid Redox Signal. 2015 Feb 20; 22(6): 465–485. doi: 10.1089/ars.2014.5899

Olschewski A, Papp R, Nagaraj C, Olschewski H. Ion channels and transporters as therapeutic targets in the pulmonary circulation. Pharmacol Ther. 2014 Dec;144(3):349-68. doi: 10.1016/j.pharmthera.2014.08.001. Epub 2014 Aug 6.

Orie NN, Ledwozyw A, Williams DJ, Whittle BJ, Clapp LH. Differential actions of the prostacyclin analogues treprostinil and iloprost and the selexipag metabolite, MRE-269 (ACT-333679) in rat small pulmonary arteries and veins. Prostaglandins Other Lipid Mediat. 2013 Oct;106:1-7. doi: 10.1016/j.prostaglandins.2013.07.003. Epub 2013 Jul 18.

Paffett ML, Walker BR. Vascular adaptations to hypoxia: molecular and cellular mechanisms regulating vascular tone. Essays Biochem. 2007;43:105-19.

Pankey EA, Thammasiboon S, Lasker GF, Baber S, Lasky JA, Kadowitz PJ. Imatinib attenuates monocrotaline pulmonary hypertension and has potent vasodilator activity in pulmonary and systemic vascular beds in the rat. Am J Physiol Heart Circ Physiol. 2013 Nov 1;305(9):H1288-96. doi: 10.1152/ajpheart.00329.2013. Epub 2013 Aug 30.

Paulin R, Michelakis ED. The metabolic theory of pulmonary arterial hypertension. Circ Res. 2014 Jun 20;115(1):148-64. doi: 10.1161/CIRCRESAHA.115.301130.

Perez A, Gonzalez-Manzano S, Jimenez R, Perez-Abud R, Haro JM, Osuna A, Santos-Buelga C, Duarte J, Perez-Vizcaino F. The flavonoid quercetin induces acute vasodilator effects in healthy volunteers: correlation with beta-glucuronidase activity. Pharmacol Res. 2014 Nov;89:11-8. doi: 10.1016/j.phrs.2014.07.005. Epub 2014 Jul 27.

Perez-Vizcaino F, Bishop-Bailley D, Lodi F, Duarte J, Cogolludo A, Moreno L, Bosca L, Mitchell JA, Warner TD. The flavonoid quercetin induces apoptosis and inhibits JNK activation in intimal vascular smooth muscle cells. Biochem Biophys Res Commun. 2006 Aug 4;346(3):919-25. Epub 2006 Jun 9.

Perez-Vizcaino F, Cogolludo A, Moreno L. Reactive oxygen species signaling in pulmonary vascular smooth muscle. Respir Physiol Neurobiol. 2010 Dec 31;174(3):212-20. doi: 10.1016/j.resp.2010.08.009. Epub 2010 Aug 24.

Perez-Vizcaino F, Duarte J, Andriantsitohaina R. Endothelial function and cardiovascular disease: effects of quercetin and wine polyphenols. Free Radic Res. 2006 Oct;40(10):1054-65.

Perez-Vizcaino F, Duarte J, Jimenez R, Santos-Buelga C, Osuna A. Antihypertensive effects of the flavonoid quercetin. Pharmacol Rep. 2009 Jan-Feb;61(1):67-75.

Perez-Vizcaino F, Duarte J. Flavonols and cardiovascular disease. Mol Aspects Med. 2010 Dec;31(6):478-94. doi: 10.1016/j.mam.2010.09.002. Epub 2010 Sep 15.

Pérez-Vizcaíno F, Villamor E, Moro M, Tamargo J. Pulmonary versus systemic effects of vasodilator drugs: an in vitro study in isolated intrapulmonary and mesenteric arteries of neonatal piglets. Eur J Pharmacol. 1996 Oct 24;314(1-2):91-8.

Potter LR. Guanylyl cyclase structure, function and regulation. Cell Signal. 2011 Dec;23(12):1921-6. doi: 10.1016/j.cellsig.2011.09.001. Epub 2011 Sep 10.

Pratheeshkumar P, Budhraja A, Son YO, Wang X, Zhang Z, Ding S, Wang L, Hitron A, Lee JC, Xu M, Chen G, Luo J, Shi X. Quercetin inhibits angiogenesis mediated human prostate tumor growth by targeting VEGFR- 2 regulated AKT/mTOR/P70S6K signaling pathways. PLoS One. 2012;7(10):e47516. doi: 10.1371/journal.pone.0047516. Epub 2012 Oct 18.

Price LC, Wort SJ, Perros F, Dorfmüller P, Huertas A, Montani D, Cohen-Kaminsky S, Humbert M. Inflammation in pulmonary arterial hypertension. Chest. 2012 Jan;141(1):210-21. doi: 10.1378/chest.11-0793

Pugliese SC, Poth JM, Fini MA, Olschewski A, El Kasmi KC, Stenmark KR. The role of inflammation in hypoxic pulmonary hypertension: from cellular mechanisms to clinical phenotypes. Am J Physiol Lung Cell Mol Physiol. 2015 Feb 1;308(3):L229-52. doi: 10.1152/ajplung.00238.2014. Epub 2014 Nov 21.

Quintela AM, Jiménez R, Gómez-Guzmán M, Zarzuelo MJ, Galindo P, Sánchez M, Vargas F, Cogolludo A, Tamargo J, Pérez-Vizcaíno F, Duarte J. Activation of peroxisome proliferator-activated receptor-β/-δ (PPARβ/δ) prevents endothelial dysfunction in type 1 diabetic rats. Free Radic Biol Med. 2012 Aug 15;53(4):730-41. doi: 10.1016/j.freeradbiomed.2012.05.045. Epub 2012 Jun 7.

Rabinovitch M, Guignabert C, Humbert M, Nicolls MR. Inflammation and immunity in the pathogenesis of pulmonary arterial hypertension. Circ Res. 2014 Jun 20;115(1):165-75. doi: 10.1161/CIRCRESAHA.113.301141.

Rabinovitch M. Molecular pathogenesis of pulmonary arterial hypertension. J Clin Invest. 2012 Dec;122(12):4306-13.

Ralevic V, Dunn WR. Purinergic transmission in blood vessels. Auton Neurosci. 2015 Sep;191:48-66. doi: 10.1016/j.autneu.2015.04.007. Epub 2015 Apr 25.

Ramos M, Lamé MW, Segall HJ, Wilson DW. Monocrotaline pyrrole induces Smad nuclear accumulation and altered signaling expression in human pulmonary arterial endothelial cells. Vascul Pharmacol. 2007 Jun;46(6):439-48. Epub 2007 Feb 2.

Reid HM, Kinsella BT. Prostacyclin receptors: Transcriptional regulation and novel signalling mechanisms. Prostaglandins Other Lipid Mediat. 2015 Sep;121(Pt A):70-82. doi: 10.1016/j.prostaglandins.2015.04.008. Epub 2015 Apr 30.

Revermann M, Schloss M, Mieth A, Babelova A, Schröder K, Neofitidou S, Buerkl J, Kirschning T, Schermuly RT, Hofstetter C, Brandes RP. Levosimendan attenuates pulmonary vascular remodeling. Intensive Care Med. 2011 Aug;37(8):1368-77. doi: 10.1007/s00134-011-2254-9. Epub 2011 May 31.

Ried M, Potzger T, Neu R, Sziklavari Z, Szöke T, Liebold A, Hofmann HS, Hoenicka M. Combination of sildenafil and bosentan for pulmonary hypertension in a human ex vivo model. Cardiovasc Drugs Ther. 2014 Feb;28(1):45-51. doi: 10.1007/s10557-013-6499-0.

Robbins IM, Barst RJ, Rubin LJ, Gaine SP, Price PV, Morrow JD, Christman BW. Increased levels of prostaglandin D(2) suggest macrophage activation in patients with primary pulmonary hypertension. Chest. 2001 Nov;120(5):1639-44.

Robbins IM, Kawut SM, Yung D, Reilly MP, Lloyd W, Cunningham G, Loscalzo J, Kimmel SE, Christman BW, Barst RJ. A study of aspirin and clopidogrel in idiopathic pulmonary arterial hypertension. Eur Respir J. 2006 Mar;27(3):578-84.

Rothermund L, Friebe A, Paul M, Koesling D, Kreutz R. Acute blood pressure effects of YC-1-induced activation of soluble guanylyl cyclase in normotensive and hypertensive rats. Br J Pharmacol. 2000 May;130(2):205-8.

Roura-Ferrer M, Solé L, Martínez-Mármol R, Villalonga N, Felipe A. Skeletal muscle Kv7 (KCNQ) channels in myoblast differentiation and proliferation. Biochem Biophys Res Commun. 2008 May 16;369(4):1094-7. doi: 10.1016/j.bbrc.2008.02.152. Epub 2008 Mar 10

Ryan J, Dasgupta A, Huston J, Chen KH, Archer SL. Mitochondrial dynamics in pulmonary arterial hypertension. J Mol Med (Berl). 2015 Mar;93(3):229-42. doi: 10.1007/s00109-015-1263-5. Epub 2015 Feb 13.

Ryan MJ, Didion SP, Mathur S, Faraci FM, Sigmund CD. PPAR(gamma) agonist rosiglitazone improves vascular function and lowers blood pressure in hypertensive transgenic mice. Hypertension. 2004 Mar;43(3):661-6. Epub 2004 Jan 26.

Rybalkin SD, Yan C, Bornfeldt KE, Beavo JA. Cyclic GMP phosphodiesterases and regulation of smooth muscle function. Circ Res. 2003 Aug 22;93(4):280-91.

Saglam M, Vardar-Yagli N, Calik-Kutukcu E, Arikan H, Savci S, Inal-Ince D, Akdogan A, Tokgozoglu L. Functional exercise capacity, physical activity, and respiratory and peripheral muscle strength in pulmonary hypertension according to disease severity. J Phys Ther Sci. 2015 May;27(5):1309-12. doi: 10.1589/jpts.27.1309. Epub 2015 May 26.

Sahara M, Sata M, Morita T, Hirata Y, Nagai R. Nicorandil attenuates monocrotaline-induced vascular endothelial damage and pulmonary arterial hypertension. PLoS One. 2012;7(3):e33367. doi: 10.1371/journal.pone.0033367. Epub 2012 Mar 30.

Salom JB, Barberá MD, Centeno JM, Ortí M, Torregrosa G, Alborch E. Comparative relaxant effects of the NO donors sodium nitroprusside, DEA/NO and SPER/NO in rabbit carotid arteries. Gen Pharmacol. 1999 Jan;32(1):75-9.

Sánchez M, Galisteo M, Vera R, Villar IC, Zarzuelo A, Tamargo J, Pérez-Vizcaíno F, Duarte J. Quercetin downregulates NADPH oxidase, increases eNOS activity and prevents endothelial dysfunction in spontaneously hypertensive rats. J Hypertens. 2006 Jan;24(1):75-84.

Sandifer BL, Brigham KL, Lawrence EC, Mottola D, Cuppels C, Parker RE. Potent effects of aerosol compared with intravenous treprostinil on the pulmonary circulation. J Appl Physiol (1985). 2005 Dec;99(6):2363-8. Epub 2005 Sep 1.

Sato K, Li J, Metais C, Bianchi C, Sellke F. Increased pulmonary vascular contraction to serotonin after cardiopulmonary bypass: role of cyclooxygenase. J Surg Res. 2000 May 15;90(2):138-43.

Savai R, Pullamsetti SS, Kolbe J, Bieniek E, Voswinckel R, Fink L, Scheed A, Ritter C, Dahal BK, Vater A, Klussmann S, Ghofrani HA, Weissmann N, Klepetko W, Banat GA, Seeger W, Grimminger F, Schermuly RT. Immune and inflammatory cell involvement in the pathology of idiopathic pulmonary arterial hypertension. Am J Respir Crit Care Med. 2012 Nov 1;186(9):897-908. doi: 10.1164/rccm.201202-0335OC. Epub 2012 Sep 6.

Schermuly RT, Dony E, Ghofrani HA, Pullamsetti S, Savai R, Roth M, Sydykov A, Lai YJ, Weissmann N, Seeger W, Grimminger F. Reversal of experimental pulmonary hypertension by PDGF inhibition. J Clin Invest. 2005 Oct;115(10):2811-21.

Schermuly RT, Stasch JP, Pullamsetti SS, Middendorff R, Müller D, Schlüter KD, Dingendorf A, Hackemack S, Kolosionek E, Kaulen C, Dumitrascu R, Weissmann N, Mittendorf J, Klepetko W, Seeger W, Ghofrani HA, Grimminger F. Expression and function of soluble guanylate cyclase in pulmonary arterial hypertension. Eur Respir J. 2008 Oct;32(4):881-91. doi: 10.1183/09031936.00114407. Epub 2008 Jun 11.

Seferian A, Chaumais MC, Savale L, Günther S, Tubert-Bitter P, Humbert M, Montani D. Drugs induced pulmonary arterial hypertension. Presse Med. 2013 Sep;42(9 Pt 2):e303-10. doi: 10.1016/j.lpm.2013.07.005. Epub 2013 Aug 22.

Selej M, Romero AJ, Channick RN, Clozel M. Development of macitentan for the treatment of pulmonary arterial hypertension. Ann N Y Acad Sci. 2015 Nov;1358(1):68-81. doi: 10.1111/nyas.12856. Epub 2015 Aug 20.

Sellers MM, Stallone JN. Sympathy for the devil: the role of thromboxane in the regulation of vascular tone and blood pressure. Am J Physiol Heart Circ Physiol. 2008 May;294(5):H1978-86. doi: 10.1152/ajpheart.01318.2007. Epub 2008 Feb 29.

Sepúlveda FV, Pablo Cid L, Teulon J, Niemeyer MI. Molecular aspects of structure, gating, and physiology of pH-sensitive background K2P and Kir K+-transport channels. Physiol Rev. 2015 Jan;95(1):179-217. doi: 10.1152/physrev.00016.2014.

Shao D, Park JE, Wort SJ. The role of endothelin-1 in the pathogenesis of pulmonary arterial hypertension. Pharmacol Res. 2011 Jun;63(6):504-11. doi: 10.1016/j.phrs.2011.03.003.

Shimokawa H, Rashid M. Development of Rho-kinase inhibitors for cardiovascular medicine. Trends Pharmacol Sci. 2007 Jun;28(6):296-302. Epub 2007 May 7.

Simonneau G, Robbins IM, Beghetti M, Channick RN, Delcroix M, Denton CP, Elliott CG, Gaine SP, Gladwin MT, Jing ZC, Krowka MJ, Langleben D, Nakanishi N, Souza R. Updated clinical classification of pulmonary hypertension. J Am Coll Cardiol. 2009 Jun 30;54(1 Suppl):S43-54. doi: 10.1016/j.jacc.2009.04.012.

Smyth EM. Thromboxane and the thromboxane receptor in cardiovascular disease. Clin Lipidol. 2010 Apr 1;5(2):209-219.

Sobey CG. Potassium channel function in vascular disease. Arterioscler Thromb Vasc Biol. 2001 Jan;21(1):28-38.

Sommer N, Dietrich A, Schermuly RT, Ghofrani HA, Gudermann T, Schulz R, Seeger W, Grimminger F, Weissmann N. Regulation of hypoxic pulmonary vasoconstriction: basic mechanisms. Eur Respir J. 2008 Dec;32(6):1639-51. doi: 10.1183/09031936.00013908.

Soubrier F, Chung WK, Machado R, Grünig E, Aldred M, Geraci M, Loyd JE, Elliott CG, Trembath RC, Newman JH, Humbert M. Genetics and genomics of pulmonary arterial hypertension. J Am Coll Cardiol. 2013 Dec 24;62(25 Suppl):D13-21. doi: 10.1016/j.jacc.2013.10.035.

Spiekerkoetter E, Tian X, Cai J, Hopper RK, Sudheendra D, Li CG, El-Bizri N, Sawada H, Haghighat R, Chan R, Haghighat L, de Jesus Perez V, Wang L, Reddy S, Zhao M, Bernstein D, Solow-Cordero DE, Beachy PA, Wandless TJ, Ten Dijke P, Rabinovitch M. FK506 activates BMPR2, rescues endothelial dysfunction, and reverses pulmonary hypertension. J Clin Invest. 2013 Aug;123(8):3600-13. doi: 10.1172/JCI65592. Epub 2013 Jul 15.

Stanbrook HS, Morris KG, McMurtry IF. Prevention and reversal of hypoxic pulmonary hypertension by calcium antagonists. Am Rev Respir Dis. 1984 Jul;130(1):81-5.

Stenmark KR, Fagan KA, Frid MG. Hypoxia-induced pulmonary vascular remodeling: cellular and molecular mechanisms. Circ Res. 2006 Sep 29;99(7):675-91.

Stenmark KR, Meyrick B, Galie N, Mooi WJ, McMurtry IF. Animal models of pulmonary arterial hypertension: the hope for etiological discovery and pharmacological cure**.** Am J Physiol Lung Cell Mol Physiol. 2009 Dec;297(6):L1013-32. doi: 10.1152/ajplung.00217.2009. Epub 2009 Sep 11.

Stewart DJ, Levy RD, Cernacek P, Langleben D. Increased plasma endothelin-1 in pulmonary hypertension: marker or mediator of disease? Ann Intern Med. 1991 Mar 15;114(6):464-9.

Stoclet JC, Chataigneau T, Ndiaye M, Oak MH, El Bedoui J, Chataigneau M, Schini-Kerth VB. Vascular protection by dietary polyphenols. Eur J Pharmacol. 2004 Oct 1;500(1-3):299-313.

Stork PJ, Schmitt JM. Crosstalk between cAMP and MAP kinase signaling in the regulation of cell proliferation. Trends Cell Biol. 2002 Jun;12(6):258-66.

Sung JY, Choi HC. Nifedipine inhibits vascular smooth muscle cell proliferation and reactive oxygen species production through AMP-activated protein kinase signaling pathway. Vascul Pharmacol. 2012 Jan-Feb;56(1-2):1-8. doi: 10.1016/j.vph.2011.06.001. Epub 2011 Jun 25.

Sutliff RL, Kang BY, Hart CM. PPARgamma as a potential therapeutic target in pulmonary hypertension. Ther Adv Respir Dis. 2010 Jun;4(3):143-60. doi: 10.1177/1753465809369619.

Swenson ER. Hypoxic pulmonary vasoconstriction. High Alt Med Biol. 2013 Jun;14(2):101-10. doi: 10.1089/ham.2013.1010.

Sylvester JT, Shimoda LA, Aaronson PI, Ward JP. Hypoxic pulmonary vasoconstriction. Physiol Rev. 2012 Jan;92(1):367-520. doi: 10.1152/physrev.00041.2010.

Tabima DM, Frizzell S, Gladwin MT. Reactive oxygen and nitrogen species in pulmonary hypertension. Free Radic Biol Med. 2012 May 1;52(9):1970-86. doi: 10.1016/j.freeradbiomed.2012.02.041. Epub 2012 Mar 6.

Takeda Y, Miyamori I, Furukawa K, Inaba S, Mabuchi H. Mechanisms of FK 506-induced hypertension in the rat. Hypertension. 1999 Jan;33(1):130-6.

Tanner FC, Meier P, Greutert H, Champion C, Nabel EG, Lüscher TF. Nitric oxide modulates expression of cell cycle regulatory proteins: a cytostatic strategy for inhibition of human vascular smooth muscle cell proliferation. Circulation. 2000 Apr 25;101(16):1982-9.

Tantini B, Manes A, Fiumana E, Pignatti C, Guarnieri C, Zannoli R, Branzi A, Galié N. Antiproliferative effect of sildenafil on human pulmonary artery smooth muscle cells. Basic Res Cardiol. 2005 Mar;100(2):131-8. Epub 2004 Nov 24.

Teixeira CE, Priviero FB, Webb RC. Molecular mechanisms underlying rat mesenteric artery vasorelaxation induced by the nitric oxide-independent soluble guanylyl cyclase stimulators BAY 41-2272 [5-cyclopropyl-2-[1-(2-fluorobenzyl)-1H-pyrazolo[3,4-b]pyridin-3-yl]pyrimidin-4-ylamine] and YC-1 [3-(5'-hydroxymethyl-2'-furyl)-1-benzyl Indazole]. J Pharmacol Exp Ther. 2006 Apr;317(1):258-66. Epub 2005 Dec 13.

Teunissen BE, Smeets PJ, Willemsen PH, De Windt LJ, Van der Vusse GJ, Van Bilsen M. Activation of PPARdelta inhibits cardiac fibroblast proliferation and the transdifferentiation into myofibroblasts. Cardiovasc Res. 2007 Aug 1;75(3):519-29. Epub 2007 May 3.

Thenappan Thenappan, W Prins, Marc R Pritzker, John Scandurra, Karl Volmers, and E Kenneth Weir. The Critical Role of Pulmonary Arterial Compliance in Pulmonary Hypertension. 21 Jan 2016 as DOI: 10.1513/AnnalsATS.201509-599FR

Thomas BJ, Wanstall JC. Alterations in pulmonary vascular function in rats exposed to intermittent hypoxia. Eur J Pharmacol. 2003 Sep 12;477(2):153-61.

Thomas M, Ciuclan L, Hussey MJ, Press NJ. Targeting the serotonin pathway for the treatment of pulmonary arterial hypertension. Pharmacol Ther. 2013 Jun;138(3):409-17. doi: 10.1016/j.pharmthera.2013.02.002. Epub 2013 Feb 14.

Thorsen LB, Eskildsen-Helmond Y, Zibrandtsen H, Stasch JP, Simonsen U, Laursen BE. BAY 41-2272 inhibits the development of chronic hypoxic pulmonary hypertension in rats. Eur J Pharmacol. 2010 Nov 25;647(1-3):147-54. doi: 10.1016/j.ejphar.2010.08.032. Epub 2010 Sep 7.

Toque HA, Teixeira CE, Priviero FB, Morganti RP, Antunes E, De Nucci G. Vardenafil, but not sildenafil or tadalafil, has calcium-channel blocking activity in rabbit isolated pulmonary artery and human washed platelets. Br J Pharmacol. 2008 Jun;154(4):787-96. doi: 10.1038/bjp.2008.141. Epub 2008 Apr 21.

Townsley MI. Structure and composition of pulmonary arteries, capillaries, and veins. Compr Physiol. 2012 Jan;2(1):675-709.

Tribolo S, Lodi F, Winterbone MS, Saha S, Needs PW, Hughes DA, Kroon PA. Human metabolic transformation of quercetin blocks its capacity to decrease endothelial nitric oxide synthase (eNOS) expression and endothelin-1 secretion by human endothelial cells. J Agric Food Chem. 2013 Sep 11;61(36):8589-96. doi: 10.1021/jf402511c. Epub 2013 Aug 28.

Tsai BM, Turrentine MW, Sheridan BC, Wang M, Fiore AC, Brown JW, Meldrum DR. Differential effects of phosphodiesterase-5 inhibitors on hypoxic pulmonary vasoconstriction and pulmonary artery cytokine expression. Ann Thorac Surg. 2006 Jan;81(1):272-8.

Tsang SY, Yao X, Wong CM, Au CL, Chen ZY, Huang Y. Contribution of Na^+ -Ca^{2+} exchanger to pinacidil-induced relaxation in the rat mesenteric artery. Br J Pharmacol. 2003 Feb;138(3):453-60.

Tuder RM, Cool CD, Geraci MW, Wang J, Abman SH, Wright L, Badesch D, Voelkel NF. Prostacyclin synthase expression is decreased in lungs from patients with severe pulmonary hypertension. Am J Respir Crit Care Med. 1999 Jun;159(6):1925-32.

Upton PD, Morrell NW. The transforming growth factor-β-bone morphogenetic protein type signalling pathway in pulmonary vascular homeostasis and disease. Exp Physiol. 2013 Aug;98(8):1262-6. doi: 10.1113/expphysiol.2012.069104. Epub 2013 May 3.

van Albada ME, van Veghel R, Cromme-Dijkhuis AH, Schoemaker RG, Berger RM. Treprostinil in advanced experimental pulmonary hypertension: beneficial outcome without reversed pulmonary vascular remodeling. J Cardiovasc Pharmacol. 2006 Nov;48(5):249-54.

Veit F, Pak O, Brandes RP, Weissmann N. Hypoxia-dependent reactive oxygen species signaling in the pulmonary circulation: focus on ion channels. Antioxid Redox Signal. 2015 Feb 20;22(6):537-52. doi: 10.1089/ars.2014.6234.

Vildbrad MD, Andersen A, Holmboe S, Ringgaard S, Nielsen JM, Nielsen-Kudsk JE. Acute effects of levosimendan in experimental models of right ventricular hypertrophy and failure. Pulm Circ. 2014 Sep;4(3):511-9. doi: 10.1086/677366.

von Kügelgen I. Pharmacological profiles of cloned mammalian P2Y-receptor subtypes. Pharmacol Ther. 2006 Jun;110(3):415-32. Epub 2005 Oct 28.

Wakino S, Hayashi K, Tatematsu S, Hasegawa K, Takamatsu I, Kanda T, Homma K, Yoshioka K, Sugano N, Saruta T. Pioglitazone lowers systemic asymmetric dimethylarginine by inducing dimethylarginine dimethylaminohydrolase in rats. Hypertens Res. 2005 Mar;28(3):255-62.

Walker EH, Pacold ME, Perisic O, Stephens L, Hawkins PT, Wymann MP, Williams RL. Structural determinants of phosphoinositide 3-kinase inhibition by wortmannin, LY294002, quercetin, myricetin, and staurosporine. Mol Cell. 2000 Oct;6(4):909-19

Wang PG, Xian M, Tang X, Wu X, Wen Z, Cai T, Janczuk AJ. Nitric oxide donors: chemical activities and biological applications. Chem Rev. 2002 Apr;102(4):1091-134.

Wang RN, Green J, Wang Z, Deng Y, Qiao M, Peabody M, Zhang Q, Ye J, Yan Z, Denduluri S, Idowu O, Li M, Shen C, Hu A, Haydon RC, Kang R, Mok J, Lee MJ, Luu HL, Shi LL. Bone Morphogenetic Protein (BMP) signaling in development and human diseases. Genes Dis. 2014 Sep;1(1):87-105.

Wanstall JC, Kay CS, O'Donnell SR. Pinacidil-induced relaxation in pulmonary arteries isolated from pulmonary hypertensive and normotensive rats and pre-contracted with different spasmogens. Pulm Pharmacol. 1994 Dec;7(6):401-8.

Wanstall JC, O'Donnell SR. Responses to vasodilator drugs on pulmonary artery preparations from pulmonary hypertensive rats. Br J Pharmacol. 1992 Jan;105(1):152-8.

Ward JP, McMurtry IF. Mechanisms of hypoxic pulmonary vasoconstriction and their roles in pulmonary hypertension: new findings for an old problem. Curr Opin Pharmacol. 2009 Jun;9(3):287-96. doi: 10.1016/j.coph.2009.02.006. Epub 2009 Mar 16.

Weimann J, Ullrich R, Hromi J, Fujino Y, Clark MW, Bloch KD, Zapol WM. Sildenafil is a pulmonary vasodilator in awake lambs with acute pulmonary hypertension. Anesthesiology. 2000 Jun;92(6):1702-12.

Weir EK, Olschewski A. Role of ion channels in acute and chronic responses of the pulmonary vasculature to hypoxia. Cardiovasc Res. 2006 Sep 1;71(4):630-41. Epub 2006 Apr 27.

Wharton J, Davie N, Upton PD, Yacoub MH, Polak JM, Morrell NW. Prostacyclin analogues differentially inhibit growth of distal and proximal human pulmonary artery smooth muscle cells. Circulation. 2000 Dec 19;102(25):3130-6.

Wharton J, Strange JW, Møller GM, Growcott EJ, Ren X, Franklyn AP, Phillips SC, Wilkins MR. Antiproliferative effects of phosphodiesterase type 5 inhibition in human pulmonary artery cells. Am J Respir Crit Care Med. 2005 Jul 1;172(1):105-13. Epub 2005 Apr 7.

Wiklund A, Kylhammar D, Rådegran G. Levosimendan attenuates hypoxia-induced pulmonary hypertension in a porcine model. J Cardiovasc Pharmacol. 2012 May;59(5):441-9. doi: 10.1097/FJC.0b013e31824938f0.

Wilkins MR, Wharton J, Grimminger F, Ghofrani HA. Phosphodiesterase inhibitors for the treatment of pulmonary hypertension. Eur Respir J. 2008 Jul;32(1):198-209. doi: 10.1183/09031936.00124007.

Wilkins MR. Pulmonary hypertension: the science behind the disease spectrum. Eur Respir Rev. 2012 Mar 1;21(123):19-26. doi: 10.1183/09059180.00008411.

Wilson SJ, Dowling JK, Zhao L, Carnish E, Smyth EM. Regulation of thromboxane receptor trafficking through the prostacyclin receptor in vascular smooth muscle cells: role of receptor heterodimerization. Arterioscler Thromb Vasc Biol. 2007 Feb;27(2):290-6. Epub 2006 Nov 16.

Wozney JM1, Rosen V, Celeste AJ, Mitsock LM, Whitters MJ, Kriz RW, Hewick RM, Wang EA.. Novel regulators of bone formation: molecular clones and activities. Science 1988;242:1528–34.

Xie W, Wang H, Ding J, Wang H, Hu G. Anti-proliferating effect of iptakalim, a novel KATP channel opener, in cultured rabbit pulmonary arterial smooth muscle cells. Eur J Pharmacol. 2005 Mar 28;511(2-3):81-7.

Xu EZ, Kantores C, Ivanovska J, Engelberts D, Kavanagh BP, McNamara PJ, Jankov RP. Rescue treatment with a Rho-kinase inhibitor normalizes right ventricular function and reverses remodeling in juvenile rats with chronic pulmonary hypertension. Am J Physiol Heart Circ Physiol. 2010 Dec;299(6):H1854-64. doi: 10.1152/ajpheart.00595.2010. Epub 2010 Oct 1.

Yanagisawa M, Kurihara H, Kimura S, Tomobe Y, Kobayashi M, Mitsui Y, Yazaki Y, Goto K, Masaki T. A novel potent vasoconstrictor peptide produced by vascular endothelial cells. Nature. 1988 Mar 31;332(6163):411-5.

Yasutsune T, Kawakami N, Hirano K, Nishimura J, Yasui H, Kitamura K, Kanaide H. Vasorelaxation and inhibition of the voltage-operated Ca2+ channels by FK506 in the porcine coronary artery. Br J Pharmacol. 1999 Feb;126(3):717-29.

Yoshizumi M, Tsuchiya K, Suzaki Y, Kirima K, Kyaw M, Moon JH, Terao J, Tamaki T. Quercetin glucuronide prevents VSMC hypertrophy by angiotensin II via the inhibition of JNK and AP-1 signaling pathway. Biochem Biophys Res Commun. 2002 May 24;293(5):1458-65.

Young TE, Lundquist LJ, Chesler E, Weir EK. Comparative effects of nifedipine, verapamil, and diltiazem on experimental pulmonary hypertension. Am J Cardiol. 1983 Jan 1;51(1):195-200.

Yu PB, Beppu H, Kawai N, Li E, Bloch KD. Bone morphogenetic protein (BMP) type II receptor deletion reveals BMP ligand-specific gain of signaling in pulmonary artery smooth muscle cells. J Biol Chem. 2005 Jul 1;280(26):24443-50. Epub 2005 May 9.

Yuan JX, Aldinger AM, Juhaszova M, Wang J, Conte JV Jr, Gaine SP, Orens JB, Rubin LJ. Dysfunctional voltage-gated K+ channels in pulmonary artery smooth muscle cells of patients with primary pulmonary hypertension. Circulation. 1998 Oct 6;98(14):1400-6.

Yuan Z, Long C, Junming T, Qihuan L, Youshun Z, Chan Z. Quercetin-induced apoptosis of HL-60 cells by reducing PI3K/Akt. Mol Biol Rep. 2012 Jul;39(7):7785-93. doi: 10.1007/s11033-012-1621-0. Epub 2012 May 4.

Zhang D, Wang G, Han D, Zhang Y, Xu J, Lu J, Li S, Xie X, Liu L, Dong L, Li M. Activation of PPAR-γ ameliorates pulmonary arterial hypertension via inducing heme oxygenase-1 and p21(WAF1): an in vivo study in rats. Life Sci. 2014 Mar 7;98(1):39-43. doi: 10.1016/j.lfs.2013.12.208. Epub 2014 Jan 8.

Zhang WH, Liu CP, Zhang YJ, Ji YQ, Lu WX, Zeng Q. Additive effect of tadalafil and simvastatin on monocrotaline-induced pulmonary hypertension rats. Scand Cardiovasc J. 2012 Dec;46(6):374-80. doi: 10.3109/14017431.2012.729272. Epub 2012 Sep 28.

Zhao L, Mason NA, Morrell NW, Kojonazarov B, Sadykov A, Maripov A, Mirrakhimov MM, Aldashev A, Wilkins MR. Sildenafil inhibits hypoxia-induced pulmonary hypertension. Circulation. 2001 Jul 24;104(4):424-8.

Zhu Y, Zhang S, Xie W, Li Q, Zhou Y, Wang H. Iptakalim inhibited endothelin-1-induced proliferation of human pulmonary arterial smooth muscle cells through the activation of K(ATP) channel. Vascul Pharmacol. 2008 Feb-Mar;48(2-3):92-9. doi: 10.1016/j.vph.2008.01.001. Epub 2008 Jan 16.

Zhuplatov SB, Masaki T, Blumenthal DK, Cheung AK. Mechanism of dipyridamole's action in inhibition of venous and arterial smooth muscle cell proliferation. Basic Clin Pharmacol Toxicol. 2006 Dec;99(6):431-9.

Zippel N, Malik RA, Frömel T, Popp R, Bess E, Strilic B, Wettschureck N, Fleming I, Fisslthaler B. Transforming growth factor-β-activated kinase 1 regulates angiogenesis via AMP-activated protein kinase-α1 and redox balance in endothelial cells. Arterioscler Thromb Vasc Biol. 2013 Dec;33(12):2792-9. doi: 10.1161/ATVBAHA.113.301848. Epub 2013 Sep 26.